

## The Hipparcos and Tycho Catalogues



SP-1200  
June 1997

# The Hipparcos and Tycho Catalogues

Astrometric and Photometric Star Catalogues  
derived from the  
ESA Hipparcos Space Astrometry Mission

A Collaboration Between  
the European Space Agency  
and  
the FAST, NDAC, TDAC and INCA Consortia

and the Hipparcos Industrial Consortium led by

Matra Marconi Space

and

Alenia Spazio

European Space Agency  
Agence spatiale européenne

Cover illustration: an impression of selected stars in their true positions around the Sun, as determined by Hipparcos, and viewed from a distant vantage point. Inset: sky map of the  $B-V$  colour index from the Tycho Catalogue, in galactic coordinates.

*Published by:* ESA Publications Division, c/o ESTEC, Noordwijk, The Netherlands

*Scientific Coordination:* M.A.C. Perryman, ESA Space Science Department  
and the Hipparcos Science Team

*Composition:* Volume 1: M.A.C. Perryman  
Volume 2: K.S. O'Flaherty  
Volume 3: F. van Leeuwen, L. Lindegren & F. Mignard  
Volume 4: U. Bastian & E. Høg  
Volumes 5–11: Hans Schrijver  
Volume 12: Michel Grenon  
Volume 13: Michel Grenon (charts) & Hans Schrijver (tables)  
Volumes 14–16: Roger W. Sinnott  
Volume 17: Hans Schrijver & W. O'Mullane  
  
Typeset using  $\text{\TeX}$  (by D.E. Knuth) and dvips (by T. Rokicki)  
in Monotype Plantin (Adobe) and Frutiger (URW)

*Film Production:* Volumes 1–4: ESA Publications Division, ESTEC, Noordwijk, The Netherlands  
Volumes 5–13: Imprimerie Louis-Jean, Gap, France  
Volumes 14–16: Sky Publishing Corporation, Cambridge, Massachusetts, USA

*ASCII CD-ROMs:* Swets & Zeitlinger B.V., Lisse, The Netherlands

*Publications Management:* B. Battrick & H. Wapstra

*Cover Design:* C. Haakman

©1997 European Space Agency  
ISSN 0379-6566  
ISBN 92-9092-399-7 (Volumes 1–17)

*Price:* 650 Dfl (\$400) (17 volumes)  
165 Dfl (\$100) (Volumes 1 & 17 only)

Volume 4

# Construction of the Tycho Catalogue

Compiled by:

U. Bastian & E. Høg

with the support of

members of the TDAC Data Reduction Consortium



# Volume 4: Construction of the Tycho Catalogue

## Contents

Foreword . . . . .	xi
--------------------	----

### Section A: Background to the Tycho Data Analysis

1. Introduction . . . . .	1
1.1. Overview . . . . .	1
1.2. Pre-Launch Preparations . . . . .	2
1.3. Organisation of the TDAC Consortium . . . . .	3
1.4. Relevant Properties of the Mission and the Star Mapper . . . . .	5
1.5. Calibration Inputs . . . . .	7
1.6. Detection and De-Censoring . . . . .	10
2. Overview of the Tycho Data Processing . . . . .	15
2.1. Introduction . . . . .	15
2.2. Tycho Input Catalogue . . . . .	16
2.3. Prediction of Group Crossings . . . . .	16
2.4. Detection of Star Transits . . . . .	17
2.5. Recognition of Stars . . . . .	25
2.6. Transit Identification . . . . .	26
2.7. Photometry . . . . .	26
2.8. Astrometry . . . . .	27
2.9. Double and Multiple Stars . . . . .	28
2.10. Five Stages of Processing . . . . .	28
3. The Tycho Input Catalogue . . . . .	31
3.1. Introduction . . . . .	31
3.2. The Production of the Tycho Input Catalogue . . . . .	32
3.3. Cross-Matching the Guide Star Catalog with the INCA Data Base . . . . .	33
3.4. The Contents of the Tycho Input Catalogue . . . . .	37
3.5. The Tycho Input Catalogue Revision . . . . .	40
3.6. Publication of the Tycho Input Catalogue . . . . .	41

## Section B: Analysis Procedures and Intermediate Results

4. Satellite Data Processing . . . . .	43
4.1. Prediction of Group Crossings . . . . .	43
4.2. Background Determination . . . . .	51
4.3. Detection of Star Transits . . . . .	55
4.4. Estimation of Transit Parameters . . . . .	63
4.5. Verification Methods . . . . .	64
5. Recognition of Stars . . . . .	73
5.1. Introduction . . . . .	73
5.2. General Outlines . . . . .	73
5.3. Preparation of the Input Data . . . . .	74
5.4. The Search for Companion Stars . . . . .	76
5.5. The Search for Serendipity Stars . . . . .	81
5.6. Estimation of the Magnitudes of the Stars . . . . .	84
5.7. Properties of the Tycho Input Catalogue Revision . . . . .	87
6. Updating and Identification of Transit Data . . . . .	91
6.1. Prediction Updating-2 . . . . .	91
6.2. Prediction Updating-3 . . . . .	93
6.3. Identification of Transits . . . . .	96
6.4. Verification Methods . . . . .	99
7. Astrometric Analysis of Transit Data . . . . .	103
7.1. Theoretical Basis of the Astrometric Reduction . . . . .	103
7.2. Processings, Identification, Parasites . . . . .	107
7.3. Geometric Calibration of the Star Mapper . . . . .	111
7.4. Astrometric Parameters and Quality Classes . . . . .	117
8. Photometric Analysis of Transit Data . . . . .	123
8.1. Theoretical Basis . . . . .	123
8.2. Instrument Calibration . . . . .	126
8.3. Verification Methods . . . . .	128
9. De-Censored Magnitudes of Faint Stars . . . . .	133
9.1. Introduction . . . . .	133
9.2. The Statistical Model . . . . .	134
9.3. The Adaptation of the Model to the Actual Data . . . . .	136
9.4. The De-Censoring Procedure . . . . .	138
9.5. Verification of the Results of the De-Censoring . . . . .	144
10. Reprocessing of the Satellite Data . . . . .	149
10.1. Introduction . . . . .	149
10.2. The Tycho Input Catalogue Update . . . . .	151
10.3. Prediction of Group Crossings . . . . .	153
10.4. Prediction for Solar System Objects . . . . .	154
10.5. Detection of Transits . . . . .	156
10.6. Identification of Transits . . . . .	156
10.7. Verification Methods . . . . .	157

11. Production of the Tycho Catalogue . . . . .	159
11.1. Production of the Astrometric Catalogue . . . . .	159
11.2. Merging . . . . .	161
11.3. Completing Steps of the Catalogue Production . . . . .	164
11.4. Production of the Tycho Epoch Photometry . . . . .	174
11.5. Photometric Part of the Tycho Catalogue . . . . .	178
12. Tycho Processing Summary . . . . .	181
12.1. Introduction . . . . .	181
12.2. Raw Data and Pre-Reduction . . . . .	182
12.3. Sorting and Catalogue Preparation . . . . .	184
12.4. Catalogue Production . . . . .	185

### Section C: The Off-Line Tasks

13. Photometric Standard Stars . . . . .	187
13.1. The Preliminary Standard Star Catalogue . . . . .	187
13.2. The Revised Standard Star Catalogue . . . . .	188
14. Special Treatment of Double and Multiple Systems . . . . .	191
14.1. Introduction . . . . .	191
14.2. Close Double Stars from Catalogues . . . . .	192
14.3. Candidate Double Stars from Tycho Observations . . . . .	195
14.4. Astrometric Reduction of Close Double Stars in Reprocessing . . . . .	197
14.5. Double-Peak Detection in Reprocessing . . . . .	203
14.6. Photometric Duplicity Search . . . . .	204
15. Special Astrometry and Photometry of Solar System Objects . . . . .	205
15.1. General Overview of Planetary Data Treatment . . . . .	205
15.2. Reduction of Planet Observations . . . . .	207
15.3. Accuracy and Precision . . . . .	208

### Section D: Properties of the Final Tycho Catalogue

16. Contents of the Tycho Catalogue . . . . .	219
16.1. Overview of the Tycho Catalogue . . . . .	219
16.2. Astrometric Content . . . . .	220
16.3. Photometric Content . . . . .	233
16.4. The Tycho Epoch Photometry Annex . . . . .	239
17. Verification of the Tycho Catalogue: Stellar Content . . . . .	243
17.1. Introduction . . . . .	243
17.2. Completeness of the Tycho Catalogue at the Bright End . . . . .	243
17.3. Completeness of the Tycho Catalogue at the Faint End . . . . .	250
17.4. Cross References . . . . .	252
17.5. Concluding Remarks . . . . .	252

yr t r s g l a b y t i o i t a f i r e

sc of Ed S r i a n t s 1 2  
 e g l a t e c r a p h i c i n s i n g 1 8  
 e g l a t e c r a p h i c i n s i n g 1 8  
 s o i t i s o n 1 8 . . . . . 2 2  
 s o i t i s o n 1 8 . . . . . 2 2

18.6. Tycho Parallaxes . . . . . 265

19. Verification of the Tycho Catalogue: Photometry . . . . . 267

19.1. Tycho Mean Magnitudes . . . . . 267

19.2. Doubtful Standard Stars . . . . . 268

19.3. Tycho Suspected Variable Stars . . . . . 271

19.4. Comparison of Tycho and Hipparcos Epoch Photometry for Algol . . 275

19.5. Tycho Photometry of Double Stars . . . . . 279

20. Future Prospects . . . . . 283

20.1. Proper Motions Derived by Means of the Astrographic Catalogue . . 283

20.2. Reductions of Photographic Plates and CCDs using the Tycho Catalogue 285

20.3. Search for New Variables in the Epoch Photometry . . . . . 285

20.4. The Second Tycho Processing . . . . . 286

Appendices

Appendix A. References . . . . . 289

Index . . . . . 295

## FOREWORD

The Tycho experiment was not part of the Hipparcos mission approved by ESA in March 1980, nor had it been considered during the previous feasibility studies of the mission. The star mapper slit system was only intended for observation of the transit times of bright reference stars with known positions when they crossed the slits. These transit data were to be used to determine the satellite attitude in real time, as required for the observation of the planned 100 000 stars on the main modulating grid, and for the later accurate Hipparcos data reductions on ground.

It was during a study in March 1981 to define suitable meridian circle observations of reference stars for the attitude determination that the Tycho project was conceived by this author. The great potential of the star mapper for astrometric and photometric observations became clear and was immediately presented to the Hipparcos Science Team in three short technical notes. Incidentally, it gave rise to a project that looked more like a competitor to meridian circles than a helper. Since then the limiting magnitude of meridian circles has however improved from visual magnitude 10 to about 16 mag, whereas the limit for Tycho is about 11 mag.

Later, in 1981, ESA formally approved the Tycho project after a detailed assessment of the scientific return versus cost had been presented to the Science Programme Committee. At that time it aimed at determining magnitudes and positions for at least 400 000 stars. Had the Tycho proposal come a couple of months later, the satellite design would have been frozen, and the idea of the Tycho project would have been a lost opportunity. This wonderful idea would have been difficult to forget about, even though we were immersed in the fascination of the main mission, and in all the work it gave us.

The Tycho project required a very different approach to the data reductions to that of the main mission. The Tycho Consortium had to be set up, a very difficult task since practically all European astrometric expertise was busy with the main mission. But new dedicated teams were formed at Copenhagen, Heidelberg, Strasbourg, and Tübingen, and we obtained unfailing support from members of the Hipparcos Science Team, and from the FAST, INCA and NDAC Consortia, in defining the data reduction scheme, supplying photometric standard stars, satellite attitude, mathematical formulations, instrument calibrations, and other early access to results and data bases. We had to invent the data reduction scheme which in principle was very simple, but in practice became very complex, partly because satellite observations are never simple, partly because the Tycho astrometry had to be closely tied to the Hipparcos reference frame, and partly because we wanted to utilize every bit of information contained in the data. The extensive data simulations carried out before launch were very useful, but the real satellite data immediately posed many unforeseen problems, such as ‘spikes’ in the photon counts, and the complexities of the background determination. A quick response to new ideas was paramount to our work, whilst keeping a focused and concerted effort on the timely reduction of the 100 Gigabytes of data.

The care and optimisation invested in the data analysis were rewarded with a final Tycho Catalogue of more than one million stars. The timely reduction also succeeded, and the Tycho results were eventually finalized about one year earlier than expected before launch. This was early enough to allow the common completion, verification, and publication of both catalogues, and the introduction of the  $V_T$  magnitude, and the derived  $B - V$  and  $V - I$ , into the main Hipparcos Catalogue. The addition of the

colour indices from Tycho greatly enhances the astrophysical value of the Hipparcos parallaxes, supplying otherwise missing accurate abscissae in the Hertzsprung-Russell diagram for about half of the Hipparcos Catalogue stars.

The late addition of the Tycho project meant that particular efforts, not foreseen during the Phase A study, had to be mobilized rapidly. This was accomplished within the European Space Agency, the scientific community around Hipparcos, and their supporting institutes and space agencies. The support of the four institutes where the main Tycho data reduction was carried out deserves our special gratitude: Astronomisches Institut, Tübingen; Astronomisches Rechen-Institut, Heidelberg; Centre de Données astronomiques de Strasbourg; and Copenhagen University Observatory. The support of the Space Telescope Science Institute in providing early access to the Guide Star Catalog for the Tycho Input Catalogue production was crucial for the Tycho project.

The scientific utilisation of the Tycho results has barely begun, with all available effort to date having been devoted to the catalogue completion and publication. The Tycho Catalogue will be central to the astrometric reductions of photographic plates and CCD images, at the same time providing a dense net of two-colour photometric reference stars. The derivation of accurate proper motions for all Tycho stars by means of observations at earlier epochs, especially the Astrographic Catalogue, has started. The discovery of new variable stars by means of the Tycho epoch photometry has just begun, and the study of colour variation in known variable stars has been envisaged.

Despite the thorough reduction of the observations carried out by the Tycho Consortium it is possible to do more, because the one million star catalogue is now available as a starting point, and because modern fast computers and large disk arrays have become available. A second Tycho reduction has begun in a collaboration between Copenhagen and Heidelberg and is expected to measure about 3 million stars. The immense potential of space astrometry has been opened up.

E. Høg, Tycho Consortium Leader

# 1. INTRODUCTION

*In the Tycho project astrometric and photometric data of 1 052 000 stars to a limit of  $V_T = 11.5$  mag were derived. The brightest 99 per cent of the stars obtained magnitudes in two passbands  $B_T$  and  $V_T$ . A precision (median standard error) of 7 mas was achieved in astrometry (positions, annual proper motions and parallaxes) for stars with  $V < 9$  mag, and 25 mas for all stars. The median precision in photometry is 0.012 mag for  $V_T$  of the bright stars and 0.06 mag for the whole catalogue. Double stars with separation larger than 2 arcsec have been resolved, and duplicity down to 0.4 arcsec has been detected. The results were obtained by appropriate treatment of the continuous data records generated by the Hipparcos satellite's star mapper which provides simultaneous measurements in two spectral channels. The processing was based on predicted star transits using its own 'Tycho Input Catalogue'. The data treatment was carried out by the Tycho Data Analysis Consortium (TDAC), using calibration and satellite attitude information from the Hipparcos data reduction consortium, NDAC, and photometric standard stars from the FAST Consortium. An overview of the data reductions and of the astrometric and photometric results is given. Raw observation data and their numerical treatment are described.*

---

## 1.1. Overview

---

The astrometry satellite Hipparcos was launched by the European Space Agency on 8 August 1989 into an elliptical transfer orbit, from which observations were carried out in the period November 1989 to August 1993, instead of from the intended geostationary orbit. A major consequence of this was that some 50 per cent of the data were lost for the Tycho project due to enhanced background counts during passage through the van Allen belts resulting in the loss of accurate attitude determination. Nevertheless, the Tycho Catalogue (TYC) from the 'revised' mission of 37 months surpassed the expected number of stars by a factor of 2.5, and exceeded the precision predicted before launch.

The photon counts from the star mapper of the Hipparcos astrometry satellite were processed to detect star transits exceeding a certain signal-to-noise ratio. These detections or transits, collected throughout the mission, were identified with stars contained in a Tycho Input Catalogue of 3 million stars. Stars down to a limiting magnitude of  $V = 11.5$  mag, depending on star colour, were recognized within small areas of 40 arcsec diameter centred on each Tycho Input Catalogue position, leading to the final Tycho

Catalogue of a million stars. The typical (median) astrometric and photometric precision of a mean value in the Tycho Catalogue is 0.025 arcsec and 0.06 mag, respectively. This is also the typical precision at the median magnitude  $V_T = 10.5$  mag. Annual proper motions and parallaxes were obtained with the same precision. The standard errors of positions and magnitudes roughly decrease by a factor of 2 per magnitude towards brighter stars, reaching a roughly constant level of about 2 mas for stars brighter than  $V_T = 6$  mag. The Tycho Catalogue content is described in Chapter 16 and in Volume 1, Section 2.2. The complete stellar content is mapped in Volumes 14–16.

Photometry for individual transits is given in the Tycho Epoch Photometry Annex A for a selection of about 34 000 stars, on average 170 epochs per selected star (see Section 2.7). Annex A is made available on a CD-ROM, while an Annex B with epoch photometry for 481 000 stars is available from the Centre de Données astronomiques de Strasbourg (CDS). Double stars with separations larger than about 2 arcsec are resolved. For separations down to 0.4 arcsec, duplicity was recognized from a correlation between the position angle of the slit and the estimated magnitude.

---

## 1.2. Pre-Launch Preparations

---

When the Hipparcos project was approved by ESA early in 1980, it had not been realized that the star mapper could be used as a powerful astrometric and photometric device. Soon afterwards, in 1981, the idea was explored by E. Høg in notes to ESA. It was shown that the star mapper could give very important scientific results (Høg, Jaschek & Lindegren 1982). Indeed, the results would by far outweigh all ground-based observations of all meridian circles already made during the present century, meridian circles being the principal source of fundamental astrometric observations. It would, furthermore, represent the largest and most homogeneous photometric catalogue ever produced.

The primary purpose of the Hipparcos star mapper was to observe the transit time of bright reference stars of known position when they crossed the slits. By means of known positions and transit times, the attitude of the satellite was determined. The satellite attitude had to be known with an accuracy of about 1 arcsec during the mission in order to point the light-sensitive area of the main detector at the individual programme stars as they crossed the main field of view. A good attitude knowledge is also required at a later stage to achieve the best astrometric accuracy in the data analysis for the programme stars, and here the attitude must be known with an accuracy of 0.1 arcsec; in fact 0.03 arcsec was achieved on average perpendicular to the scan direction, and 0.002 arcsec along the scan direction.

Since stars used for the satellite real-time attitude determination are a small subset of all stars brighter than the star mapper detection limit, it is evident that observations of transit times for many stars, other than those required for attitude determinations, can be exploited to derive the positions of these stars. The photometric results are obtained from the analysis of the stellar photon flux at the slit transits.

In 1981, ESA formally approved the Tycho project which then aimed at determining magnitudes and positions for at least 400 000 stars. The hardware changes required were the introduction of dichroic beam splitters and a pair of redundant photomultiplier tubes into the science payload, and the provision to transmit all photon counts from

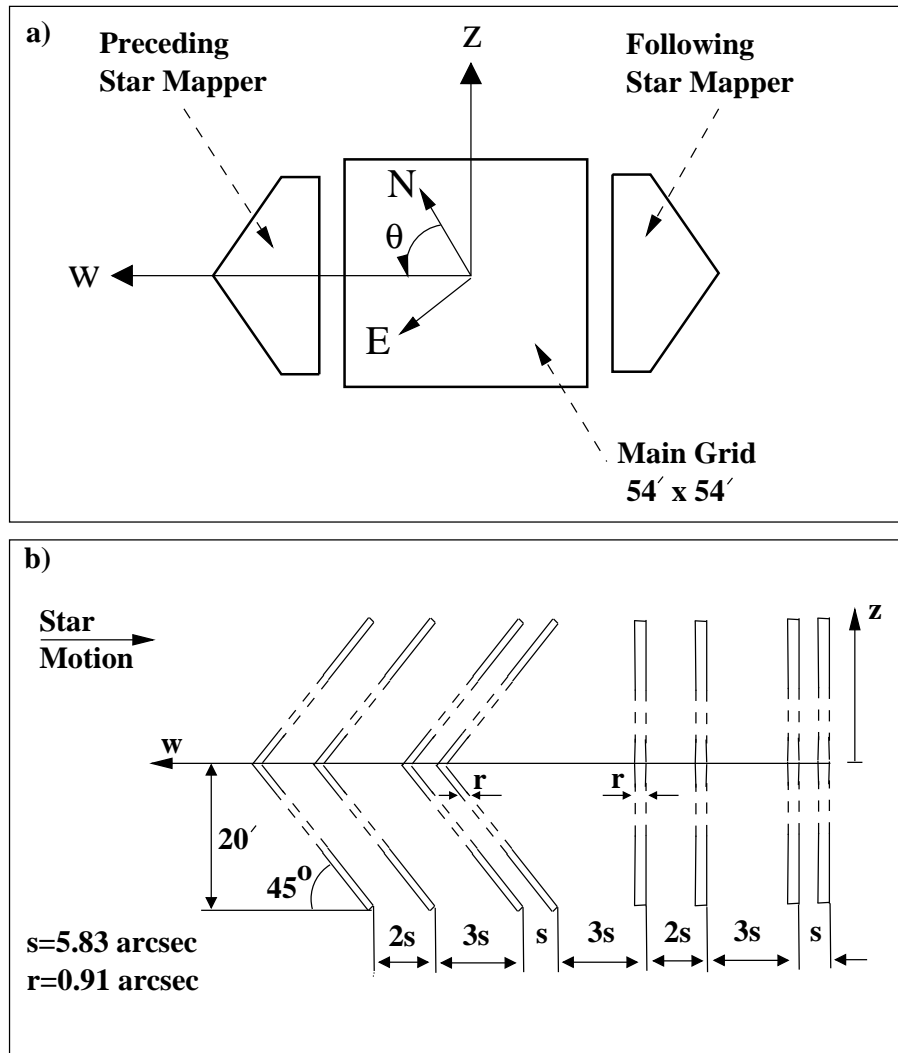


**Figure 1.1.** The slit systems at the focal plane. (a) Arrangement of the star mappers and the main grid; definition of the  $w, z$  coordinate system and the position angle  $\theta$  relative to celestial north and east ('N' and 'E' in the figure). (b) The preceding star mapper; the following star mapper is redundant and was in fact never used. The 'vertical' slits of the star mapper are perpendicular to the motion of the stars, while the 'chevron' slits are inclined by  $45^\circ$ . The light from the whole star mapper area is divided by a dichroic beam splitter into two photomultiplier tubes which count the photoelectrons simultaneously in two bands:  $B_T$  and  $V_T$ .

these tubes to the ground—not only during the time intervals when a reference star required for the attitude reconstruction was crossing the star mapper slits (Figure 1.1).

---

### 1.3. Organisation of the TDAC Consortium

---

In 1982, ESA called for commitments to perform the Tycho scientific data analysis which resulted in the formation of the Tycho Data Analysis Consortium (TDAC) with participation from most ESA countries and the USA. The participation in TDAC before

launch appears in Appendix C in Perryman *et al.* (1989, Vol. III). The title pages of Volume 1 specify in detail the participation during the mission and catalogue production.

The following contains an overview of the data analysis, illustrated in Figure 1.2, as it was actually carried out. It is, however, worth recalling briefly how the concepts of the data analysis changed considerably from the first ideas in 1981 through the studies before launch and the practical experience with real observations.

The first idea was already based on detection of a stellar transit over a group of four slits, and this feature was maintained throughout. The usefulness of an input catalogue for the Tycho data reduction was briefly discussed by Høg, Jäschek & Lindegren (1982), but no uniform catalogue with more than 400 000 stars existed at that time. In the summer of 1982 an unexpected possibility appeared when the plan for the Guide Star Catalog (GSC) of 20 million stars for the Hubble Space Telescope became known. Enormous savings in computational efforts would be made if the mapping of the detections could be limited to very small areas centred on the positions of the brightest 1 or 2 million GSC stars. This idea implied that the Tycho Catalogue would then not be truly unbiased in terms of the stellar content, but this was not considered too serious a handicap. The idea of a Tycho Input Catalogue based on the Guide Star Catalog was quickly accepted.

The following time was busy with the design of the data analysis for the main Hipparcos mission, but in 1984 the detection of star transits on the star mapper was studied by Høg (1985) and the quality of various estimators for the detection was discussed by Yoshizawa *et al.* (1985). In 1985 the concept of mapping in a small area was presented by Grewing & Høg (1986). Numerous meetings of the Tycho participants helped develop the concepts. Simulations of the processes were made and described in internal technical reports. Internal Tycho reports reached the total number of 265 in 1995, not including a thousand short messages by electronic mail. The development of ideas up to the time of launch is also recorded in Høg (1985), and in Perryman *et al.* (1989, Vol. III, Sections 10 and 11).

The first real photon counts from the satellite revealed that three problems had not obtained an optimal solution before launch: (1) determination of the background level; (2) suppression of side lobes generated by the four slits; and (3) suppression of narrow spikes caused by cosmic events. The solutions were found and implemented by A. Wicenec in early 1990. This was reported in Høg & Wicenec (1991) with the other good news that the stellar count rates were 20 per cent higher than predicted, the typical background was slightly lower than expected, and the effect of the background noise was decreased by the new determination method. This implied that a million stars could perhaps be detected, in spite of the 50 per cent loss of effective observing time due to passage through the van Allen belts and at perigee. This is indeed the number of stars finally included in the Tycho Catalogue. The astrometric accuracy of 0.03 arcsec predicted in 1982 for stars of  $B = 10$  mag, or  $V = 9.3$  mag, is obtained for stars one magnitude fainter.

The apparent complexity of the Tycho data processing results from three main features: (i) the large number of faint stars with poor *a priori* positions to  $\pm 1$  arcsec (source confusion in the photon counts); (ii) the possibility of the transit arising from either field of view and from different slit systems; (iii) the relatively poor early knowledge of the satellite attitude of  $\pm 1$  arcsec.

These conditions lead to an iterative data processing approach, and as a result the raw photon counts from the star mapper underwent a sequence of processing steps. Firstly,

the 'detection' process was used to detect slit transits above a certain signal-to-noise threshold, and to estimate the epoch, amplitude and background associated with each such transit. Each transit was identified or associated with a star by means of a series of processes explained below: prediction, recognition and identification. The 'Identified Transits' (IT in Figure 1.2) were finally analyzed to yield the astrometric results. The photometric results were produced by means of the identified transits and a data set of 'All Transits' (AT in Figure 1.2) containing the information on how close each transit is to the star defined by the astrometric processing.

The astrometric and photometric results were merged into the main Tycho Catalogue, containing mean values for each star and some external data, e.g. the identification numbers of stars in the Hipparcos Catalogue.

---

#### **1.4. Relevant Properties of the Mission and the Star Mapper**

---

The Hipparcos satellite observed from an elliptical orbit with the apogee at the geostationary distance as a result of the apogee boost motor failure. The spin axis pointed at an angle of  $43^\circ$  from the Sun, and moved with nearly constant angular velocity around the Sun 6 times per year in the so-called revolving scanning mode. The spin rate was 11.25 revolutions per day or 168.75 arcsec per second, with variations up to 1 per cent. With a sampling frequency of 600 Hz for the star mapper the stars moved about 0.281 arcsec/sample. Payload characteristics are given in Table 1.1. Chapters 2, 3, 5, 7, 9, 10 and 14 of Volume 2 contain further information on the star mapper.

Calibration of the star mapper properties was obtained from a combination of laboratory measurements and in-flight calibrations based on the routine star observations; no special observations were performed for the purpose of calibration alone. The slits of the modulating grid have been manufactured by electron beam scanning thus ensuring utmost accuracy, (see the grid specifications in Volume 2, Table 2.6), so that star observations were sufficient to provide the final high accuracy. Some of the calibration parameters varied with time during the mission, e.g. due to changes of the telescope focal length and the orientation of the grid in the telescope.

The single-slit response functions, giving the light curve as a star crosses a slit, were obtained from star observations and are given in Section 1.5. Such functions were used in every signal amplitude estimation of the transit of a star over a group of four slits (see Section 4.4).

The spectral transmission curves are discussed in Section 1.5. The slits did not have ideally constant width along their length and the optics were not ideally transparent. The photometric sensitivity therefore had to be calibrated by means of star observations as described in Chapter 8.

The positions of the slits in the focal plane were known beforehand so that the time of transit for stars with known positions could be predicted by means of the satellite attitude. For highest precision the positions of the slits in the focal plane and their deviation from being ideally straight had to be calibrated by the astrometric star observations. This so-called geometric calibration is described in Section 7.3.

## TYCHO DATA FLOW - main processing

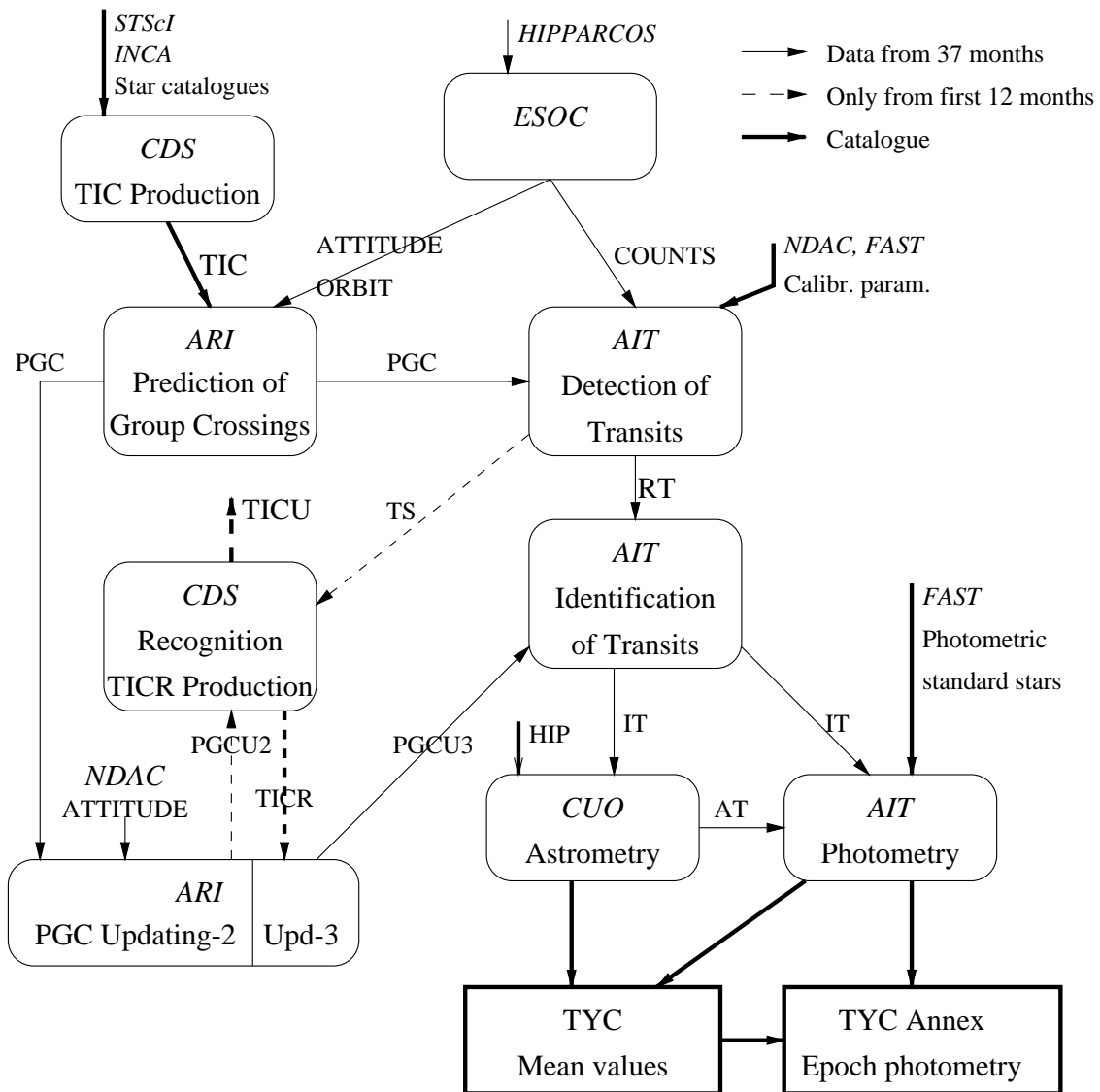


**Figure 1.2.** The data flow of Tycho main mass processing. Further explanation is given throughout these chapters on Tycho. A more complete representation of the data flow and processes and their distribution on the participating institutes is given in Figure 12.1. The main institutes, in italics, are situated in: Darmstadt (ESOC), Strasbourg (CDS), Heidelberg (ARI), Tübingen (AIT) and Copenhagen (CUO). Abbreviations for data are: TIC = Tycho Input Catalogue, TICR = TIC Revision; the output catalogues are HIP = Hipparcos Catalogue and TYC = Tycho Catalogue; PGC = Predicted Group Crossing, PGCU = PGC Updating, RT = Raw Transit, IT = Identified Transit, TS = Transit Summary, AT = All Transits.

**Table 1.1.** Hipparcos and Tycho payload characteristics from Volume 2, Table 2.1.

<b>Optics:</b>	Telescope configuration	All-reflective Schmidt
	Field of view	$0^{\circ}9 \times 0^{\circ}9$
	Separation between fields	$58^{\circ}$
	Diameter of primary mirror	290 mm
	Focal length	1400 mm
	Scale at focal surface	$6.8\mu\text{m}$ per arcsec
	Mirror surface accuracy	$\lambda/60$ rms (at $\lambda = 550$ nm)
<b>Primary Detection System:</b>	Modulating grid	2688 slits
	Slit period	1.208 arcsec ( $8.2\mu\text{m}$ )
	Detector	Image dissector tube
	Photocathode	S20
	Scale at photocathode	$3.0\mu\text{m}$ per arcsec
	Sensitive field of view	38 arcsec diameter
	Spectral range	375–750 nm
	Sampling frequency	1200 Hz
<b>Star Mapper (Tycho) System:</b>	Modulating grid	4 slits perpendicular to scan 4 slits at $\pm 45^{\circ}$ inclination
	Detectors	Photomultiplier tubes
	Photocathode	Bi-alkali
	Spectral range ( $B_T$ )	$\lambda_{\text{eff}} = 430$ nm, $\Delta\lambda = 90$ nm
	Spectral range ( $V_T$ )	$\lambda_{\text{eff}} = 530$ nm, $\Delta\lambda = 100$ nm
	Sampling frequency	600 Hz

---

## 1.5. Calibration Inputs

---

### Single-Slit Response Functions

Figures 1.3(a) and 1.3(b) show response functions for the inclined slits and illustrate the significant difference between the preceding field of view and the following field for these slits. Such a difference does not exist for the vertical slits as appears from Figure 1.3(c).

The inclined slits, but not the vertical, show a considerable asymmetry for the preceding field: For  $z < 0$  shown in Figure 1.3(a) the trailing side, i.e. the side with larger sample number, is higher than the leading side. This is reversed for  $z > 0$ . This phenomenon would be observed if the stellar image in the preceding field is accompanied by a fainter ‘ghost’ image at about 1 arcsec smaller  $z$ -value. It is noted that the direction of the  $z$ -axis is defined in Figure 1.1, in accordance with Equations 1.15 and 1.16 in Volume III of Perryman *et al.* (1989) and Figures 2.7.4 and 2.7.6 of Volume 1 (Perryman *et al.* 1989).

All functions in the figures are for the  $B_T$  channel and  $z < 0$ . The functions for  $V_T$  are essentially identical. In practice 16 combinations of vertical/inclined, preceding/following,  $B_T/V_T$ , and  $z < 0 / > 0$  were determined and used in the photometric signal estimation.

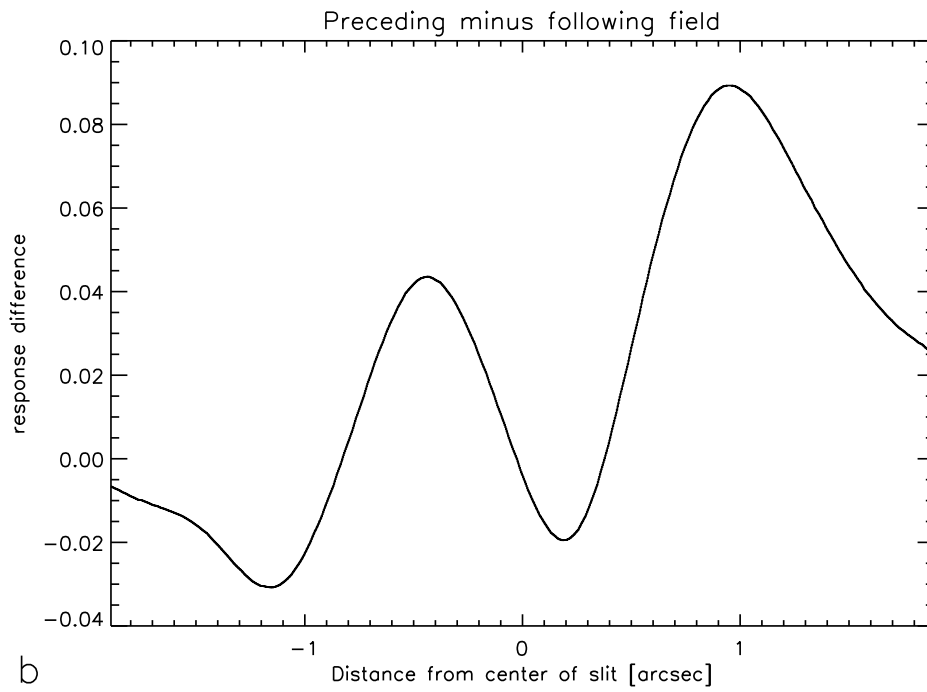
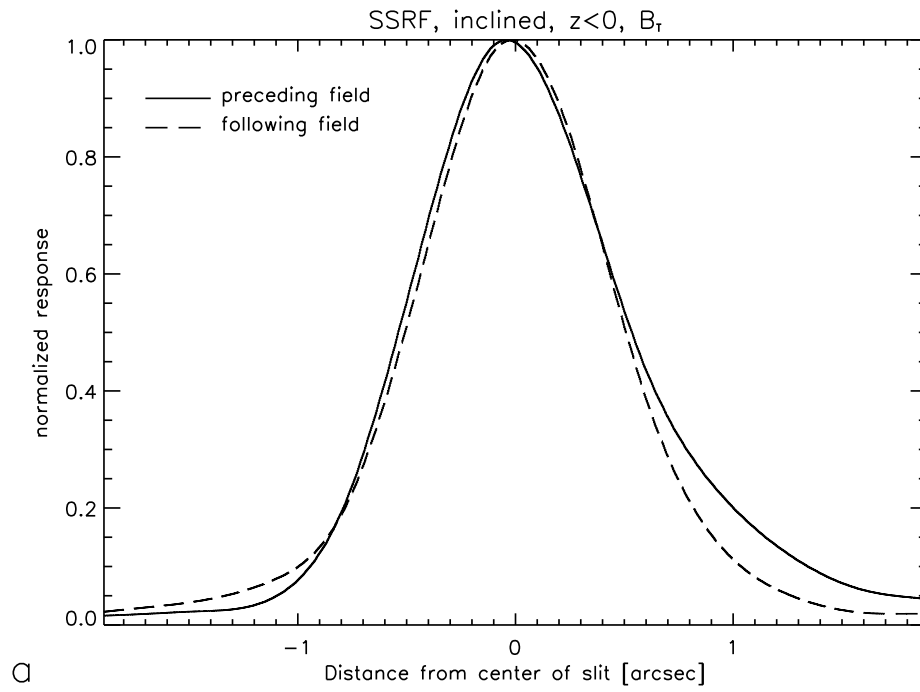


**Figure 1.3(a,b).** Slit response functions for inclined slits: (a) preceding and following fields, (b) the difference. The abscissa corresponds to increasing sample number.

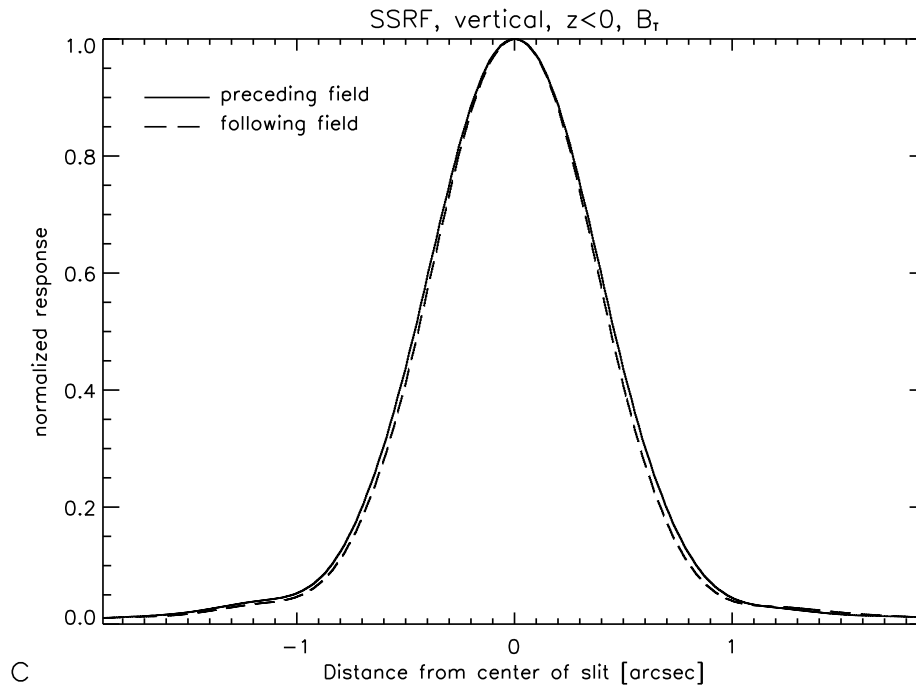


**Figure 1.3(c).** Slit response functions for vertical slits.

### Preliminary Payload Geometry Calibration

Tycho reductions started using an on-ground star mapper geometry provided by ESA. It was implemented in the form of a calibration file provided by FAST. Due to the strong rotation of the grid in the focal plane, this had very soon to be replaced by an updated version, which was then used for the initial steps of Tycho data reductions throughout the mission (see Section 4.1).

For the iteration steps, however, calibration files from NDAC were used, for reasons explained in Chapter 6. The NDAC calibration files were based on the on-ground calibration of the so-called ‘medium-scale irregularities’ provided by ESA (Figure 1.4), complemented by 11 low-order distortion terms derived by NDAC from in-orbit data. Both the medium-scale irregularities and the distortion terms were recalibrated in the Tycho astrometry processing (Chapter 7).

The on-ground data described the actual shape of the star mapper slits quite well. The maximum value of the medium-scale irregularities in Figure 1.4 is about 180 mas; the maximum value of the Tycho corrections is only about 10 mas, see Figure 7.4.

### Spectral Response and Photometric Standard Stars

Spectral transmission curves from laboratory measurements are given in Tables 2.3, 2.4 and Figure 2.19 of Volume 2. The  $B_T$  and  $V_T$  magnitudes in the Tycho passbands for available photometric standard stars were derived before launch by M. Grenon corresponding to these transmission values. It is noted that the transmissions were not otherwise used in the Tycho data reduction. More accurate spectral passbands for  $B_T$  and  $V_T$  were derived after launch from observations as given in Volume 1, Table 1.3.1

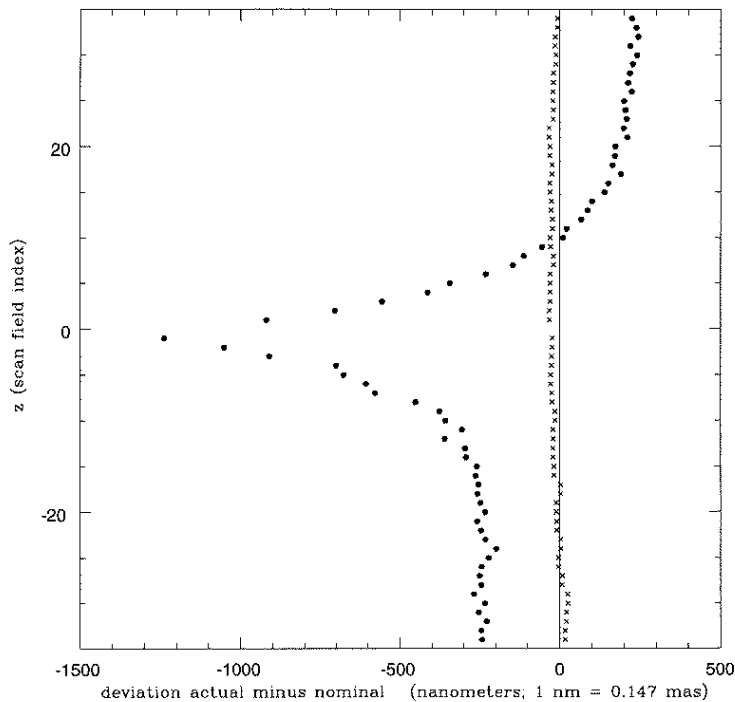


**Figure 1.4.** On-ground calibration of the medium-scale irregularities of the star mapper grid. The electron beam etching of the star mapper grid was done in 68 small segments called ‘scan fields’, each having a size of about 0.6 arcmin perpendicular to the scanning direction. The figure shows the mean displacement of the actual slits in the direction of the scanning motion relative to their nominal location on the grid substrate, for each of the scan fields. Crosses refer to the vertical slits, filled hexagons to the inclined slits. The maximum value of  $-1239$  nm (at the tip of the lower branch of the inclined slits) corresponds to  $182$  mas at the focal length of Hipparcos. The vertical scale in the figure represents the numbering of the scan fields ( $-34$  to  $-1$ , and  $+1$  to  $+34$ ).

and Figure 1.3.1. They were inferred by M. Grenon from Tycho observations of the photometric standard stars. The redetermination of the spectral passbands resulted in a redefinition of the standard star magnitudes, as described in Chapters 8 and 13.

---

## 1.6. Detection and De-Censoring

---

A part of Section 2.2 of Volume 1, related to the Tycho data reduction, is repeated here in slightly modified form. It introduces some main concepts and methods, thus complementing the more detailed description in Chapter 2 of the various work tasks.

**Transits, detections, measurements:** In the terminology of the Hipparcos Catalogue, a star ‘transit’ is defined as a crossing of the star across the main modulating grid ( $2688$  slits covering a field of view of approximately  $0.9 \times 0.9$ ). In the terminology of the Tycho Catalogue, a ‘transit’ refers to the crossing of the star across a star mapper slit system (either of a set of four vertical or inclined slits of  $40$  arcmin length, located at the edge of the main field of view, and used primarily for the satellite real-time attitude determination). Such a transit is defined irrespective of whether or not such a crossing

yields ‘useful’ astrometric and/or photometric information. The transit yields useful astrometric and/or photometric information when the star is not too faint, when the background was below a certain limit, when an accurate attitude determination was available, and when the observations were not perturbed by nearby bright stars.

All relevant transits related to a given star have been combined to provide the astrometric data and the summary photometric data contained in the main Tycho Catalogue, and individual transit records (providing ‘epoch photometry’) are contained in the Tycho Epoch Photometry Annex. The summary photometric data provide median magnitudes for bright stars and ‘de-censored mean magnitudes’ for fainter stars, and a set of parameters and flags giving an overview of the variability. The Tycho Epoch Photometry Annex includes details of each transit including background, observation epoch, and related quantities and flags.

In practice, the detection process giving a signal amplitude and a transit time was carried out on a signal where the photon counts in the  $B_T$  and  $V_T$  channels had been added, forming the so-called  $T$  channel. The term ‘detected transit’ is used to refer to a transit containing a significant signal belonging to the relevant star, and this signal itself is called a detection. When a signal was detected above a signal-to-noise ratio of 1.5 in the  $T$  channel an estimation (or measurement) of the signal amplitude was carried out in the  $B_T$  and  $V_T$  channels separately whenever possible. If no such measurement was available, a flag (see Table 2.6.2 of Volume 1) indicates that the magnitude could not be measured in one or other of the separate channels.

**Valid and invalid transits for photometry:** Transits were used for Tycho (mean value) photometry irrespective of whether or not the object was actually detected in the predicted ‘transit interval’ of a few arcsec length for the corresponding slit group—the condition for using the transit being simply that the relevant data interval was considered to be ‘valid’. Such a transit interval could contain several detections (either real detections due to the predicted star or to another star, or false detections due simply to photon noise) or it could contain no detection at all.

Certain transit intervals were considered as ‘invalid’, and subsequently excluded from use in Tycho photometry, for a variety of reasons:

- (a) if the satellite attitude was poorly known, or if (attitude-control) jet firings were affecting the satellite attitude estimation at the moment of the observations;
- (b) if the detector background was high, for example as a result of a passage of the satellite through the van Allen radiation belts—a higher background was acceptable for astrometry than for photometry;
- (c) because the star crossed the star mapper slit system too close to the end of the slit, or to the  $90^\circ$  angle of the inclined slits—in such cases, attitude uncertainties may have made it infeasible to distinguish between ‘uncaptured’ transits, and transits where the signal was below the detectability threshold.

**Non-detections and de-censored magnitudes:** A valid transit interval was classified as ‘non-detected’ or ‘censored’ if it contained no detection, in the  $T$  channel, close enough to the predicted transit time for the relevant star. The criterion for rejection was that all residuals of detections in the astrometric adjustment of the transit interval were larger than given limits.

Limits used in astrometry for the rejection of detections were  $|\Delta u| > 1.0$  arcsec or  $|\Delta u| > 3\sigma_u$ , where  $\Delta u$  is the difference between the observed and computed transit times (converted to an angular distance using the instantaneous satellite scan speed across the slit group), and  $\sigma_u$  is the standard error of  $\Delta u$ . A single limit was used in the de-censoring analysis,  $|\Delta u| > 0.6$  arcsec. Since transit detection was based on preliminary predicted transit times, which were sometimes in error by a large amount, the real transit occasionally occurred outside the predicted transit interval. Such detected transits were not assigned to the appropriate star and were thus lost, even when the improved transit times were introduced at a later stage. As a consequence, non-detections were occasionally associated even with bright stars. This problem was accommodated within the mathematical model for the de-censoring analysis by assuming that there was a probability of 6 per cent that a predicted Tycho star transit resulted in a non-detection even for a bright star. This is referred to as the assumption of 6 per cent ‘spurious non-detections’, and users of the Tycho epoch photometry should be aware of this deficiency. Photometric standard star observations were used for checking the validity of the de-censoring analysis and for correcting final small biases, as described in further detail in Chapter 9.

The use of non-detected transits has two reasons. First, because detectability depends on the signal-to-noise ratio of a given transit, mean or median magnitudes have not simply been constructed from the detected transits—rather, a ‘de-censored mean magnitude’ in  $B_T$  and  $V_T$  was constructed, using model-based inferred magnitudes in place of transits which were either not detected in the  $T$ -channel, or detected but not measured in the  $B_T$  or  $V_T$  channels. All valid transits were thus taken into account, whether detected or not (see Chapter 9 for details). Second, non-detected transits may be relevant in variability studies, where it may be important to identify whether a photometric data point is absent because the object’s magnitude fell below the threshold at that epoch, or simply because no data were acquired at that epoch. But a non-detection is not always an indication that the star was too faint to be detected due to the 6 per cent spurious non-detections described above.

For bright stars with  $B_T \leq 8.5$  mag and  $V_T \leq 8.0$  mag a median magnitude was derived from the measured signal in the  $B_T$  and  $V_T$  channels respectively. This median magnitude is equivalent, within 0.005 mag, to a de-censored mean magnitude because bright stars resulted in very few non-detections. The median magnitude was adopted for bright stars since the median could also be constructed for variable stars, while the de-censoring analysis was based on the assumption that the star is constant.

**Parasites:** Some transits have been flagged as disturbed by a ‘parasite’, i.e. a fairly bright star which was close in transit time to that of the star considered, according to calculations based on the stars in the Tycho Input Catalogue Revision, described in further detail in Chapter 7. Such transits were rejected in the astrometric adjustment, and (partly) in the de-censoring analysis since these analyses were sensitive to outlying observations. They are however included and properly flagged in the Tycho Epoch Photometry Annex if none of the conditions (a–c) discussed under ‘Valid and Invalid Transits for Photometry’ also caused a rejection in the astrometric adjustment. The flag was not used in the construction of median magnitudes since the median is only weakly affected by outliers, and since such transits in fact often do not suffer from any significant photometric disturbance.

**Number of transits:** The number of valid transits for a given Tycho Catalogue entry, including the non-detections, is denoted by  $N_{\text{transits}}$ . The Tycho Epoch Photometry Annex contains this number of transits for the selected stars (see Section 16.4 for details).

The final astrometric and photometric results for each star have typically been constructed from different numbers of star transits in each case—individual transits having been used, or rejected, for the final catalogue for a variety of reasons. The number of transits used in the astrometric adjustment,  $N_{\text{astrom}}$ , is given in the main Tycho Catalogue. It excludes non-detections and detections affected by parasites.

The number of transits used in Tycho mean value photometry,  $N_{\text{photom}}$ , is given in the main Tycho Catalogue.  $N_{\text{astrom}}$  and  $N_{\text{photom}}$  are about 25 per cent less than  $N_{\text{transits}}$ . The number of valid transits was slightly lower for photometry than for astrometry because a higher background was acceptable in astrometry. The process of photometric de-censoring used both detections which were unaffected by parasites, and the non-detections. Therefore, for stars brighter than  $V_T \simeq 10$  mag with few non-detections the ratio  $N_{\text{photom}}/N_{\text{astrom}} \simeq 0.80$ , while for fainter stars with many non-detections the ratio may be as large as 1.5. For median magnitudes only detections were used, including those affected by parasites, since these were too few to have any significant effect on the median.

E. Høg



## 2. OVERVIEW OF THE TYCHO DATA PROCESSING

*An overview is given of the main Tycho data processing up to the completion of the main Tycho Catalogue of astrometric and photometric mean values for one million stars, and the Tycho Epoch Photometry Annex for a selection of fairly bright stars. The simulations before the satellite launch and the test processing during the first part of the mission are mentioned, but the emphasis is on the final main processing. In particular the basic signal processing with digital filtering and signal detection is described in detail.*

---

### 2.1. Introduction

---

Some main concepts and methods of the Tycho data reduction have been introduced in Section 1.6 as a complement to the following description of the various work tasks. The Tycho processing described before launch (Høg 1989) has not been changed with respect to the main architecture. The data flow for the main processing is shown in Figure 1.2. Volume 4 is divided as follows:

Chapter 3: The Tycho Input Catalogue of 3 million stars, and its role in Tycho data analysis, is described.

Chapter 4: The satellite data processing divides into two processes: 'prediction' and 'detection'. The 'prediction' process calculates the time of each slit group crossing by means of previously known star positions and satellite attitude. In the 'detection' process a background value is normally determined for intervals of 10 seconds since the background varies quite slowly. The background contains 'spikes' which are eliminated from the raw counts by means of a non-linear filtering.

Chapter 5: In 'star recognition' a mapping of the whole sky is carried out from one year of observations giving the Tycho Input Catalogue Revision.

Chapter 6: The transit identification process determines the final correspondence between each detected transit and the stars on the sky, using the accurate on-ground attitude reconstruction and the stars in the Tycho Input Catalogue Revision. The resulting identified transits serve as input for the final photometry and astrometry processing.

Further chapters describe the astrometric and photometric processing and the final catalogue production and verification.

---

## 2.2. Tycho Input Catalogue

---

The Tycho Input Catalogue (TIC in Figure 1.2) consists of the three million brightest stars on the sky selected at the Centre de Données astronomiques de Strasbourg, to a limit of  $B = 12.8$  mag or  $V = 12.1$  mag from a merging of the Hubble Space Telescope Guide Star Catalog (GSC), and the Hipparcos Input Catalogue Data Base, INCA (see Chapter 3). The accuracy of positions in the Tycho Input Catalogue at the epoch of Tycho observations is in general 1–2 arcsec rms. The catalogue contains information on stars of different categories: 40 000 astrometric reference stars, some 12 000 good photometric standard stars, double stars, variables, non-stellar objects etc.

The Tycho Input Catalogue greatly facilitated the on-ground analysis of the photon recordings and was used as input to all TDAC processes. It was however not used to control the observations on-board the satellite. The transits found in the photon record by analysis on the ground were identified with real stars by means of the transits predicted from the Tycho Input Catalogue.

Many of the stars in the Tycho Input Catalogue were too faint to be recognized, but the complete Tycho Input Catalogue of three million stars was retained throughout the mission in ‘prediction’ and ‘detection’ in order to keep a uniform data set.

---

## 2.3. Prediction of Group Crossings

---

The ‘prediction process’ was carried out at the Astronomisches Rechen-Institut (ARI) in Heidelberg by means of the Tycho Input Catalogue, the satellite’s real-time attitude and position in the orbit, and a description of the star mapper geometry. The transit time for the central position of each slit group was predicted for all stars in time sequence. The resulting ‘predicted group crossings’ (PGC in Figure 1.2) were used as input to the detection processing of the raw photon counts provided by ESOC, the European Space Operations Centre in Darmstadt.

Three stages of ‘prediction’ and ‘prediction updating’ based on successive improvements of the attitude and the Tycho Input Catalogue are distinguished.

### First Prediction

The first pass through the data used the Tycho Input Catalogue and the satellite’s real-time attitude. It was therefore uncertain by about 1 arcsec.

### Updating-2 by Attitude

A better estimate of the attitude was derived by the main Hipparcos data analysis groups, NDAC and FAST, for their own data reduction. The uncertainty of the first version of this attitude was about 0.2 arcsec at the ‘chevron’ or inclined slits. The attitude relevant

for the vertical slits is directed along the scan and was determined from the ‘great circle solution’. It had an accuracy of about 0.005 arcsec in all ‘prediction updatings’.

The attitude was used to update the prediction. The result was used to update the ‘transit summary’ (TS in Figure 1.2) from which the recognition process produced the Tycho Input Catalogue Revision of some 1 million stars with accuracy about 0.15 arcsec.

### **Updating-3 with Tycho Input Catalogue Revision and Final Attitude**

The prediction was again updated using this catalogue and the final satellite attitude with an accuracy of about 0.035 arcsec at the inclined slits. This resulted in predictions only for the recognized stars having an uncertainty of about 0.2 arcsec, including the uncertainty of the star positions. These data were used for transit identification which produced the final input for photometry and astrometry.

The satellite attitude used for Updating-2 was delivered by NDAC between December 1991 and February 1992. The final satellite attitude with uncertainty at the chevron slits of about 0.035 arcsec was received from NDAC between May 1993 and June 1994. This final attitude was originally expected after the end of mission, and the much earlier delivery helped to complete the Tycho Catalogue on the same schedule as the Hipparcos Catalogue.

---

## **2.4. Detection of Star Transits**

---

A star appears in the data stream as four rather narrow peaks superposed on a practically constant background. An example is shown in Figure 2.1. The Tycho magnitudes  $B_T$  and  $V_T$  were derived from the signal amplitudes in the  $B_T$  and  $V_T$  channels respectively, and sometimes a  $T$  magnitude was derived from the amplitude of the added signal  $B_T + V_T$ . In the following,  $B_T$  and  $V_T$  refer to Tycho specific magnitudes, while  $B$  and  $V$  may be used where the distinction between the Tycho and Johnson magnitudes is unimportant ( $B_J$  and  $V_J$  are used for the Johnson  $B$  and  $V$  magnitudes where the distinction is stressed).

In order to detect the star signal and accurately estimate its amplitude and location in time it was important to determine also the background and possible non-stellar signals. Disturbing non-stellar signals were the spikes, usually having a width of only one sample.

### **Background**

A ‘format’ background value was determined (see Chapter 4) from 6400 samples = 10.66... s, defined as a telemetry format. For each format the distribution functions of the counts in the two channels  $B_T$  and  $V_T$  were determined and these were in fact nearly Poissonian. The background was determined from the median value of the distribution function. Figure 2.2 shows the background in  $B_T + V_T$  for 12 hours of data (roughly five revolutions) in the elliptical orbit. The background increased when the satellite was in the van Allen belts, but between the inner and outer belts the background was sometimes as low as around apogee. Information on position in the

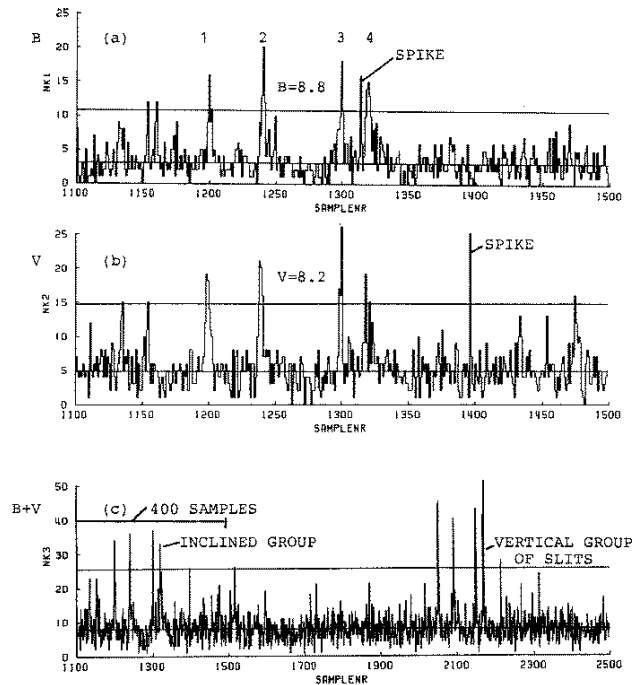


**Figure 2.1.** Typical Tycho counts. (a, b) 400 samples in the  $B_T$  and  $V_T$  channels. The four peaks of a star and a few spikes are marked. Horizontal lines mark the background and the threshold for spikes in the background. (c) 1400 samples in the added counts  $B_T + V_T$ . The star is in fact seen crossing the 'inclined' group of 4 slits and then the 'vertical' group.

orbit was contained in the data sets for photometry and astrometry, e.g. for eliminating less reliable observations between the two belts.

The background arose from different sources: sky background of faint stars, Cerenkov radiation, stray light from the Sun, and dark current in the photomultiplier. Nebulosities contributed relatively little because the star mapper slits were very narrow and extended over two times 40 arcmin on the sky. Table 2.1 lists the background as observed around apogee during about 40 per cent of the time, and the background expected from an analysis before launch. It appears that the apogee background was somewhat lower than expected which gave an advantage in the detection of faint stars. Stars brighter than about 8 mag could usually be detected as close to the Earth as the outer radiation belt. Sometimes, however, the outer belt extended so far out that it increased the background even at apogee.

It appears from Figures 2.2(a) and 2.2(b) that the background varied so slowly that one background value per 10 s was normally sufficient. The typical variation was about 0.3 counts per sample per 10 s, and only very rarely was it 3 times larger, even at a background as high as 40 counts per sample. The wings of stars brighter than 7.5 mag were so prominent that a 'local background' was determined based on 0.32 s of data. In this way it became possible to detect companion stars at separations about 5 arcsec and larger.

The high wing of the distribution function of counts is determined by bright stars and spikes, but the vast majority of samples appear to belong to a Poisson distribution. Significant deviations from this typical behaviour were found in the van Allen belts only, but not always. Figure 2.3(a) shows such a large deviation due to spikes. But

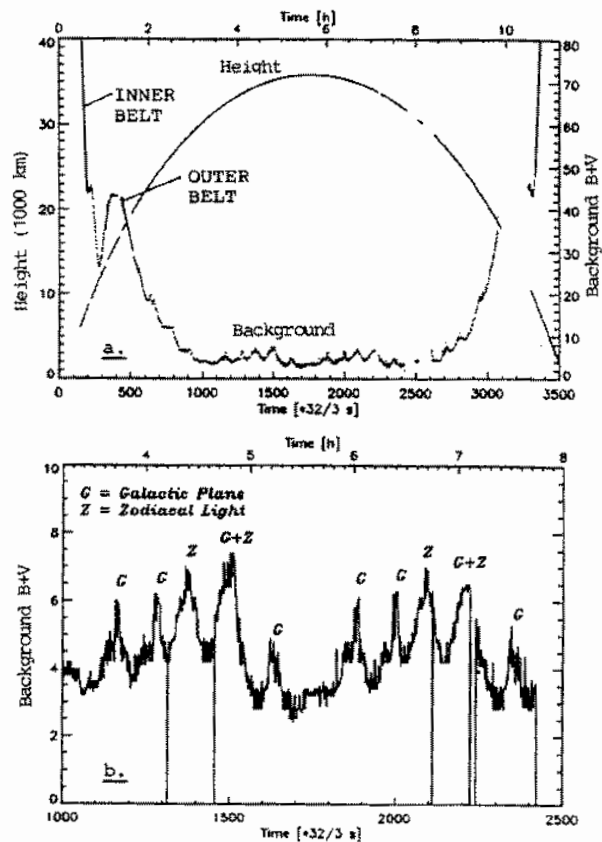


**Figure 2.2.** Typical Tycho background as a function of time. (a) Top: the height above the Earth, and the background in  $B_T + V_T$ , during one orbit = 10.667 hours. Note the high background in the Earth's radiation belts and the missing signal when the telescope is pointing at the Earth, or when the background is high. (b) Bottom: magnified view of a small section. The background was low for about 40 per cent of the orbit around apogee. Some features are marked: G = galactic plane, Z = zodiacal light. Unit: 1 format = 10.66...s.

Figure 2.3(b) observed 70 s earlier, also between the inner and outer belt, shows much less deviation from a Poissonian, and most of it is probably due to the presence of a dozen bright stars up to 6 mag.

## Spikes

A spike was defined as a count which was significantly higher than could be expected from photon statistics in the light coming from background plus stars. In the Tycho detection process (see Chapter 4) the threshold for spike detection has been chosen so that the nominal probability was about 1/6000 per sample for a 'false spike', i.e. a spike due to pure photon statistics. The definition of the threshold took the actual, sometimes non-Poissonian distribution, into account so that the nominal false spike probability was obtained. With the typical background of 4 in  $B_T$  and  $V_T$  the spike threshold became about 12 counts per sample.

It was characteristic for spikes that they did not occur simultaneously in  $B_T$  and  $V_T$  which shows that they must be due to light generated behind the dichroic beam splitter.

**Table 2.1.** Background counts  $b$ . Average values observed around apogee, and expected before launch. Unit of  $b$ : counts per sample. 1 sample =  $1/600$  s  $\simeq 0.281$  arcsec of scan. The last two lines give, in addition, the observed maximum and minimum values at apogee.

	Observed		Expected	
	$B_T$	$V_T$	$B_T$	$V_T$
Sky background	1	1	<4	<4
Cerenkov radiation	1	1	<2	<2
Straylight, max	<1	<1	<1	<1
Dark current	<1	<1	0.5	0.5
Total	3	4	6	6
Total, minimum	0.8	1.2	–	–
Total, maximum	10	10	–	–

The duration of low spikes was usually one sample, but higher spikes may be wider, even up to 5 samples, requiring a physical phenomenon lasting a few milliseconds. This excluded Cerenkov radiation of a single electron because such an event may well generate many photons, but within a time shorter than the dead time of the detector, which was about 300 ns. The result was therefore only one count, no matter how many photons hit the cathode. The origin of the light is assumed to be fluorescence in the glass of the photomultiplier tubes caused by high-energy cosmic ray protons.

Statistics of spikes in the background between stars has been determined. Figure 2.4 shows the number,  $N(H)$ , of spikes in channel  $B_T$  which are higher than  $H$  counts per sample during the observing period illustrated in Figure 2.2. Thus, e.g.  $N(16) = 1.7$  spikes per second. The statistic for  $V_T$  was very similar. The function appears to follow a power law distribution:

$$N(H) = aH^b \quad [2.1]$$

with two different values of the exponent  $b$  in the interval  $1.2 < \log(H) < 2.8$ .

With the frequency distribution of spikes given in Figure 2.4 it can be shown that only a few per cent of the transits of a star were disturbed significantly and that more than 90 per cent did not suffer any disturbance at all. Thus, the spikes were not a very serious problem for the Tycho mission, but serious enough not to be neglected. Therefore, a method described in the following subsection was developed at Tübingen to eliminate significant spikes in the detection process and in the estimation of transit time and photon flux.

### Detection and Estimation

The ‘detection’ process (see Chapter 4) treated the photon records of the  $B_T$  and  $V_T$  channels in parallel with the output from the ‘prediction’ process containing the predicted group crossing epochs and other information. The ‘detection’ process included both the detection of statistically significant transits and the estimation of their epochs and signal amplitudes.

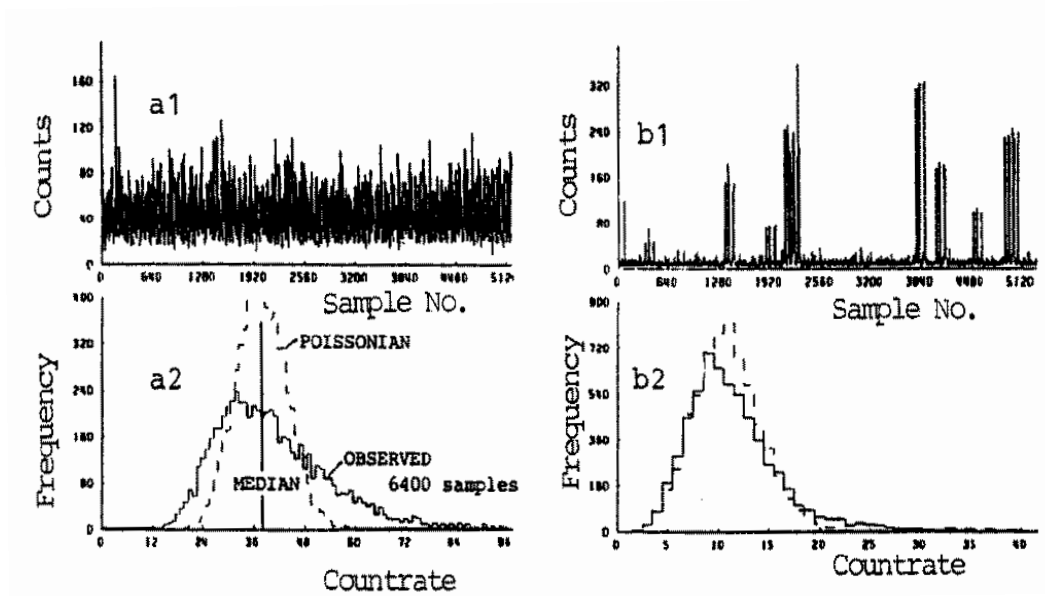


**Figure 2.3.** Extreme cases of Tycho counts obtained between the inner and outer van Allen belts are shown in the upper figures, with the distribution functions below from 6400 samples. (a) Strongly non-Poissonian distribution due to spikes. (b) Many bright stars and low background, but nearly Poissonian distribution.

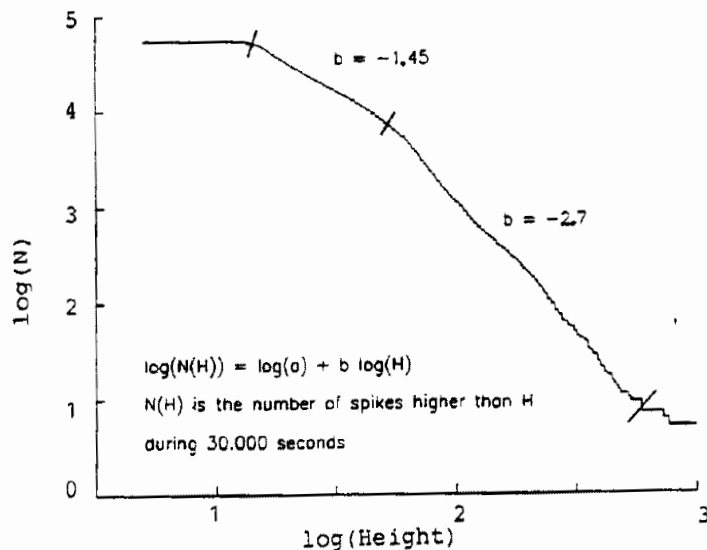


**Figure 2.4.** Distribution of spikes higher than the height  $H$  for channel  $B_T$  in the background shown in Figure 2.2(a). The levelling-off at small spikes with less than 12 counts is due to the present definition of a spike rather than to the absence of low-amplitude disturbances.

A ‘predicted group crossing interval’ is an interval of time corresponding to 12 arcsec centred on the predicted group crossing epoch. The true group crossing for a star will nearly always lie within the predicted group crossing interval of 12 arcsec, even if the accuracy of the Tycho Input Catalogue is 2 arcsec rms. If the detection of transits in the photon record was limited to such a small time interval, detections down to a signal-to-noise ratio of about 1.5 could be retained without getting too many false detections caused by photon noise. Simulations had shown that this limit gave about one false detection in each predicted group crossing interval of 12 arcsec, and the observations produced an average total of 1.5 detections in such an interval.

The bias in the flux of faint stars resulting from the neglect of transits with a signal below the detection limit was corrected in the photometric analysis, see Chapter 9.

The detection was carried out on the complete star mapper data stream, using the  $B_T + V_T$  counts, i.e. on the combined counts from the  $B_T$  and  $V_T$  channels, which were sampled simultaneously. If a detection in  $B_T + V_T$  with a signal-to-noise ratio larger than 1.8 was found, an estimation in the  $B_T$ ,  $V_T$  and  $B_T + V_T$  channels was made, irrespective of whether or not the detection lay within a predicted group crossing interval. This will only give a relatively small number of false detections. If the signal-to-noise ratio was smaller, but still larger than 1.5, an estimation was carried out only if the detection was inside a predicted group crossing interval. These latter estimates were recorded as ‘raw transits’ (RT in Figure 1.2) under the heading of the appropriate star. In cases of overlapping predicted group crossing intervals, the estimates were carried out and recorded under two or more stars of the Tycho Input Catalogue. Such multiple or double recordings occurred in about 30 per cent of cases with a Tycho Input Catalogue of three million stars.

The detections outside predicted group crossing intervals were referred to as ‘serendipity detections’, and may be due to photon noise or to true stars missing from the Tycho Input Catalogue, the latter referred to as ‘serendipity stars’. With the signal-to-noise ratio limits given above and a Tycho Input Catalogue of three million stars, the total number of false detections was about equal to the number of true detections from stars, and this was acceptable.

### The Filtering Process

The raw photon counts were subject to a filtering process which was basically linear, but became non-linear when significantly bright stars or spikes were present in the counts. The non-linear filtering had the desirable effect that significant spikes and prominent side lobes of bright stars were removed in the filtered output, whereas they would be quite disturbing for a purely linear filtering.

Figure 2.5 illustrates the detection process by means of numerical filters. The left-hand side of Figure 2.5 shows the raw counts  $N_k$  in  $B_T + V_T$  of two cases where one or more bright stars are involved. The 4 peaks corresponding to the 4 slits were in the case of a linear filtering superposed by means of a 4-peak filter  $w_j$  which was equal to 1 at four correctly spaced values, corresponding to the spin velocity of the satellite.

Thus, strictly linear filtering is defined as:

$$P_k = \sum_j w_j N_{k+j} \quad [2.2]$$

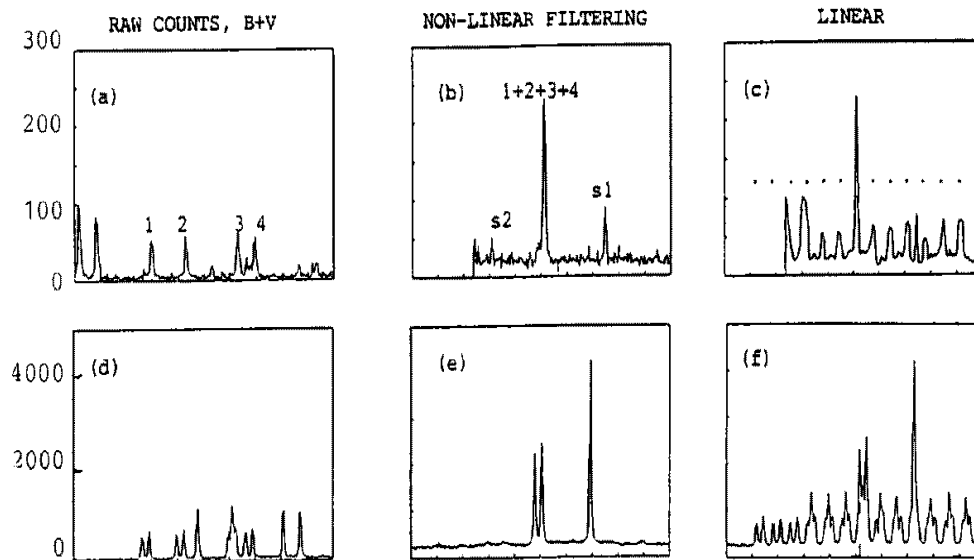


**Figure 2.5.** Filtering of raw photon counts. Unit: counts per sample. Spikes and side lobes of bright stars were eliminated with a non-linear filter, but not with a linear 4-peak filter. Faint stars were in fact only subject to linear filtering. (a) Raw counts with 4 peaks of a bright star (7.5 mag). (b) Output from a non-linear filter. (c) Output from a linear filter giving a main lobe as in (b) and 12 side lobes at positions marked by dots (.) which may disturb main lobes of other stars. (d, e, f) Similarly for a complicated triple system.

where the index of  $N$ , here  $k + j$ , is the number of a sample.

The result shown in Figure 2.5(c) contains the main lobe of the bright star as it should, but surrounded by several disturbing features. At the 12 positions marked by dots are side lobes, each arising when one of the filter peaks passed one of the lobes in  $N_k$ . These 1+12 lobes result from all stars in  $N_k$ .

The devastating effect of the strictly linear filtering on a bright triple star is illustrated in Figure 2.5(f) where the many side lobes disturb the detection of transits.

The improvement by non-linear filtering (see Section 4.3) in these two cases is illustrated in the Figure 2.5(b) and 2.5(e), respectively. In Figure 2.5(b) the main lobe of the bright star appears in the middle, 4 times higher than each of the lobes in  $N_k$ . The lobes from two fainter stars appear at  $s1$  and  $s2$ . The non-linear filtering in Figure 2.5(e) clearly reveals the three stellar components. They are in fact due to  $\epsilon$  Lyrae with four components: the fainter D and C are the first from left, while A and B are superposed because they are oriented along the slits.

This non-linear filtering, described in Chapter 4, is a simple modification of the linear filtering described above. It was carried out by a comparison of the 4 samples selected by the filter. If some of the samples were significantly larger than the smallest one, they were replaced by the mean value of the three other samples before they were added. The resulting bias of the amplitudes is very small due to the ensured low probability of a false spike (see above). A count may be too high for two reasons other than pure statistics: it may be a spike, or it may belong to one of the 4 lobes of a bright star. No distinction can be made between these two cases.

**Table 2.2.** The amplitude of a star, i.e. the counts at the centre of a slit, observed by TDAC, and expected before launch, for a star of magnitude  $B_T = V_T = 10$  mag. The ratio of inclined/vertical is given, and of observed/expected counts.

Quantity	Slits	Observed		Expected	
		$B_T$	$V_T$	$B_T$	$V_T$
Amplitude (counts per sample)	inclined	3.56	2.55	3.97	1.98
Amplitude (counts per sample)	vertical	4.75	3.62	4.88	2.79
Inclined/Vertical	–	0.75	0.71	0.81	0.71
Observed/Expected	vertical	0.97	1.30	–	–

On the typical background of 4 counts per sample an additional count of 8 is ‘significant’ in the present context. This required a star brighter than about  $B = 9.3$  mag or  $V = 8.9$  mag at the centre of a vertical slit in the  $B_T$  and  $V_T$  channels, as may be deduced from Table 2.2. In  $B_T + V_T$  the limit was somewhat fainter. Stars fainter than these magnitudes in  $B$  and  $V$  were consequently subject to a strictly linear filtering. The same is true for the fainter parts of the wings of brighter stars.

The net effect of the non-linear filter was to use only the undisturbed parts of lobes of a star in the observations  $N_k$ . Spikes and bright side lobes, (see Figure 2.5), did not appear in the result. Fainter spikes and side lobes which were border cases may be included in the result, and act as a slight increase of the photon noise as a result of the statistical criteria defining the filter. Another non-linear (multiplicative) filtering for star mapper data reduction was developed by F. van Leeuwen for the NDAC Consortium (Section 3.6 of Canuto *et al.* 1989). The FAST consortium determined the four transit times through each slit independently and combined them afterwards (Volume 3, Section 6.5).

The Tycho detection processing consisted of the following steps. First, derive  $P_k$  from the  $B_T + V_T$  counts by non-linear 4-peak filtering. Second, locate the peaks by maximum cross correlation with a slit response function. Third, for each of these peaks or detections the signal-to-noise ratio was determined and the estimation was carried out in  $P_k$  of  $B_T$ ,  $V_T$  and  $B_T + V_T$  as described above.

The accurate estimation of position and amplitude was carried out with maximum likelihood estimators, though sometimes simplified in order to save computing time. The simplifications introduced a certain loss of accuracy, but never more than 3 per cent in the mean error.

Using values for the background,  $b$ , and the amplitude,  $a$ , from Tables 2.1 and 2.2 a theoretical limiting magnitude for the Tycho processing was derived, defined as the magnitude giving an average signal-to-noise ratio in  $B_T + V_T$  of 1.5. For stars of the typical colour index  $B - V = 0.7$  mag we obtained limits of  $B = 11.6$  mag expected before launch of Hipparcos, and  $B = 12.1$  mag expected from the observed count rates. This agreed with the practical limit reported by Halbwachs *et al.* (1992). There are 1.2 million stars on the sky brighter than  $B = 12.0$  mag, and in fact most of these are contained in the final Tycho Catalogue.

The improvement by 0.5 mag is due to three equally important reasons. First, the more precise format background, replacing the 9-peak background (see Høg 1989). Second, the lower observed background of 7 counts per sample in  $B_T + V_T$ , instead of the expected 12. Third, the 14 per cent higher sensitivity of the detector system for  $B_T + V_T$ , which appears from the last line of Table 2.2.

Based on the inspection of the first observed data it was safe to state in June 1990 (Høg & Wicenc 1991) that the original expectations could be surpassed with the revised mission extending for 3 years, in spite of the fact that Tycho observations on a low background of less than 10 counts per sample were only obtained during about 40 per cent of the time, instead of the 90 per cent expected before launch.

---

## 2.5. Recognition of Stars

---

The ‘recognition’ processing, see Chapter 5, was based on one year of transit data. It combined the observed detections for each Tycho Input Catalogue position and performed a mapping of a small area in order to ‘recognize’ one or several stars in the area. In most cases no sufficiently bright star was found because a rather faint limiting magnitude was chosen for the Tycho Input Catalogue in order to account for the uncertainty of, for example, the magnitudes in the Tycho Input Catalogue.

The data were delivered to the recognition process as the ‘transit summary’ (TS in Figure 1.2) containing records with the transit times from ‘prediction’ and ‘detection’. The transit times from the prediction process were at first based on the real-time satellite attitude having an accuracy about 1 arcsec. Before these transit times were used for the recognition process they were updated by means of the improved attitude from the on-ground processing of the main Hipparcos data, see ‘updating-2’ in Section 2.3. The attitude accuracy at this stage was expected to be better than 0.2 arcsec.

Recognition means that a mapping was performed for a circular area of 40 arcsec diameter centred on each Tycho Input Catalogue position for the first 12 months of mission data. In many cases several components were found, with a resolution of 2–3 arcsec. Eventually, however, many of these new components were found to be false, and were eliminated by use of proper measures of significance.

An additional process was the serendipity recognition mapping which searched for stars outside these small circles that were bright enough to give a rather high signal-to-noise ratio. The serendipity recognition was performed in maps of half a square degree arranged in a network covering the whole sky uniformly. In order to save computing time and to limit the amount of data, only the detections with a signal-to-noise ratio higher than 3.5 and which were detected outside small circles around the bright stars of the Tycho Input Catalogue were taken into account in this process.

The result of the recognition process was a Tycho Input Catalogue Revision of 1 270 000 stars, completed in September 1992. The accuracy of positions was about 0.15 arcsec. This catalogue contained many thousands of suspected serendipity stars and new components, but most of them were later found to be insignificant or redundant with other stars so that the final Tycho Catalogue includes only about 160 serendipity stars and 6600 new components found within 20 arcsec of the Tycho Input Catalogue positions.

---

## 2.6. Transit Identification

---

The ‘transit identification’ process determined which detected transits in the photon records corresponded to which stars on the sky, given in the Tycho Input Catalogue Revision.

For this purpose the predicted group crossing epochs were improved by means of the accurate on-ground attitude reconstruction and an improved geometric calibration of the slit system. Also, the more accurate positions of the stars in the Tycho Input Catalogue Revision were taken into account for the resulting ‘predicted group crossing updates-3’, see Section 2.3, to be used for transit identification.

The transit identification process started in 1993 and converted the ‘raw transits’ into ‘identified transits’ (totalling about 15 Gigabytes) to be used for the final astrometric and photometric data processing. In the process each raw transit was considered. It was included as an identified transit if it was within 3.0 arcsec of a predicted group crossing position of a star in the Tycho Input Catalogue Revision, no matter whether it agreed or not in magnitude. The further decisions to use a particular transit for astrometry and photometry were taken by these processing tasks and are discussed in more detail in the corresponding chapters. The decision in astrometry was based entirely on astrometric arguments, not on the amplitude, or magnitude, of the transit, but a statistical weight was assigned in accordance with the amplitude. During the photometric processing it was known whether a particular transit was accepted for use in astrometry by way of information supplied by the ‘All-Transits’ data set (AT in Figure 1.2). A detection was flagged as false if it was far from any star, and in this case it was not passed on to the final astrometric and photometric data processing. If other stars were close enough to disturb a transit the amplitude of these were recorded in the process ‘parasite recording’ giving information to be utilized by astrometry and photometry.

---

## 2.7. Photometry

---

The signal amplitudes obtained in the estimation process are measures of the stellar photon flux in the (Tycho)  $B_T$  and  $V_T$  bands, which resemble the Johnson  $B$  and  $V$  bands. The estimated amplitudes in the  $B_T + V_T$  counts gave the Tycho  $T$  magnitude. This was useful for faint stars since  $T$  may be available even if  $B_T$  or  $V_T$  is too faint to be estimated. A calibration of the observed amplitudes (Scales *et al.* 1992) was required to transform to an internally consistent magnitude system, taking into account the small sensitivity variations with time, with field coordinate, etc. This was done by means of some 20 000 photometric standard stars provided by the Geneva Observatory as measured from the ground, but with calculated magnitudes in the passbands of  $B_T$  and  $V_T$ ; see Section 1.5.

Provisional photometric calibrations, but not astrometric, were derived from the raw transits, which became available shortly after the observations. The final calibration required the identified transits because they were less affected by false detections and nearby transits of other stars.

An average star obtained 170 valid group crossings or ‘transits’ during the revised mission of 37 months, though this number was highly dependent on e.g. ecliptic latitude, due to the special scanning law of the satellite. A valid transit is a predicted transit where the satellite attitude was well known, the detector background was not too high, and the star was not too close to the ends of the slits, (see Section 1.6 for further explanation). This resulted on average in 130 accepted transit times and magnitudes per star in  $T$ ,  $B_T$  and  $V_T$  for stars bright enough to be detected at every crossing. Thus, on average 25 per cent of the valid transits ( $\simeq 40$  transits per star) were rejected for various reasons: the transit time residual exceeded certain limits in the astrometric processing ( $\simeq 10$  per cent); the transit was disturbed by a parasite, i.e. another fairly bright star crossing the slits nearly at the same time ( $\simeq 10$  per cent); or the background was not determined. The Tycho  $T$  magnitude was used during the astrometric processing since transit times from the  $B_T + V_T$  signal were used for astrometry. But  $T$  magnitudes are given in only 1333 cases in the final Tycho Catalogue of mean magnitudes, and only when  $V_T$  is not available. A median precision of 0.06 mag was obtained at  $V_T = 10.5$  mag for the mean value of the measurements for each star, see Table 16.3.

The ‘mean’ values of  $B_T$  and  $V_T$  for each star were computed as median values for bright stars or by a special ‘de-censoring’ analysis in order to take into account that many transits for a faint star were censored, i.e. not detected because its signal-to-noise ratio was below the adopted limit of 1.5. The detected transits were the brightest ones, so that a simple mean or median value of these would give a biased (too bright) magnitude for the star. The de-censoring analysis, described in Section 1.6 and in detail in Chapter 9, took into account the known number of non-detections for each star and was able to reduce the bias to a negligible amount for the faintest stars.

The two independent photometric observations at the vertical and inclined slit groups were separately calibrated and reduced, and were not combined in the final Tycho Catalogue. The Tycho Epoch Photometry Annexes A and B contain magnitudes of individual transits for about 480 000 selected stars, (see Section 2.6 of Volume 1). The individual transits may be used to detect and to study variability of the stars.

---

## 2.8. Astrometry

---

The transit time at a slit group is a one-dimensional measure of the star position in the direction perpendicular to the slit (either vertical or inclined), provided that the satellite attitude and the grid geometry are known. In the 37 months an average of 170 valid transits were obtained, and some 130 of these were accepted for astrometry using very similar criteria of acceptance as the photometric processing, explained in the preceding section. These observations were used to derive the five astrometric parameters for each star, and their covariance matrix (see Chapter 7). A typical (median) precision of 26 mas was obtained for the position components for stars of  $V_T = 10.5$  mag, see Table 16.2.

The astrometric quality of the results for a given star is characterized by various numbers. The formal standard error is one such number which has been shown to agree within a few per cent with the external standard error obtained by comparison with the much more accurate Hipparcos astrometric results. But for faint stars the formal error may be up to 40 per cent too small (see Chapter 18). A rather small formal standard error is however not enough to ensure that especially the faint objects are real and are

undisturbed by the background or by possible neighbouring stars. Therefore a signal-to-noise ratio,  $F_s$ , of the star image was computed.  $F_s$  is defined in Section 7.4 and is a combined measure of the number of detected transits and their concentration within a distance of 1.4 arcsec of the central position. Finally, three numbers were used to define an astrometric quality index  $Q$ : the largest of the five formal errors  $\sigma_{\max}$ , the  $F_s$ , and the formal standard error of the single observation. This integer value from 1 to 9 (with  $Q = 1$  as the best) was used to divide the Tycho stars into quality classes, see Section 7.4.

---

## 2.9. Double and Multiple Stars

---

Stars with separations smaller than 3 arcsec were usually not separated in the one year transit data processing (see Chapter 5), although this limit is almost ten times wider than the diffraction limit of the telescope. In particular the integration by the 0.9 arcsec wide slits limited the practical resolution. In the reprocessing, a particular effort was made in applying an adequate treatment to the double stars and to suspected double stars of an input catalogue containing 22 000 stars. The close double stars were eventually detected in different ways, according to their separations: between 1.5 and 3 arcsec, both components may be detected separately, and the individual positions were derived. In summary descriptions it is stated conservatively that pairs with separations of 2 arcsec and about equal magnitudes are resolved in the Tycho Catalogue. For separations between 0.4 and 1.5 arcsec, a duplicity could often be detected from an analysis of the magnitude versus the slit angle. In the case of a significant detection the position angle of the system was determined, modulo  $180^\circ$ , but is not published within the Tycho Catalogue. This method was applied to the  $\simeq 500\,000$  brightest stars of the Tycho Catalogue. The special treatment of double and multiple stars is described in Chapter 14.

---

## 2.10. Five Stages of Processing

---

The whole analysis of Tycho data can logically be divided into five ‘stages’ or ‘passes’, starting before launch with the analysis of simulated observations. After launch the analysis began with test processing of selected pieces of data. This led to software improvements, and by March 1991 sufficient confidence had been obtained to start the mass processing of all observations obtained since December 1989.

### Simulations

Realistic simulated observations were produced before launch to test all processes from reception of the satellite data, prediction, detection and recognition to photometry and astrometry. They were based on the expected satellite performance and orbit. The detection software in particular had to be almost completely rewritten after the problems of background and spikes were found in the real observations obtained in the unintended orbit. Between 1981 and 1989 there were at first simulations for each of the five processes, but later on the simulations were based on simulated data in downlink format. These were produced at the Royal Greenwich Observatory with a simulation program developed for the NDAC consortium and used on a realistic map of the sky, including high star densities, and covering a few hours of satellite scanning. Such

observations, called Tycho 'data streams' were passed through all processes to ensure as far as possible the correctness of processes and the interfaces between these. The simulated data were produced by an 'instrument model' from 'true' values on which a noise model was applied. The 'true' values were provided for comparison with the 'estimated' values from each process.

### **Test Processing**

The test processing started in TDAC in November 1989 when the first real observations were received from ESOC and it lasted for about two years, partly overlapping with the main mass processing. These and many following 'provisional ESOC tapes' contained selected pieces of data and were treated almost immediately by prediction and detection. The results, reported soon after, were relevant for improving the software of TDAC and the interfaces with ESOC. The output tapes containing 'raw transits' have been used for photometry and astrometry since December 1989.

A qualitatively new test began in October 1990 when attitude from NDAC was used to produce 'update-2' prediction. These data were needed for recognition in the mass processing (Figure 1.2), but they were also well suited for 'provisional identified transits' in the test processing. Many stars in the Tycho Input Catalogue had a positional accuracy of better than 0.5 arcsec, sufficient for most tests, but the resolving of double stars could only be tested with a Tycho Input Catalogue Revision by which final predictions (update-3 and 'real identified transits') were produced.

The provisional ESOC tapes contained 12 weeks of observations spread over 8 months of mission data, and they were the basis for the first results reported by Høg *et al.* (1992). All of these data had been processed by prediction and detection, whereas only one to three weeks of observations had been analyzed by the other tasks. About December 1990 the first 'provisional identified transits' for photometry and astrometry were produced and the recognition task received the first 'transit summaries'.

Similar test processing was carried out by NDAC and FAST and extensive comparisons between the results were made, including TDAC. Finally, in January 1991 it was decided to start ESOC's mass production for all consortia of the first 6 months of the mission.

### **Main Mass Processing**

The main mass processing of prediction and detection lasted from March 1991 to April 1994, after the end of the 37-month mission in August 1993. The Tycho Input Catalogue Revision was completed in September 1992. This catalogue was needed for transit identification from which astrometry and photometry produced the final catalogue in early 1996.

Before launch it was planned to handle the observations in weekly batches. With the backlog in April 1991 of more than one year it was practical to work with batches of several months.

### **Reprocessing**

The main processing of the Tycho raw data was a compromise between the wish to complete an output catalogue within a given (short) time and with the given resources

of computing power and manpower on the one hand, and the wish for optimum scientific exploitation of the data on the other. Some of the drawbacks on data quality stemming from this compromise were eliminated for some groups of celestial objects by the first reprocessing, as described in Chapter 10.

For this purpose, a special list of stars to be treated again, the 'Tycho Input Catalogue Update' was compiled from the Tycho Input Catalogue Revision and other sources. It was used as input to analogues of the prediction, detection/estimation and transit identification steps of the main processing. This reprocessing of all the original raw data was a moderate effort, since the star list contained only 300 000 entries (less than 10 per cent of the Tycho Input Catalogue), and since the iterative parts of the main processing (Predicted Group Crossing updating, star recognition and most of transit identification) could be omitted. It started in September 1994 and was completed in January 1995. The subsequent astrometric and photometric reductions were done in the same way as for the main processing. End results from the main processing and reprocessing were then merged into the Tycho Catalogue, as appropriate.

The reprocessing included all solar system objects as well. The result was included in the transit identification, astrometry and photometry processing.

E. Høg

## 3. THE TYCHO INPUT CATALOGUE

*A specific Tycho Input Catalogue was constructed, before the launch, as an essential preparatory task for the Tycho data reduction. This catalogue of three million stars brighter than  $V = 12.1$  mag resulted from the cross-matching of a subset of the Hubble Space Telescope Guide Star Catalog with the Hipparcos INCA Data Base. Estimated external errors of the Tycho Input Catalogue positions, at the epoch of the Hipparcos satellite observations, were in the range 1 to 2 arcsec. This was sufficient to allow the Hipparcos star mapper transits to be identified at the epochs when a ‘Tycho star’ was predicted to be transitting the star mapper slits.*

---

### 3.1. Introduction

---

The strategy for the Tycho data analysis was based on a Tycho Input Catalogue (Egret *et al.* 1989; Egret *et al.* 1992) which was used to identify the detections of star transits with real stars, a process complicated by the fact that the photon counts of a given detection may be due to a star anywhere on the 40 arcmin long inclined or vertical star mapper slits, in either of the two fields of view. For this purpose, the Tycho Input Catalogue was thus constructed to be complete to the limit of detection of the instrument, and even beyond, in order to take into account the uncertainty on the stellar magnitudes.

The reasons for using a Tycho Input Catalogue, and not reducing the Tycho records in a pure survey mode, have been discussed by Høg (1985). The main advantages, besides the savings in data processing, are an easier identification of the detected transits with real stars, and the possibility to work to a fainter limiting magnitude.

Producing such a complete catalogue was made possible by using as a basis the Hubble Space Telescope Guide Star Catalog, a survey of about 20 million objects, complete at the fainter magnitude limit to some 13–15 mag, depending on galactic latitude. At the bright end, the catalogue was completed for the stars missing in the Guide Star Catalog (roughly those brighter than 7 mag) by merging with the Hipparcos INCA Data Base, with stars common to both data sets being identified and flagged accordingly.

The Tycho Input Catalogue contains the positions of 3 154 204 objects, to a magnitude limit of  $V = 12.1$  mag or  $B = 12.8$  mag.

The present chapter concentrates on a description of the production of the Tycho Input Catalogue, followed by a description of its contents and format.

---

### 3.2. The Production of the Tycho Input Catalogue

---

#### The Guide Star Catalog

The primary source for constructing the Tycho Input Catalogue was the Guide Star Catalog, compiled at the Hubble Space Telescope Science Institute for the needs of the Hubble Space Telescope. A detailed description is given in a series of three papers, by Lasker *et al.* 1990; Russell *et al.* 1990; Jenkner *et al.* 1990.

The Guide Star Catalog (the version used is GSC 1.0, published in June 1989, and distributed as a set of two CD-ROMs) contains 25 126 027 entries for 18 819 291 objects in the 7–16 mag range, of which more than 15 million are classified as stars. The star positions were obtained by scanning some 1500 Schmidt plates covering the whole sky at epochs around 1980. The expected accuracy is 1 arcsec rms for the positions (3 arcsec in the worst case, near the plate edges) and 0.7 mag for the magnitudes. Internal errors are about 0.25 arcsec and 0.15 mag, respectively, within an individual plate.

As a result of an agreement between the Space Telescope Science Institute and the Tycho project, the Centre de Données astronomiques de Strasbourg (CDS) was given early access to the first version of the Guide Star Catalog in order to be able to produce the Tycho Input Catalogue in time. This access, prior to publication, consisted of the delivery of a subset of the Guide Star Catalog, prepared at the Space Telescope Science Institute, limited to 13 mag, and containing 7 026 931 entries for 5 907 922 stars.

#### The INCA Data Base

The INCA Data Base (215 000 stars of interest for the Hipparcos mission; see Turon *et al.* 1989, Gómez *et al.* 1989) was used to complete the Guide Star Catalog towards the bright end, and to improve the positions and magnitudes, at least for the brightest stars. The INCA Data Base is essentially complete to between  $V = 7.3$  and 9.0 mag (depending on galactic latitude, colour index and spectral type). Additional fainter stars, down to  $V \simeq 12.5$  mag, were included from all programmes proposed in 1982 for Hipparcos observations.

The INCA Data Base was originally derived from the SIMBAD astronomical data base (Egret *et al.* 1991), but has evolved independently, including new ground-based measurements, new compilations, and many corrections introduced by the Hipparcos Input Catalogue Consortium (Turon *et al.* 1991). The INCA Data Base contains all the bright stars supposed to be absent from the Guide Star Catalog, and a large number of stars of astrometric or astrophysical interest for the Tycho project, such as large proper motion and variable stars (Turon *et al.* 1992).

Early access to the INCA Data Base, in March 1989, prior to publication, was made possible through an agreement with the Hipparcos Input Catalogue Consortium.

## Selection of the Tycho Input Catalogue Stars

The first step of the Tycho Input Catalogue production was the selection of the subset of stars observable by Tycho from the catalogue received from the Space Telescope Science Institute. The original plans were to include the 2 million brightest stars of the sky, of which 400 000 to 1 million were expected to be actually detected. It was thus possible to take into account the uncertainty on the magnitude.

In a first approach, the corresponding adopted magnitude limit was  $V = 11.7$  mag or  $J = 12.4$  mag, according to the magnitudes available in the Guide Star Catalog which are  $V$  in the northern hemisphere (Palomar Quick  $V$  survey, north of  $\delta = +3^\circ$ ) and  $J$  in the southern hemisphere (the letter  $J$  refers to the  $J$  plates of the ESO/SERC Schmidt survey, giving a photographic passband close to the  $B$  filter). The limits in  $V$  and  $J$  were optimized for a mean colour  $B - V = 0.7$  mag.

Later on, an analysis of the first results of the Hipparcos-Tycho mission showed that the actual magnitude limit was fainter than anticipated. It was then decided to extend the Tycho Input Catalogue by adding one million stars up to the new limit of  $V \leq 12.1$  mag or  $J \leq 12.8$  mag. For this extension no further cross-matching was attempted with the INCA Data Base (there are, in any case, only a small number of stars from the INCA Data Base in this magnitude range).

Although all Guide Star Catalog entries with magnitudes brighter than the limit given above were included, the resulting catalogue is not fully complete to this limit, because of possible misclassifications (see below), and because the new list is getting close to the effective limit of the Guide Star Catalog in some areas, especially for objects with large magnitude uncertainties or extreme colour indices.

## Average Positions in the Overlap Regions of the Guide Star Catalog Plates

The Guide Star Catalog was originally produced by merging the scans from individual Schmidt plates, for which there is a small overlap: nominally  $0^\circ.4$  in the north and  $1^\circ.4$  in the south, for  $6^\circ.4 \times 6^\circ.4$  plates. In principle (with exceptions, including some high proper motion stars), each redundant entry in the overlap zones is identified by the same key GSC number.

In the Tycho Input Catalogue, the individual plate positions stored in the Guide Star Catalog were used for computing a mean position. This led to an intermediary catalogue (hereafter called the GSC/Tycho file) of 2 022 607 stars brighter than  $J = 12.4$  mag to which the cross-matching described in the following section was applied.

---

### 3.3. Cross-Matching the Guide Star Catalog with the INCA Data Base

---

The cross-matching of Guide Star Catalog stars with an astronomical data base was necessary because the original Guide Star Catalog did not include the brightest stars (which cannot be properly measured on the Schmidt plates) and because for the stars brighter than about  $V = 9$  mag, better positional and photometric parameters could be expected from the existing astrometric catalogues than from the Guide Star Catalog

itself, due to the saturated images on the Schmidt plates. Another result of this cross-referencing was the flagging of variable stars and high proper motion stars for which the parameters given in the Guide Star Catalog may have changed at the time of the mission. Other lists or catalogues of astrophysical interest (for example, photometric and astrometric standards, and the Hipparcos Input Catalogue) were also cross-identified.

The use of the INCA Data Base, constructed for the Hipparcos Input Catalogue preparation (some 220 000 stars), rather than the SIMBAD Data Base, was the result of a compromise which made it possible to perform the cross-matching in a limited amount of time. The whole SIMBAD Data Base, containing 600 000 stars at that time, was not used because that task appeared too ambitious within the tight schedule left after the completion of the Guide Star Catalog (Didelon & Egret 1987; Egret, Didelon & McLean 1988).

An 'INCA/Tycho master file' was produced in April 1990 by extracting the required information from the INCA Data Base. At that time the number of entries in the data base was 214 754. For 10 915 multiple systems within the INCA Data Base, the entries of close components (closer than 10 arcsec) had been merged into one single entry. For all systems with distances between two components larger than 3 arcsec (according to the data base), the individual components were restored. As a result, the total number of entries in the master file increased to 220 352.

It should be noted that the positions included in the INCA Data Base for all multiple systems at that time were still on the FK4 system, not on the J2000 FK5 system of the other catalogue positions (they were transformed to the FK5 before the publication of the Hipparcos Input Catalogue, but too late for inclusion into the Tycho Input Catalogue).

A total of 4547 complementary entries from the Catalogue des Données Astrométriques (CDA, produced at Astronomisches Rechen-Institut, Heidelberg for the Input Catalogue consortium, Jahreiß 1989) were also added to the master file: these comprised all known stars with proper motion larger than 0.15 arcsec/year and not already included in the INCA Data Base.

### **The Cross-Matching Procedure**

The cross-matching between the Guide Star Catalog file and the INCA master file was made through a comparison of celestial positions and magnitudes. When the positions of objects from both files matched within an error box corresponding to the internal standard errors, the cross-identification was considered acceptable. In case a better match with another INCA entry was found later on, an iterative procedure deleted the previous cross-identification. Due to the characteristics of the Tycho data reduction, whenever some doubt arose about an entry, it was preferable to keep a spurious entry (not related to a real star) rather than risk missing a star. False entries were eliminated in the course of the Tycho data reductions.

The cross-identification was always assigned to the closest object, unless there was a better choice for that (the closest) object. An estimated error box was derived from the standard errors given in the Guide Star Catalog and the INCA Data Base (hereafter

abbreviated as  $G$  and  $I$ ) for positions and magnitudes, with a minimum value of 1 arcsec and 1 mag, respectively:

$$E_{\text{pos}} = \max(1 \text{ arcsec}, \sigma_{\text{pos}_G}, \sigma_{\text{pos}_I}) \quad [3.1a]$$

$$E_{\text{mag}} = \max(1 \text{ mag}, \sigma_{\text{mag}_G}, \sigma_{\text{mag}_I}) \quad [3.1b]$$

When the distances were smaller than three times the estimated errors:

$$|\text{pos}_G - \text{pos}_I| < 3E_{\text{pos}} ; |\text{mag}_G - \text{mag}_I| < 3E_{\text{mag}} \quad [3.2]$$

the cross-identification was considered acceptable. When the distance was between three and four times the error, the cross-identification was still accepted, but the entries were flagged accordingly.

For stars with large proper motion the comparison procedure included the computation of the position to a common epoch: the mean epoch of the Guide Star Catalog plates (i.e. 1983 for stars with  $\delta > -17.0^\circ$  and 1975 for stars with  $\delta < -17.0^\circ$ ). For the identified stars, the position recorded in the Tycho Input Catalogue is the position at epoch 1990 (and equinox J2000).

The non-cross-matched INCA or CDA entries (generally bright stars absent from the Guide Star Catalog, or components of multiple systems, see below) were added to the Tycho Input Catalogue, when their magnitude was brighter than the adopted limit of  $B = 12.4$  mag. In the operational version of the Tycho Input Catalogue the positions recorded for the non-cross-matched stars with proper motions larger than 0.15 arcsec/year were inadvertently given at the Guide Star Catalog plate mean epoch instead of at epoch 1990. This error was corrected as part of the reprocessing procedure described in Chapter 10, and in the published version of the Tycho Input Catalogue (Egret *et al.* 1992).

### The Cross-Matching Results

A satisfactory cross-matching was found for 198 360 out of the original 224 899 entries in the INCA master file (88 per cent). After omission of the stars actually fainter than the adopted  $B = 12.4$  mag limit, the remaining 19 264 entries constituted the additional INCA/CDA stars to be added to the Guide Star Catalog stars.

The non-cross-matched stars can be roughly divided into three subsets. Approximately 8000 stars are the bright stars actually missing in the Guide Star Catalog because they generated large images on the Schmidt plates. This includes all the stars brighter than  $V = 6.0$  mag and an additional fraction of stars between 6–8 mag. Another large subset (about 6250) comprises the components of multiple systems not recorded in the Guide Star Catalog, in general because a faint component was masked by a bright primary star. The third part (about 5000 objects) contains stars missed on the Guide Star Catalog plates (for instance stars close to an extended object) and also possible errors or uncertainties in the INCA master file (this is especially true for the stars not selected for the Hipparcos Input Catalogue, for which positional data possibly remained inaccurate).

### Flagging of Specific Objects

The cross-identification was also useful for flagging ‘peculiar objects’, namely:

- known proper-motion stars;
- known high-proper-motion stars (larger than 0.2 arcsec/year);

- stars with known parallax;
- known variable stars;
- known multiple systems as described below;
- non-stellar images in the Guide Star Catalog (this flag indicates a doubtful classification); misclassification is estimated to be about 1 per cent in uncrowded fields and about 3 per cent in crowded ones (Lasker *et al.* 1990).

Of course, these flags could only be provided when the ‘peculiarity’ was known to INCA; this was generally not the case for the faintest stars. Some specific lists were also flagged within the Tycho Input Catalogue, namely:

- reference stars for astrometry (FK5, IRS);
- standard stars for photometry (from multicolour photometric systems);
- monitor stars (to be used during the data reduction for monitoring the processing);
- stars from the Hipparcos Input Catalogue (about 120 000 stars);
- INCA stars (when additional information is available for these objects from INCA).

Additional flags concern discrepancies found while cross-matching the Guide Star Catalog and the INCA Data Base:

- position discrepancy (larger than  $3\sigma$ );
- magnitude discrepancy (larger than  $3\sigma$ );
- position and magnitude discrepancy.

As a result of the cross-identification with the INCA Data Base, the following actions were taken:

- bright objects from the INCA Data Base not included in the Guide Star Catalog were added to the Tycho Input Catalogue; this list of additional stars was provided to the Space Telescope Science Institute for operational use (the stars brighter than 7.5 mag have been included in GSC 1.1 and later versions);
- bright objects from the Guide Star Catalog not found in the INCA Data Base were checked and kept when no error was detected.

Finally, an attempt was made to flag double stars according to separation and data origin. The resulting flags were the following:

- close pair with separation less than 3 arcsec in the INCA Data Base;
- component of pair in the INCA Data Base with separation less than 10 arcsec;
- double or multiple system from the Catalogue of Components of Double and Multiple Stars (CCDM), with any separation (see Dommanget 1989b);
- component of Tycho Input Catalogue pair whose separation is less than 20 arcsec.

It should be understood that this task remained an ‘automatic’ flagging (through computer software) and was certainly not an extensive study of multiple systems which, in any case, was not necessary as far as the Tycho Input Catalogue was concerned. This was made from existing information in the INCA Data Base and CCDM Catalogue concerning double stars, and for the last flag, through an analysis of the neighbourhood of the Tycho Input Catalogue stars.

---

### 3.4. The Contents of the Tycho Input Catalogue

---

The Tycho Input Catalogue contains the items listed in Tables 3.1 and 3.2: identification; J2000 coordinates, mean errors; magnitudes, mean errors; flags.

#### The Tycho Input Catalogue Identification

This identification is the common key of all data streams in the Tycho data reduction. It is also used in the auxiliary files. The original Guide Star Catalog is organised into regions so that the Guide Star Catalog identification for an object consists of the region number and a sequential number within the region. To determine the region limits, the sky is divided into approximately square areas of 50 square degrees which are subdivided, depending on the star density, into 4, 9, 16 or 25 regions. The total number of regions is 9537.

The identification system adopted for the Tycho Input Catalogue keeps the Guide Star Catalog identification described above. There are gaps in the running numbers because objects fainter than the magnitude limit adopted for Tycho are omitted.

In the operational version, additional stars (e.g. bright stars absent from the Guide Star Catalog) were numbered with a region number corresponding to the Guide Star Catalog region in which the star appears and a running number starting from 10001. This was later replaced by a running number provided by the GSC team, and consistent with their scheme. Only this improved numbering scheme is used in the final Tycho Catalogue.

Solar system objects were given a dummy region number equal to zero.

#### The Coordinates

Equatorial coordinates are given at equinox J2000 (both in the Guide Star Catalog and the Tycho Input Catalogue). Positions coming from the INCA Data Base are corrected to the epoch 1990 by means of proper motions. The epoch of a position from the Guide Star Catalog is generally (by definition) that of the Schmidt plates used for the Catalog, i.e. around 1980. The epoch difference is significant for the high-proper-motion stars (for which a 10- or 15-year motion is larger than the confidence interval of 2 or 3 arcsec) and was handled by adding to the Guide Star Catalog position the proper motion, when known. The estimated error on position given in the Guide Star Catalog (Russell *et al.* 1990) was kept, but sometimes updated from the INCA Data Base.

#### *B* and *V* Magnitudes

The *V* magnitude, and its estimated error, are from the Guide Star Catalog (or INCA) in the northern hemisphere, or from INCA or (most frequently) unknown in the south. The *B* magnitude, and its estimated error, are from the Guide Star Catalog (or INCA) in the southern hemisphere, or from INCA or (most frequently) unknown in the north. The source (Guide Star Catalog or INCA) is given by a flag.

**Table 3.1.** The Tycho Input Catalogue format (binary). The record length is 28 bytes.

Name	Offset	Length	Unit	Range	Short Description
TICID1	0	2	-	0-9537	Guide Star Catalog region number
TICID2	2	2	-	1-32767	Running number in region
TICRA	4	4	0.01 arcsec	0-1296×10 <sup>5</sup>	Right ascension J2000, epoch 1990
TICSPD	8	4	0.01 arcsec	0-648×10 <sup>5</sup>	South polar distance ( $\delta + 90^\circ$ )
TICPOSE	12	2	0.01 arcsec	0-32767	Error on position
COMPI	14	1	-	-	Reserved for catalogue revision
-	15	1	-	-	Spare
TICBE	16	1	0.01 mag	0-255	Error on <i>B</i> mag (0 if absent)
TICB	17	1	0.05 mag	0-255	<i>B</i> magnitude (0 if absent)
TICVE	18	1	0.01 mag	0-255	Error on <i>V</i> mag (0 if absent)
TICV	19	1	0.05 mag	0-255	<i>V</i> magnitude (0 if absent)
TICFL	20	4	-	-	31 one-bit flags (see Table 3.3)
TICDRA	24	2	-	-	Reserved for catalogue revision
TICDDEC	26	2	-	-	Reserved for catalogue revision

**Table 3.2.** The Tycho Input Catalogue format (ASCII). The record length is 80 bytes.

Name	Bytes	Format	Unit	Range	Short Description
TICID1	1-4	I4	-	0-9537	Guide Star Catalog region number
TICID2	6-10	I5	-	1-32767	Running number in region
TICRA	11-20	I10	0.01 arcsec	0-1296×10 <sup>5</sup>	Right ascension J2000, epoch 1990
TICSPD	21-29	I9	0.01 arcsec	0-648×10 <sup>5</sup>	South polar distance ( $\delta + 90^\circ$ )
TICPOSE	31-34	I4	0.01 arcsec	0-32767	Error on position
TICBE	36-38	I3	0.01 mag	0-255	Error on <i>B</i> mag (0 if absent)
TICB	39-43	I5	0.01 mag	0-255	<i>B</i> magnitude (0 if absent)
TICVE	45-47	I3	0.01 mag	0-255	Error on <i>V</i> mag (0 if absent)
TICV	48-52	I5	0.01 mag	0-255	<i>V</i> magnitude (0 if absent)
TICFL	54-80	27I1	-	-	Flags 1 to 27 (see Table 3.3)

**Table 3.3.** Tycho Input Catalogue flags. For each flag, the number of entries for which the flag value is set to 1 is given within parentheses.

---

F00	Zero (most significant bit)
F01	FK5 star (3564)
F02	IRS star (38 775)
F03	Standard star for photometry (21 559)
F04	Random set of Tycho Input Catalogue stars (15 776)
F05	Problem stars ('sick objects'), selected by flags (9340)
F06	Signature stars, individually selected (707)
F07	Stars with good quality photometry in auxiliary file (42 103)
F08	Monitor stars (logical OR of F01 to F06) (82 012)
F09	Discrepancy while attempting Guide Star Catalog/INCA cross-identification (2468)
F10	Bright stars: $V < 11.3$ mag or $B < 12.0$ mag (1 068 730)
F11	Magnitude discrepancy in Guide Star Catalog/INCA cross-identification (116)
F12	INCA or CDA star without Guide Star Catalog counterpart (19 320)
F13	Source of position (0=Guide Star Catalog, 1=INCA) (211 526)
F14	Source of $B$ magnitude (0=Guide Star Catalog, 1=INCA) (204 122)
F15	Source of $V$ magnitude (0=Guide Star Catalog, 1=INCA) (212 251)
F16	Non-stellar Guide Star Catalog image (classification = unknown) (480 709)
F17	Component of Tycho Input Catalogue pair (there is at least one companion with a separation smaller than 20 arcsec) (48 910)
F18	Close pair with one single entry (usually separation $< 3$ arcsec) from INCA (9346)
F19	One component of INCA pair (separation $< 10$ arcsec) (8353)
F20	INCA Data Base star (cross-identification available in auxiliary file) (217 625)
F21	Known proper motion; correction to epoch 1990 applied to the position (193 065)
F22	Known high proper motion (larger than 0.15 arcsec/year) (12 627)
F23	Known parallax (from INCA) (5548)
F24	Known variable (from INCA) (7406)
F25	Known multiple system (any separation) from INCA (30 995)
F26	Hipparcos Input Catalogue star from INCA/IC5 (117 778)
F27	CDA star (Catalogue des Données Astrométriques) (4474)
F28	zero (reserved for TICR)
F29	Additional faint Guide Star Catalog star (1 112 277)
F30	Guide Star Catalog star with a rejected cross-match (5300)
F31	Spare

---

## Flags

The flags associated with the Tycho Input Catalogue are described in Table 3.3. Auxiliary files, described in the next section, are associated with some of these flags.

Additional faint Guide Star Catalog stars (flag 29) have all other flags set to zero, except the following: 4, 8 and 16 which may be 0 or 1. The Tycho Input Catalogue pair flag 17 has not been computed for these stars.

## The Auxiliary Files

The general format of the auxiliary files is the following: the key is the Tycho Input Catalogue identification and the record contains the information related to the flag (generally extracted from the INCA Data Base). The following auxiliary files were produced:

- known proper motions (flags 21 and 22);
- photoelectric photometry:  $B_T$  and  $V_T$  in the Tycho system are computed from observations in multicolour photometric systems (flag 7, and flag 3 for standard stars);
- known double and multiple systems (flag 25);
- known parallaxes (flag 23);
- known variable stars (flag 24);
- Hipparcos Input Catalogue; more precisely 'IC5', the provisional version of the Hipparcos Input Catalogue available at the time of finalisation of the Tycho Input Catalogue (flag 26);
- cross-identification from the INCA Data Base (flag 20);
- signature stars: stellar nebulae, or stars associated with extended regions, specially selected for their expected response; this constitutes a subset of the monitor stars (flag 6).

---

### 3.5. The Tycho Input Catalogue Revision

---

The Tycho Input Catalogue Revision is the intermediate catalogue derived from the first twelve months of satellite observations, as described in Chapter 5. It includes a reduced number of stars (only those definitely detected), additional serendipity stars, and companion stars detected around the Tycho Input Catalogue stars. It also includes a number of false (spurious) stars which were discarded in later steps of the data processing. The revised positions have an accuracy better than 0.15 arcsec rms (Halbwachs *et al.* 1992).

---

### 3.6. Publication of the Tycho Input Catalogue

---

The Tycho Input Catalogue as circulated within the Tycho consortium is stored in compact binary format, convenient for a working file on disk. It was released in 1992 (Egret *et al.* 1992) and made available in electronic form at the Centre de Données astronomiques de Strasbourg and other data centres in 1993.

The additional bright stars ( $V < 7.5$  mag) from the INCA Data Base were subsequently included into the Guide Star Catalog for the release GSC 1.1 in 1992. Such entries are designated by the plate identifier +056 in GSC.

When the list of stars observed by Tycho was made available (Halbwachs *et al.* 1994), the related flag for 1 049 971 stars actually observed was added to the distributed version of the Tycho Input Catalogue.

D. Egret



## 4. SATELLITE DATA PROCESSING

*The Tycho data processing chain started with two very large processes: the 'prediction of group crossings', and the 'detection of transits', treating the raw data from the satellite, as delivered by the European Space Operations Centre (ESOC). The general role of the two processes was outlined in Chapter 2. They are described in more detail in this chapter.*

---

### 4.1. Prediction of Group Crossings

---

The prediction process was executed at Astronomisches Rechen-Institut, Heidelberg. Its task was to calculate expected times of group crossings of celestial objects from input data giving:

- the attitude (i.e. pointing on the sky) of the satellite as a function of time;
- the orbital position and velocity vectors of the satellite as functions of time;
- the apparent positions of the celestial objects, depending on time and on the orbital position and velocity of the satellite;
- the precise optical geometry of the telescope and grid assembly, i.e. the geometric instrument calibration.

A 'group' is a set of four parallel star mapper slits in the focal plane of the Hipparcos telescope (see Figure 1.1). A group crossing is the transit of a star's image across a fiducial line defining the centre of gravity of the four slits in the direction of the motion of the star images across the focal plane. This fiducial line is called the centre line of the group.

The celestial objects to be treated by the prediction process included the 3.15 million entries (mainly stars) of the Tycho Input Catalogue, plus 59 solar system objects: Venus, Mars, Jupiter, Saturn, Uranus, Neptune, the 4 Galilean moons, Titan, and the 48 brightest Minor Planets.

The actual Tycho data processing chain contained several iterative steps of 'prediction' and 'prediction updating'. The present section is restricted to what in Chapter 2 was called 'first prediction'. The various steps of iteration will be described in Chapters 5, 6 and 9.

## Basic Algorithm

The basic task of the prediction process is simple. The attitude of the satellite is a time-dependent rotation matrix, transforming celestial coordinates into field coordinates in the Hipparcos focal plane. It is given in some tabular form, with the entries of the table being valid for a dense set of (spacecraft-defined) instants of time. Two such instants  $(t_1, t_2)$  define a short time interval (1.067 s in the case of ‘first prediction’) within which the attitude can be linearly interpolated with sufficient accuracy. For any such time interval, prediction does the following:

- get attitude and satellite status data for  $t_1$  and  $t_2$ . Use the satellite status data to decide whether scientifically useful observations may possibly be performed during the interval  $(t_1, t_2)$ . If not, skip the interval;
- select all celestial objects that may experience a group crossing during the interval  $(t_1, t_2)$  in either of the two fields of view of the telescope (this is the most complex part of the software);
- calculate the satellitocentric apparent positions of these objects for  $(t_1 + t_2)/2$ , i.e. the interval mid-time (this is the most time-consuming part of the software);
- transform the apparent positions into field coordinates in the focal plane of the Hipparcos telescope, for times  $t_1$  and  $t_2$ , using the corresponding attitude matrices;
- check (for each object) whether it has crossed the centre line of any of the slit groups between  $t_1$  and  $t_2$ . If so, compute the predicted transit time by linear interpolation of the field coordinates;
- for each transit found, compute auxiliary data (such as the instantaneous scan speed, the instantaneous direction of scanning, the field coordinates at transit time, jet firings of the attitude control system etc.) and create the output records for the PGC (‘predicted group crossing’) data stream. There is one such record per predicted group crossing;
- sort the records according to the predicted transit time;
- write everything to magnetic tape.

In spite of this basically simple task, the actual prediction software was large and complex. Its complexity was enforced by the sheer computational size of the task. The selection of the objects to be treated in each time interval (see second item above) was a complicated multi-stage process. It had to be very efficient, since it decided on the number of apparent positions to be computed. The computation of one high-precision apparent position for a star took about 1 ms on the IBM mainframe computer at Astronomisches Rechen-Institut, Heidelberg.

Thus, even if only  $10^{-4}$  of all Tycho Input Catalogue entries would have been considered in each time interval, the prediction processing would have been slower than the satellite observations. Likewise, the actual retrieval of the selected objects from the magnetic-disk Tycho Input Catalogue file had to be organized very efficiently. This was necessary because, from the point of view of catalogue access, Hipparcos scanned the sky in a highly erratic fashion.

## Input Data

Prediction had to treat several types of input data, which will be described very briefly in this section. The largest amount of input data was provided by the European Space Operations Centre (ESOC), in the form of roughly 1300 magnetic tapes with raw telemetry from Hipparcos. Slightly more than one big tape reel (2400 feet), corresponding to about 150 Megabytes of data, was produced by the satellite on each day of scientific operations. The sum of all other types of input data together amounted to less than one per cent of this volume.

The real-time satellite attitude was provided in the so-called ‘attitude and orbit control system’ files on the telemetry tapes. The orientation of Hipparcos in space was given in the form of three ‘error angles’ relative to the nominal scanning law. The nominal scanning law itself was not tabulated on the tapes, since its definition was part of the mission specification. The rotation matrices mentioned in the previous section were derived from the attitude and orbit data.

A variety of satellite status data were also derived from the attitude and orbit data files and from the so-called Data Catalogue file on each telemetry tape. The relevant data included gas jet firings, shutter and electronic switch positions, orbital correction manoeuvres, bad telemetry signal levels, the two free parameters of the nominal scanning law, etc. Some of these were used to decide on the usefulness of the telemetry (i.e. to switch the prediction process on and off), and some of them were just copied to the output stream as warnings to the users.

Geocentric orbital ephemerides of the Hipparcos satellite were provided by ESOC, as a separate file on each of the telemetry tapes. Instantaneous position and velocity vectors of Hipparcos were computed from a Chebychev polynomial representation of its orbital motion.

Different sorts of ephemerides had to be used for different groups of solar system objects. The standard Development Ephemeris DE200 of the Jet Propulsion Laboratory (Pasadena, USA) was used for the major planets, including Earth. Special ephemerides on *ad hoc* formats were provided for the minor planets and for the moons of the major planets by A. Bec-Borsenberger and J. Arlot, respectively, of Bureau des Longitudes, Paris. More details on these and on their usage are given in Section 10.4.

The primary inputs provided by the Tycho Input Catalogue were the mean positions, proper motions and parallaxes for the computation of apparent positions of stars. Besides these, the Tycho Input Catalogue provided magnitudes, flags etc., which were simply copied to the output data stream of the prediction process. In addition to the 3.15 million Tycho Input Catalogue objects, a list of almost 100 000 so-called serendipity points was used for the serendipity process, as described in Section 5.5.

Last but not least, prediction had to make use of a precise model of the optical geometry of the telescope and grid assembly. For Tycho, this model essentially consisted of the field coordinates of the centre lines of the various slit groups in the Hipparcos focal plane, plus the precise value of the basic angle between the two fields of view. The pre-flight calibration provided by ESOC turned out to be too imprecise for prediction. Thus, early in-orbit calibrations produced by the FAST consortium were used throughout the mission.

The specifications of all input data except the Tycho Input Catalogue and DE200 are unpublished, as are the data themselves. The telemetry data were defined in the ESOC 'Data Delivery Interface Document for Hipparcos'. The interpretation of the satellite orbit file is described in an additional letter by ESOC's Attitude and Orbit Division. The ephemerides for minor planets and moons are described in letters from their originators only. The FAST instrument geometry description is defined in an internal document called 'FAST Calibration Document', and that of NDAC in NDAC-internal interface documents titled 'Great-Circle Interface Document 7' and 'C-238'. These facts are mentioned here in order to explain the absence of references to published material in the present section.

## Output Data

The output of 'first prediction' consisted mainly of the Predicted Group Crossing (PGC) data stream, indicated in Figure 1.2, plus some protocol and log files. The PGC data stream was used in the 'detection' process and the various 'prediction updating' processes. It mainly contained time-ordered PGC records, one for each predicted group crossing. In addition, there was a header record every 10.66... s of operational mission and a Data Catalogue file roughly every day of mission, both giving auxiliary data on satellite status, timing, orbit etc. The precise description of the data stream is given in a Tycho-internal booklet under the title 'Tycho Interface Document'. The total data volume of the PGC data stream for the entire mission was roughly 200 magnetic tapes of 2400 feet each, corresponding to about 30 Gigabytes.

## Computation of Apparent Positions

Satellitocentric apparent positions of celestial objects were computed to an accuracy of better than 1 mas. The relevant physical effects included in the calculations are, for stars: proper motion, stellar aberration (due to the orbital motion of the Earth around the Sun, and of the satellite around the Earth), annual parallax, relativistic light bending by the Sun and the Earth (but not the other planets; they are irrelevant for Tycho). The astronomical and mathematical basis of the procedure was described by Walter *et al.* (1986).

Prediction used the following model for proper motions: The mean positions given in the Tycho Input Catalogue (TIC) were used in the form of cartesian position vectors  $(x, y, z)$ . These referred to a fixed epoch  $t_{\text{TIC}} = \text{J1990.0}$ . The Input Catalogue proper motion components (in right ascension and declination) were used in the form of time derivatives  $(x', y', z')$  of the cartesian position vector. The position vector of an object at a given epoch  $t$  was calculated in two steps. First an intermediate vector  $(x, y, z) + (x', y', z') \times (t - t_{\text{TIC}})$  was computed. Then this vector was normalized to unit length to give the position vector of the object at epoch  $t$ . Consistent application of this proper motion model was necessary in the 'astrometry' task, especially for nearby stars with large proper motions and for stars close to the celestial poles.

## Retrieval of Tycho Input Catalogue Objects from Magnetic Disk

Within an attitude time interval  $(t_1, t_2)$ , the centre lines of the slit groups in each field of view swept across a part of the celestial sphere having the shape of a symmetric right-angled pentagon (see Figure 4.1). Only objects lying within that part of the sky

could possibly produce a group crossing within the given time interval. For each time interval there were exactly two such pentagons on the sky: one for each field of view. Their location and orientation on the sphere were determined by the satellite attitude at time  $t_1$ ; their length in the direction of scan was determined by  $t_2 - t_1$ . Each of the pentagons comfortably fits into a circle of radius  $r = 23$  arcmin (for  $t_2 - t_1 = 1.067$  or  $2.13$  s) around a central point  $P$  on the line of symmetry (see Figure 4.1). This fact was utilized for efficient TIC access in the following way.

The celestial sphere was divided into small ‘regions’ in a special way. A running number  $n$  was assigned to each of these regions. For any point on the sky (e.g. a Tycho Input Catalogue object or the central point  $P$ ), this region number can be determined by a simple algorithm. The main point is the following (see Figure 4.2): For any position on the sky, situated in an arbitrary region  $n$ , the circle of a fixed radius  $s$  around that position is entirely contained in that region  $n$  and the immediately adjacent regions (shaded in Figure 4.2). The numbers of the adjacent regions can again be determined by a simple algorithm. The ‘characteristic size’  $s$  of the regions is chosen slightly larger than the above-defined radius  $r$  of the pentagon.

To utilize this concept the Tycho Input Catalogue file on magnetic disk was organized and indexed according to these regions on the sky. Retrieval of the Tycho Input Catalogue objects necessary for one field of view in a time interval  $(t_1, t_2)$  started with the computation of the region number  $n$  for the central point  $P$  of the pentagon, and the region numbers of all the immediately adjacent regions. Then all objects within these regions (typically a few hundred to a few thousand) were read into computer main storage. But these objects were still too many for the computation of apparent positions. The next selection step, therefore, simply transformed the Tycho Input Catalogue positions to field coordinates (using the attitude matrix for time  $t_1$ ), and kept only those objects situated close to the pentagon or its forward extension (bold dashed lines in Figure 4.2).

Once this retrieval procedure had been executed for the time interval  $(t_1, t_2)$  it did not need to be repeated as long as the central point  $P$  remained situated in the same region during subsequent time intervals. For a reasonable ‘characteristic size’  $s$  this condition held, on average, for about 10 consecutive time intervals of 1.067 s each. During this time, the selection of objects was permanently refined in order to save even more computation of apparent positions. For instance, every object having crossed the vertical slit group was removed from the selection for following time intervals. It could not produce another group crossing during this particular transit across the field of view.

The sole purpose of this mechanism, which occupies a large fraction of the entire prediction program code, was the saving of computing time for apparent positions. Just for the sake of completeness this paragraph is concluded with the recipe for the division of the sphere into regions having a ‘characteristic size’  $s$ :

- let the regions be rectangles in  $(\alpha, \delta)$  space. Choose their size in the direction of  $\delta$  (i.e. declination) as  $s = \pi / (2N)$ , where  $N$  is an integer, such that  $s$  is slightly larger than  $r$ ;
- take as region number 1 a circle around one pole with radius  $s$  (this is also a rectangle in  $(\alpha, \delta)$  space);
- add circular declination zones, each having width  $s$ ;
- divide the first such zone into six regions of identical shape, with one of the north-south boundaries being at  $\alpha = 0$ ;

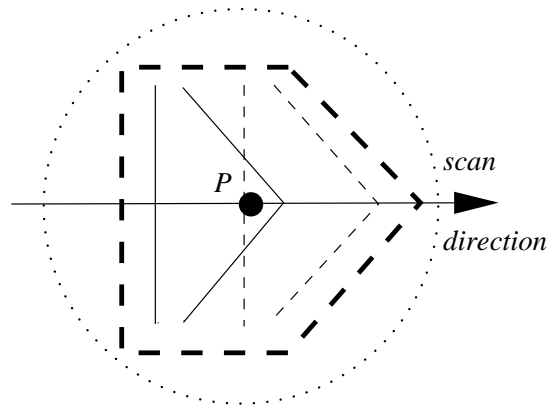


**Figure 4.1.** The scanning pentagon on the sky. The figure shows the centre lines of the various slit groups projected onto the celestial sphere, for two instants of time (in one of the two fields of view only). Their location at time  $t_1$  is given as thin full lines, that at time  $t_2$  as thin broken lines. The horizontal shift between the full and the broken lines is equal to the time difference  $(t_2 - t_1)$ , multiplied by the scanning velocity  $v$  of the satellite. The bold dashed lines indicate the symmetric right-angled pentagon which is discussed in the text. Its central point  $P$  is indicated by the filled circle. The pentagon contains all celestial objects that can possibly produce a group crossing in the time interval  $(t_1, t_2)$  for the particular field of view. The enclosing circle, which is discussed in the text, is also shown (dotted).

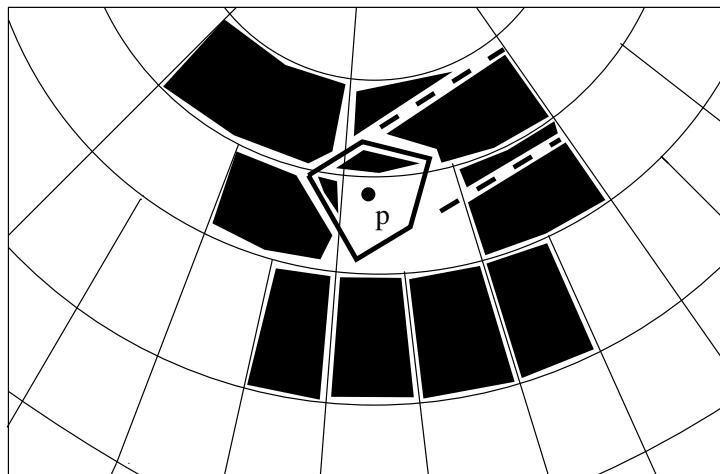


**Figure 4.2.** Principle of Tycho Input Catalogue access. The figure shows a part of the celestial sphere, divided into the 'regions' (thin lines), as described in the text. The pentagon for a given instant of time is shown in bold lines, the corresponding central point  $P$  as a filled circle. The region containing  $P$  is evident. 'Immediately adjacent' regions are those having a common corner or boundary line with this first one. They are shaded in the figure. The 'forward extension' of the pentagon is outlined by dashed lines.

- divide all the remaining zones analogously into  $6 \times 2^m$  regions, where  $m$  is an integer chosen such that:
  - the regions are as small as possible, but
  - the shortest distance between any two rectangle ‘corners’ is at least  $s$ .
- assign a serial number to each individual region by starting at one pole with number 1, proceeding from zone to zone and numbering the regions within each zone according to the value of  $\alpha$  at their centres.

This recipe leads to a simple algorithm for the computation of a region number from a given celestial position, and of the numbers of the immediately adjacent regions.

## Solar System Objects

The treatment of the solar system objects in the prediction process was quite different from that of the Tycho Input Catalogue objects. Its description is deferred to the chapter on Tycho reprocessing (Section 10.4), since only reprocessing data was used for the solar system objects. The astronomical results on the solar system objects are described in Chapter 15.

## Consistency between Geometric Instrument Calibration and Attitude

Prediction combined the real-time satellite attitude and a precise model of the instrument geometry to compute star transits across the star mapper slit groups. The attitude, in turn, was determined on board the satellite from actually observed transits—implicitly using some instrument geometry as input. The on-board instrument model was chosen by ESOC to optimize the satellite operations for the main grid. The Tycho prediction model, on the other hand, was chosen to give the best possible predictions for the star mappers. Any inconsistency between the two instrument models would necessarily lead to systematic offsets of the predicted crossing times from the actual crossings of stars. Such offsets were indeed observed during the mission.

Prediction was started using the best available pre-launch instrument geometry. The predicted group crossings were compared with actual crossings (as observed by Tycho’s detection process). Very large systematic deviations were found, caused mainly by the big rotation of the grid assembly relative to its nominal position inside the telescope. That rotation was taken account of by an early in-orbit geometry (‘Version 2’) produced by the FAST consortium. A constant offset ‘observed minus predicted’ of about 2 arcsec remained, which was removed by an *ad hoc* correction to the FAST geometry.

Beginning with 23 January 1990 (i.e. 2 months after the start of scientific observations) ESOC implemented the grid rotation into the on-board instrument model. This greatly improved the precision of the real-time attitude, but again introduced large deviations in the predicted group crossings. A small part of these deviations was compensated by a change to an improved FAST geometry (‘Version 3’). However, the major part was due to a systematic attitude offset of the kind discussed in the first paragraph of this subsection. Its character was such that it could not reasonably be remedied by another correction to the instrument geometry. Instead, it was removed by an *ad hoc* correction to the attitude. This gave satisfactory results throughout the mission. The remaining systematic deviations were smaller than 0.1 arcsec, which is irrelevant for the ‘first prediction’. The *ad hoc* attitude correction consisted of a constant rotation

by  $-5.9$  arcsec and  $-0.65$  arcsec, respectively, around the satellite's  $x$  and  $z$  axes (for a definition of the axes see Volume 2, Section 8.1).

### **Actual Processing**

Trial and verification runs started on 9 November 1989, when the first provisional telemetry tape with real Hipparcos data was delivered by ESOC. The final mass processing started in March 1991, and was completed in April 1994.

All computing was done at Astronomisches Rechen-Institut, Heidelberg, using the IBM-3090 computer of the computing centre of the University of Heidelberg.

### **Prediction Redoing**

For most of the Hipparcos mission the real-time attitude provided by the satellite had its nominal precision, i.e. about 1 arcsec, which was sufficient for the purpose of 'first prediction'. This was not true, however, for the very first and very last parts of the mission. The attitude was much worse for data collected before 23 January 1990 (i.e. for 63 days of scientific operations) and after 7 July 1992 (169 days of scientific operations), with errors frequently exceeding 5 arcsec. The start of the mission was impaired by the initially unsatisfactory instrument geometry model and by still sub-optimal attitude control. The end of the mission suffered from the rapid deterioration of the  $z$ -axis gyro and, after its total failure, from the reduced attitude information provided by the two-gyro operational mode. However, during both time intervals Hipparcos did actually collect high-quality star mapper observations.

Bad real-time attitude meant the loss of part of these observations, simply because the 'predicted group crossing interval' (see the paragraph on detection and estimation in Section 2.4) extended only 6 arcsec on either side of the predicted group crossing epoch. Therefore it was decided that the bad parts of real-time attitude should be replaced by on-ground attitude for the purpose of first prediction. This decision created the task of 'prediction redoing', and analogous tasks for detection of transits, prediction updating and transit identification. The repeat of about 20 per cent of these processes was considered affordable within the agreed Tycho time schedule. Software capable of doing prediction with on-ground attitude had been planned in any case (for the 'reprocessing' step, see Chapter 10). Thus, the prediction redoing task was executed immediately after the reprocessing software and the necessary on-ground attitude became available in autumn 1994.

The usage of on-ground attitude instead of on-board real-time attitude made prediction redoing more precise and reliable than the original prediction, and in addition it made it also quicker, for reasons explained in Chapter 10. The on-ground attitude files did not provide some of the information contained in the telemetry tapes. This is why the data interfaces between the various Tycho processing steps had to be slightly modified for redoing. In consequence, the software for detection of transits and for prediction updating also had to be modified for the redoing step.

---

## 4.2. Background Determination

---

The detection and estimation process, including the background determination, is the very core of the Tycho data reduction scheme. Therefore it was described at some length in the overview in Chapter 2. This section and the following two sections give additional details.

### Introduction

The raw Tycho signal is the sum of photon counts produced by transiting stars and a background. The quality and efficiency of the detection and estimation processes, and thus of the whole data reduction chain, depend strongly on the quality of the background determination. This is mainly because the signals of most of the star transits used by Tycho were not far above the background level.

Background determination was carried out during the initial data preparation for the detection process. It was the first piece of TDAC software looking into details of the Tycho raw data. In general, the method of background determination was independent of star transits and the normal data reduction. The background was derived and provided for any given stretch of data and for both channels of the Tycho experiment. Moreover, all background data were stored in a self-contained data base giving access to information about the satellite environment, the sky background and the zodiacal light during the mission for all data used by TDAC. The whole background data base together with some orbital data of the satellite is publicly available. It can be used for studies of the variations of the van Allen belts or of the influence of solar flares on the environment of satellites (see Wicenc & Bässgen 1992; Wicenc & van Leeuwen 1995).

### Mathematical Principle

The background used by Tycho was based on the median value of a set of count rates, where the number of count rates in the set depended on the non-stellar disturbances in the raw counts (see below). If a set of count rates is sorted, the median is defined as the middle value in the case of an odd number of count rates. In the case of an even number of count rates the median is determined by interpolation between the two middle values (Spiegel 1961).

The very low detection limits used by the detection process (signal-to-noise ratio = 1.8 for transits outside the predicted group crossing intervals, and signal-to-noise ratio = 1.5 for transits inside these intervals) yield some problems due to disturbances by spikes (see Chapter 2) or dense star fields. These were circumvented by the usage of median (rather than mean) values for the definition of the background. Any set of count rates is a statistical representation of the distribution function  $F_d$  of the counts. Normally one would expect  $F_d$  to be a Poissonian distribution for the type of independent processes detected with the Tycho photomultipliers. However  $F_d$  is disturbed by stars and spikes. In the actual satellite data, both the background level and the strength of the deviations from Poissonian statistics varied strongly (see Figure 2.3).

Even the median value is sensitive to a long tail of the distribution function (Press *et al.* 1986), i.e. to an excessive asymmetry of  $F_d$  due to a large number of spikes or a high density of faint stars. Such effects slightly shift the derived background to higher values. This bias was deliberately accepted by Tycho. It was utilized in the detection process to limit the number of false transits in heavily disturbed formats.

Several statistical estimators in addition to the median were used to judge the disturbance of the distribution function and to decide how long the set of counts could be chosen for the background determination. These include the lower and upper quartile of the distribution function of the count rates in the set and the mean of the four maximum count rates. For a set size of 6400 samples, i.e. 10.66... s of data, the difference of the median background to one estimated from the lower quartile was less than 1 per cent (indicating very little disturbance) for about 90 per cent of the data. It increased to the order of 10 per cent for the highest star densities, where both estimates of the background had an internal uncertainty of more than 50 per cent. Faint stars of the Milky Way band which are not resolved by Tycho as well as all clusters of resolved stars caused a bias of the background level by disturbing the distribution function.

### Format Background

The so-called ‘format background’ was derived in the manner described above from sets of 6400 samples each, corresponding to one telemetry format, or 10.66... s of data. Usually the background varied very slowly, being essentially constant over periods much longer than one telemetry format. Thus, for at least 75 per cent of the sky (low to moderate star densities) and 50 per cent of the orbit (apogee region), the format background was applicable.

### Local Background

Whenever the condition of essentially constant background was violated, the so-called ‘local background’ was used instead of the format background. It was computed by exactly the same method as the latter, but with the size of the data set reduced to 192 samples, corresponding to 0.32 s of time, or 54 arcsec on the sky. Cases where the local background had to be used included:

- transits of very bright stars ( $m < 5$ ), of dense open star clusters and of dense Milky Way regions;
- scanning of the zodiacal light;
- crossing of the van Allen belts and strong variations of the energetic-particle background due to magnetic storms, solar flares etc.;
- straylight produced in the instrument by a very bright extended object.

The variation time scales in these cases ranged from some 100 samples to several formats. Careful studies of Tycho data showed that the shortest background variation time scales were due to bright stars and internal reflections where the latter ones had their source in very bright extended objects such as Venus, Jupiter or Saturn and therefore occurred very seldom. Figure 4.3 shows the lower part of a transit of a star with  $B_T = V_T = 2.2$  mag after the nonlinear folding of the detection process (see Section 4.3). The very wide extension of the ‘wings’ of the main peak may disturb transits with a separation up to approximately  $\pm 150$  arcsec, or about 500 samples, in scan direction. If

the format background would have been used in these cases the detection process would have produced lots of ‘false’ and too bright transits respectively, because the amplitude estimation for transits on such wings would result in an overestimation of the signal due to the local excess of the background. This effect was detected for stars down to  $B_T \simeq 5$  mag and for open clusters. The local background was used therefore, in order to avoid ‘holes’ around bright stars in the Tycho Catalogue.

The length of 192 samples for the definition of the local background was chosen because about 200 samples cover the main peak of a bright star. The usage of the local background yielded accurate results for the cases of bright stars, high star densities and bright extended objects. Figure 4.4 shows the count rates of one telemetry format (filling the white area) and the local background derived for each sample of that format (black line). The variation of the local background exceeds  $\pm 10$  counts, while the format background is about 16 counts. The variations are due to many (mostly faint) star transits while both fields of view are scanning the galactic plane. The number of predicted transits is around 600 in this format.

### Tycho Background Features

The van Allen belts produced the most prominent features in the background data (see Figure 4.5). They appear as high steep peaks above the ‘level’ of the apogee background. Normally there should be four peaks during every orbit, but the two inner peaks are not complete, because of the telemetry loss during perigee. In the apogee region one may recognize numerous little peaks. They are due to the crossings of one or both of the telescopes’s fields of view of the galactic plane, other regions of high star density or the zodiacal light.

The apogee zone, which was most interesting for Tycho, was not free of disturbance. The combined background level in the  $B_T$  and  $V_T$  channels, (called  $b_{B_T+V_T}$  in the following) varied from 5 to 30 counts per sample. The time interval around the apogee which was not affected by the van Allen belt slopes, varied between some 10 minutes and about 5 hours. This duration was directly correlated with the height above the Earth where the van Allen belts begin to disturb the background. The maximum height was nearly equal to the apogee height of the satellite (36 000 km above ground), whereas the minimum height lay around 20 000 km. The variations within the undisturbed apogee zone amounted to approximately  $\pm 3$  counts per sample with a mean value of about 6 counts per sample in  $b_{B_T+V_T}$ .

The peaks of the outer van Allen belts sometimes showed a ‘bifurcation’ (see Figure 4.6). This effect has been reported by Frank *et al.* (1964). It is due to a series of geomagnetic storms where the effects of a later one is superimposed on the previous, resulting in a doubling of the outer van Allen belt. These effects were known to last for a couple of days, which is in agreement with the Tycho data.

Figure 4.7 shows a different representation of the  $b_{B_T+V_T}$  data. The count rates are given in counts per second (logarithmic scaling) versus the length of the satellite’s location vector in units of the Earth radius ( $R_e$ ). The different locations of the minima between 2 and 3  $R_e$  indicate the passage of the satellite at the day and night side, respectively. The minima between the two belts sometimes were nearly as low as the count rates in the apogee region. However, studies of the spike density showed that the data between the belts had to be treated very carefully, and data in the range of the van Allen belts were not usable for TDAC at all. Moreover it turned out that the height of the satellite

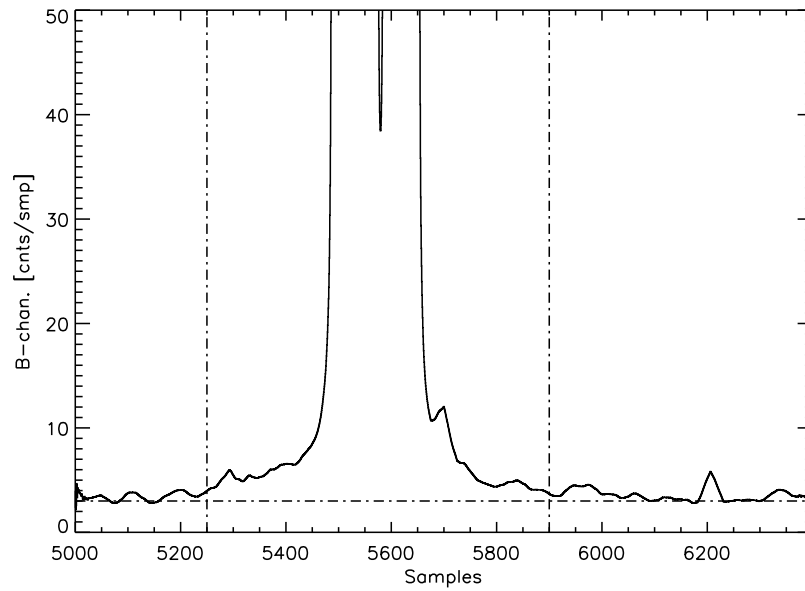


**Figure 4.3.** Lower part of the count rates of a bright star transit. The wide wings of the instrument response function extend to about  $\pm 500$  samples, corresponding to about  $\pm 150$  arcsec on the sky.

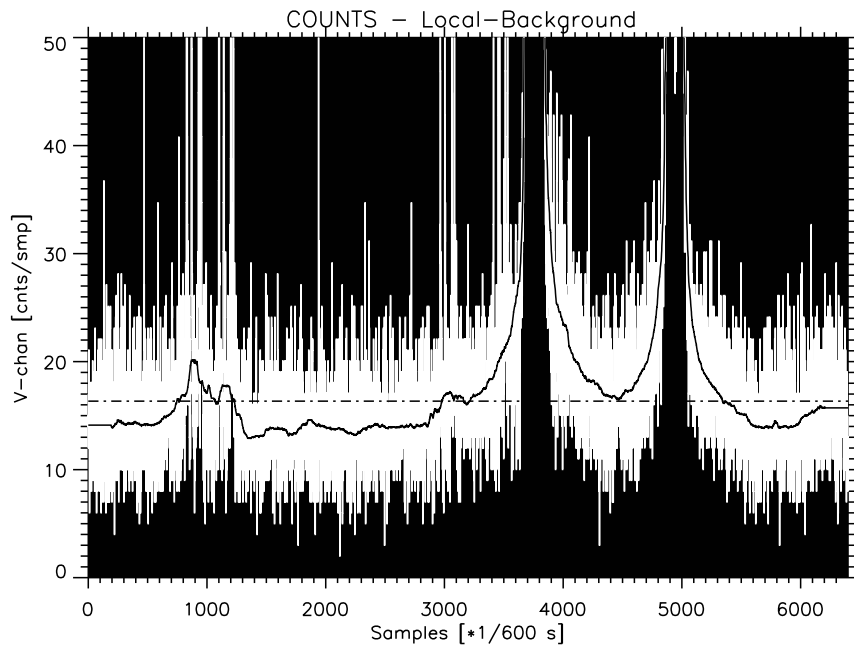


**Figure 4.4.** Count rates and local background of one format of Tycho data where both fields of view are scanning in the galactic plane. Full line: local background; dash-dotted line: format background; white area: individual count rates.

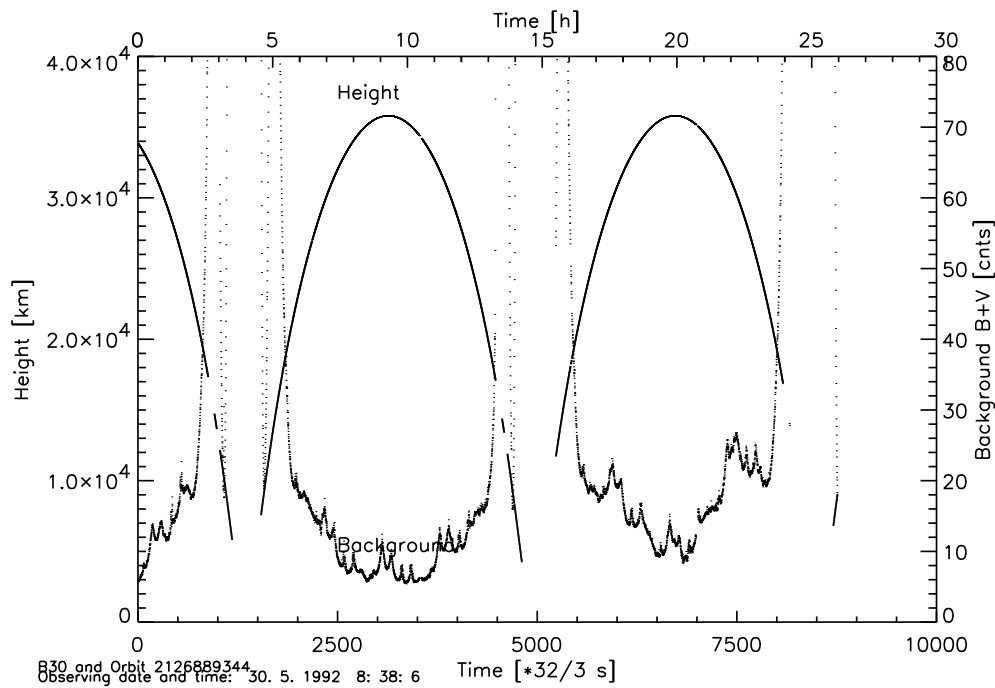


**Figure 4.5.** The Tycho background  $b_{B_T+V_T}$  level (small dots) compared to the height of the satellite above ground, for about 2 successive orbits. The individual features are discussed in the text.

alone could not be used as an indicator of ‘good’ data. This was made impossible by the strong variations of the background level at apogee and of the height of the disturbing belts due to the solar activity.

---

### 4.3. Detection of Star Transits

---

The task of detection was to find signals due to any star-like object on the sky in the Tycho data stream, and to estimate the precise observed group crossing times and amplitudes of the signals from input data giving:

- the predicted group crossing times and auxiliary data from prediction;
- the raw photon counts from the  $B_T$  and the  $V_T$  channel of the Tycho experiment, called the Tycho data stream hereafter;
- calibration data.

Most of the complexity of the Tycho data reduction scheme stemmed from the very low limits used to detect predicted signals from starlike objects. The limits were chosen and adjusted in a way to allow about one or two false detections per one true detection. A detection is fully described by a transit time, the signal amplitudes, the backgrounds and the signal-to-noise ratios in both channels, accompanied by some auxiliary data which originated in the Tycho Input Catalogue (TIC), in the prediction process and in the Tycho data stream.

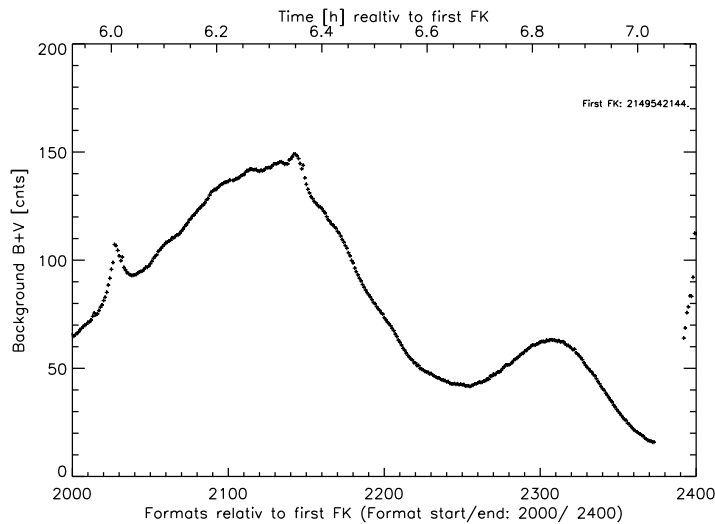


**Figure 4.6.** One peak of the outer van Allen belt showing the bifurcation effect referred to in the text. The small peaks at the extreme left and on top of the main peak are caused by crossings of the galactic plane by the preceding and following field of view respectively. The scale along the top of the figure gives the time in hours with respect to an arbitrary origin, the bottom scale is an 'internal' timescale.

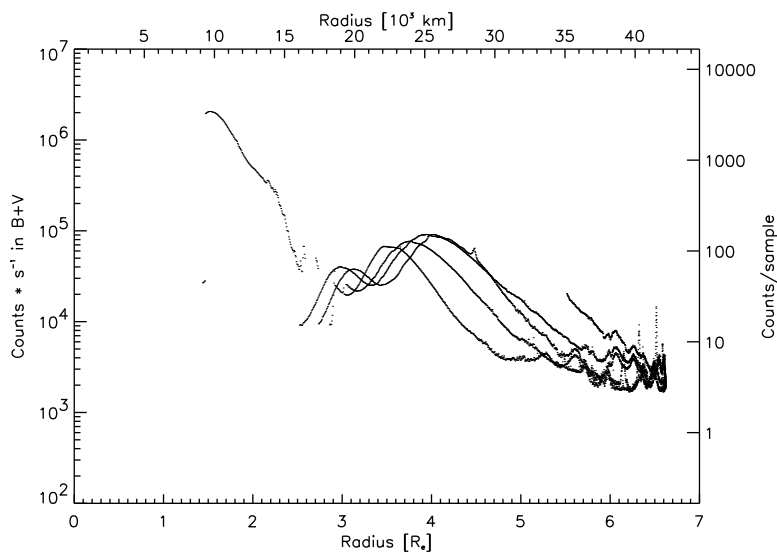


**Figure 4.7.** The background count rates as a function of the satellite's distance from the centre of the Earth, for several consecutive orbits. The individual features are discussed in the text.

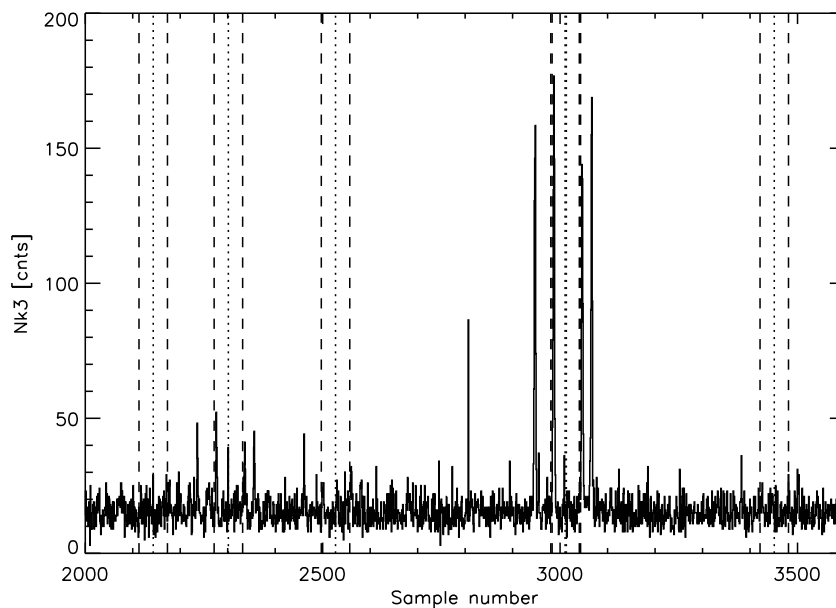


**Figure 4.8.** Raw photon count rates ( $N_{k3}$ ) in  $B_T + V_T$ . The stretch of data covers about 450 arcsec in scan direction, where some brighter stars are visible. For stars brighter than 10 mag in either of the two colours, the Predicted Group Crossing (dotted) and the corresponding Predicted Group Crossing intervals (dashed) are shown.

## Input Data Bases

The Tycho data stream contained the photon count rates in  $B_T$  and  $V_T$ , sampled at 600 Hz, plus information about the timing of the observations, and flags describing their quality. The photon count rates were given in compressed one-byte values in a semi-logarithmic form. They were decompressed after reading.

The Predicted Group Crossing (PGC) data stream gave, for each predicted group crossing: the identification of the Tycho Input Catalogue entry concerned; the PGC epoch; the type of the slit group (inclined or vertical); the field of view (preceding or following) in which the object was expected to appear; the vertical coordinate on the slits, and the actual scanning velocities (or rather the image velocities of the star) along the nominal scanning direction and its orthogonal direction, plus information originating from the Tycho Input Catalogue, e.g. ground-based magnitudes in  $B$  and  $V$ . Figure 4.8 shows an extracted part of raw photon counts with the location of some predicted group crossings for some transits, and the corresponding predicted group crossing intervals.

Calibration data included the decompression tables for the photon count rates, the geometric calibration of the star mapper slit groups, and single-slit response functions for the different slit groups (vertical/inclined, upper/lower half of slit, preceding/following field of view,  $B_T/V_T$  channel). The detection process used the photon count rate decompression tables given by ESOC, and the geometric star mapper calibration and single-slit response functions derived by the NDAC team at the Royal Greenwich Observatory.

## Output Requirements

The subsequent tasks: recognition (Chapter 5), astrometry (Chapter 7) and photometry (Chapters 8 and 9), required the following from detection and estimation:

- background values in  $B_T$  and  $V_T$ ;
- transit time estimates in  $B_T$ ,  $V_T$  and  $B_T + V_T$ ;
- $B_T$ ,  $V_T$  and  $B_T + V_T$  signal amplitude estimates;
- signal-to-noise ratio for each detected transit;
- auxiliary data copied from the Predicted Group Crossing and Tycho signal data streams and from the Tycho Input Catalogue.

Separate  $B_T$ ,  $V_T$  and  $B_T + V_T$  transit time and amplitude estimates were obtained using the  $B_T$  and  $V_T$  count rates and the sum of both. The times were the result of an inverse interpolation in the folded counts, the amplitudes were the result of a maximum likelihood iteration procedure.

## Principle and Strategy of Detection

Whenever the image of a star crossed a star mapper slit group, the pattern of the raw photon counts showed four signal peaks spaced at intervals 2:3:1 (Figures 4.9(a) and 2.1). The principle of detecting such patterns was simple: Take an integer filter consisting of zeroes and four unit values which are spaced at the same mutual distances as the four signal peaks. Fold the data with this filter, called 4-peak filter hereafter. Find peaks with a signal-to-noise ratio exceeding a certain limit, called the detection limit, in the folded data. Calculate the exact time and amplitude of this peak. Such a detected peak is called a detection, the estimated group crossing time is called transit time. The estimated amplitude is called signal amplitude.

The detection was carried out in all the Tycho data, using the sum of the simultaneously sampled counts from the  $B_T$  and  $V_T$  channels. The signal-to-noise ratio for the  $B_T + V_T$  counts should usually be higher or at least equal to the signal-to-noise in a single channel. In the following we will call the  $B_T$  count rate data  $N_{k1}$ , the  $V_T$  data  $N_{k2}$ , and the  $B_T + V_T$  data  $N_{k3}$ . The 4-peak folded counts in  $B_T$  will be denoted  $P_{k1}$ , in  $V_T$   $P_{k2}$ , and in  $B_T + V_T$   $P_{k3}$ .

In the real Tycho data a simple filtering and detection scheme would have encountered several difficulties:

- the spacing of the signal peaks depended on the scanning velocity, the real star mapper geometry and the response function of the single slits;
- the method of folding the raw photon counts (additive or multiplicative) would have resulted in problems with side lobes (additive) or a loss of faint transits (multiplicative, see Volume 3, Sections 6.3–6.5);
- the expected Poisson distribution of photon count rates was disturbed by spikes (spikes are non-stellar signals not expected before launch, whose origin is inside the satellite and usually of one sample width, see Chapter 2);

- the background was highly variable and sometimes did not follow a Poisson distribution. This effect appeared regularly for background values larger than some 200 counts per sample (see Chapter 2).

The methods described below were developed to circumvent or at least limit these difficulties.

### Motivation of the Non-linear 4-Peak Filter

The need of a new filtering method arose during the investigation of the first real satellite data. It immediately turned out that there were spikes in the data, i.e. photon count rates considerably higher than expected from Poisson statistics, originating from isolated events in the telescope optics. About 0.1 per cent of the data were spikes, regardless of the height of the background. Figures 4.9(a) and 2.1 show extracted parts of photon count rates in  $B_T + V_T$ , containing signal peaks due to a star and some spikes. Because the photon count rates were disturbed by spikes, a linear additive filtering (which in principle means just adding four samples) would have disturbed a considerable quantity of signals. Signal amplitudes would have been increased and the estimated transit times would have been disturbed.

The non-linear filtering method was at first developed to derive quantitative numbers for the spike distribution and amplitudes. Thus the filter was originally designed to do the opposite of what would be done in the normal data reduction: finding spikes, and suppressing signals from stars. However it was obvious that this logic could afterwards be turned around, i.e. that such a filter could analogously isolate star transits from spikes and, in addition, free star transits from the influence of spikes, side lobes and multiple ('parasitic') star transits.

The basic idea underlying the non-linear 4-peak filter is described by the following sentence: When the linear 4-peak filter is applied to the raw photon counts in  $B_T + V_T$  ( $N_{k3}$ ), the counts at the four samples  $p_1$ ,  $p_2$ ,  $p_3$ , and  $p_4$  picked by the 4-peak filter should not differ more than given by Poisson statistics, loosely speaking:

$$N_{k3}(p_1) \pm m\sigma = N_{k3}(p_2) \pm m\sigma = N_{k3}(p_3) \pm m\sigma = N_{k3}(p_4) \pm m\sigma \quad [4.1]$$

where  $m$  is a parameter defining the allowed deviation of the count rates and  $\sigma$  is the scatter of the count rates expected from pure Poisson statistics (both quantities will be defined precisely in the following). Equation 4.1 is also true when the filter passes the four signal peaks of a star, because each filter point  $p_k$  corresponds to the same position on the single-slit response function (see below). Equation 4.1 is not true if the filter touches upon only one signal peak (thus producing a side lobe) or when a spike disturbs the data. Any violation of the assumption made in Equation 4.1 thus indicates the occurrence of spikes, parasitic star transits and side lobes above a certain limit.

### Characterisation of the Non-linear Filter

The mechanism of the non-linear 4-peak filter is as follows: Before combining  $N_{k3}(p_1)$ ,  $N_{k3}(p_2)$ ,  $N_{k3}(p_3)$ , and  $N_{k3}(p_4)$  it is checked that none of them are outliers (i.e. spikes or side lobes). None must exceed a certain limit  $uplim$ , where  $uplim$  is derived from the lowest of the four count rates,  $N_{k3}(p_{\min})$ , which is supposed to be the least disturbed. The value of  $uplim$  sets the limit of the non-linearity of the filter:

$$uplim = N_{k3}(p_{\min}) + m\sqrt{N_{k3}(p_{\min})} \quad [4.2]$$

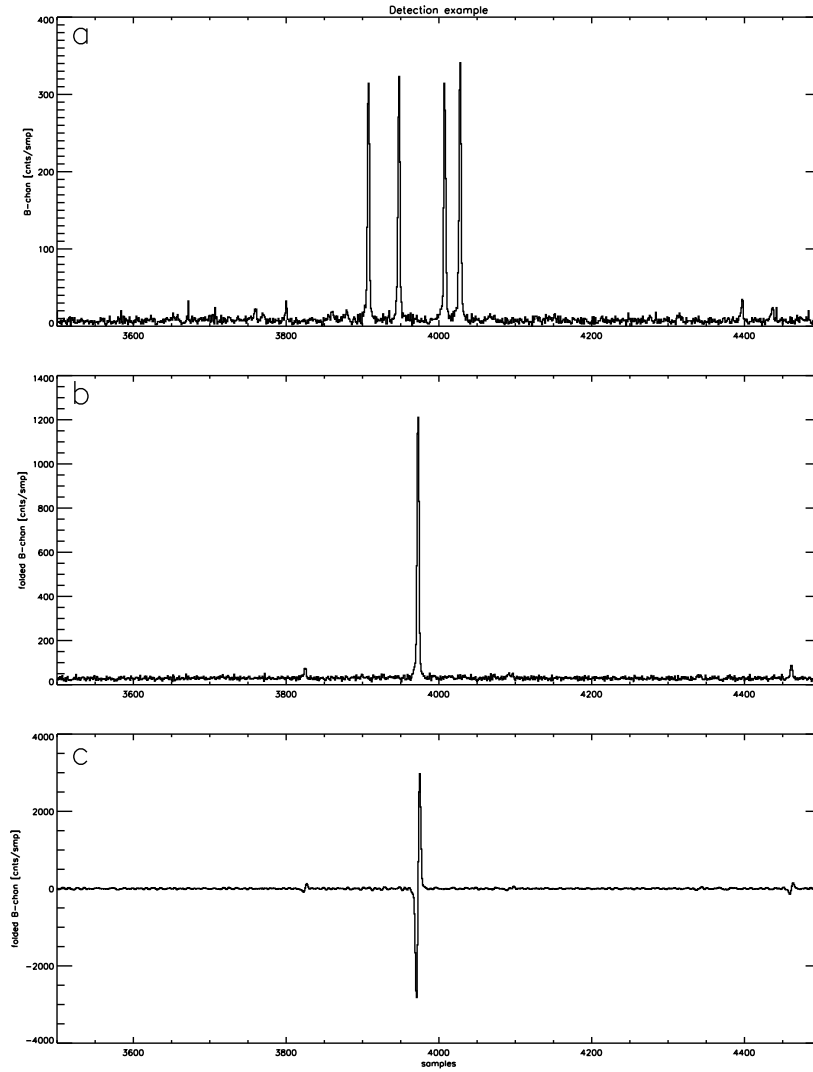


**Figure 4.9.** The three main steps of the detection process. (a) The summed raw count rates ( $N_{k3}$ ) of the  $B_T$  and  $V_T$  channels for 1000 telemetry samples (approximately 4.7 arcmin of scan). This stretch of data contains the transit of a bright star. (b) The same stretch of data folded by the non-linear filtering technique, resulting in  $P_{k3}$ . (c)  $P_{k3}$  folded with the 7-point transit filter, resulting in  $Q_{k3}$ .

If the lowest value  $N_{k3}(p_{\min})$  is less than the background value in  $B_T + V_T$ ,  $uplim$  is derived from the background instead of  $N_{k3}(p_{\min})$ .

If one of the four count rates exceeds  $uplim$ , it is set to the mean of the other three values. But if one or more of the other three count rates are disturbed by spikes or lobes from parasitic stars, this mean value may also exceed  $uplim$ . In this case the count rate is set to  $uplim$ . When replaced, the new values  $N_{k3}(p_k)$  are thus given by:

$$N_{k3}(p_k) = \min \left( 1/3 \sum_{\substack{i=1 \\ i \neq k}}^4 N_{k3}(p_i), uplim \right) \quad \text{for } k = 1 \dots 4 \quad [4.3]$$

These new  $N_{k3}(p_k)$  are then combined to form the folded  $P_{k3}$ . Thus spikes and side lobes are bound to an amplitude which lies in a range allowed by Poisson statistics.

This non-linear filter used by detection uses the knowledge of the expected relative height of the four peaks of the signal. The difference of this filter to a purely additive (linear) filter is determined by Poisson statistics. Applying this filter to the data makes the implicit assumption, that the lowest count rates are not disturbed by any cause. Note that the filter needs a precise value for the background in order to work properly. As described in Section 4.2, either the format background or the local background was computed during the preparation of the data. The background which was actually used in the detection and estimation procedure is called the ‘actual background’,  $b$ , in the following. In general it is the format background.

The non-linear 4-peak filter may cause a bias of the estimated amplitudes, because count rates are never raised but sometimes lowered. This bias is very small and is of the order of a tenth of the overall amplitude error. On the other hand, a linear filter would cause an unknown bias towards higher amplitudes due to the presence of arbitrarily high spikes and disturbing parasitic stars.

The non-linearity of the filter starts only above a certain limit (given by  $m$  in Equation 4.1) in order to avoid disturbances or a bias while detecting very faint transits. This limit had to satisfy two requirements:

- an erroneous spike due to pure Poisson noise should be obtained with a probability of some 1/6000 (1 erroneous spike per format);
- transits fainter than  $\simeq 10.5$  mag should not be affected by the non-linearity of the filter; they were to be treated with a purely linear filter.

The appropriate value of  $m$  was found to be 4.5, i.e. the non-linearity started  $4.5 \times \sigma$  above the expected count rate.

### Practical Realisation

Despite the theoretical simplicity of the 4-point filter, the straightforward implementation of the procedure was limited by computing-time constraints. Since the filtering had to be carried out on the complete Tycho data stream of approximately  $7 \times 10^{10}$  data points, the practical implementation was split into two main intermediate steps. These steps introduced some arbitrary levels of significance for star transits, where the limits were chosen in a way to secure that only very few transits were lost compared to the straightforward implementation. Using this two-step procedure it was possible to decide by rather crude (and fast) criteria whether to really search for and estimate a detection or not:

(1) signal-to-noise criterion: a rough signal-to-noise ratio was computed using four neighbouring count rates around each of the filter points,  $p_k$ , of the linear 4-peak filter. If it exceeded a provisional detection limit of  $0.8 \times F_{\text{det}}$  (where  $F_{\text{det}}$  is the actual detection limit applied afterwards), i.e. only if at this place a detection could possibly be found, these data were submitted to the second step;

(2) the non-linear filtering: the second step consisted of the non-linear filtering as described above.

## Searching Transits

Transits were searched in the  $P_{k3}$  stream by folding  $P_{k3}$  with the integer transit filter:  $[1, 1, 1, 0, -1, -1, -1]$  spaced over seven samples, giving  $Q_{k3}$ :

$$Q_{k3}(i) = P_{k3}(i-1) + P_{k3}(i-2) + P_{k3}(i-3) - (P_{k3}(i+1) + P_{k3}(i+2) + P_{k3}(i+3)) \quad [4.4]$$

where  $i$  is the number of a sample. A change in  $Q_{k3}$  (Figure 4.9(c)) from negative to positive values indicates a transit. A transit was accepted (i.e. turned into a detection), if its signal-to-noise ratio was above the detection limit  $F_{\text{det}}$ . But before this could be done, the rough signal-to-noise ratio had to be replaced by a more accurate evaluation.

The rough signal-to-noise ratio was computed by using four points centred on the possible transit position. If it was above 50 per cent of  $F_{\text{det}}$ , the transit time was computed by inverse interpolation in  $Q_{k3}$ . At this transit time a least-squares estimation of the  $B_T + V_T$  signal amplitude  $a$  (see Section 4.4) was carried out. Taking the resulting signal amplitude  $a$  and the actual background  $b$ , a more accurate signal-to-noise ratio  $F_{B_T+V_T}$  was calculated as:

$$F_{B_T+V_T} = a / \sqrt{0.15(a+b)} \quad [4.5]$$

where the factor 0.15 is a trivial consequence of the normalisation of  $a$  and  $b$ . If  $F_{B_T+V_T}$  was above the detection limit  $F_{\text{det}}$ , the transit was accepted. The detection limit used inside a Predicted Group Crossing interval ( $F_{\text{det}} = 1.5$ ) was different from that outside ( $F_{\text{det}} = 1.8$ ). These limits were chosen in order not to get too many false detections and not to lose many true transits. For stars with  $V_T = 11.5$  about half of the true transits were found, the other half being censored. One accidental false detection was found per Predicted Group Crossing interval. Due to the higher detection limit outside these intervals a smaller amount of false detections was found there.

The detection of a transit, as described above, included the estimation of the  $B_T + V_T$  transit time and amplitude. The  $B_T + V_T$  amplitude obtained from  $P_{k3}$  could be slightly underestimated due to the not exactly spaced 4-peak filter, as explained below. The transit time estimate remained unaffected, because the barycentre of the 4-peak filter still corresponded to the barycentre of the signal peaks, and any deformation of the folded peak remained symmetric. For amplitude estimations in  $B_T$  and  $V_T$ ,  $N_{k1}$  and  $N_{k2}$  were folded separately, with the inexact spacing of the 4-peak filter taken into account (see below). Thus  $B_T$  and  $V_T$  amplitudes were not disturbed by this effect.

## Folding of the B and V Photon Counts

After the search for transits in  $N_{k3}$  and the  $B_T + V_T$  transit time estimation, the folding of  $N_{k1}$  and  $N_{k2}$  was carried out. No further signal-to-noise check was done, because a transit was supposed to be there. Once the transit time was fixed, the integer spacing of the 4-peak filter could be taken care of. Due to the undersampling of the Tycho data the gradient of the count rates was rather steep, especially for bright stars. Thus in extreme cases the non-linear filter could have found count rates exceeding the *uplim* criterion just because of the integer filter positions. To prevent these cases the following procedure was implemented: using the (known) transit time, the actual scanning velocity and the precise slit group geometry for each filter point, the approximate position on the corresponding slit, i.e. the value of the single-slit response function at the filter point positions, was computed. In principle, the folding was done in the same way

as the  $N_{k3}$  folding. But while applying the non-linear filter, the four points under consideration were normalized to the same value of the single-slit response function. Before combining the points, the normalisation had to be reversed, of course, in order to preserve the original shape of the signal.

---

#### 4.4. Estimation of Transit Parameters

---

##### Transit Time Estimation

$B_T$  and  $V_T$  transit times were estimated separately by using the same integer filter method as for  $B_T + V_T$  transit times, but operating on  $P_{k1}$  and  $P_{k2}$ , which result from the non-linear filtering in  $B_T$  and in  $V_T$ . It was shown by Yoshizawa *et al.* (1985) that a maximum cross-correlation filter method for the estimation of transit times is not more accurate than this simple integer filter method.

##### Signal Amplitude Estimation

Yoshizawa *et al.* (1985) showed that for the signal amplitude estimation a maximum-likelihood method is superior to a least-squares fit. Thus, the  $B_T$  and  $V_T$  amplitudes were evaluated using a maximum likelihood iteration, the starting values being the results of a least-squares fit. Input required for the amplitude estimation were the actual background, the transit time estimate, and the relevant response function (vertical/inclined slit group, preceding/following field of view, upper/lower half of slits,  $B_T/V_T$  channel) and folded photon counts in the  $B_T$  and  $V_T$  channels.

**Preparing the single-slit response function:** For the fitting procedure a folded slit response function  $F_p$  had to be prepared to correspond to the 4-peak folded data. This means the following: Assume the estimated transit time  $p$  corresponds to the barycentre of the four slit signals. Knowing the actual scanning velocity and the slit geometry, the distances of the four slit signals (in units of samples) and the approximate position of each sampling point on the corresponding slits can be computed. Thus it is possible to reconstruct the real signal peak at the transit time by adding the relevant values of the single-slit response functions. The shape of the resulting folded slit response function  $F_p$  depends on the fraction of  $p$  ( $p$  in units of samples) and on the actual scan speed.

**Least-squares estimation for amplitudes as starting value:** The result of a least-squares fit of the folded response function to 10 points of the 4-peak folded data was used as the starting value for the final maximum likelihood amplitude estimation. The least-squares fit determined only the signal amplitude  $a$ , keeping the previously determined background and transit time fixed. The minimum of the sum  $\sum_i (aF_p(i) + 4b - P_k(i))^2$  over 10 data points was determined as:

$$a = \frac{\sum_i (P_k(i) - 4b)F_p(i)}{\sum_i F_p^2(i)} \quad [4.6]$$

where  $i$  denotes the indices of the 10 data points.

Whenever this amplitude estimate resulted in a zero or negative value, the shape of the signal did not fit the expected one. In this case the transit was either disturbed or it was a false detection. If this occurred while estimating the  $B_T + V_T$  amplitude during the

search for transits, these transits were not accepted. If it occurred while estimating  $B_T$  or  $V_T$  amplitudes, the transit was flagged ‘bad’ in the corresponding channel, and no further estimation was done in this channel.

**Maximum likelihood estimation of final amplitude:** The final maximum likelihood amplitude estimation was an iterative method, giving the most probable amplitude  $a$ , assuming the previously determined transit time  $p$  and the background  $b$  to be correct. Photon count rates were supposed to be Poisson distributed. The result was obtained by a Newton-Raphson iteration process (Silvey 1970):

$$a_n = a_{n-1} + \sum_i (P_k(i)/P_{n-1}(i) - 1)F_p(i) / \sum_i F_p^2(i)/P_{n-1}(i) \quad [4.7]$$

where  $i$  denotes the indices of the 10 data points,  $P_{n-1}$  is the theoretical  $P_k$ , i.e.  $P_{n-1} = 4b + a_{n-1}F_p(i)$ .

The iteration was stopped as soon as  $a_n$  and  $a_{n-1}$  differed by less than 0.1 per cent. Again, if the amplitude iteration did not converge, the transit was flagged ‘bad’ in the corresponding channel.

---

## 4.5. Verification Methods

---

The verification of the software used for the prediction and detection tasks, and of their output data streams, was a continuous process. It started well before the launch of the satellite and ended only after a first preliminary Tycho output catalogue had been produced by the astrometry task. It had to be an iterative procedure, primarily because of the gradual development of the software, but also because of the iterative nature of the Tycho data reduction chain itself. Verification efforts before launch included the trial processing of simulated satellite data provided by NDAC. After launch, the verification processes were interleaved with the calibration of the instrument, using actual mission data.

The prediction and detection processes are so intimately connected that much of the verification of prediction could only be done with the output of detection in hand. Thus the verification of either of these processes was at no stage independent from the other one. Verification of prediction was furthermore made difficult by the fact that prediction had to be accurate to the milliarcsec level in order not to degrade the final Tycho astrometry. But, due to the low precision of the real-time satellite attitude and of the Tycho Input Catalogue, the actual agreement between predicted and observed group crossings could initially be tested to the level of a few tenths of an arcsec only. This situation only gradually improved with the advent of on-ground attitude, of more precise star mapper calibrations, and finally with the first preliminary Hipparcos output catalogues. More details can be found in Chapters 7 and 10.

The remainder of this section briefly outlines some of the early verification steps, starting with different aspects of the prediction software, and proceeding to the detection task later on.

## Satellite Orbit Comparison

A correct interpretation of the satellite ephemerides (which were provided on each of the telemetry tapes, see Section 4.1), was crucial to the computation of stellar aberration and (for the solar system objects) of parallax. Shortly after launch, the European Space Operations Centre provided a sample orbit file to the Data Reduction Consortia, along with a numerically tabulated interpretation of the Chebychev polynomials into satellite position vectors and velocity vectors, in the different relevant coordinate systems, for some specific instants of time. These data were compared with the output of the relevant subroutines in the operational prediction software.

## Apparent Positions Comparison

The computation of apparent star positions from stellar data (mean position, proper motion and parallax), solar system ephemerides and satellite position and velocity vectors was verified by comparisons among the different Data Reduction Consortia and the European Space Operations Centre. In 1990, a set of *ad hoc* comparison inputs was produced by NDAC (the Royal Greenwich Observatory group), and successfully passed by all parties. In 1992, another comparison was performed by extracting apparent positions actually computed during the operational runs of the data reduction programs of FAST, NDAC and TDAC. For this purpose, a few particular stars and a few hours of mission time were selected at random. The analysis of the resulting sample outputs showed agreement on the 0.1 mas level among all four participating parties.

## Star Selection for Prediction

The most complicated part of the prediction software concerned the Tycho Input Catalogue access, i.e. the selection of those stars that may produce group crossings within a certain small time interval. If this procedure had been imperfect, the Tycho data reduction chain would have lost part of the observations. This could not be fully verified before launch. It was partly tested by, for example, manually constructing the run of the star mapper slits over a part of the Input Catalogue sky, and comparing with the actual Predicted Group Crossing data stream. Final verification came much later by checking (over a significant part of the mission) that essentially none of the actually observed transits of bright stars (by the detection process) remained without corresponding Predicted Group Crossing data. Still another check was to look for 'holes' in the sky distribution of all stars having Predicted Group Crossing records. The only 'holes' found after a few months of mission corresponded to 'holes' in the Input Catalogue, which in turn could be verified as real by comparison with the printed photographic sky surveys. Another verification of the completeness of prediction came from the star recognition process described in Chapter 5. The few bright ( $V < 8.5$  mag) stars missing from the Tycho Input Catalogue Revision were thoroughly investigated. None were due to missing Predicted Group Crossings.

## 'Cloud Plots'

Plots of the individual transit time differences 'detected minus predicted' versus the  $z$  coordinate along the slits were referred to as 'cloud plots'. Figure 4.10 shows a few

examples. Each of the tiny  $\times$  symbols corresponds to one detection inside a Predicted Group Crossing interval. The height of the plots is slightly less than the full width of the interval. Units on the vertical scale are  $1/600$  s, the time interval of one Tycho photon counts sample. On the sky, this corresponds to 0.281 arcsec for the vertical slits (right half of the figure), and to 0.199 arcsec for the inclined slits (left half), at the nominal scan speed of  $168.75$  arcsec  $s^{-1}$ . The detections in the dense 'clouds' are those that are really related to the predicted star transits, while the homogeneous background of detections on either side of the clouds are due to photon noise peaks, and to unrelated stars crossing the slits at about the same time.

The cloud plots were one of the major diagnostic tools for prediction and detection. The width of the clouds are indicative of the combined precision of the attitude and input catalogue. Any offset of the clouds from the centre of the Predicted Group Crossing intervals, on the other hand, shows errors or inconsistencies in the interpretation of the attitude and/or instrument geometry. The examples in Figure 4.10 were chosen to illustrate some of the early improvements achieved at the start of the mission. They do not all belong to the mass production phase of prediction and detection, but to the extensive trial runs with real satellite data that were performed during 1990.

The two plots at the top contain the first results on a stretch of data collected before 23 January 1990. The inclination and offset of the clouds are caused by the unexpected rotation of the grid assembly relative to its nominal position in the focal plane. The 'jump' of the inclined slits at  $z = 0$  is also caused by this effect. The rms width of the clouds is about 0.9 arcsec, which is mainly due to the imprecise real-time attitude at this early stage of the mission. This state of affairs is clearly unsatisfactory: some real star transits are being missed at the edges of the Predicted Group Crossing intervals, especially at large negative  $z$  coordinates (lower left in the plots).

The two plots in the centre show analogous data, but with the grid rotation (and a systematic attitude offset) taken into account in the prediction process. This removed the systematic offsets, but could not improve the random errors of the attitude, i.e. the width of the clouds.

The two plots at the bottom show data collected after 23 January 1990, when the grid rotation had been implemented into the on-board instrument model. The improvement is evident. It is due to the improved real-time satellite attitude. The rms width of the clouds is about 0.6 arcsec for the inclined slits, and 0.4 arcsec for the vertical slits. It is apparent that the instrument model used in the prediction process for these data caused a slight overcorrection of the 'jump' in the inclined slits at  $z = 0$ . However, the defect was sufficiently small not to disturb the subsequent Tycho data reduction steps.

### **Standard Quality Control in Detection**

During the mass processing of detection a set of standard tools were used in order to monitor the quality of the input and output data. These standard tools used statistical data collected during the routine processing. A total of about 0.5 Gigabytes of such data were produced and regularly inspected. Besides the 'cloud plots' described previously, a set of 10 different sorts of plots were provided by the so-called 'Diagnostic Package' reading the statistical data sets. Some of these plots are presented and described hereafter for one arbitrarily selected stretch of satellite observations. The plots show the typical properties of the input and output of the detection and estimation process for reprocessing data.

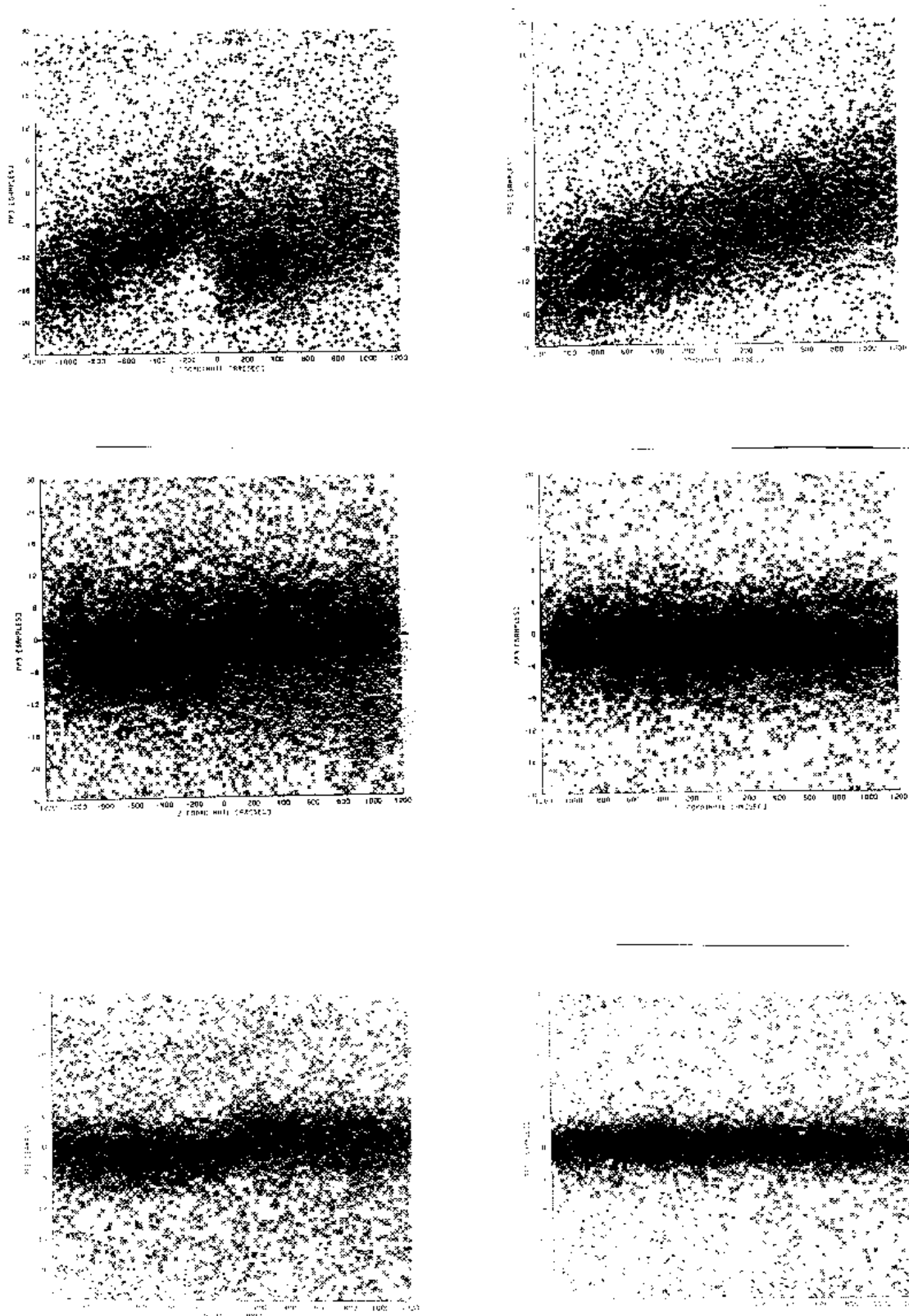


**Figure 4.10.** Sample 'cloud plots' from the early stages of trial processing of prediction and detection. The height of the plots corresponds to 12 arcsec on the sky, i.e. the width of the Predicted Group Crossing intervals. The horizontal axis spans the 40 arcmin length of the star mapper slits. Details are described in the text. The improvement from top to bottom is evident.

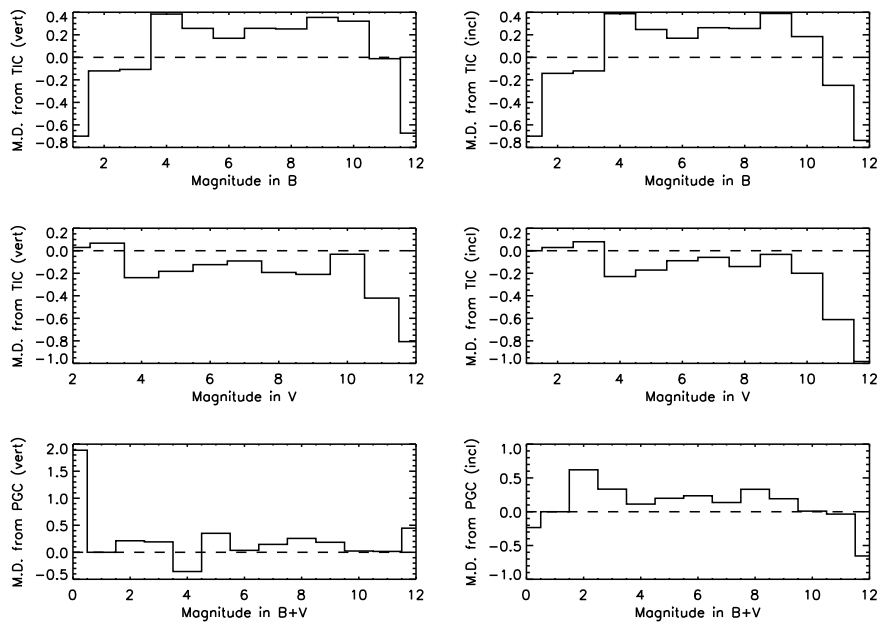


**Figure 4.11.** The mean difference between the observed and the Tycho Input Catalogue magnitudes (derived from a crude calibration) is shown for different magnitude bins in  $B_T$  (top) and  $V_T$  (centre), for the vertical (left) and inclined (right) slit groups. The roughly constant values throughout the centre of the plots indicate linearity of the estimation process. The number of bright stars is very low. Thus the strong variations at extreme left are due to small-number statistics. At extreme right, i.e. at very faint magnitudes, the effect of the censoring causes a drop of the plotted curves, but again small-number statistics modifies the effect. The lower panels show the mean difference between the predicted and the measured transit times versus  $B_T + V_T$  magnitude in the vertical (left) and the inclined (right) slit group, respectively, in units of samples (corresponding to 0.281 arcsec on the sky).

**Mean deviation from input catalogue magnitudes:** The signal amplitudes derived by the estimation process were converted to magnitudes, using a crude calibration formula provided by the photometry task. For a linear photometric system, the mean of the differences between the measured magnitudes and the Tycho Input Catalogue magnitudes should not depend on the magnitude (the mean value itself is of no importance; it is just the error of the crude calibration zero point used). Since the photometric calibration did not use a magnitude-dependent term (see Table 8.2), any magnitude dependence (i.e. non-linearity) in estimation would be reflected in the finally reduced magnitudes. Plots like the one shown in Figure 4.11 were used to check the linearity (i.e. constancy of the offset versus magnitude).

**Predicted minus observed transit times:** The detection process depended very much on the accuracy of the predicted group crossings. Thus the monitoring of the quality of prediction was vital for the whole data reduction. One kind of quality control was the production of the ‘cloud plots’, see Figure 4.10. However, the production of these plots was quite time-consuming and thus impractical for daily use. So-called ‘PDI-plots’ (Figure 4.12) were used as a quick-look utility on the same parameters, namely the difference between the measured and the predicted crossing, but without resolution along the  $z$  axis.

**Goodness-of-fit:** During the estimation process the goodness-of-fit (chi-square per degree of freedom,  $\chi^2/f$ ) was determined for every detected transit. In an ideal instrument, the frequency distribution of the goodness-of-fit should follow a normalized

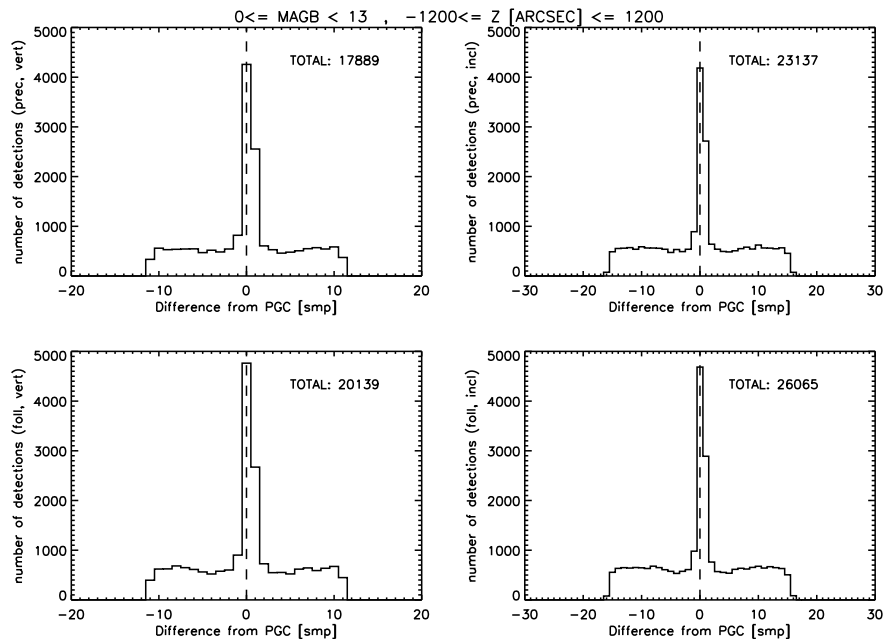


**Figure 4.12.** Histograms of the differences between the observed  $B_T + V_T$  transit times and the Predicted Group Crossing epochs are shown for the vertical (left) and inclined (right) slit groups, and for the preceding (top) and following (bottom) field of view. The width of the plots corresponds roughly to the Predicted Group Crossing interval. The peaks in the centres are due to the predicted star transits, while the broad plateaux are due to unrelated ('parasitic') stars and photon noise ('false') detections. Only in the reprocessing are the peaks as narrow as shown here. In the main processing stage their total width was of the order of  $\pm 4$  samples for the vertical slits.

$\chi^2 / f$  distribution with a peak around  $\chi^2 / f = 1$ . In a more realistic case, the distribution of the mean goodness-of-fit versus magnitude should show a smooth behaviour. The actual distribution for the Tycho data depended on a number of parameters such as the background and the magnitude distribution of the stars contained in a specific data set. The actual values derived in the estimation process showed a strong dependence on the magnitude. At faint magnitudes where the differences between observed and modelled count rates were dominated by photon noise, the actual goodness-of-fit roughly corresponded to the ideal expectations. The strong increase towards bright magnitudes (Figure 4.13), is due to the fact that there the photon noise becomes negligible compared to other error sources. The increase is due to, for example, small errors of the model response functions, the undersampling of the response functions, and other effects, which are all more disturbing for bright than for faint stars. For stars brighter than about  $V_T = 4.5$  mag or  $B_T = 5$  mag, the goodness-of-fit usually reached and even exceeded 12.7, the maximum value which could be stored in the range provided by the output formats. This is the reason for the high plateau in the top and centre panels of Figure 4.13, and for the narrow peak in the two lower panels.

**Signal-to-noise ratio:** The signal-to-noise ratio of detected transits should obviously depend on the magnitude of the observed stars. This is confirmed by the upper part of Figure 4.14 (the levelling-off of the curve for stars brighter than about 7.5 mag is due to a cutoff imposed by the data format, as in the case of Figure 4.13). However, it should not strongly depend on the background, at least within the background range used by photometry. This requirement was monitored by plots like the ones shown in the lower part of Figure 4.14.

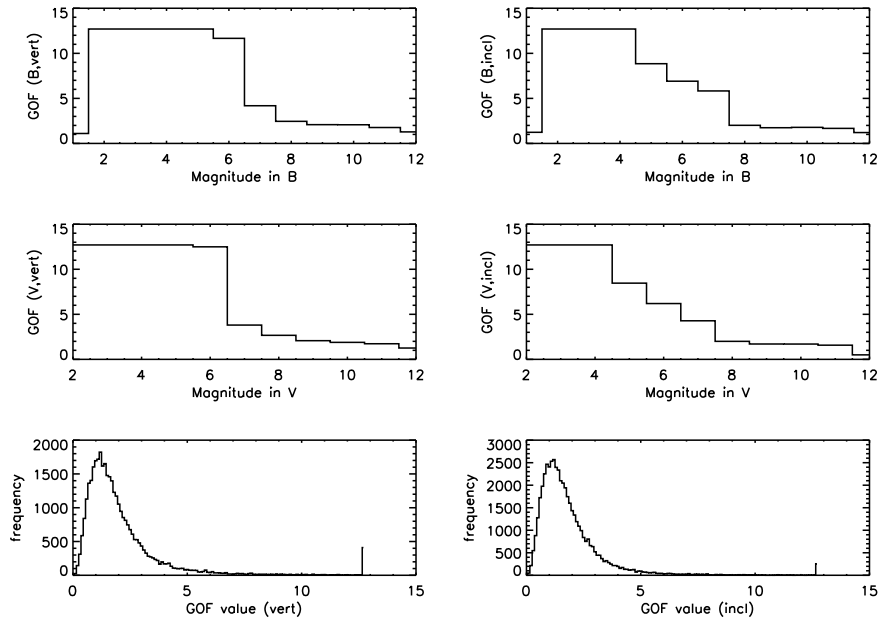


**Figure 4.13.** The mean values of the goodness-of-fit (chi-square per degree of freedom) in  $B_T$  (upper) and in  $V_T$  (middle) is shown versus magnitude for the vertical (left) and inclined (right) slit groups. The excess towards brighter magnitudes results from the very high sensitivity of the fits to the steep slopes of the response function. The overall distribution of the goodness-of-fit is shown in the lower two panels, again for the vertical (left) and inclined (right) slit groups. Details are explained in the text.

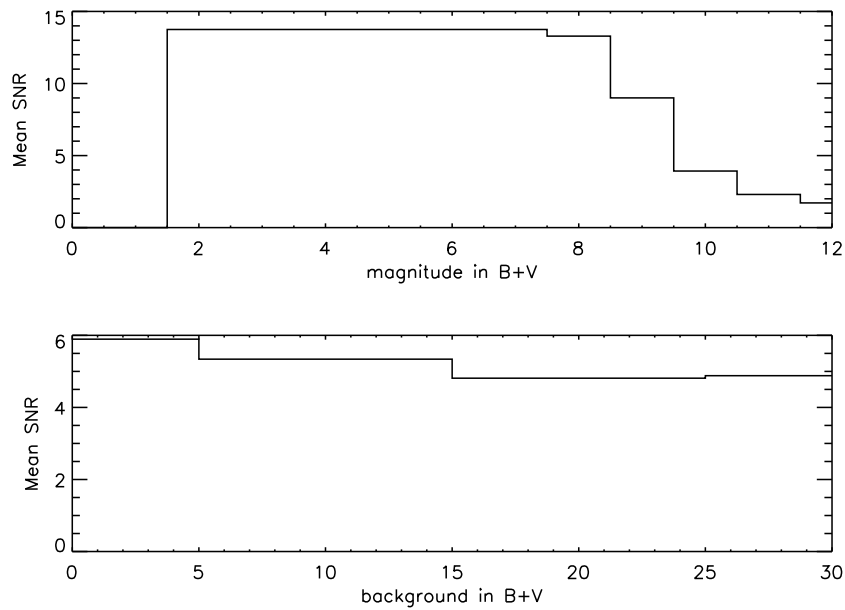


**Figure 4.14.** The mean signal-to-noise ratio versus  $B_T + V_T$  magnitude is shown in the upper graph. In the lower graph, the mean signal-to-noise ratio versus background is shown.

**Background:** The background observed in the Tycho detectors was one of the worst consequences of the highly elliptical orbit of the revised Hipparcos mission. Usability of the raw data was almost solely a function of the background. Thus the distribution of the background level was one of the most important quantities to be monitored. Within the 'Diagnostic Package' there were two kinds of plots which gave an instant overview of this parameter. In addition, there was a quite extensive external toolset for off-line visualising and investigation of the background. Some of the results of this toolset are shown in Figures 4.3 to 4.7.

**Step-by-step reduction:** Another very important diagnostic tool was a special version of the complete detection and estimation (plus rough photometric reduction) software package providing a manually controlled step-by-step treatment of the data for a single, freely selectable star, for a given stretch of satellite observations. It provided the possibility of visualising details of each processing step. This tool proved invaluable in finding software errors, investigating data anomalies and interpreting problem stars.

U. Bastian, A. Wicenec



## 5. RECOGNITION OF STARS

*The observations of the first year of mission of the Tycho program were used for revising the Tycho Input Catalogue in the process called 'recognition of stars'. The Tycho Input Catalogue Revision essentially defined the list of objects in the final Tycho Catalogue. The stars were searched with three different processes, according to their distances from the positions in the Tycho Input Catalogue. The main process concerned stars closer than 6 arcsec. Stars with separations between 6 and 20 arcsec were searched too, but the threshold in detection was slightly brighter than in the main process. Stars absent from the input catalogue were also searched, but with an even higher threshold in detection. At the same time, the mean uncertainty of the positions was improved from about 1 arcsec in the Tycho Input Catalogue to about 0.15 arcsec.*

---

### 5.1. Introduction

---

The basic strategy of Tycho required an input catalogue with accurate positions, in order to relate the stars and their signals in photon counts. The Tycho Input Catalogue, presented in Chapter 3, was the first step for this purpose; its accuracy was about 1 arcsec on average, but this was not sufficient. Due to the uncertainty of the magnitudes, it contained slightly more than three million stars, but the Tycho team expected that only about one million stars would be retained in the final selection. Moreover, since the Tycho Input Catalogue was partly based on Schmidt plates, many faint stars were expected to be missing, such as stars close to a bright companion illuminating the plate, or stars lying in a nebulous area. The revision of the input catalogue was done in the process called 'recognition of stars', which is the subject of this chapter. Its aim was to find all the stars lying in areas centered on the positions of the Tycho Input Catalogue entries, and to determine precise positions for them.

---

### 5.2. General Outlines

---

The Tycho Input Catalogue Revision was produced from observations with the satellite and the Tycho Input Catalogue. Predictions of the times of star transits were used for selecting the signals from the stars. The discrepancies between predicted epochs and actual ones were converted into offsets in the star positions, taking into account the

scanning law of the satellite. This basic principle was used in all the Tycho reductions. The main difference between the recognition of stars and the final astrometric reduction is the length of the time interval around each predicted transit where the signal was searched. In the recognition of stars, the interval corresponds to a wide area on the sky, where several stars may be found.

Before searching stars, the observations around each entry of the Tycho Input Catalogue were gathered (the term ‘entry’ is preferred over ‘stars’, since it refers hereafter to positions and identifications, but not to astronomical objects). The entries of the Tycho Input Catalogue were then treated, one after the other, and the stars were searched. Three different processes were used, differing in the time interval where the signal was searched:

- the search for ‘close companions’ was the first of the three processes. It concerned stars that are closer than 6 arcsec to the positions in the Tycho Input Catalogue. It covered only 0.065 per cent of the sky, since the Tycho Input Catalogue contains 3.15 million entries. This search was performed using a low threshold in the signal-to-noise ratio of the detections;
- the second process was dedicated to the ‘wide companions’, having distances from the positions in the Tycho Input Catalogue between 6 arcsec and 20 arcsec. The detection threshold of the observed transits was taken a bit brighter. This process covered 0.66 per cent of the sky;
- the third process was the search for ‘serendipity stars’, which was based on any bright transits not produced by stars in the Tycho Input Catalogue. These transits were related to a network of points covering the whole sky, in order to be sure that all bright stars missing from the Tycho Input Catalogue could be found in the Tycho Input Catalogue Revision.

Subsequent steps of the recognition process removed the redundant stars and estimated the magnitudes. When a star was found by different processes, a rule of selection was used to decide which solution had to be considered as the most reliable one, and the others were discarded. An estimation of a broad-band magnitude called  $T$  was also derived from the added signal amplitudes in the  $B_T$  and  $V_T$  bands.

---

### 5.3. Preparation of the Input Data

---

The input data for the recognition of stars were the ‘transit summary’ file and a corresponding file of updated predictions of group crossings of the first year. These data are denoted ‘TS’ and ‘PGCU-2’, respectively in Figure 1.2.

#### **The Transit Summary File**

The transit summaries are combinations of predictions of the time of transits (the so-called ‘predicted group crossings’) with actually detected transits (for brevity, these will be called ‘detections’ in the following). The predicted group crossings were derived from the on-board attitude of the satellite and from the Tycho Input Catalogue. They were computed at Astronomisches Rechen-Institut in Heidelberg. A prediction consists of:

- the identification of the star in the Tycho Input Catalogue;
- information about the scanning motion of the satellite;
- the position on the star mapper of the transit of the star, assuming the coordinates in the Tycho Input Catalogue;
- the predicted epoch of that transit.

This description of the conditions of observation is completed by the photon noise background level, which was provided by the detection process.

The predictions were sent to Astronomisches Institut of Tübingen. The transits of stars were then searched in the tapes of photon counts around the epochs of the predictions. A detection consists of:

- the offset in epoch between the detection and the prediction;
- the signal-to-noise ratio;
- the photon noise background level.

In the detection process, the detections were related to the predictions according to two modes. The first mode was the search for signals within 'prediction intervals'. A prediction interval is an interval in time centred on a prediction epoch, and having a length permitting the detection of a star as long as the offset in position is not larger than 6 arcsec (this is the limit of the search for close companion stars). This means that when a crossing of the vertical slit group is considered, the length of the interval corresponds to the scanning of  $2 \times 6$  arcsec. This corresponds to 71.11 ms when the average scanning velocity of  $168.75 \text{ arcsec s}^{-1}$  is assumed. For a crossing of the chevron slit group, the size of the interval is  $\sqrt{2}$  times larger in time. The detection threshold within the prediction intervals for the signal-to-noise ratio of peaks in the photon counts is 1.5.

All the detections found were related to the current prediction. When two prediction intervals were overlapping, detection was processed twice in the overlapping part, and the detections in that part appeared in duplicate in the transit summary file, since they could belong to either of the two predictions. If no detection was found, the prediction was still transmitted to the transit summary file, in order to count the predictions of each entry of the Tycho Input Catalogue.

The second mode of detection concerned the observations done outside the prediction intervals. The detection threshold for these was set to 1.8, and the detections were related to the first prediction that followed.

The recognition of stars was based on the observations collected during the first 368 days of the scientific mission, beginning the end of November 1989. The transit summary file prepared at Astronomisches Institut of Tübingen corresponded to 310 full days of observation. The 3.15 million entries of the Tycho Input Catalogue received 244 million predictions, and the transit summary file was written on 152 high-density magnetic tapes. These tapes were sent to the Centre de Données astronomiques de Strasbourg (CDS) to be used for the star recognition process.

## Updating and Selection of the Predictions

The prediction updating process performed a re-calculation of the predictions using on-ground determinations of the attitude of the satellite and of the star mapper calibration. The updated predictions became available about one year later than the on-board attitude, and it was therefore not possible to use them in the detection step. The accuracy of the updated predictions was around 0.2 arcsec instead of 1 arcsec for the original predictions used for detection. For the recognition of stars, Astronomisches Rechen-Institut at Heidelberg prepared 44 high-density magnetic tapes of updated predictions (PGCU-2) that were sent to the star recognition task at the Centre de Données astronomiques de Strasbourg.

The predictions in the transit summary file were replaced by the updated predictions, and the differences of epochs between the predictions and the detections were recomputed. The transits getting an updated prediction with an uncertainty larger than 1 arcsec were discarded from the process. The predictions corresponding to a large background could not help for the detection of faint stars, but might well have added false detections. For that reason, transits having a background larger than 20.7 counts per sample were also discarded. The remaining data contained 155 million predictions and the related detections, giving an effective rate of 53 per cent of the covered time of satellite flight. On average, each entry of the Tycho Input Catalogue received 49 predictions. However, the actual number was highly variable from one entry to another: 2091 entries got less than 4 predicted group crossings, and no search for stars was performed around them. At the other extreme, one entry got 322 predicted group crossings.

---

## 5.4. The Search for Companion Stars

---

As explained above, the so-called ‘companion stars’ are the stars searched around the entries of the Tycho Input Catalogue. Close companions are closer than 6 arcsec from them; wide companions have distances between 6 and 20 arcsec, the latter being searched with a brighter threshold for the detections. The searches for the close and for the wide companion stars were processed together.

### Gathering the Transits Related to the Same Entry of the Tycho Input Catalogue

In the original transit summary file, the detections were related to predictions within intervals corresponding to the search for close companion stars. This assignment was reconsidered in the recognition of stars, taking into account the updated epochs of predictions. The detections with signal-to-noise ratios between 1.5 and 1.8 which fell outside the prediction intervals were discarded.

On the other hand, detections with signal-to-noise ratios larger than 1.8 were related to the predictions whenever they were within a ‘wide companion interval’. Since the wide companion stars were to be searched within areas of 20 arcsec radius instead of 6 arcsec for the close companions, the wide companion intervals had to be chosen 20/6 times larger than the original prediction intervals.

On average, every prediction finally received 6 detections, although only one third of the Tycho Input Catalogue entries actually corresponded to detectable stars. As expected, the vast majority of all detections were due to noise: Poissonian fluctuations in the photon counts, spikes, background stars, and ghost detections due to the side lobes generated by bright stars. The rate of true detections per prediction was 0.3. The distribution of the detections around the positions in the Tycho Input Catalogue is shown in Figure 5.1. It appears that the standard deviation of the true detections from the prediction corresponds to 0.5 arcsec. The total amount of data was 991 million 24-byte records, or 23.8 Gigabytes. This file was stored with a cartridge system on the IBM-3090 computer of the Centre de Calcul CNRS de Strasbourg-Cronenbourg. For gathering the transits of each entry in the Tycho Input Catalogue, it was sorted according to the star identifications, with a method perfected by the Centre de Calcul CNRS.

### The Search for Stars around the Positions in the Tycho Input Catalogue

The searches for the close companion and for the wide companion stars were processed in two steps: a preliminary search in a digital map and an iterative least-squares computation. The input data were the transits, converted to detection lines (Figure 5.2). A detection line is the position of the slit group relative to the predicted group crossing at the time of the actual detection (the detected star can be anywhere on this line). The detection lines were calculated in a cartesian coordinate system with the origin at the Tycho Input Catalogue position. The parameters of each detection line were derived from the scanning direction and from the offset between prediction and detection epoch, assuming that the scanning velocity is  $168.75 \text{ arcsec s}^{-1}$ . Each detection line received a weight equal to the square of the signal-to-noise ratio of the detection. In order to avoid false stars generated by detections due to bright stars outside the map, the weights were limited to 9 and 12.25 for the close companions and for the wide companions, respectively. The weights of the brightest detections were thus only about 4 times larger than those of the faintest detections.

Digital maps were built in order to determine approximate positions of the stars. A digital map is a grid of 0.5 arcsec-sized pixels, with sides of 13 arcsec in the search for close companions and 41 arcsec for the wide companions. Since stars were to be searched in circular areas, only the pixels covering a disc inscribed in the square grid were considered. Each pixel received the sum of the weights of the detection lines crossing a diamond having its corners in the middles of the sides of the pixel. In the case of the wide companions, only the detections having a signal-to-noise ratio larger than 1.8 were taken into account. The grid points, i.e. the intersections of the lines that define the pixels, were considered next. Each grid point received the sum of the weights of the four surrounding pixels. The position of the intersection getting the largest weight was finally taken as input for an iterative least-squares computation.

The purpose of the least-squares calculation is to find the point which minimizes the weighted sum of squares of orthogonal distances to the detection lines. Let  $x$  and  $y$  denote the coordinates in the cartesian reference system,  $a_i$ ,  $b_i$ , and  $c_i$  the parameters of the detection lines, and  $w_i$  the corresponding weight. The equation of a line is:  $a_i x + b_i y = c_i$ . Then the position  $(X, Y)$  of the star is given by the normal equations:

$$\begin{pmatrix} \sum a_i^2 w_i & \sum a_i b_i w_i \\ \sum a_i b_i w_i & \sum b_i^2 w_i \end{pmatrix} \begin{pmatrix} X \\ Y \end{pmatrix} = \begin{pmatrix} \sum a_i c_i w_i \\ \sum b_i c_i w_i \end{pmatrix} \quad [5.1]$$

where the left-hand matrix is the normal-equation matrix.

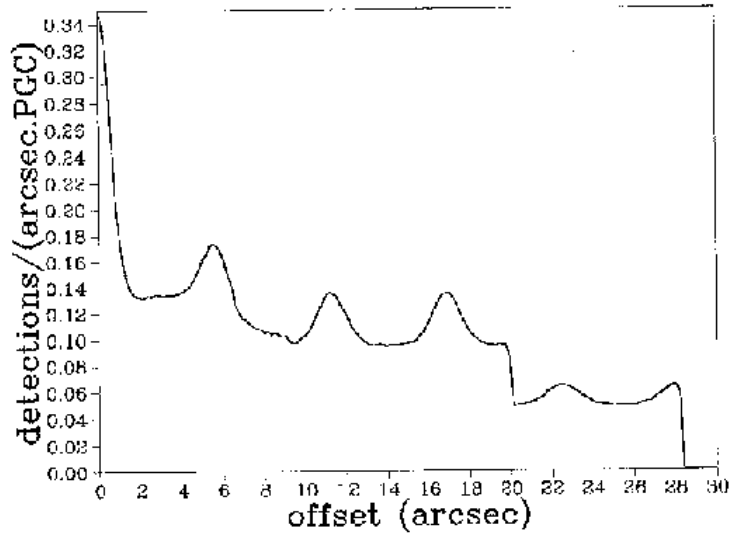


**Figure 5.1.** Frequency of detections according to their distances from the positions in the Tycho Input Catalogue. The ordinate is the number of detections per arcsec and per predicted group crossing. The figure is derived from a subsample of 6.5 million detections related to 1.1 million predictions. The main peak contains the detections of the stars of the Tycho Input Catalogue. The secondary peaks are due to side lobes as expected from the configuration of the slit groups.

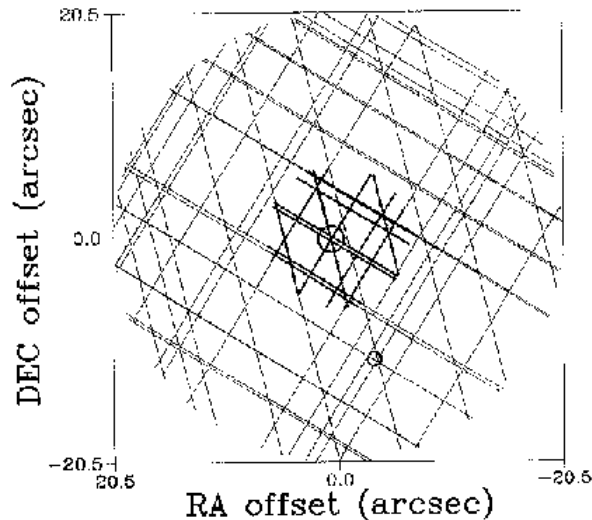


**Figure 5.2.** A map of detection lines. The central area has a diameter of 13 arcsec, and the diameter of the large circular area is 41 arcsec. The thick lines interrupted at the border of the central area correspond to detections taken into account in the search for close companion stars. The circles indicate the positions of the stars selected by the computation. The central star is ADS 13 909 C (magnitude: 9.60). The wide companion is the D component (magnitude: 11.25). For clarity of the figure, the number of predicted group crossings is only 6, instead of 49 on average. The significance of the two circled points is therefore not apparent to the eye.

The weight  $w_i$  of each line was set to be the product of the weight coming from the signal-to-noise ratio and of a weight coming from the distance between the line and the input position. This last weight was set to  $1/(1 + d^4)^2$ , where  $d$  is the orthogonal distance of the line in arcseconds. The calculation of the position of the stars was repeated iteratively. Each time a position had been derived, it was used for determining the weights of the detection lines for the next iteration. The calculation stopped as soon as one of the two following conditions was satisfied: (a) the new position is closer than 0.03 arcsec to the preceding one, or, (b) the number of iterations is 6.

When a star was found, it was verified that at least 3 detection lines were closer than 0.5 arcsec from its position; otherwise the star was assumed to be false. Other false stars were generated by intersections between closely parallel detection lines produced by a star outside the map and a single background line having a different slope. These were eliminated by rejecting the solution when the condition number of the  $2 \times 2$  normal-equation matrix,  $\mathbf{A}$ , was greater than 7:

$$\text{cond}(\mathbf{A}) = \frac{\|\mathbf{A}\|^2}{\det \mathbf{A}} > 7 \quad [5.2]$$

Many false stars were still generated by background detection lines, but they were removed by considering the total weights of the detection lines closer than 0.5 arcsec from the solution (only the weights derived from the signal-to-noise ratios of the detections were considered here). These weights were compared to thresholds depending on the numbers of predicted group crossings. The initial thresholds had deliberately been chosen too small, their refinement will be discussed further below. When the weight of a star was above the threshold, the star was provisionally recorded, otherwise it was rejected.

Whenever the least-squares calculation yielded a star that could not be accepted, the four pixels that had provided its preliminary position were set to zero. On the other hand, when a star was accepted, the detection lines closer than 1 arcsec to the calculated position were removed from the digital map and were discarded from the computations of the positions of more stars. This was done to avoid false stars generated by intersections between detection lines related to a star and background detection lines. The search for stars was processed again until the weight of the subsequent preliminary position became less than 1.6 times the acceptance threshold of the least-squares solution.

False stars could have appeared if the close companions and the wide companions had been searched independently: the detection lines of a close companion star might then have generated false stars in the surrounding area where wide companions were searched, and vice versa. This possibility was largely avoided by the following rule: The search for close companions was processed first, and the detection lines closer than 1 arcsec to the stars were discarded. The wide companions were searched afterwards, on the basis of the detections with signal-to-noise ratios larger than 1.8 that were not discarded previously. When one or more wide companions were found, the search for close companions was completely carried out again, discarding all the detection lines that were closer than 1 arcsec to the wide companions.

This process, based on preliminary selection thresholds, provided 1.31 million stars: 1.23 million close companions, and 76 000 wide companions. The next step was to redetermine the acceptance thresholds in order to remove most of the false stars. For that purpose, it was first necessary to remove the redundant stars.

## Search for the Redundant Companion Stars

The Tycho Input Catalogue contains some components of double or multiple stars whose separation is smaller than the size of the digital maps. A component of such a multiple system could then appear in several maps, and it could be recorded several times as close or as wide companion stars, that were in fact redundancies of the same object.

For searching redundancies, the equatorial coordinates of the stars were derived by adding the coordinates in the Tycho Input Catalogue to their positions relative to the map centres. The selection of the redundant entries was based on the following algorithm:

- when two stars were closer to each other than the 'redundancy threshold', one of them was flagged as redundant; the rule was to flag the star with the largest distance from the centre of the map where it was found; the redundancy threshold was chosen as the closest separation between two stars found in the same map: 1.22 arcsec;
- when a star had been flagged as redundant, it was no longer considered for searching other redundant stars; but,
- when a star became redundant, the redundancy flags of the stars that it had made redundant before were reconsidered.

This iterative process converged rapidly. About 27 000 stars were discarded from the determination of the definitive thresholds because they were redundant.

## The Definitive Selection of Companion Stars

The choice of the selection thresholds depended on the number of false stars that was considered acceptable in the Tycho Input Catalogue Revision. It was decided that the search for close companions and the search for wide companions may each generate about 60 000 false stars, corresponding to a proportion of 2 per cent of the entries of the Tycho Input Catalogue. The number of false stars was crudely estimated, assuming that it corresponds to the number of stars more than 2 arcsec from the positions in the Tycho Input Catalogue. The thresholds were determined in order to get, for each process, about 2 per cent false stars among the entries of the Tycho Input Catalogue having the same number of predicted group crossings. The total number of stars having weights above the thresholds finally adopted was 1 166 500.

This amount was further reduced by applying a final criterium: the maximum number of stars found in the same map was 21, but it was not considered realistic that so many stars could be correctly found within a 40 arcsec diameter area; therefore only the 8 brightest stars were kept. This resulted in a final file of 1 163 399 stars, among which 26 356 stars were still redundancies. When these are not counted, 1 078 889 close companions remained. 61 973 of them were between 2 and 6 arcsec from the positions in the Tycho Input Catalogue. The number of wide companions was 58 154. These numbers are both reasonably close to the target of 60 000 'false stars' introduced in the preceding paragraph. The distribution of the close companion stars as a function of their distances to the positions in the Tycho Input Catalogue is presented in Figure 5.3. The stars having the most accurate positions in the Tycho Input Catalogue are the astrometric standards. The uncertainty of their positions is 0.14 arcsec on average,

and the distance from the stars actually found is on average 0.16 arcsec. This similarity indicates a very good accuracy for the revised positions. A comparison with the positions derived from Hipparcos provided an average offset of 0.07 arcsec for the Hipparcos stars (which are brighter on average, and thus measured more precisely than a ‘typical’ Tycho star).

The final Tycho Catalogue contains 6920 stars that were found by the search for companion stars at more than 3 arcsec away from any entry of the Tycho Input Catalogue. This number looks small when compared to the whole catalogue, but the importance of the companion processes appears when the double stars are considered: about 20% of the Tycho double stars with separations closer than 20 arcsec have at least one component among the 6920 stars above. Moreover, the entries of the Input Catalogue that were split into two close companion stars are not counted in this statistic. In fact, half of the Tycho Catalogue double stars closer than 10 arcsec and with unbiased ( $B_T$ ,  $V_T$ ) magnitudes have a component that was added in the companion processes.

---

### 5.5. The Search for Serendipity Stars

---

The vast majority of detections in the transit summary file were not related to companion stars. While the detections with small signal-to-noise ratios were generally not due to stars, but to noise or to artefacts, the bright ones could possibly be due to stars missing in the Tycho Input Catalogue. These bright detections are called ‘serendipity detections’, and they were processed to search for the ‘serendipity stars’.

#### The Network of Serendipity Points

As with the other modes, the search for the serendipity stars was based on predictions of group crossings of positions in an input catalogue, and on detections in the photon counts around the predicted epochs. The fundamental difference is that the input positions now are no longer positions of stars, but positions arbitrarily chosen, hereafter called ‘serendipity points’. These points were used as the centers of big square maps of detection lines that cover the whole celestial sphere. Since the vertical slit group of the star mapper is 40 arcmin long, it was decided to use maps with 40 arcmin sides. To make sure that no stars be lost at the boundaries, the 40-arcmin maps were chosen to have overlaps of at least 6 arcsec. The serendipity points were arranged on 273 parallel circles on the sphere, the median one being the equator. The total number of serendipity points was 94 575.

#### The Predictions in the Serendipity Process

The updating and selection process of the predictions, described in Section 5.3, provided 4.6 million predictions of transits of the serendipity points. Contrary to the search for companion stars, these predictions were not sufficient for collecting all the star detections in the 40-arcmin maps: the maps were now as large as the star mapper slits, but the predictions referred only to their centers; a star somewhere in a map could yet have been detected when the slit group was scanning a strip that did not contain the center. In order to take into account the scanning of any part of the maps, additional predictions were calculated, assuming that the slits are lengthened by  $\sqrt{2} \times 20$  arcmin at each extremity.

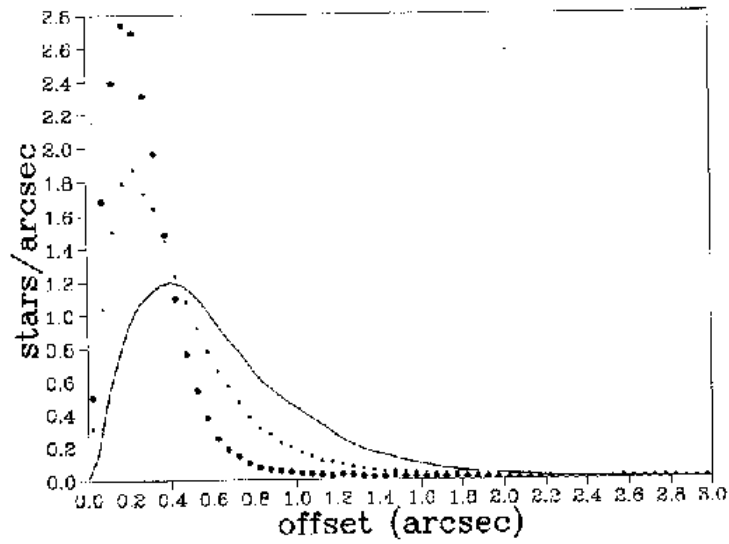


**Figure 5.3.** Frequency of the accepted stars as a function of distance to the Tycho Input Catalogue positions. The large dots refer to the astrometric standard stars in the Tycho Input Catalogue, the small dots refer to the stars of the Hipparcos programme, and the line refers to all the accepted stars. The frequencies are normalized in order to facilitate the comparison.

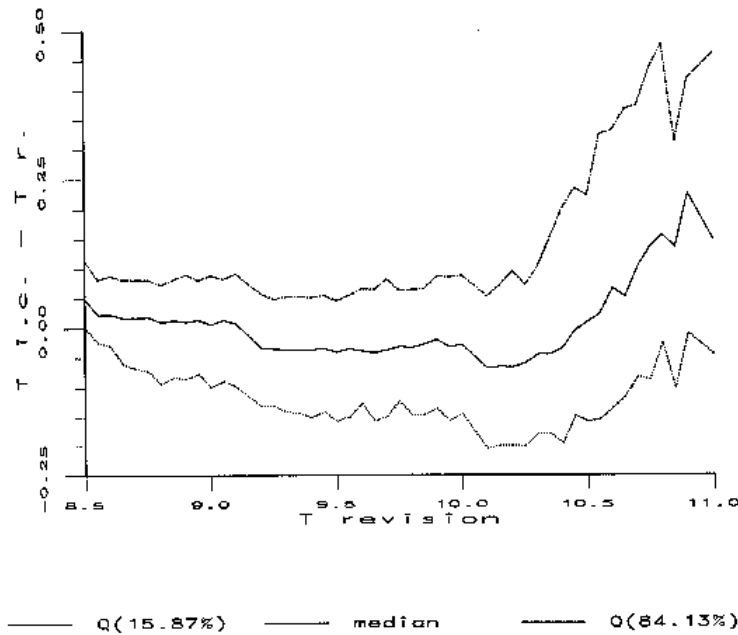


**Figure 5.4.** Relation between the  $T$  magnitudes estimated in the Tycho Input Catalogue Revision, and their offset with respect to the magnitudes in the Tycho Input Catalogue. The solid line indicates the median of the difference between the magnitudes derived from the Tycho Input Catalogue and the magnitudes obtained from the observations. The dotted line refers to the quantile 15.87 per cent, and the dots and dashes to the quantile 84.13 per cent. Only the photometric standards with known  $B$  and  $V$  are considered.

This computation was done by interpolating the predictions for the centers of the maps as long as the rotation of the satellite was not affected by jet firings. Whenever a jet firing occurred between two original predictions, the computation was an extrapolation from the unaffected side. The result was then less accurate, but this concerned only 3 per cent of the additional predictions.

The additional predictions were slightly less accurate than the original ones: for 5.8 million predictions derived by interpolation, the standard deviation is about 1.2 arcsec instead of 0.2 arcsec. The computation of the additional predictions was carried out at the Centre de Données astronomiques de Strasbourg. The final number of predictions was 10.6 million.

### **The Serendipity Transits**

The 'serendipity transits' were extracted from the transit summary file, and related to the predictions for the serendipity points, calculated above. Only detections with signal-to-noise ratios larger than 3.5 were taken into account. Moreover, detections closer than 3 arcsec to the entries of the Tycho Input Catalogue were discarded, since they were probably due to the stars already found with the close companion process. The remaining serendipity detections (9.4 million) were then assigned to the 10.6 million predictions. Each assignment was accepted only when no jet firing modified the rotation velocity of the satellite between the detection and the prediction. Each detection was related to several predictions, since it might have come from the preceding as well as from the following field of view, from the chevron as well as from the vertical slit group, and since the slit groups were usually crossing more than one digital map at a time. For these various reasons, the final file of serendipity transits contained 94.1 million records, i.e. ten times the number of detections. These records were sorted in order to gather the transits of each serendipity point.

### **The Mapping Process in the Search for Serendipity Stars**

Since the size of the digital maps in the serendipity process was much larger than in the search for companion stars, the preliminary positions of the stars were derived in two steps:

- the 40-arcmin map was digitized in  $50 \times 50$  square pixels of 48 arcsec size. For each transit, the position of the related slit group was recorded on the map. The calculation was different from the case of the companion stars, since the detections were no more represented by a single line crossing the whole map; the extremities now had to be taken into account, as well as the shape of the chevron slit group. The detections received a weight equal to the square of the signal-to-noise ratio, as in the search for companion stars. The value of the weight was limited to 36. The map was used for a rough localisation of a possible star, with the method of the grid points already described in Section 5.4;
- the selected grid point was used as the centre of a second  $50 \times 50$  pixels map, but now with a pixel size of 2 arcsec. This map corresponds to the four pixels of the first map that were around the selected grid point. The detection lines were recorded in the second map, and the position of the star was searched again.

The preliminary position derived in this way was used as input for an iterative least-squares calculation based on the detection lines of the second map. This calculation

was similar to that of the positions of companion stars, with some adaptations, since the uncertainty of the transits was a bit larger still. The weight of each line was again multiplied by a term depending on the orthogonal distance from the input position, but this distance was now reckoned in units of 2.3 arcsec. The total weights of the stars were derived from the lines closer than 1.15 arcsec to the derived positions (the limit was 0.5 arcsec for the companion stars). When a star was found, the detections closer than 3.45 arcsec were discarded (instead of 1 arcsec in the companion processing).

The preliminary selection threshold for the serendipity stars was quite underestimated, since somewhat more than half a million stars were found. It was obvious that the large majority of these objects could not be stars missing in the Tycho Input Catalogue, but were only false alarms.

### Final Stages of the Search for Serendipity Stars

As for the classes of companion stars, the number of serendipity stars to be selected was arbitrarily fixed to 60 000, i.e. 0.63 star per serendipity point. Again, the minimum weight of the stars to be selected was a function of the number of predicted group crossings, in order to obtain a constant rate. The redundant stars in the overlapping parts of the maps were removed assuming a redundancy threshold of 2 arcsec. The serendipity stars closer than this limit to companion stars were also considered as redundancies and were discarded.

The final file of serendipity stars contained 57 933 stars. In the end, only 162 of these were later found to be true stars which were retained in the Tycho Catalogue, see Chapters 10 and 11. This small number is in no way to be regarded as a failure of the serendipity recognition but, on the contrary, as indicative of a highly successful Tycho Input Catalogue.

---

## 5.6. Estimation of the Magnitudes of the Stars

---

The last step in the recognition of stars was the evaluation of the magnitudes of the stars from a rough photometric reduction. Each time a star was found, the related detections were used to derive the average amplitude of the photon counts. Since the photon counts used in the process were the sum of those obtained through the  $B_T$  and the  $V_T$  filters, the resulting magnitude, called  $T$ , refers to a combination of  $B_T$  and  $V_T$ . The transformation of the averaged amplitudes to  $T$  magnitudes was calibrated using the photometric standard stars in the Tycho Input Catalogue.

### Calibration of the Magnitudes using Standard Stars

The Tycho Input Catalogue does not provide the  $T$  magnitudes of standard stars, but only  $B$  and  $V$  magnitudes. These magnitudes are even different from  $B_T$  and  $V_T$ , but this difference is neglected here.  $T$  was defined such that  $T = B_T = V_T$  when  $B_T - V_T = 0$ . The  $T$  magnitudes of standard stars were thus derived applying this constraint and using star mapper count rates estimated before launch:

$$T = V - 2.5 \log(0.74 + 10^{-0.4(B_T - V_T)}) + 0.6 \quad [5.3]$$

(This formula is practically equivalent to  $T = (B_T + V_T)/2$ , if the colour index  $B_T - V_T$  is not extreme, but the mathematical mean of two magnitudes is in fact meaningless.)

The relation between the average amplitudes of the detections and  $T$  was derived from the above-defined  $T$  magnitudes of the standard stars. Stars brighter than 8.5 mag were not taken into account, since the available amplitudes were truncated. For the others, a least-squares calculation gave the relation:

$$T = 12.30 - 2.65 \log \langle S \rangle \quad [5.4]$$

where  $\langle S \rangle$  is the average amplitude of the star (in Tycho-internal units). This calibration is rather rough, but it was sufficiently accurate for the purpose of the Tycho Input Catalogue Revision. It appears in Figure 5.4 that, for stars brighter than 10.2 mag, the true relation is perfectly linear with the slope  $-2.5$ . This confirms that the amplitudes are proportional to the fluxes. The estimation of magnitudes fainter than 10.2 leads to underestimations: faint stars are not detected at every predicted group crossing, and the missing detections are not taken into account in the calculation. The 11 mag stars therefore appear about 0.2 mag brighter than they are.

### Calculation of the Magnitudes of Bright Close Companion Stars

The calibration, Equation 5.4, was used to compute the magnitudes of the stars. However, due to the truncation of amplitudes, no magnitude brighter than 8.5 could reliably be derived. Whenever a magnitude brighter than 8.5 was found for a close companion, it was investigated whether it might be preferable to keep an estimation of the magnitude derived from  $B$  and  $V$  in the Tycho Input Catalogue. In these cases an alternative magnitude was derived from Equation 5.3 (when only one of the magnitudes  $B$  and  $V$  was available, the color index  $B - V = 0.7$  was assumed) and compared to that derived from the calibration, Equation 5.4. The brightest was kept in the Tycho Input Catalogue Revision.

### Distribution of the Magnitudes

The cumulative frequencies of the stars found with the different processes are shown in Figure 5.5. In a logarithmic plot a straight line would be expected for the distribution when the sample is complete. It appears that the limits of completeness are about 10.7, 10.6 and 10.2 mag for the searches of close companion, wide companion and serendipity stars respectively (the differences reflect the different thresholds in detection, since the wide companions and the serendipity stars are generally not stars but false alarms).

The Tycho Input Catalogue contains about 590 000 stars brighter than 10.725 mag, among which 44 786 have no companion star closer than 3 arcsec. Some of these stars probably have erroneous positions in the input catalogue, others are probably variable stars, but still others could have been missed due to inhomogeneities in the observations: some stars got only very few predicted group crossings, or have observations disturbed by spikes or high background. For these reasons, the 44 786 entries not found, but brighter than 10.725 mag were kept in the selection and included into the Tycho Input Catalogue Revision.

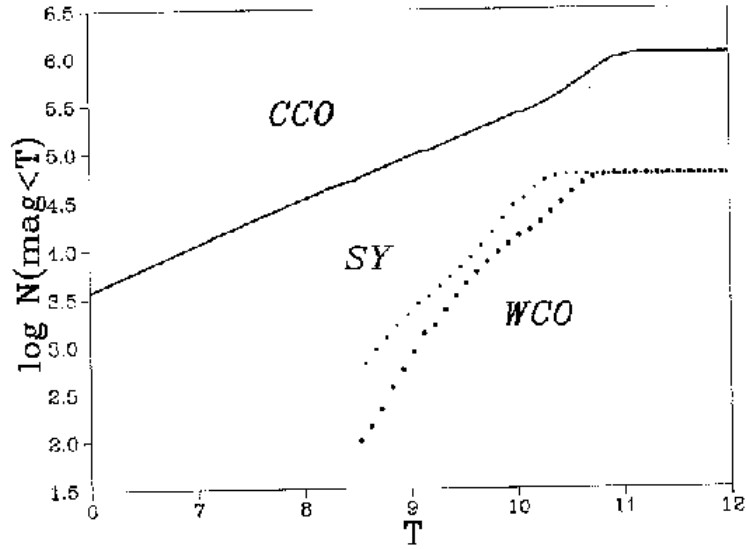


**Figure 5.5.** The cumulative distribution of  $T$  magnitudes of the non-redundant stars. The upper line is the distribution for the close companion stars. The large dots refer to the wide companion stars, and the small dots to the serendipity stars.

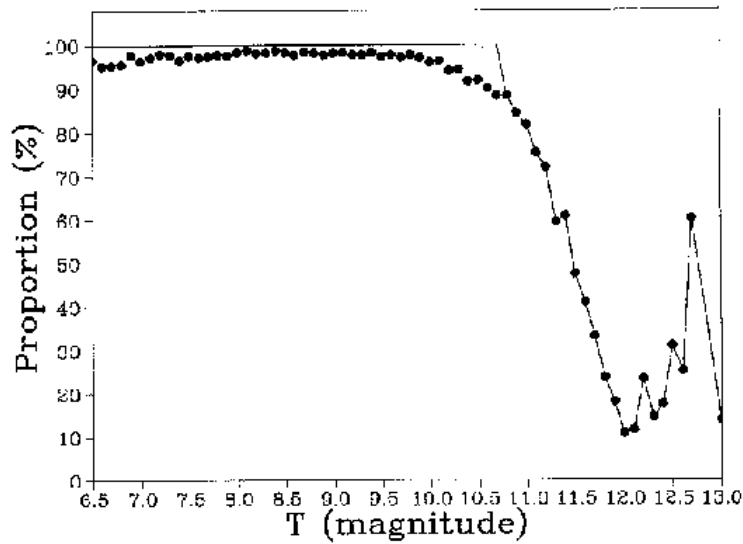


**Figure 5.6.** Proportion of Tycho Input Catalogue entries found with the close companion process, versus the  $T$  magnitude. Only stars with accurate data in the Tycho Input Catalogue are considered. The dots give the success rate of the process proper; the line refers to the proportion of stars finally selected for the Tycho Input Catalogue Revision (the stars brighter than 10.725 mag in the Tycho Input Catalogue were kept even when they were not found in the process).

---

## 5.7. Properties of the Tycho Input Catalogue Revision

---

### Content of Tycho Input Catalogue Revision

The Tycho Input Catalogue Revision finally contains:

- 1 078 889 non-redundant stars found by the search for close companions. Among these stars, 1 016 916 are closer than 2 arcsec to positions given in the Tycho Input Catalogue, and are very probably true stars;
- 58 154 non-redundant stars found by the search for wide companions. An undetermined proportion of these are in fact false stars, generated by background detections (actually, this proportion was subsequently determined by the final steps of the Tycho data reductions described in Chapters 7 and 11);
- 26 356 redundancies, due to overlapping between maps centered on closely neighbouring Input Catalogue entries;
- 57 933 serendipity stars, with a large proportion of false stars among them;
- 44 786 entries of the Tycho Input Catalogue, corresponding to stars brighter than 10.725 mag that were not found in the search for close companions.

The total number of entries is 1 266 118, including 178 060 candidate new stars. The efficiency of the search for new stars is investigated hereafter, based on our knowledge shortly after the recognition process had been carried out. The final stellar content of the Tycho catalogue will be discussed in Chapters 17 and 19.

### Efficiency of the Close Companion Process

The efficiency of the search for close companion stars was investigated on the basis of the stars having the most accurate data in the Tycho Input Catalogue: stars from the INCA Data Base that are not members of binary systems, and for which the  $B$  and  $V$  magnitudes are known. The proportion of entries for which a companion star was found closer than 2 arcsec is given in Figure 5.6. This proportion is close to 100 per cent for stars brighter than 10 mag, and still larger than 90 per cent for stars brighter than 10.725 mag.

### Efficiency of the Wide Companion Process

Although the wide companion process produced a lot of entries that must be assumed to be false alarms but not stars, it had to be verified that the stars actually missing in the Tycho Input Catalogue were effectively found. The efficiency of the process could be estimated thanks to a bug in the operational version of the Tycho Input Catalogue: some stars having large proper motions received positions corresponding to an erroneous epoch (this bug is corrected in the published version). The efficiency of the wide companion process was estimated from the stars for which the positions at the epoch of the observations were between 6 and 20 arcsec from the positions used for the search. It is assumed that a star was correctly found when a companion star is less than

3 arcsec from the correct position. Results are given in Table 5.1. This statistic refers to stars with proper motions between 0.4 and 2.9 arcsec/year, that are not easily found since their transits are scattered. It is an underestimation of the efficiency of the search for the missing stars with the wide companion process.

### **Efficiency of the Serendipity Process**

The case of the search for serendipity stars was investigated with the same method as for the wide companions. 47 stars have proper motions so large that their actual positions would be more than 20 arcsec away from their positions in the operational version of the Tycho Input Catalogue. 28 serendipity stars were found closer than 3 arcsec from these 47 actual positions. Results are given in Table 5.2. As for the wide companions, they give an underestimation of the efficiency of the process, since these stars have proper motions larger than 1.3 arcsec/year and their transits are scattered.

### **The Search for Secondary Components with the Companion Processes**

The companion processes were dedicated to the search for stars missing in the Tycho Input Catalogue which are close to a brighter star that is included. For evaluating how well this goal was achieved, the double stars of the INCA Data Base were considered. The pairs with secondary components fainter than 10.5 mag were discarded from the statistic, since such stars were incompletely found even when they are single. The proportion of secondary stars for which a companion star was found closer than 3 arcsec is given in Table 5.3.

The small proportion of secondary components that were found when the separations are closer than 3 arcsec comes essentially from the limit in detection. In this process, two stars could be separated with certainty only when the projection of the position difference along the scanning direction was larger than 2 arcsec. Since several detection lines with different directions are necessary for a successful recognition, the effective limit for separating two stars is  $\sqrt{2} \times 2 = 2.8$  arcsec. Some pairs closer than this limit were separated however, since stars as close as 1.2 arcsec were sometimes separated by detection. On the other hand, things are worse when the scattering of the predicted group crossings is large. Under these conditions, the detection lines of two close components, when they are reported on a digital map, do not reveal two stars but only a large patch roughly corresponding to the photocentre of the system.

When the separation is large, the search for the secondary star is even less efficient than the search for a single star. This is due to the detection threshold of the wide companion process, but also to another reason: bright primary components generate side lobe transits with distances equal to harmonics of the basic step of the slit groups, which is 5.625 arcsec (see Figure 5.1). The intersections of these side lobe lines with the detection lines of the secondary components sometimes generate a false star that looks brighter than the secondary. When such a false star is found and accepted by the reduction algorithm, the neighbouring detection lines are discarded, including those coming from the true star. The remaining detection lines may then be too few to permit the selection of the secondary star. For these reasons, an off-line treatment of double stars was added to the Tycho data reduction scheme. This process is described in Chapter 14.

**Table 5.1.** The stars with erroneous positions in the operational version of the Tycho Input Catalogue (the so-called ‘TIC stars’ here) which were found with the wide companion process.

T magnitudes	<10.5	10.5–11.0	11.0–12.0	>12.0
TIC stars	134	21	60	13
Companions	111	9	10	0
Proportions (per cent)	83	43	17	0

**Table 5.2.** The stars with erroneous positions in the operational version of the Tycho Input Catalogue (the so-called ‘TIC stars’ here) which were found with the serendipity process.

T magnitudes	<8.5	8.5–10.5	>10.5
TIC stars	22	8	17
Serendipity Stars	16	3	0
Proportions (per cent)	73	37	0

**Table 5.3.** The double stars of the INCA Data Base for which the secondary components were found. Only pairs with components brighter than  $T=10.5$  mag are considered.

Separations	<3''	3–6''	6–12''	12–20''
INCA double stars	306	799	868	630
Secondary components found	64	549	621	490
Proportions (per cent)	21	69	72	78

**Conclusions**

The Tycho Input Catalogue Revision contains all the stars of the Tycho Input Catalogue down to a magnitude of  $T=10.7$  mag. Any stars brighter than this limit and missing in the Tycho Input Catalogue, but located close to an Input Catalogue entry, were found with a very good efficiency by the companion processes. The serendipity process, in addition, found a significant proportion of such stars even if they were far from any Input Catalogue position. The typical precision of the positions in the Tycho Input Catalogue Revision is about 0.15 arcsec, as shown in Figure 5.3.

J.-L. Halbwachs

## 6. UPDATING AND IDENTIFICATION OF TRANSIT DATA

*The present chapter describes the prediction updating processes (Sections 6.1 and 6.2), and how their output was used to improve the identification of observed peaks in the photon counts with the transits of specific stars (Section 6.3). The role of these processes, and of transit identification, is to replace some or all of the imprecise inputs used in first prediction and transit detection (namely the Tycho Input Catalogue, the on-board satellite attitude and preliminary instrument geometry calibrations) by better data.*

---

### 6.1. Prediction Updating-2

---

The second prediction step in the iterative Tycho data reduction scheme was called prediction updating-2. Its main role was to replace the imprecise on-board satellite attitude by an improved on-ground attitude for the purposes of the star recognition process (i.e. the Tycho Input Catalogue Revision) described in Chapter 5. The central problem of that process was to distinguish true stars from chance crossings of detection lines in its digital line maps. The ability to solve this problem crucially depended on the scatter of the transit lines about the true position of a star—and this scatter could not possibly be smaller than the uncertainty of the satellite attitude. Without prediction updating, the recognition process could not have used line map pixels as small as 0.5 arcsec. Instead it would have had to use pixels of about 3 arcsec. This would have created a 36 times higher rate of background detection line crossings per pixel, which in turn would have buried the true line crossings of all the fainter Tycho stars.

The basic task of prediction updating was much the same as that of the first prediction process, which was to provide a time-ordered list of expected group crossings of celestial objects, along with some auxiliary data. Despite this basic similarity, the actual process was completely different, and very much quicker. The first prediction process was controlled by the availability of on-board attitude and certain satellite status indicators. The most complex and time-consuming parts of the software were the selection of candidate stars for group crossings and the computation of satellitocentric apparent positions for these. Both could be avoided in prediction updating. This was made possible by a careful design of the Predicted Group Crossing (PGC) data stream.

## Basic Algorithm

The prediction updating process was controlled by the Predicted Group Crossing (PGC) data stream, i.e. the output of the first prediction process. The original PGC tapes were sent from Heidelberg to Tübingen to be used in the detection process. Copies of them were also kept at Heidelberg to be used in prediction updating. They were processed in strict time sequence, with one predicted group crossing being treated at a time. The basic algorithm consisted of the following actions:

- read one predicted group crossing from the PGC data stream;
- check whether on-ground attitude is available for the appropriate instant of time;
- if so, use the apparent position of the object under consideration (which is included in the input PGC record), and the on-ground attitude to directly compute a new transit time. This is done exactly as in prediction, by linear interpolation between neighbouring pivotal points of the attitude (see Section 4.1);
- recompute some of the auxiliary data and flags (such as the instantaneous scan speed, the field coordinates at transit time, jet firings of the attitude control system etc.);
- compute the mean error of the updated transit time from the mean errors of the on-ground attitude alone (i.e. disregarding the uncertainty of the star position);
- create the output record for the PGC Updating-2 data stream and write it to tape.

No real updating could be done if no on-ground attitude was available for a particular predicted group crossing. But still a record was written to the PGC Updating-2 data stream in that case. It was flagged as non-updated, and furthermore marked by a large dummy value (corresponding to 1 arcsec on the sky) of the transit time mean error.

Note that this basic algorithm implied a number of approximations, all of which however, had negligible effects on the quality of its output. First, the apparent positions were not recomputed. This was possible because the original and updated predicted transit times differed by at most a few times 0.01 s, and because the apparent positions change only slowly (the biggest effect being the change of aberration due to the satellite's geocentric acceleration, at most  $1 \text{ mas s}^{-1}$ ). Second, the search for transiting stars was not repeated. Due to the change in attitude it might have happened that a star had just missed the ends of the star mapper slits in the original prediction process, but now caused a transit (or vice versa). This possibility was avoided by using a star mapper model with slits that were somewhat longer than the real ones, both in first prediction and in prediction updating. Thus, no transits could be lost. Spurious transits produced in this way were easily recognized by their  $z$  coordinate being outside the actual slit boundaries after updating. Third, the originally predicted transit time might have fallen into the time interval between two pivotal points of the on-ground attitude, but slightly outside that interval after updating. In such cases the updating was performed as usual, which implied a very small extrapolation of the attitude (instead of the usual interpolation).

## Input Attitude for Prediction Updating-2

The Tycho consortium was ready to use on-ground attitude from either NDAC or FAST, depending on availability. In practice, on-ground attitude from NDAC was

available sooner (the first few months of attitude with sufficient precision of 0.2 arcsec were delivered by NDAC in December 1991). Thus, this was used for updating-2.

As explained in Section 4.1, it is important that an instrument geometry model consistent with the attitude determination is used in any computation of Tycho group crossings. This was automatically ensured by the presence of a special NDAC star mapper geometry file on each of the attitude tapes.

### **Output Data**

The output of updating-2 consisted mainly of the PGC Updating-2 data stream, indicated in Figure 1.2, plus some protocol and log files. The output tapes were sent to Strasbourg, where they were used for the production of the Tycho Input Catalogue Revision, as described in Chapter 5.

### **Actual Processing**

A series of test runs for prediction updating-2 was performed during 1991, using provisional on-ground attitude from both NDAC and FAST. This resulted in the discovery and removal of software errors, and also provided the opportunity to monitor the gradual progress in the quality of the on-ground attitude. The final production runs for prediction updating-2 were started on 21 February 1992, and completed 7 weeks later.

---

## **6.2. Prediction Updating-3**

---

The role of prediction updating-3 was to replace both the originally used attitude and the star catalogue used for the first prediction. There were two reasons for using the Tycho Input Catalogue Revision instead of the Tycho Input Catalogue for a prediction updating. First, the number of stars was greatly reduced, from 3.15 million to 1.26 million. Second, the mean errors of the star positions were greatly reduced. Both of these differences resulted in a better agreement between predicted and actually observed transit times of stars, which was needed to improve the elimination of unrelated background transits and photon noise peaks in the final astrometry and photometry tasks.

### **Direct-Access Tycho Input Catalogue Revision Installation**

While prediction updating-2 needed no star catalogue access at all, updating-3 needed an efficient access to the Tycho Input Catalogue Revision. The organisation and indexing of the Tycho Input Catalogue into a direct-access magnetic-disk file according to small regions on the sky was described in Chapter 4. That organisation was optimized for the needs of first prediction processing. To make it usable for prediction updating-3, the sequential record numbers of the Tycho Input Catalogue objects in that direct-access file were also included in the Predicted Group Crossing records. The Tycho Input Catalogue Revision itself was brought into the same sequence (with dummy records filling the 2 million gaps produced by the 'unrecognized' Tycho Input Catalogue stars). The resultant direct-access Tycho Input Catalogue Revision records did not include the improved positions for the Tycho Input Catalogue Revision objects, but the differences

between the Tycho Input Catalogue Revision and Tycho Input Catalogue positions, represented by three-dimensional cartesian difference vectors. The dummy records were marked by a flag.

This organisation allowed the PGC-controlled retrieval of the Tycho Input Catalogue Revision data with a single magnetic-disk access, but only for those Tycho Input Catalogue entries having zero or one corresponding entry ('companion') in the Tycho Input Catalogue Revision. Those Tycho Input Catalogue entries yielding more than one companion in the star recognition process (Chapter 5) were managed in the following way. In the Tycho Input Catalogue Revision, the different companions to a particular Tycho Input Catalogue entry were distinguished by a running 'companion number'. The ordered direct-access Tycho Input Catalogue Revision record described in the preceding paragraph was occupied by the companion with the highest companion number. A pointer at the end of the record contained the physical record number where the companion with the next-lower number could be found, and so on, until the companion with the companion number 1 was reached. The extra records for the additional companions were simply added at the end of the direct-access Tycho Input Catalogue Revision file.

In this way the PGC-controlled retrieval of the Tycho Input Catalogue Revision data with a single magnetic-disk access per object was achieved even in the case of multiple companions, as explained below.

### **Basic Algorithm**

The basic algorithm of prediction updating-3 was similar to that of prediction updating-2, with a few additional actions caused by the change of the star list from the Tycho Input Catalogue to the Tycho Input Catalogue Revision. Again the selection of candidate stars for group crossings and the computation of satellitocentric apparent positions were avoided by the design of the input PGC data stream and the above-described special installation of the Tycho Input Catalogue Revision. The individual steps were as follows:

- read one predicted group crossing from the PGC data stream;
- check whether on-ground attitude is available for the appropriate instant of time;
- if so, use the direct-access record number (from the PGC record) to read Tycho Input Catalogue Revision data. Check whether a dummy Tycho Input Catalogue Revision record was found;
- if not, use the apparent position of the Tycho Input Catalogue object under consideration (from the PGC record), add the position difference (from the Tycho Input Catalogue Revision record) and directly compute a new transit time from the on-ground attitude, as in prediction updating-2;
- recompute some of the auxiliary data and flags (such as the instantaneous scan speed, the field coordinates at transit time, jet firings of the attitude control system etc.);
- compute the mean error of the updated transit time from the mean errors of the on-ground attitude alone (i.e. disregarding the uncertainty of the star position);
- create the output record for the PGC Updating-3 data stream, including flags and magnitudes from the Tycho Input Catalogue Revision, and write it to tape;

- if the component number under consideration is larger than 1, get the Tycho Input Catalogue Revision data for the next-lower component number, and repeat the preceding four steps.

This algorithm implies the same approximations as in prediction updating-2. In addition, there is an approximation by using the apparent position for the Tycho Input Catalogue object to get that for the Tycho Input Catalogue Revision companion(s). This is well justified, since the difference vector between a mean and an apparent position is a very slowly varying function of the location on the celestial sphere. The biggest effect is produced by the annual aberration. Its maximum possible derivative is about 0.1 mas per arcsec. So, for position updates (Tycho Input Catalogue Revision minus Tycho Input Catalogue) of a few arcsec, it is completely negligible in Tycho data reductions (larger offsets were taken care of in the Tycho reprocessing, Chapter 10).

A more important effect of this approximation is that implicitly the same proper motions and parallaxes were assumed for all companions of a Tycho Input Catalogue entry. This does not cause any problems, since the Tycho astrometric data are derived independently for all companions in the astrometry processing (Chapter 7).

### **Input Attitude for Prediction Updating-3**

An NDAC-provided on-ground attitude was used throughout the mission. The particular set of 11 attitude tapes used for the final production runs of prediction updating-3 were all based on the 18-month NDAC Hipparcos sphere solution. That is, the attitude was the orientation of the satellite with respect to the celestial coordinate system defined by that preliminary Hipparcos catalogue. The typical rms errors of the attitude angles were 35 mas perpendicular to the scan direction, and a few mas along the scan direction.

### **Output Data**

The output of updating-3 consisted mainly of the PGC Updating-3 data stream, indicated in Figure 1.2, plus some protocol and log files. While PGC Updating-2 contained an output record for every input PGC record, PGC Updating-3 was smaller by about a factor of 3, because there were no output records for the 2 million Tycho Input Catalogue entries missing in the Tycho Input Catalogue Revision. The PGC Updating-3 tapes were sent to Tübingen, where they were used for the identification of transits, as described in Section 6.3.

### **Actual Processing**

A series of test runs for prediction updating-3 was performed during 1992, using provisional on-ground attitude from both NDAC and FAST, partly with a provisional Tycho Input Catalogue Revision and partly with the operational one.

The operational attitude (described above) was delivered to Heidelberg in small portions between May 1993 and August 1994. The final production for prediction updating-3 started in July 1993, and most of it was completed in February 1994. Updating-3 was an even quicker process than updating-2, due to the much smaller number of objects to be treated. It quickly caught up with the still running prediction process, then proceeded closely following the prediction process.

### **Prediction Updating-3 Redoing**

The ‘prediction redoing’ process (see last paragraph of Section 4.1) produced a PGC data stream based on the final on-ground attitude, for the parts of the mission with bad real-time attitude. But it still used the Tycho Input Catalogue as input star catalogue. Therefore, a prediction updating step for redoing was still necessary in order to replace:

- (a) the imprecise Tycho Input Catalogue positions by the more precise Tycho Input Catalogue Revision positions; and
- (b) the object list and object numbering system of the Tycho Input Catalogue by that of the Tycho Input Catalogue Revision.

Thus, prediction updating-3 was run on the redoing PGC data stream (with slightly modified software to accommodate the changes in the data interfaces, see Section 4.1). The resulting special PGC Updating-3 tapes were also sent to Tübingen, to be used in the redoing transit identification.

---

### **6.3. Identification of Transits**

---

The role of transit identification was to connect the prediction updating-3 data stream (Section 6.2) with the raw transit data stream produced in the detection process (Section 4.3). It had to perform two major tasks: assigning actual detections to the predicted group crossings given by updating-3 (and thus to stars on the sky), and to record potential disturbances caused by nearby other transits.

#### **Assignment of Transits**

The assignment of detections to the predictions given by updating-3 was carried out using the raw transit data stream (RT in Figure 1.2). No second analysis of the photon count data was done. The output of the process consisted of the identified transits data stream (IT in Figure 1.2). Each identified transit record contained most of the combined information of the corresponding updating-3 and raw transit data. Therefore it was 25 per cent bigger than a raw transit record. The complete amount of data however produced by the identification process was only about 30 per cent of the raw transit data stream. Due to the reduced error sources of updating-3 compared to the first prediction, the width of the time interval in which detections could be assigned to a certain prediction was only half of that used in the detection process. Furthermore, all raw transits which had been assigned to Tycho Input Catalogue objects not present in the Tycho Input Catalogue Revision were discarded. In that way a much cleaner input data stream for the following astrometric and photometric processing was produced.

In order to be assigned to a specific prediction, a detection from the raw transit data stream had to fulfill two conditions: (a) it had to lie inside the assignment interval; (b) the updated prediction (PGC Updating-3) had to be the update of the original (first) prediction to which the detection had been assigned in the detection process.

The second criterion was introduced to make sure that, for example, detections which had been assigned to a Predicted Group Crossing on the inclined slit group, and thus

been treated by a specific geometric calibration parameter set in the estimation of their amplitude, would not turn into identified transits assigned to a Predicted Group Crossing Update on the vertical slit group, and vice versa. The same holds for the two fields of view and for the upper and lower slit branches.

As described in Sections 5.4 and 6.2, an original Tycho Input Catalogue object could be split into several Tycho Input Catalogue Revision companions, all carrying the original Tycho Input Catalogue identification number, distinguished only by a running companion number. In the terms of the second criterion, all companion predictions for the same Tycho Input Catalogue identification were treated as an update of the first prediction. So, a single detection could be assigned to all companion predictions if it was inside all assignment intervals.

For each identified transit an identity probability was computed, decreasing with increasing difference between predicted and actual transit time and with increasing difference between the Tycho Input Catalogue Revision magnitude and actual magnitude.

### **Parasite Recording**

The second main task for the transit identification process was the so-called parasite recording. Parasites are transits (either detections or predicted group crossings; details are given in Section 7.2) above a limiting magnitude which are close enough to a given detection to produce a significant astrometric or photometric disturbance. The basic idea of their recording is to provide, for each potentially disturbed identified transit, the sum of the disturbing amplitudes. The decision whether to use the disturbed transit in the catalogue production is postponed to the astrometry and photometry processes.

A theoretical analysis of the relative additional positional scatter introduced by parasites of different brightness to detections of different brightness had shown that this scatter depends only on the brightness of the parasites (see Section 7.2). It had also been shown that recording all parasites brighter than the limiting magnitude of 10.5 was the best compromise between discarding too many detections and neglecting too many disturbances.

Parasitic amplitudes were recorded differently in the identified transit records, depending on their time distance to the detection under consideration. For distances greater than 9 samples, these amplitudes were taken directly from the raw transit data (i.e. from actual detections of other objects). For smaller distances one has to be aware that the parasite might be disturbed as well as the detection under consideration; for very small distances there may even be only one (combined) transit. So the parasitic disturbance in an interval of 18 samples centred on the detection under consideration was determined from the prediction data alone, recalculating only the parasitic amplitude from the Tycho Input Catalogue Revision magnitude given in the PGC Updating-3 data.

### **Basic Algorithm**

The transit identification process was controlled by the PGC Updating-3 data stream. It was not possible, however, to treat the input data record by record, i.e. to read one predicted transit time, assign all appropriate raw transits, write the output data and step to the next prediction. The reason for this was that for the calculation of the parasitic amplitudes for a specific transit all detections and predictions within the

parasite recording range had to be known, including those which followed the currently considered detection. Furthermore, although the prediction updating-3 process was controlled by the strictly time-ordered PGC data stream, it did not produce strictly time-ordered predictions (due to the treatment of the different Tycho Input Catalogue Revision companions described in Section 6.2). As the position of two companions of a Tycho Input Catalogue Revision star on the sky could differ by about 40 arcsec (see Section 5.4), detections and predictions of a time interval of about 150 samples in both directions had to be considered to be sure that no potential parasite was lost. But, on the other hand, in order to keep processing time as short as possible, all input records had to be read only once.

These complex and partly conflicting requirements made the transit identification software much more complicated than its basically simple task suggests. The working principle was to read the complete input data into a number of memory arrays, the 'record arrays'. Furthermore some additional arrays were used in which each element represents a time interval of one sample. These 'sample arrays' were filled during processing with amplitude data and with pointers to the corresponding PGC Updating-3 and raw transit record array elements. Internally they were split into three parts, the central part and the lower and upper buffer. The size of these buffers was set big enough to make sure that all records which could possibly contribute parasitic influences to any transit in the central region were always available.

The data processing consisted of the following actions:

- read PGC Updating-3 data until the end of the sample array is reached;
- read raw transit data for the same time interval. By filling up the raw transit sample array, identical transits can be identified. They are created in the transit detection process when a transit is assigned to more than one prediction (see Section 4.3). If two predictions belong to, for example, different slitgroups, different geometric calibration values are used in transit parameter estimation (see Section 4.4), so transit times of identical transits may differ slightly. Two transits were regarded as identical if their transit time difference was below 1 sample;
- treat the prediction records one by one in the sequence given by the PGC Updating-3 file;
- assign all appropriate raw transits for the actual prediction;
- calculate the parasitic amplitudes for all assigned transits, using data from the sample arrays;
- calculate the identity probability for each transit assigned to the actual prediction;
- write the data to the identified transit files;
- step to the next prediction;
- if the next prediction lies in the sample array range of the upper buffer, the contents of all sample arrays is shifted down by a certain amount of elements (or samples). Generally this amount is chosen in such a way that the next prediction to be treated is transported almost to the start of the central region. Thus all earlier possible parasites remain in the lower buffer;
- continue reading of PGC Updating-3 data.

## Transit Identification Redoing

No differences existed in the two input data streams compared to the main processing. Thus the transit identification process for redoing was done exactly as for the main processing.

## Actual Processing

During 1992, test data produced by prediction updating-3 were processed. The final production started in June 1993 and was essentially completed in March 1995, after some interruptions during which the Tübingen computers were busy with the reprocessing data (Chapter 10).

The output of the transit identification process consisted of the identified transit data stream, which was sent to Copenhagen for astrometry and stored in Tübingen for photometry. A total of 260 identified transit tapes was produced, corresponding to about 32 Gigabytes of data.

---

## 6.4. Verification Methods

---

Most of what was said in Section 4.5 about the verification of first prediction and detection equally applies (*mutatis mutandis*) for prediction updating and transit identification. In particular, it is true that the two processes can only be verified in combination, and that the accuracy of predicted group crossings can be checked in full depth (i.e. at the mas level) only in the detailed astrometric analysis of the identified transit data (see Chapter 7), using close-to-final star mapper calibrations and preliminary Hipparcos output catalogues.

The present section thus only shows an illustrative example of the improvements gained by prediction updating and transit identification. More details will be shown in Chapter 7 on astrometry processing.

Figure 6.1 displays a collection of ‘cloud plots’, showing the transit time differences ‘detected minus predicted’ versus the  $z$  coordinate along the slits, as explained in Section 4.5. The two plots at the top are repeated from Figure 4.10. They show the first results of prediction and detection on a stretch of data from the start of the mission, using as input the imprecise on-board attitude, a still unsatisfactory instrument geometry and the Tycho Input Catalogue (for more details see the description of Figure 4.10). The rms width of the ‘clouds’ is about 0.9 arcsec.

The two plots in the centre show results for a similar stretch of data, but after the application of a preliminary on-ground attitude. The rms width of the ‘cloud’ for the inclined slits (left) is 0.42 arcsec, dominated by the errors of the preliminary attitude. The attitude errors relevant for the vertical slits (right) are smaller by a factor of 20. Thus, the width of the clouds at right (0.26 arcsec rms) is entirely due to the errors of the star catalogue. Here, a small subset of the Tycho Input Catalogue, containing only stars with particularly good *a priori* positions, was used (this explains the small number

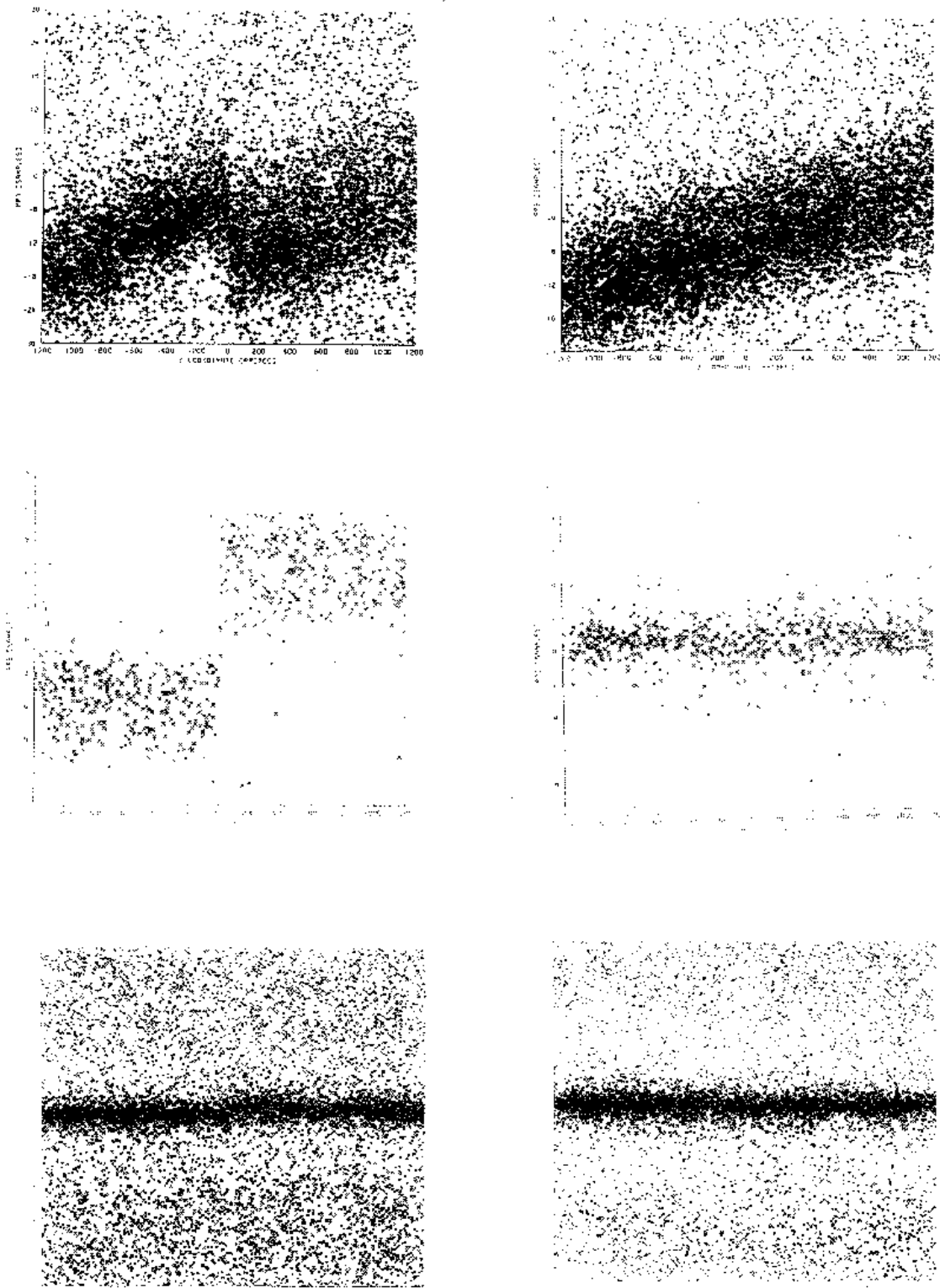


**Figure 6.1.** Sample 'cloud plots' showing the improvements gained by successive stages of prediction updating and transit identification. The height of the two plots at the top corresponds to 12 arcsec on the sky, i.e. the width of the Predicted Group Crossing intervals. The other four plots have twice the vertical scale, i.e. their height corresponds to only 6 arcsec. The horizontal axis in all six plots spans the 40 arcmin length of the star mapper slits. Details are described in the text. It is evident that the discrimination between relevant transits and background transits is much improved from top to bottom (note the enlarged vertical scale).

of points compared to the other plots). The instrument geometry has improved, but is still incorrect for the inclined slits.

The two plots at the bottom show the quality achieved by prediction updating-3 and transit identification, using as input the final on-ground attitude, a satisfactory instrument geometry, and the Tycho Input Catalogue Revision. The rms width of both clouds is 0.14 arcsec, which nicely agrees with the accuracy of the Tycho Input Catalogue Revision.

The cloud plots were produced only occasionally. Routine quality control during the mass production of transit identification was done using simple histogram plots showing the distribution of the differences between predicted and observed transit times, separately for both slit groups and fields of view. About one such plot per day of mission, covering 10 per cent of the data for that day, was checked for the occurrence of any unexpected features such as large offsets or unduly large scatter. Not a single serious alarm was raised; all (rare) cases of suspect histogram plots could be explained by disturbed data, mostly due to high radiation background.

U. Bastian, K. Wagner



## 7. ASTROMETRIC ANALYSIS OF TRANSIT DATA

*Tycho astrometric data processing is described, leading from the transit times to a geometric calibration of the slit system and to the astrometric parameters of the Tycho stars. Special quality parameters were derived for the astrometric solution of each star, in addition to the conventional internal standard errors.*

---

### 7.1. Theoretical Basis of the Astrometric Reduction

---

#### **Input Data**

The purpose of the reductions in Tycho astrometry processing is to determine the five astrometric parameters (i.e. the position and proper motion components and the parallax) for each Tycho star for which a sufficient number of observations (the ‘identified transits’, see Section 7.2 or Chapter 6) have been collected. This work combines the following information:

- (i) transit times, i.e. the observed instants at which the stars cross one of the fiducial reference lines on the focal surface of the telescope (the output of the ‘detection’ processing, described in Chapters 2 and 4);
- (ii) attitude data, describing the celestial pointing of the satellite, i.e. the coordinates of the viewing directions, as a function of time (as determined by the main mission data processing, Volume 3, Chapter 7). The attitude was supplied by NDAC, and included in the predicted transit times, as described in Chapter 6;
- (iii) star mapper calibration data, which describe the geometry of the fiducial reference lines on the grid with respect to the viewing directions, assembled from laboratory measurements of the grid and further corrections derived in the course of the astrometry task itself. These corrections were related to the transit times, the attitude and the grid in such a way that the Tycho reference system of positions was tied directly to the Hipparcos reference frame, as explained below;
- (iv) the Tycho Input Catalogue (TIC) of 3 million stars derived from ground-based catalogues;
- (v) the Hipparcos catalogue of positions, proper motions and parallaxes.

Broadly speaking, each identified transit observation defined a position line for the star, namely the projection onto the celestial sphere of the fiducial line (the centre line of the four slits) at the time of the star’s transit. This projection could be calculated from the

attitude and the grid calibration data. The intersection of several such position lines provided the astrometric position of the star, and its variation with time allowed the determination of the proper motion and parallax. In practice, a least-squares solution was made for the astrometric parameters, using linearized coordinates within a small field around the expected position. This expected position was taken from the Tycho Input Catalogue of 3 million stars (Chapter 3) in a first stage of data reduction, and from the Tycho Input Catalogue Revision of one million stars (Chapter 5) in the final processing.

It is worth noting that in principle the Tycho data reduction could have been started without an input catalogue of positions of real stars; a uniform net of about 200 000 starting positions per square degree could have been used. But the use of the much smaller Tycho Input Catalogue has greatly facilitated the data reduction. The resulting limiting magnitude in the final catalogue is fainter: without any input catalogue the acceptance limit for the signal-to-noise ratio of transits and of stars would have to be higher lest the false transits and false stars be too numerous. A ‘false star’ would be the result of a purely random concentration of position lines at a point on the sky.

### Star Mapper Geometry

The star mapper grid consisted of eight slits arranged in two groups: the vertical group ( $g = 1$ ) and the chevron or inclined group ( $g = 2$ ). The field coordinates ( $w, z$ ) represent direction cosines with respect to the orthogonal axes  $\mathbf{w}$  and  $\mathbf{z}$  as defined in Figure 1.1. For the present task the individual slits are not of particular relevance, but only the ‘fiducial line’ of each group. This line can be thought of as the centre of gravity of the four slits in a group, taken along the scanning (or  $w$ ) direction. The fiducial lines are defined, in field coordinates, by means of the equation:

$$w = w_{fg}^*(z) + \Delta w_g(z) \quad (f = \pm 1, \quad g = 1, 2) \quad [7.1]$$

where  $f = +1$  is the index for the preceding field of view of satellite rotation, and  $f = -1$  for the following field on the sky.  $\Delta w_g(z)$  is the tabulated ‘medium-scale irregularity’ derived at first from laboratory measurements of the grid. The functions  $w_{fg}^*(z)$  and corrections to the medium-scale irregularities were obtained from grid calibration by means of in-orbit observations (Section 7.3). The following representation was used:

$$w_{f1}^*(z) = (h + h_{11}z) f + w_{10} + w_{11}z \quad [7.2a]$$

$$w_{f2}^*(z) = (h + h_{21}^+z) f + w_{20} + w_{21}^+z + h_f \quad \text{if } z > 0 \quad [7.2b]$$

$$= (h + h_{21}^-z) f + w_{20} + w_{21}^-z - h_f \quad \text{if } z < 0 \quad [7.2c]$$

with Equation 7.2(a) valid for the vertical slit group, Equation 7.2(b) for the upper branch of the chevron group and Equation 7.2(c) for the lower. Apart from the terms  $\pm h_f$ , which are explained below, this representation is very similar to the one used for the attitude determination by the NDAC Consortium (Lindgren *et al.* 1992, and Volume 3, Chapter 10). Nominally, the star mapper slits are straight lines in the ( $w, z$ ) plane, with the two branches of the chevron meeting exactly at  $z = 0$ . For the preceding star mapper grid, the one shown in Figure 1.1, the nominal values of the 11 geometric parameters are:  $h, h_{11}, h_{21}^+, h_{21}^-, h_{-1}, h_{+1}, w_{11} = 0, w_{21}^+ = -1, w_{21}^- = +1, w_{10} \simeq 0.00938$  and  $w_{20} \simeq 0.01545$ ; all signs are reversed for the (redundant) star mapper on the opposite side of the main grid (the following star mapper grid), which was however never used.

The parameter  $h$  accounts for any deviation of the actual basic angle between the two fields of view on the sky from the adopted constant value  $\gamma$ , which is  $58^\circ$ . The terms  $h_{-1}$  (for the following field) and  $h_{+1}$  (preceding field) correspond to small shifts, in the  $z$  direction, of the image centroids as defined by the transit times. As mentioned above, these shifts are by definition zero in the attitude determination process. In Tycho astrometry, however, a slightly different centroid definition had to be expected due to the use of different algorithms, resulting in non-zero shifts, by a fraction of an arcsec. A similar shift in the  $w$  direction was absorbed by the parameters  $w_{10}$  and  $w_{20}$ .

The parameters  $w_{gk}$  in Equation 7.2 represent zero-points and inclinations of different parts of the slits, and the calibration gives corrections to the parameter values used in predicting the group crossing times. Only zero and first order calibration parameters were used. Second and higher order terms, representing curvature, were assumed constant over the mission and as such absorbed in a table of ‘medium scale irregularities’, discussed in Section 7.3.

A set of calibration parameters was derived from an observation period of about 24 hours, usually defined by the length of observation time contained on one tape delivered by ESOC. These parameters, suitably interpolated by splines, were used to correct the observed transit times when astrometric parameters of the stars were subsequently derived. The calibration parameters were constant over much longer stretches of time (except for e.g.  $w_{10}$  at times of refocussing), but it was decided that practically nothing could be gained by smoothing over greater lengths of time than a few days (see Section 7.3).

In the actual Tycho astrometric processing the calibration parameters were always determined as small corrections to the corresponding parameters used in the NDAC star mapper processing, since the NDAC parameters were used in the prediction updating processing (Chapter 6) together with the NDAC attitude.

### Observation Equations

The observation equations are given here, with their mathematical relation to the star mapper geometry and the astrometric parameters. The relation to the satellite attitude and to the celestial coordinates of the stars is described in Chapter 4 of this volume and in Section 1.2 of Volume 1.

All calculations of celestial directions were made in a single, well-defined coordinate system which coincided to better than 0.1 arcsec with the final system in which the Tycho Catalogue is published (the Hipparcos reference frame, which is the optical representation of the International Celestial Reference System, ICRS). At the end of the Tycho reductions all positions and proper motions were transformed, by a rigid rotation of the coordinate axes, to conform as closely as possible with the Hipparcos reference frame. Since the observations were completely decoupled from the rotation of the Earth, the effects of precession and nutation did not appear in any of the data reduction calculations.

Consider now the computation of the astrometric parameters. Let  $(w, z)$  be the field coordinates and  $f$  as defined above for an object observed at instant  $\tau$ . The object’s distance from the fiducial line of slit group  $g$  is defined as:

$$u(\tau) = w(\tau) - (w_{fg}^*(z) + \Delta w_g(z)) \quad [7.3]$$

The crossing time or transit time of the fiducial reference line for the grid is given by the equation  $u(\tau) = 0$ . The observations consist of measured transit times  $\tau_{\text{obs}}$  associated with a specific object.

The five astrometric parameters for star  $i$  are  $\alpha_i$ ,  $\delta_i$ ,  $\pi_i$ ,  $\mu_{\alpha_i}$ , and  $\mu_{\delta_i}$ . They were determined by a least-squares solution from the on average 130 observed transit times of a star. The solution is closely linked to the determination of (improved) grid parameters ( $h, w_{10}, \dots$ ) and the formulation below takes full account of this calibration.

For each observed transit  $\tau_{\text{obs}}$  of star  $i$  on slit group  $g$ , the following observation equation can be set up:

$$\begin{aligned} \frac{\partial u}{\partial \alpha_i} \Delta \alpha_i + \frac{\partial u}{\partial \delta_i} \Delta \delta_i + \frac{\partial u}{\partial \pi_i} \Delta \pi_i + \frac{\partial u}{\partial \mu_{\alpha_i}} \Delta \mu_{\alpha_i} + \frac{\partial u}{\partial \mu_{\delta_i}} \Delta \mu_{\delta_i} \\ + \frac{\partial u}{\partial h} \Delta h + \frac{\partial u}{\partial h_{11}} \Delta h_{11} + \dots + \frac{\partial u}{\partial h_{+1}} \Delta h_{+1} \\ + \text{noise} = u_{\text{obs}} - u_{\text{calc}} \end{aligned} \quad [7.4]$$

where  $u_{\text{obs}} = 0$  at time  $\tau_{\text{obs}}$  by definition, while  $u_{\text{calc}}$  is the distance calculated (predicted) from the current values of the astrometric parameters (typically the position in the Tycho Input Catalogue Revision), current grid calibration parameters, and the attitude.  $\Delta \alpha_i, \dots, \Delta h_{+1}$  are the corrections to these current parameters, to be determined by the least-squares method.

The predicted distance at time  $\tau_{\text{obs}}$  of a star from the fiducial reference line of the slit group, measured along the direction of motion, corresponds to a predicted transit time  $\tau_{\text{calc}}$ , which is related to  $u_{\text{calc}}$  through the velocity  $v_{\text{scan}}$  of the stellar image relative to the grid.  $v_{\text{scan}}$  is negative at the nominal direction of spin of the satellite  $v_{\text{scan}} = du/dt \simeq -8.18 \times 10^{-4} \text{ rad s}^{-1}$ . It is noted that the velocity component in the  $z$ -direction is relatively small, but must be taken into account. It follows that:

$$\Delta u \equiv u_{\text{obs}} - u_{\text{calc}} = -v_{\text{scan}} (\tau_{\text{obs}} - \tau_{\text{calc}}) \quad [7.5]$$

is the right-hand side of Equation 7.4.

The observation, Equation 7.4, is given in spherical coordinates, whereas a formulation using relative tangential coordinates in the vicinity of each Tycho Input Catalogue position was used in practice, thus simplifying the data reduction to a linear problem.

The uncertainty,  $\sigma_u$ , of the right-hand side of Equation 7.5 depended on two major error sources, contained in the last two terms: photon-statistical uncertainty of the observed transit time (converted to arcsec along scan),  $\sigma_\tau$ , and the attitude uncertainty. Considering the way in which the attitude was determined, it was reasonable to assume that the attitude errors in the calculated ( $w, z$ ) were uncorrelated and characterized by nearly constant standard deviations  $\sigma_w, \sigma_z$ . Then, to sufficient accuracy:

$$\sigma_u^2 = \sigma_\tau^2 + \sigma_w^2 + (g-1)\sigma_z^2 \quad [7.6]$$

where  $g-1 = 0$  for the vertical group and  $= 1$  for the chevron group, according to the definition of  $g$ .

The photon-statistical error  $\sigma_\tau$  was calculated for each transit at a slit group as a function of the estimated star and background count rates (and measured in arcsec along the scan).  $\sigma_w$  and  $\sigma_z$  are functions of time. Their average values determined from observations were about  $\sigma_w = 7 \text{ mas}$  and  $\sigma_z = 35 \text{ mas}$  which was very satisfactory since at least  $\sigma_z = 50 \text{ mas}$  error was expected for the inclined slits before launch (see Table 11.1

in Høg 1989). In practice a slightly different formulation than Equation 7.6 was used in order to accomodate variations during the mission (Equation 11.3).

Dividing Equation 7.4 by the estimated standard deviation from Equation 7.6 gives an observation equation of unit weight. Let us assume that the grid calibration requires, for a short period of the mission, a total of  $N_c$  parameters. The  $k$ -th observation equation can then be written in matrix form:

$$\mathbf{B}_k \Delta \mathbf{a}_{i(k)} + \mathbf{C}_k \Delta \mathbf{c} + v_k = e_k \quad [7.7]$$

where  $i(k)$  denotes the star  $i$  associated with observation  $k$ , and  $\Delta \mathbf{a}_{i(k)}$  and  $\Delta \mathbf{c}$  denote the column vectors of corrections to the five astrometric parameters and the  $N_c$  calibration parameters respectively.  $\mathbf{B}_k$  and  $\mathbf{C}_k$  denote the row vectors of the derivatives of  $u$  with respect to the astrometric and calibration parameters respectively, divided by  $\sigma_u$ . The  $v_k$  is a centred random variable with unit variance,  $E(v_k) = 0$ ,  $E(v_k^2) = 1$ . The right-hand side is:

$$e_k = \frac{u_{\text{obs}} - u_{\text{calc}}}{\sigma_u} \quad [7.8]$$

In addition to the scheme of weighting in Equation 7.8 some observations were completely rejected, e.g. when the background was very high, or  $|e_k| > 3$ , or  $|u_{\text{obs}} - u_{\text{calc}}| > 1$  arcsec, or when the presence of a parasitic star had been predicted (see Sections 1.6 and 7.2).

---

## 7.2. Processings, Identification, Parasites

---

### Astrometric Processing

The system of observations, given by Equations 7.7, was solved by the least-squares method, giving either astrometric parameters for the stars, or calibration parameters, but not both simultaneously. This means that the right-hand side  $e_k$  in Equation 7.7 was modified by subtracting the 1st or 2nd term on the left-hand side, calculated from the best available parameters, e.g. from a previous solution. The observation equations were used sequentially to update the upper triangular Cholesky factors, which implies that the residuals of a given solution could only be obtained as the right-hand side of the observation equations in a subsequent 'iterated' solution. The numerical method was based on Givens rotations (Lawson & Hanson 1974) thus avoiding the explicit formulation of the normal equations. (Givens rotations also have a very good numerical stability, but this was not important in the present application where the condition number was always small.)

### Sorting of Observations

The astrometric processing received the observations in chronological sequence in the form of 'identified transits'. These included timing and geometric information, the observed signal amplitude and background, and 'parasite' recording', explained below and in Chapter 6. The identified transits could have been used directly as input for the processing, but they were in fact sorted according to the star number of the catalogue. The sorting was carried out for all data from one ESOC tape (high-density 6250 bpi), corresponding to about 24 hours of observation. The purpose of the sorting was to

speed up the processing, i.e. the look-up of the star and its Cholesky factor which could then be updated with all observations for the star obtained during the 24 hours. In retrospect, we believe that the sorting gave only a doubtful advantage, and introduced a considerable complication in the software.

### **Hipparcos Reference Stars**

The observed transits of Hipparcos stars were used as input for all monitoring and calibration purposes, i.e. for provisional solutions of the astrometric parameters, for checking the quality and adequacy of the processing and of the observations.

The star mapper calibration was performed with a subset of about 105 000 stars having accurate positions, parallaxes and proper motions in the intermediate Hipparcos Catalogue, referred to as H30, derived by the two Hipparcos consortia from the first 30 months of observations. This catalogue was rotated to the N18 system derived by NDAC from 18 months of observations because the NDAC attitude was delivered in that system. Thus tying the calibration parameters to a coordinate system defined by Hipparcos positions, parallaxes and proper motions ensured that the resulting five astrometric parameters from Tycho were obtained in the N18 reference system. This catalogue was later rotated and corrected systematically to the final Hipparcos frame, as described in Chapter 11.

The status of Tycho astrometry, including the star mapper calibration after half of the mission was described by Høg *et al.* (1995). The NDAC attitude used by TDAC was given in the N18 system. This caused some problems because it suffered from global systematic differences relative to the H30 system. This inconsistency between the attitude system and the H30 system created global systematic errors in the Tycho reference system which were successfully removed, as described in Chapter 11. It was also realized that Hipparcos parallaxes had to be included in the calibration lest systematic errors would be introduced in the Tycho parallaxes. This explains why the preliminary results discussed by Høg (1995) showed Tycho parallaxes being systematically about 2.0 mas smaller than the Hipparcos values.

The set of astrometric parameters used in prediction updating were the positions from the Tycho Input Catalogue Revision and the proper motions and parallaxes from the Tycho Input Catalogue. The purpose of the astrometric processing was to compute corrections to these values, in the relative tangential coordinate system for each star. The initial 'corrections' were therefore equal to zero. For the Hipparcos reference stars, however, the initial corrections had to be non-zero in order that the stars could act as reference stars for the Tycho Catalogue. The initial corrections for these stars corresponded to the difference in position, parallax and proper motion between Hipparcos (the preliminary catalogue H30 rotated into the NDAC Consortium's intermediate N18 system) and the parameters used in prediction updating. With these values the calibration was carried out, as described in Section 7.3.

In the subsequent computation of astrometric parameters, the initial corrections for the Hipparcos stars were maintained in the iterations of the parallaxes and proper motions, whereas the positions were updated as for all other stars. The reason for not iterating the parallaxes and proper motions for the Hipparcos stars was that the time schedule of the work forbade the required considerable modification of the internal star file. The rather small penalty described in Chapter 18 is that the external standard errors calculated by

comparison with the Hipparcos Catalogue for the parallaxes and proper motions come out as nearly equal to the internal standard errors, which is too small for faint stars.

### **Main Processing and Reprocessing**

The ‘main processing’ treated the 1.3 million stars (entries) contained in the Tycho Input Catalogue Revision. In the main processing, the astrometric solution was iterated many times, using gradually larger data sets, improved values of the attitude and the star mapper calibration, and improved identifications of the transits. The connection to the other tasks in the Hipparcos and Tycho reductions is shown in Figures 1.2 and 10.1.

Following the main processing, a selection of 300 000 stars (see Chapter 10) was reprocessed, with the aim of, amongst others, obtaining improved photometry for the brighter stars, a better detection of double star components and faint stars. Also included were solar system objects. The reprocessing took less time than the main processing because the number of stars was only one tenth of the 3 million in the Tycho Input Catalogue, but the extra complication introduced by having two processings was sizeable.

### **Identification of Transits**

The raw output from the detection process could not be used for astrometric processing due to two error sources both of about 1 arcsec. This size of error was present in the real-time attitude of the satellite and in the positions given in the Tycho Input Catalogue of 3 million stars. The ‘predicted’ transit times (the above ‘calculated’  $\tau_{\text{calc}}$ ) were therefore uncertain by about 2 arcsec, which could disturb the astrometry and photometry too much, as several observed transits might be found within a few arcsec from the predicted time.

This problem was solved by means of the more accurate Tycho Input Catalogue Revision obtained from the first year of Tycho observations (Chapter 5) and the on-ground attitude produced by NDAC for its own use. This catalogue and the attitude were used in an ‘updating’ of all transit times (Chapter 6). The result was a file of ‘identified transits’, which was input for astrometry and photometry calibration and for catalogue production. The astrometric parameters and the calibration were always based on the  $B_T + V_T$  signal since it was demonstrated that the separate use of the  $B_T$  and  $V_T$  signals would give no advantage.

In reality, a PGC Updating-2 (Section 6.1) was used for a provisional identification of transits so that Tycho astrometry and photometry were able to proceed with a test processing, in particular the calibration, without having to wait for the Tycho Input Catalogue Revision. The final Tycho Catalogue is however based on final identified transits from a PGC Updating-3 (Section 6.2).

The transit identification process introduced the data from PGC Updating, and it recorded the possible disturbance from ‘parasitic’ stars as described hereafter.

### **Astrometric Disturbance by Parasitic Stars**

When a star crossed a group of four slits, it generated four peaks in the photon counts. When these counts were folded with the linear digital filter (4-peak filter) described in Chapter 2 the result was a signal with a main lobe and a total of 12 side lobes

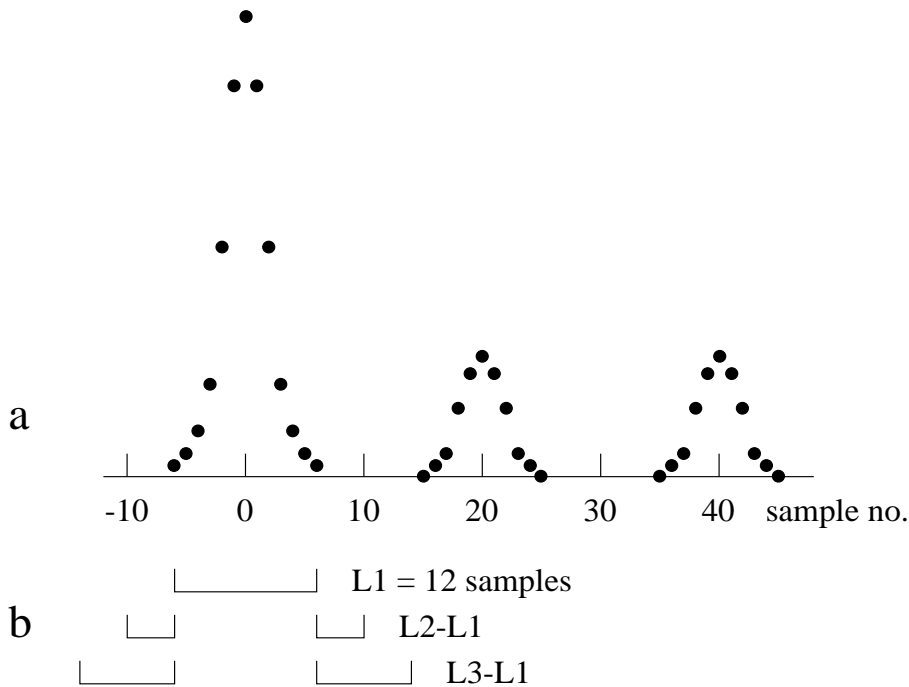


**Figure 7.1.** Strategy for parasite elimination: (a) main lobe and two of the 12 side lobes that would result if the linear filter were used in the detection of transits; the non-linear filter was used thus avoiding the side lobes. (b) An observed transit time of a main lobe was not used for astrometry if a parasite brighter than a certain limiting magnitude was present within certain intervals. A limiting magnitude  $T = 9.9$  mag was applied in a narrow interval  $L1$ , centred on the transit time corresponding to the main lobe. Brighter limits of  $T = 9.4$ ,  $8.9$  mag, respectively, were applied outside, in the intervals  $L2 - L1$  and  $L3 - L1$ , as described in the text.

having one fourth the height of the main lobe (see Figures 2.5 and 7.1). The average separation between lobes was 20 samples equivalent to 5.63 arcsec. In the Tycho detection processing a non-linear filter was used to eliminate the bright side lobes, as illustrated in Figure 2.5. The effect of the side lobes was, however, never completely removed, as was seen from the small excess of double stars with separations of an integer number of 5.63 arcsec (Figure 16.16). A main lobe from one star is called a parasite to another star if it disturbs the main lobe of that star. The added effect of the (main) lobes from several stars in a given interval was recorded for every transit during the transit identification process, where the transit time of all known stars was computed. The added intensity corresponding to the  $B_T + V_T$  signal, called the  $T$  signal, was recorded. In the inner two intervals,  $L1$  and  $L2-L1$ , of Figure 7.1 the  $T$ -magnitude of the parasitic star(s) was taken from the Tycho Input Catalogue Revision. In the outer interval  $L3-L1$ , the intensity was computed from the actual signal estimations in the  $B_T$  and  $V_T$  channels.

The parasite elimination made use of the recorded parasites. In the astrometric analysis, where the identified transits with the recorded parasites were processed, only those transits were used which had no parasites brighter than  $T = 9.9$  mag in the  $L1$ -interval. The limits were  $T = 9.4$  and  $8.9$  mag, respectively in the outer intervals. These limiting magnitudes for parasites have been shown to give a good compromise between rejecting too many transits and accepting too large disturbances.

The astrometric disturbance by parasitic lobes from other stars has been studied by theoretical models. It was shown that there would be 2.7 times as many side lobes of a given magnitude as there are main lobes if a linear filter were used, but this was much diminished by use of the non-linear filter. If nothing had been done to eliminate observations disturbed by the remaining parasitic main lobes, the resulting accuracy would have been significantly impaired, compared to the expectation for pure photon noise. A method was therefore used by which the increase of standard error due to parasites was reduced to a fairly small fraction of the photon noise error. The increase was about 5 per cent at average star density, independent of the stellar magnitude. The fraction increased only slightly to 8 per cent when one of the fields of view was on the galactic equator. If the limiting magnitude for parasites were set 1 mag brighter, the errors would have been increased by about 10 per cent, much more than the 5 per cent with the actual limits.

In the case of double stars the parasites from each star disturbed the other one, thus reducing the number of accepted transits for these stars. A special treatment of narrow double stars was therefore carried out (Chapter 14), where a more thorough analysis was able to avoid an unnecessary loss of transits.

---

### 7.3. Geometric Calibration of the Star Mapper

---

Calibration of the star mapper geometry has been carried out by means of 'identified transits' for 37 months of observations of Hipparcos stars. The results are given in Figures 7.2 and 7.3, for the main processing and the reprocessing. The figures show the numerical effect of each parameter, formally calculated at the ordinate  $z = +10$  arcmin on the grid, as a function of time. Since the parameters are obtained relative to those used by NDAC, Figures 7.2 and 7.3 should be used to discuss only the time variation and the scatter of the parameters.

Each point in the figures is derived from observations obtained over a 24 hour period. The dotted vertical lines mark a refocussing of the telescope which had a pronounced effect on the scale value, and consequently on the shifts  $w_{10}$  and  $w_{20}$ . The reason is that the satellite attitude referred to the centre of the main field of Hipparcos while the vertical slits of the star mapper were located 0.00939 rad or 32 arcmin off-centre.

On theoretical grounds one expects that  $h_{21}^+ \simeq h_{21}^- \simeq 2h_{11}$  and consequently  $h_{21}^+ + h_{21}^- \simeq 4h_{11}$ , but it appears from Figure 7.2 that the time variations of the observed parameter correction obey only the latter relation. It is noted that the time variation of Tycho parameters for, for example, basic angle and rotations cannot be directly compared with the corresponding parameters for the Hipparcos main field because the scale value of the main field is variable with time and this affects the comparison. The corresponding change of scale in the star mapper part is (mainly) absorbed in the shift parameters ( $w_{10}$ ,  $w_{20}$ ,  $h_{-1}$ ,  $h_{+1}$ ), see Figures 7.2 and 7.3.

The scatter of each parameter seen in the figures is about four times the formal standard error, but part of the scatter may be due to a real variation of the parameter. The scatter of points before  $t = 389$  days is somewhat larger than after because the attitude did not have the same quality as after that epoch, as explained in Volume 3, Section 2.1. After the interruption of observations about  $t = 1350$  days the scatter increased.

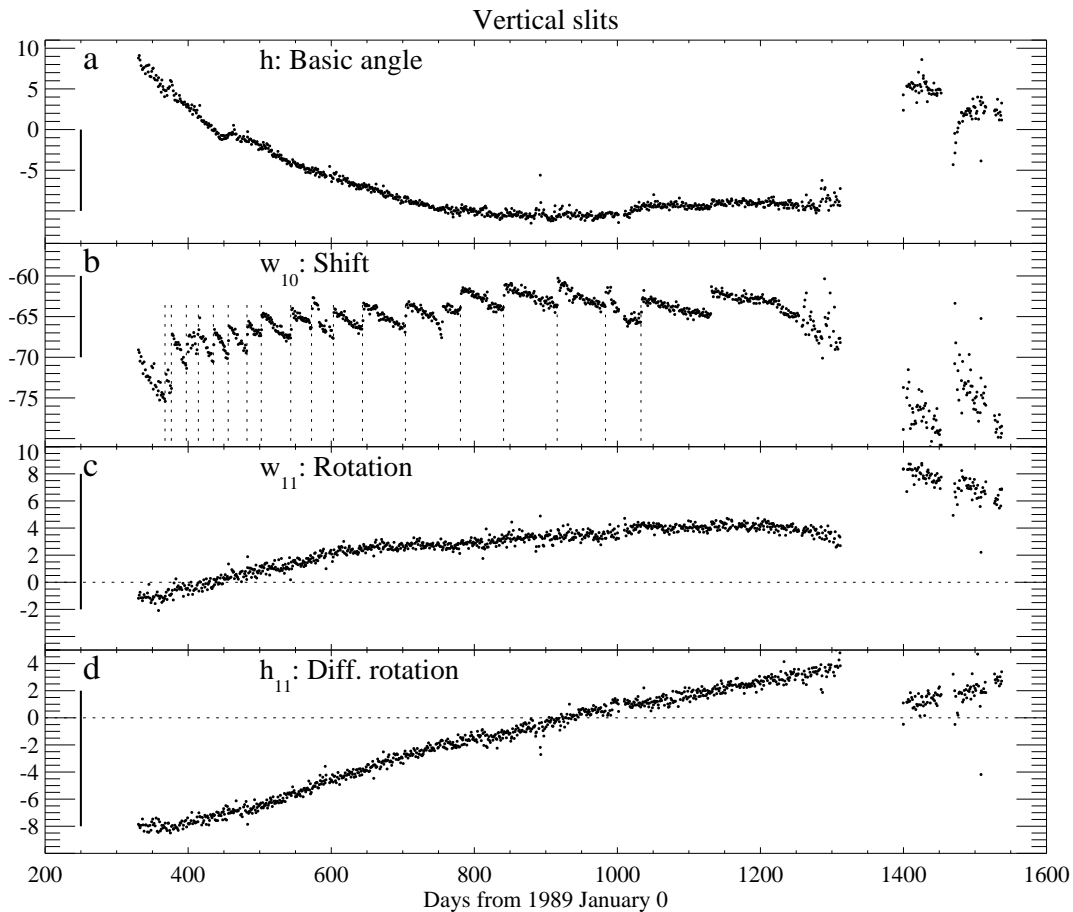


**Figure 7.2.** (a-d) vertical slits, main processing: geometric calibration parameters of the star mapper grid as a function of time. The ordinate, in mas, is the effect of each parameter at the slit coordinate  $z = 10$  arcmin, or actually, the (small) corrections to the parameters used in the prediction and attitude processing. A vertical bar of 10 mas length gives the scale in each plot. Vertical dotted lines in these figures, mark some of the times when the telescope was refocussed (see also Volume 3, Figure 2.1).

The oscillation, in Figures 7.3(f) and 7.3(g), of two parameters for the inclined slits is very conspicuous, with a peak-to-peak amplitude up to 20 mas. This is the same order of magnitude as the attitude uncertainty, but it affects the astrometric parameters more systematically. The problem was related to a small systematic defect in the reprocessing, described in Section 10.7.

It can be seen from Figure 7.2 that the scatter of the parameters during most of the mission produced a combined effect of scatter in Equation 7.2(a-c) of generally less than 1 mas for vertical and 20 mas for inclined slits. For the reprocessing a very similar scatter was found (Figure 7.3). This scatter is negligible compared with photon and attitude noise for the vertical slits, even for the average of, say, eight slit group crossings of a star, sometimes obtained in 24 hours. The 20 mas for the inclined slits is not quite negligible, compared with about 35 mas error of the attitude in the  $z$ -direction. Therefore, a piecewise spline smoothing over four days, excluding discontinuities due

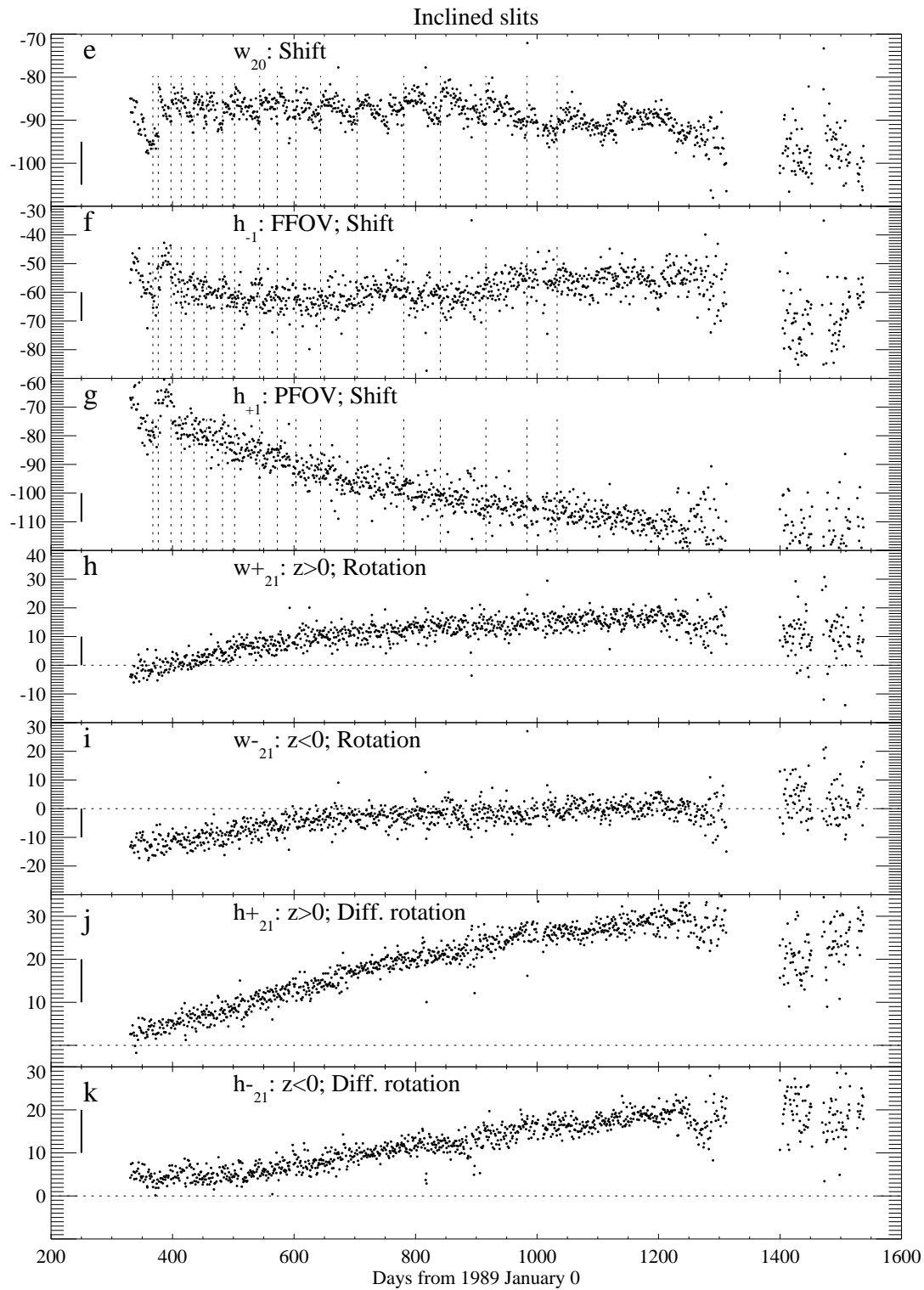


**Figure 7.2. (cont.)** (e-k) inclined slits, main processing: FFOV = following field of view; PFOV = preceding field of view.

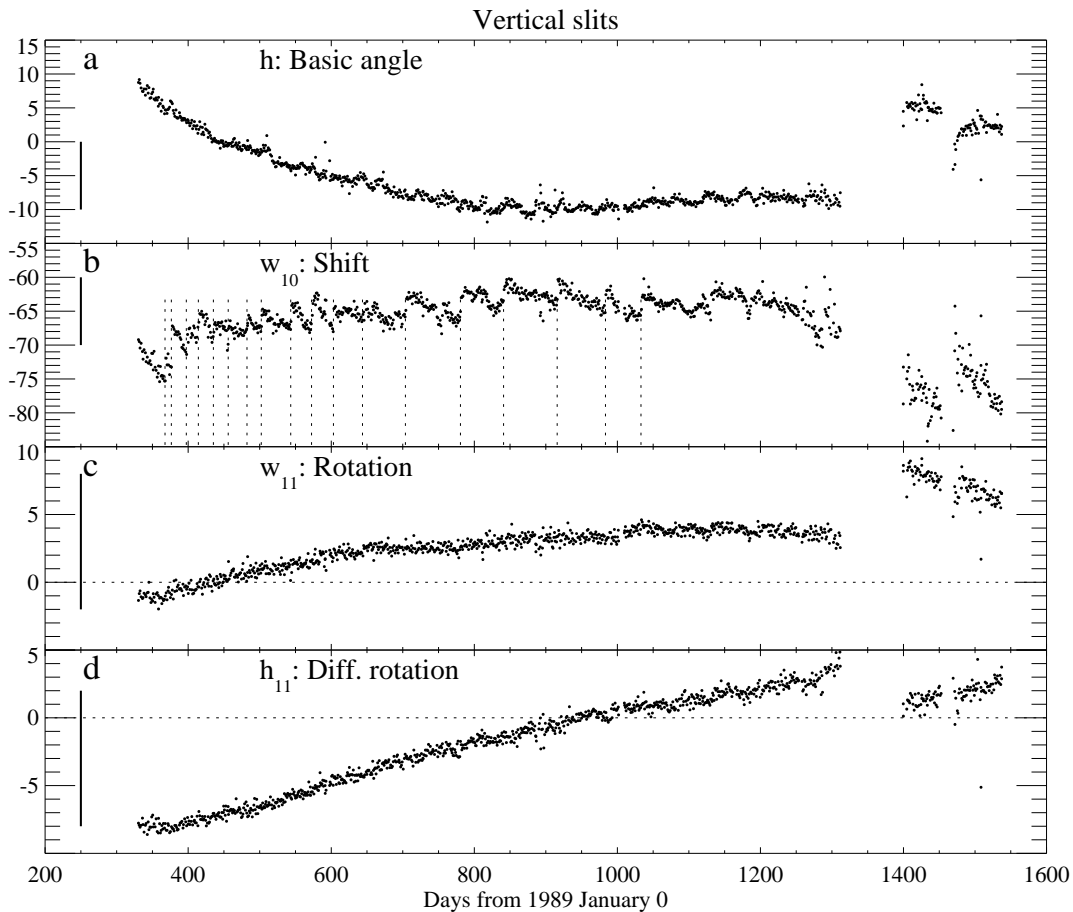


**Figure 7.3.** (a-d) vertical slits, reprocessing: geometric calibration parameters, see Figure 7.2.

to refocussing, was always applied in deriving the parameters used in star catalogue production.

### Medium-Scale Irregularities

The star mapper slits were etched by electron beam scanning on the same glass surface as the main Hipparcos grid. The etching was done one so-called ‘scan field’ at a time before moving the glass plate mechanically to the position required for the next scan field. In this way 68 fields covered the 40 arcmin in  $z$  on the chevron slit group and 34 fields covered the vertical group. The position of the slits in each scan field was measured in the laboratory, resulting in a table of medium-scale irregularities with  $2 \times 68$  values, one for each scan field, as shown in Figure 1.4. These laboratory values of up to 182 mas for the inclined slits were corrected by NDAC using in-orbit data (see Section 1.5), before they were applied in the prediction processing (see Section 4.1). The standard medium-scale irregularities discussed below are therefore corrections to these combined values. The slit errors inside each scan field were shown by laboratory measurements to be negligible. The table of medium-scale irregularities used in the

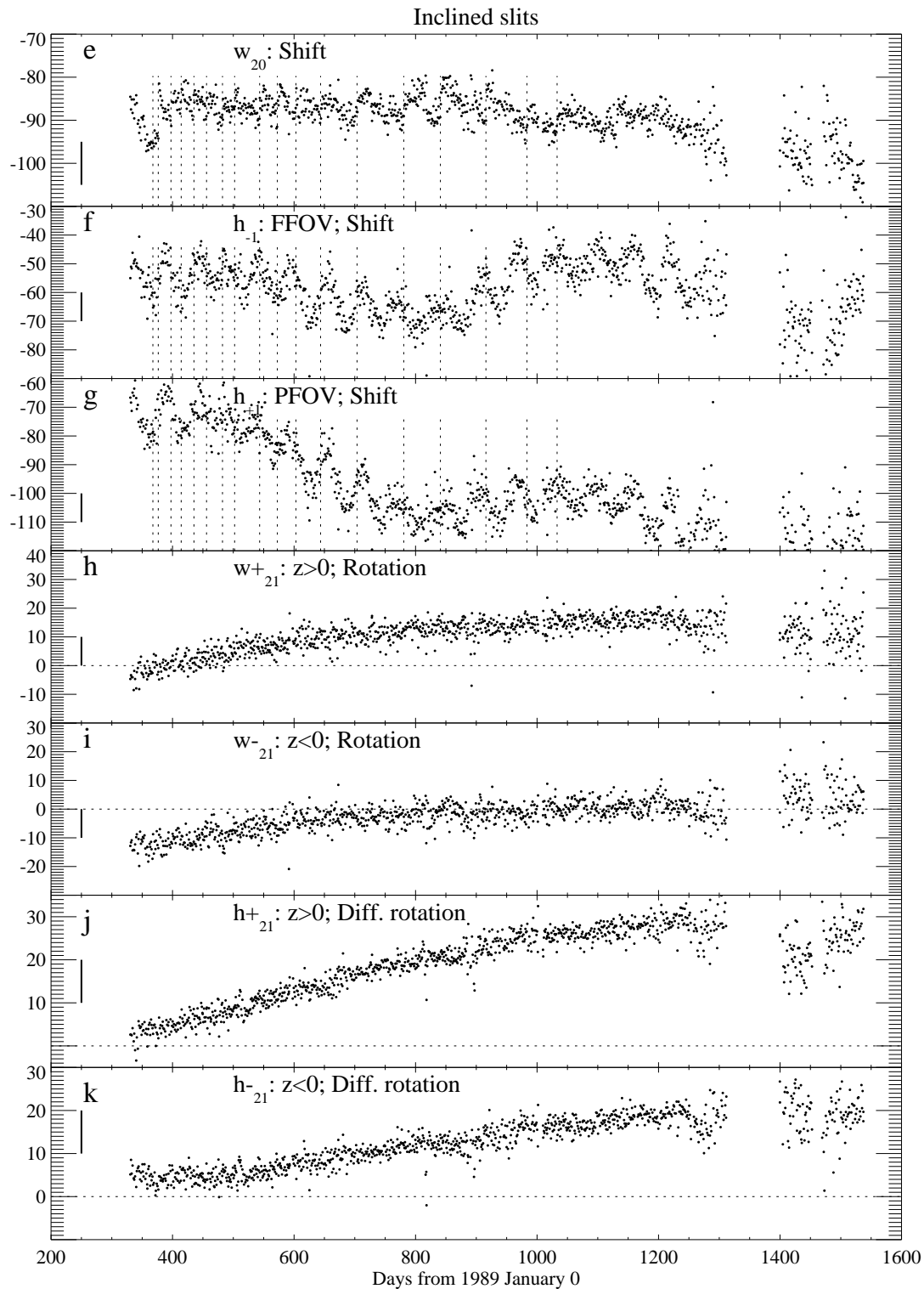


**Figure 7.3. (cont.)** (e-k) inclined slits, reprocessing: geometric calibration parameters, see Figure 7.2. FFOV = following field of view; PFOV = preceding field of view.

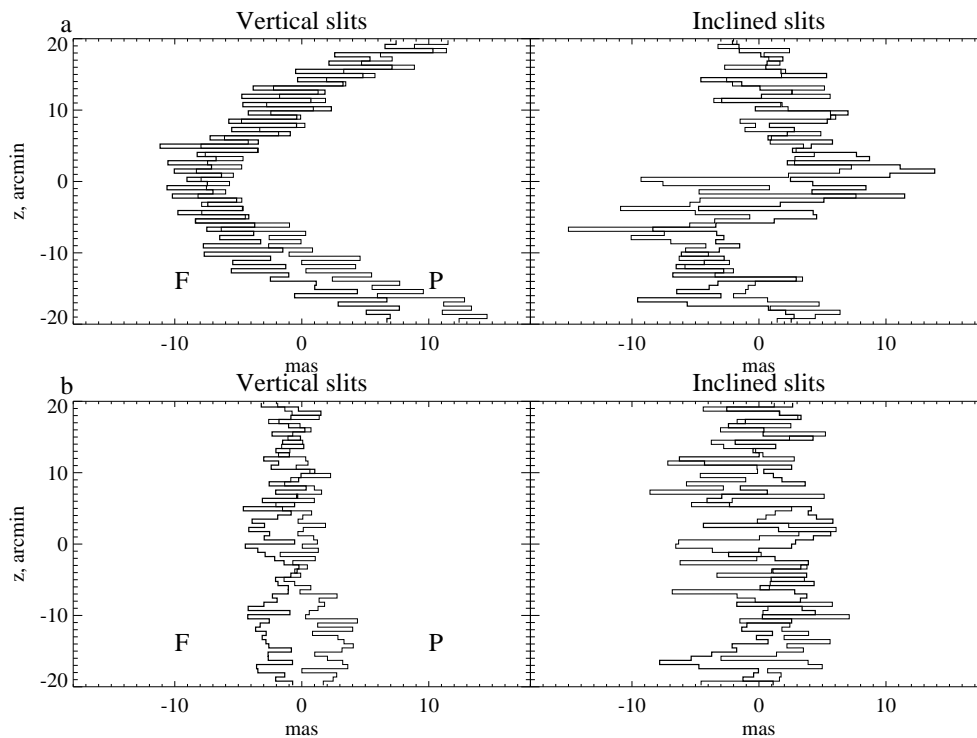


**Figure 7.4.** ‘Medium-scale irregularities’ of the star mapper grid as abscissa and the  $z$ -coordinate as ordinate. Separate values for preceding and following field on the sky are shown by thin and thick lines, marked by  $P$  and  $F$ , respectively. (a) Values determined at the epoch 1991.33; (b) Differences between values obtained at the epochs 1991.33 and 1990.20.

astrometry processing was calculated from residuals in Equation 7.2(a-c) as averages in 68 intervals along  $z$ , corresponding to the distribution of scan fields.

A ‘standard’ table of medium-scale irregularities,  $\Delta w_g(z)$ , was determined from two months of observations at the beginning of the mission and has been used for all calibration and catalogue production. The medium-scale irregularities were verified to be repeatable with another nearby data set within 1 mas systematically, and a scatter per point of 1 and 2 mas for vertical and inclined slits respectively.

Figure 7.4(a) shows the medium-scale irregularities determined for the epoch 1991.33 and for preceding and following fields of view on the sky separately, marked by  $P$  and  $F$ . Hence, it is a figure of  $\Delta w_{fg}(z)$ . A curvature of the vertical slits of 20 mas amplitude appears, and a similar amplitude for inclined slits. The variation between adjacent scan fields is smaller. The lower half of the vertical slits shows a difference about 5 mas between the two fields of view, but this is negligible for Tycho since a star was typically measured in both fields of view within 20 minutes and an average was used for star positions. It was therefore unnecessary to use different medium-scale irregularities for the two fields of view.

Figure 7.4(b) shows the change of medium-scale irregularities during one year of the mission, which appears to be negligible, especially in view of the averaging just mentioned.

---

## 7.4. Astrometric Parameters and Quality Classes

---

The five astrometric parameters for the stars were computed iteratively from the identified transits as described in Section 7.2. The computations produced standard errors, correlation coefficients, an ‘astrometric’ magnitude and various quality indicators for each star. A special file of all, accepted and not accepted, transits was produced for use in the final photometric processing.

### Astrometric Magnitude

An approximate magnitude in the photometric  $T$  channel, with standard error, was computed during one of the early stages of astrometric processing. It was based on the amplitudes given in the identified transits, using photometric calibration parameters received from the Tycho photometric processing. The resulting  $Ta$  magnitude had a considerable bias for faint stars because it was computed from an average of the amplitudes, not by de-censoring. The  $Ta$  magnitude was used for the monitoring of astrometric processing, as illustrated by Figure 7.6, long before the de-censored magnitudes became available. It was also used in the final Tycho Catalogue for 1333 stars, flagged in Field T36 (Section 2.2, Volume 1).

### Hexagon Points

In about 45 000 cases the processing of the first year of Tycho observations did not recognize any star even though the Tycho Input Catalogue contained a rather bright entry of  $< 10.725$  mag. A special effort was therefore made in the astrometric processing to find a star. Six positions were assumed in a regular hexagon with radius 0.6 arcsec, centred on the Tycho Input Catalogue position. A normal astrometric reduction was carried out for the six hexagon points and the Tycho Input Catalogue position. This resulted, after a critical analysis, in 231 further entries in the final Tycho Catalogue; these were often high proper motion stars. In many cases a bright Tycho Input Catalogue entry belonged to a nebula in the Guide Star Catalog used for the Tycho Input Catalogue. (A nebula appears with a considerable diameter and could not be distinguished from a star in the Guide Star Catalog production).

### All-Transits File

In a final astrometric processing an all-transits (AT) file was produced for use in the final photometric processing. The file mainly contained information about the distance of each detection from the final astrometric position of the relevant star, and whether the detection was used for astrometry.

The AT file contained a record for each identified transit with: Tycho star identifier; observation time; amplitude and background in the  $T$  channel; astrometric residual  $\Delta u$ ; standard error  $\sigma_u$ ; and various flags from astrometry. The flags show whether the detection was accepted for astrometry or whether parasites or a large residual were the

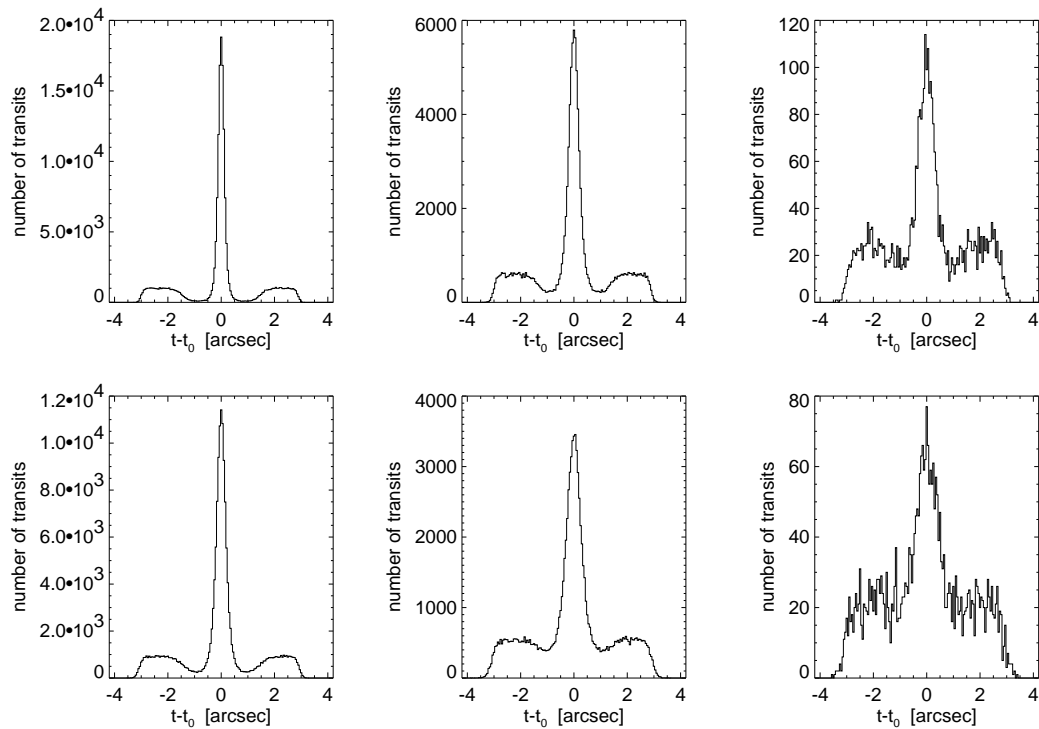


**Figure 7.5.** Accumulated distributions of astrometric residuals for stars with  $H_p$  magnitudes in an interval of 0.2 mag, centred on 9.8, 10.7 and 11.6 mag (left to right); transits on vertical slits in the upper row and on inclined slits in the lower.

reason for a rejection. Some of this information is included in the individual transit records in the Tycho Epoch Photometry Annex, see Volume 1, Table 2.6.2.

### Quality Indicators and Criteria

The standard errors of the five parameters are good quality indicators for the solution for a given star. But they were not sufficient for the present purpose, a reliable distinction of good solutions from bad ones, especially for the faint stars where the single transit could have a signal-to-noise ratio of only 1.5. Special indicators were required to measure the total signal-to-noise ratio of the combined signals from the whole mission in order to distinguish between a real star on the sky and a ‘false’ star, generated by a random accumulation of noise.

The final astrometric quality flag,  $Q$ , is mainly based on the three quality indicators  $\sigma_{\max}$ ,  $F_s$  and  $\sigma_{\text{obsf}}$  (columns 2–4 in Table 7.1).

- The Indicator  $\sigma_{\max}$ : This quantity is the largest of any of the five astrometric standard errors for a given star.
- Signal-to-Noise Ratio,  $F_s$ : This quantity was based on an examination of Figure 7.5 and was computed in a separate processing of all observations after the final astrometric parameters had already been computed.

Figure 7.5 shows the distribution of astrometric residuals,  $\Delta u$ , of Equation 7.5. The central peak in each plot is due to detections from the star, and the residuals outside

**Table 7.1.** The astrometric quality  $Q$  and associated quantities.  $N$  is the number of stars in the Tycho Catalogue of each quality class.  $\sigma_{\text{med}}$  gives the median standard error of a position coordinate at the catalogue epoch J1991.25 (the errors at the mean epoch of observation of any given star are typically 5 per cent smaller).

$Q$	$\sigma_{\text{max}}$ (mas)	$F_s$	$\sigma_{\text{obsf}}$ (mas)	$N$	$\sigma_{\text{med}}$ (mas)	Astrometric quality
1	< 5	> 5	< 300	23147	2.6	very high
2	5 – 10	> 5	< 300	70945	5.5	very high
3	10 – 25	> 5	< 300	259695	13	high
4	25 – 50	> 5	< 300	430182	26	high
5	50 – 150	> 5	< 300	146520	39	medium
6	< 150	> 5	$\geq 300$	41695	44	perhaps non-single
7	< 150	3 – 5	< 300	37821	45	low
8	< 150	3 – 5	$\geq 300$	28949	54	perhaps non-stellar
9	$\equiv 200$	–	–	13077	–	low, ‘R’ in Field T42
$\sqcup$	–	–	–	6301	–	unassigned, ‘H’ in Field T42
any	–	–	–	1058332	25	all entries

an interval from  $-0.7$  to  $+0.7$  arcsec are due to random background detections. The deficit of residuals near the ends of this interval especially for the bright stars is understood from an inspection of the slit response functions in Figure 1.3. A residual about  $0.7$  arcsec would correspond to another star at the foot of the response function where it could, however, not be detected in the presence of the brighter star. For the fainter stars to the right in Figure 7.5 the minimum is less pronounced.

The quantity  $F_s$  is defined as:

$$F_s = (n_1 - n_2) / \sqrt{n_1 + n_2} \quad [7.9]$$

where  $n_1$  is the number of detections within  $0.7$  arcsec along scan from the mean position, and  $n_2$  is the number of detections between  $0.7$  and  $1.4$  arcsec (which provides a measure of the rate of background detections). In the special but rather common case of a sharp image on a negligible background,  $n_1 \sim N_{\text{astrom}}$ ,  $n_2 \sim 0$  and  $F_s \sim \sqrt{N_{\text{astrom}}}$  where  $N_{\text{astrom}}$  is the number of accepted astrometric detections.

- Half-Width of the Image:  $\sigma_{\text{obsf}}$  is the formal standard error of the single observation, being a measure of the half-width of the star image:  $\sigma_{\text{obsf}}^2 = 0.25(\sigma_x^2 + \sigma_y^2)(N_{\text{astrom}} - 5)$ , where  $\sigma_x$  and  $\sigma_y$  are the standard errors of the two position components. A half-width larger than  $300$  mas was found to be correlated with duplicity or a non-stellar image.

### Other Indicators

- Median Standard Error:  $\sigma_{\text{med}}$  is the median standard error of a position coordinate at the catalogue epoch J1991.25. The errors at the mean epoch of observation of any given star are typically 5 per cent smaller.
- Goodness-of-Fit Parameter, F2: This number indicates the goodness-of-fit of the solution to the accepted data. For good fits F2 should approximately follow a normal distribution with zero mean value and unit standard deviation, see Figure 7.6(e). F2 values exceeding  $+2.5$  to  $+3$  thus indicate a bad fit to the data. Its construction and interpretation are explained further under Field H30 in Volume 1, Section 2.1. The

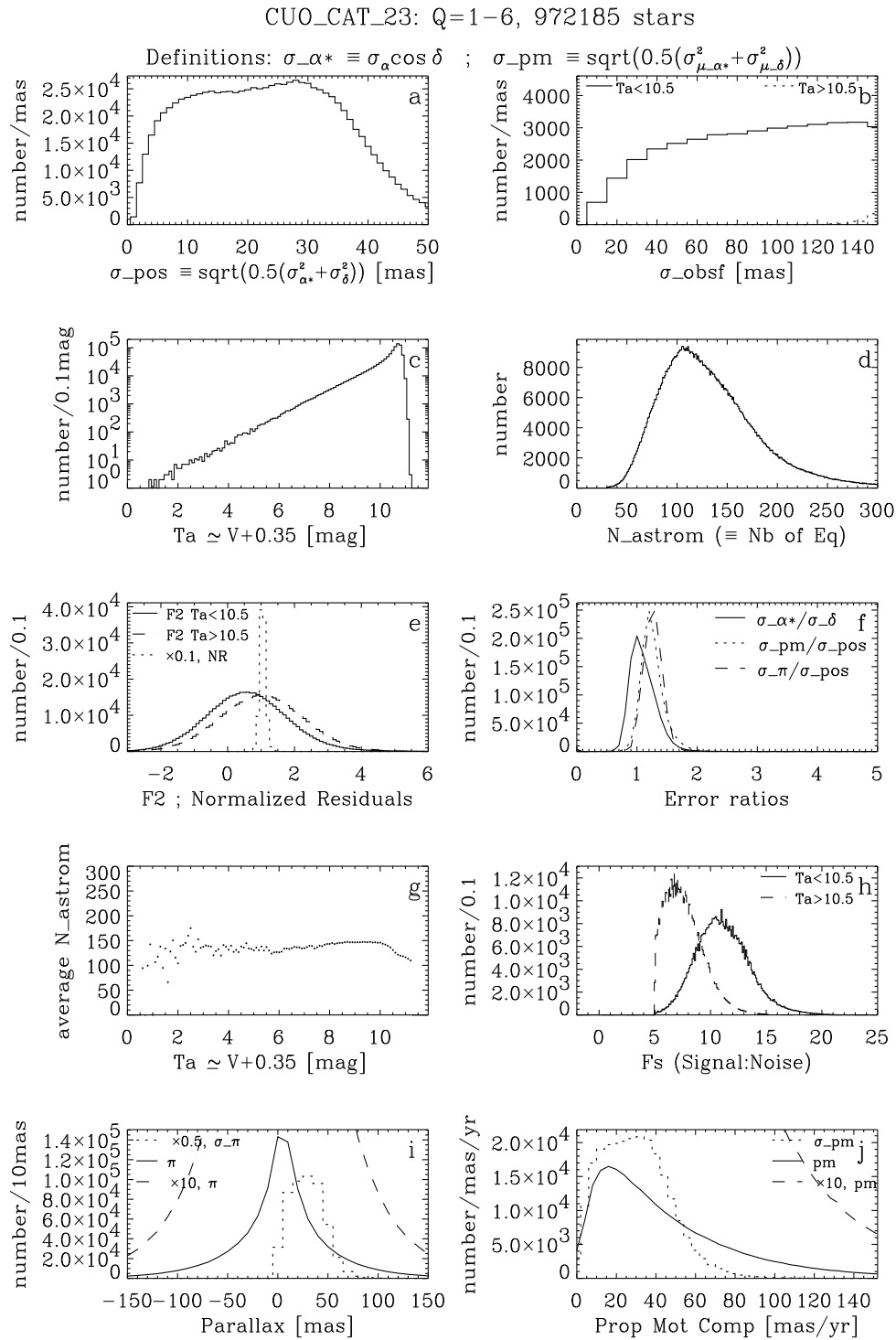


**Figure 7.6.** Distribution functions of quantities derived in the astrometric processing. Such plots for various subsets of the data were extensively used in the quality assessment. The present plot shows as an example the stars with  $Q=1-6$  in one of the intermediate (but nearly final) catalogs, numbered CUO\_CAT\_23.

F2 value was, however, not used for generating the astrometric quality flag  $Q$ , for which classification measures derived from other aspects of the data reduction were found to be more informative.

### Astrometric Quality Flag

The astrometric quality,  $Q$ , is defined for the Tycho data according to Table 7.1, where  $N$  gives the number of stars in the Tycho Catalogue of each quality class. Objects with  $Q \leq 8$  in the Tycho Catalogue all have  $F_s > 3$ ,  $\sigma_{\max} < 150$  mas,  $\sigma_{\text{obsf}} < 450$  mas, and  $N_{\text{astrom}} > 30$ . The last criterion,  $N_{\text{astrom}} \leq 30$ , had only the effect of excluding less than 100 stars of low quality, due to the  $F_s$  limit being the strongest criterion.

Objects with  $Q = 9$  have lower astrometric quality, and are included for the sake of their photometric data—these objects are flagged by ‘R’ in Field T42 (Section 2.2, Volume 1). The last line in the table shows that 6301 entries have ‘H’ in Field T42, showing that they are contained in the Hipparcos Catalogue, but were not observed by Tycho.

A flag is provided (in Field T10) showing if a star is a dubious astrometric reference star, e.g. due to suspected duplicity or dubious astrometry. The remaining approximately 900 000 stars are called ‘recommended astrometric reference stars’.

### Verification of Quality

Development of the quality criteria and their proper combination into astrometric quality classes was a long process where various tools were used. Local sky maps of the actual Tycho catalogue were compared with direct photographs or with the Digitized Sky Survey (DSS). The DSS happened to become available just as needed and it was very extensively used to distinguish stars and nebulae on the sky and compare with entries of various quality classes and false stars. Comparison with the Guide Star Catalog (Version 1.1) was also much used. Pair statistics were used, similar to Figure 16.16. Distribution functions of various quantities were plotted for selected subsets of data as shown by the example in Figure 7.6.

E. Høg



## 8. PHOTOMETRIC ANALYSIS OF TRANSIT DATA

*The purpose of the photometric calibration, described in this chapter, was to derive an accurate transformation from the signal amplitudes estimated in the  $B_T$  and  $V_T$  channels, by the detection process, into magnitudes in the Tycho  $B_T$  and  $V_T$  system. This was done for each channel separately by allowing for six independent instrument calibration parameters. Only one of these parameters was found to vary significantly during the mission.*

---

### 8.1. Theoretical Basis

---

Input data to the photometric calibration were the estimated background count rate and the estimated signal amplitudes in the  $B_T$  and  $V_T$  channel. The signal amplitudes,  $a$  (reckoned in counts per sample), came either from the main processing or from the reprocessing data stream (see below), resulting in two independent calibrations. Because calibration was done in magnitude space, the signal amplitudes were first transferred to observed raw magnitudes:

$$m_{\text{obs}} = -2.5 \log(a) + m_{\text{off}} \quad [8.1]$$

The constants  $m_{\text{off}}$  are given in Table 8.1.

The functional relationship between the observed raw Tycho magnitude  $m_{\text{obs}}$  and a ground-based magnitude from the standard star catalogue  $m_{\text{standard}}$  has the following form:

$$m_{\text{obs}} = m_{\text{standard}} + \sum_{i=1}^6 c_i X_i \quad [8.2]$$

where the  $c_i$  are the unknown calibration parameters and the  $X_i$  are the variables listed in Table 8.2.

During pre-launch simulations, time-dependent terms and higher-order mixed terms like  $(B - V - 0.7)^2 z$  and  $(B - V - 0.7) z^2$  had been included in the list of variables, but extensive tests on real data showed that they were not significant.

In order to ensure the statistical independence of the chosen variables and to add to the stability and reliability of the solution, the variables were not simply taken in their basic form but were changed to a Legendre polynomial representation. This included proper scaling of the range and units of the variables.

**Table 8.1.** Calibration constants for the photon noise. The constants  $\gamma$  and  $\delta$ , and the magnitude offsets  $m_{\text{off}}$  for the preceding and following fields of view (FOV), are described in the text.

Channel	$\gamma$	$\delta$	$m_{\text{off}}$			
			Preceding FOV		Following FOV	
			Lower	Upper	Lower	Upper
inclined $B_T$	0.12419	0.13003	11.430	11.309	11.504	11.400
vertical $B_T$	0.13223	0.11538	11.761	11.662	11.795	11.701
inclined $V_T$	0.11337	0.11115	11.071	11.046	11.028	10.998
vertical $V_T$	0.11444	0.11308	11.458	11.446	11.377	11.384

**Table 8.2.** Photometric calibration variables.

Index	Variable	Physical Meaning
1	1	zero point
2	$z$	slit abscissa
3	$z^2$	
4	$(B - V - 0.7)$	colour index
5	$(B - V - 0.7)^2$	
6	$(B - V - 0.7)z$	mixed term

The calibration was done separately for the  $B_T$  and  $V_T$  bands, both fields of view, upper and lower parts of the grid, and inclined and vertical slit groups, resulting in 16 possible combinations. The full set of parameters was computed independently for a period of time called a photoset (see Section 8.2).

Each single observation was described by the functional relationship given in Equation 8.2, relating the catalogued standard star magnitude with the observed magnitude and the unknown six calibration parameters. The catalogue error was assumed to obey a Gaussian distribution with a standard deviation equal to an adopted mean error for the particular magnitude range of the star. Using a normalisation with the standard errors of the observed magnitudes  $\sigma_{m_{\text{obs}}}$ , Equation 8.2 can be rewritten as:

$$r = p m_{\text{standard}} + \sum_{i=1}^6 q_i X_i \quad [8.3]$$

with  $p = 1/\sigma_{m_{\text{obs}}}^2$ ,  $q_i = c_i/\sigma_{m_{\text{obs}}}^2$ ,  $r = m_{\text{obs}}/\sigma_{m_{\text{obs}}}^2$ . Note that in Equations 8.2 and 8.3 the noise terms have been omitted for brevity.

This equation must be valid for each single observation and for all standard stars observed. From Equations 8.3 the design matrix of the least-squares problem was constructed, which was then multiplied by its transpose to give the normal equation matrix. Solving the normal equations gave the calibration parameters  $c_j$ . Numerically, this was done by Cholesky decomposition (Seber 1977).

### Reduction of Transit Data to the Tycho System and Error Assignment

The computed parameters  $c_j$  were used to derive magnitudes in the Tycho photometric system by inversion of Equation 8.2 for each single transit depending on field of view, part of the grid, and slit group.

To each magnitude measured in a single transit, a mean error:

$$\sigma_t = \sqrt{\sigma_{\text{pn}}^2 + \sigma_{\text{par}}^2} \quad [8.4]$$

was assigned. Here,  $\sigma_{\text{par}}$  is the parameter error resulting from the uncertainty of the calibration and  $\sigma_{\text{pn}}$  is the photon noise. The latter is given by:

$$\sigma_{\text{pn}} = \sqrt{\gamma a + \delta b/a} \quad [8.5]$$

with  $a$  being the estimated amplitude and  $b$  the background count rate in a given channel (both in counts per sample; 1 sample = 1/600 s). The constants  $\gamma$  and  $\delta$  are different for each passband and slit group. They are given in Table 8.1, which also lists the constants  $m_{\text{off}}$  for the conversion from count rates to magnitudes given in Equation 8.1. Note that  $m_{\text{off}}$  depends on the field of view (preceding/following field of view) and the branch of the slit groups (lower/upper).

The values of  $\sigma_t$  for each observed magnitude are published in the Tycho Epoch Photometry Annexes A and B, for two selections of stars. For bright stars  $\sigma_t$  is dominated by the parameter error, for faint stars by the photon noise. While the Tycho Epoch Photometry Annex gives only one value  $\sigma_t$  per magnitude, it should be noted that the photon noise  $\sigma_{\text{pn}}$  is in fact not symmetric for faint stars, as can be seen in Figure 8.2. The limits of a  $\pm 1\sigma$  interval in magnitudes must be calculated by computing Equation 8.5 in terms of count rate, and transforming:

$$a \pm \sqrt{\gamma a + \delta b} \quad [8.6]$$

to the magnitude scale, using Equation 8.1. More details are given in Chapter 9.

Further error sources not included in  $\sigma_t$  became important for certain observations. One such additional error was introduced during the data transmission from the satellite to the ground. Count rates were compressed by a semi-logarithmic algorithm; therefore the resultant magnitudes got an additional scatter. This ‘digitisation error’ had a size of several millimag. It was of importance for the brightest stars only, since for all other stars the photon noise error was much larger. Count rates for faint stars were not compressed at all. Other errors were due to variations of the scanning velocity of the satellite (Scales *et al.* 1992 and Section 8.3).

### Median Magnitudes and Standard Errors

For the analysis and verification methods described below, median magnitudes were computed. The mean error of the median magnitude is estimated by:

$$\sigma_m = s/\sqrt{2N/\pi} \quad [8.7]$$

In this formula  $N$  is the number of individual measurements, and  $s$  is a measure of the scatter of them, defined as half the difference between the 15.85th and the 84.15th percentile. For a Gaussian distribution  $s$  is equal to the standard deviation, the two selected percentiles being at  $\pm 1$  standard deviation from the mean.

---

## 8.2. Instrument Calibration

---

The Tycho photometric system consists of two channels,  $B_T$  and  $V_T$ , described in Volume 1, Section 1.3.3. During the data reductions a third broadband magnitude  $T$  was defined from the added count rates (see Großmann *et al.* 1995). The Tycho Catalogue and the Tycho Epoch Photometry Annex contain magnitudes almost entirely in the  $B_T$  and  $V_T$  photometric system.

### Selection of Standard Stars

A selection of about 30 000 standard stars was prepared in the Tycho photometric system. But the standard stars entering the observation equations were restricted to the magnitude range 4.5–9.0 mag. Brighter stars were excluded because of saturation effects of the photomultipliers, fainter stars because of the censoring problem (see Chapter 9). Members of close double stars or multiple systems were not used in order to avoid confusion. The resulting number of standards actually used in the given magnitude range was almost 10 000 for the main processing, and 13 600 for the reprocessing.

### Selection of Transits

Contrary to the case of the final selection of transits used to compute median or corrected mean magnitudes in the Tycho Catalogue, no astrometric residuals were available at the processing stage of calibration: transits were accepted according to a probability measure depending on the squared difference  $m_{\text{obs}} - m_{\text{standard}}$  and the squared difference  $t_{\text{obs}} - t_{\text{predicted}}$ , i.e. between observed and predicted transit times. Transits within 10 arcsec of the top or bottom slit ends were rejected, as were transits within 30 arcsec of the apex of the inclined slits. In addition, transits near jet-firings were not used (see Section 8.3). In order to avoid a background dependence of the calibration parameters, only transits having background count rates below 18 counts per sample entered the calibration.

### Length of the Photosets

Independent sets of calibration parameters were computed for certain periods of time called photosets. Their length was chosen such that the calibration parameters could reasonably be assumed to be constant over the period. Keeping the length constant would, however, have resulted in large variations of the parameter errors  $\sigma_{\text{par}}$ , due to sky regions with varying star densities.

For this reason the length of the photosets was adapted automatically to yield a minimum of 4500 accepted calibration transits. Thus the length varied between 3.4 and 18.0 days. Due to the higher number of stars available in reprocessing, the number of photosets covering the whole mission for this data stream was 165 compared to 138 in the main processing.

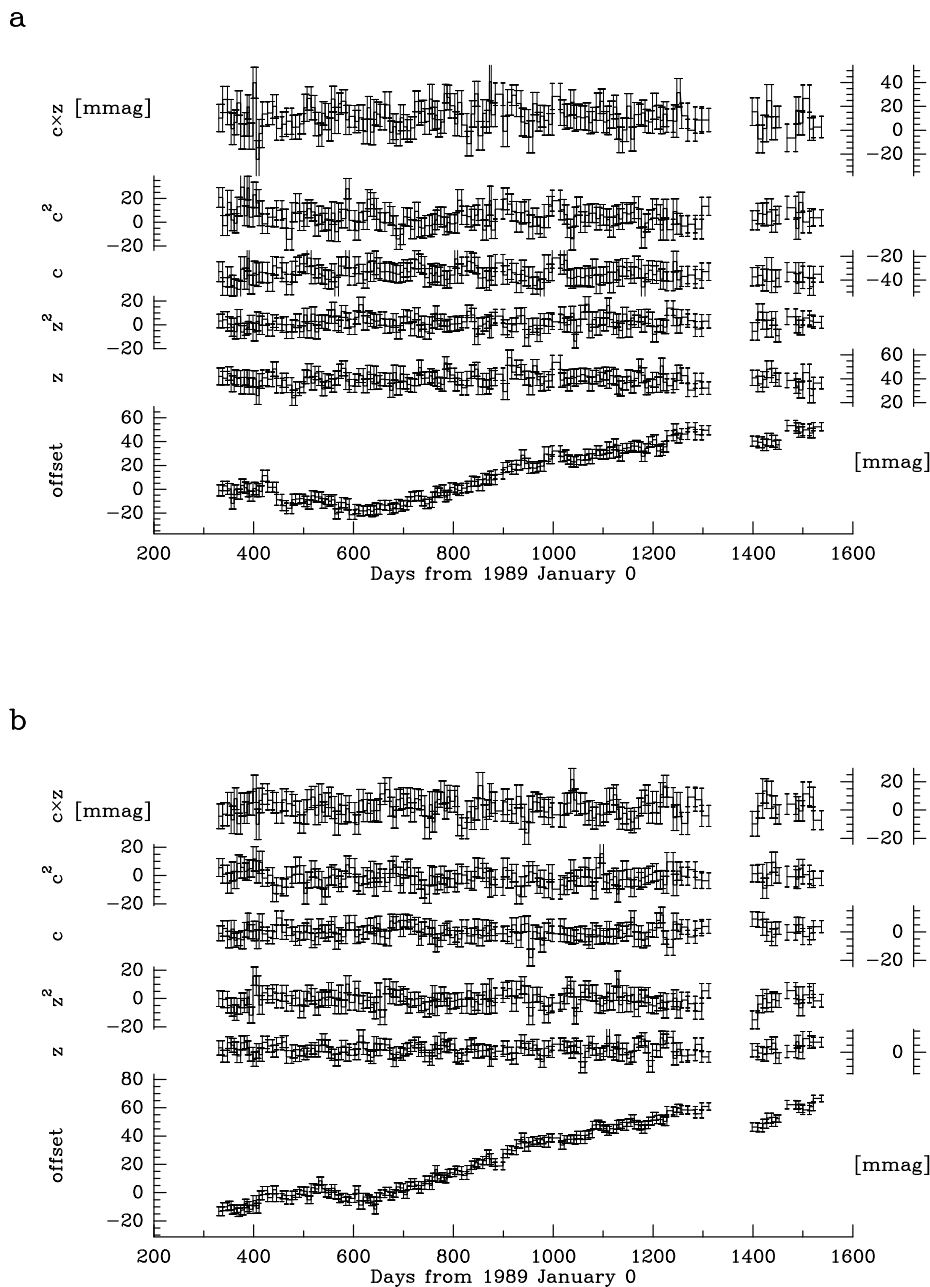


**Figure 8.1.** Results from the calibration for the whole mission, comprising 1190 days of measurements. The six calibration parameters and their mean errors are shown as a function of time: (a) for the  $B_T$  channel, and (b) for the  $V_T$  channel. The example parameter sets displayed here are for the main processing, vertical slit group, lower branch of the grid and following field of view. Note that  $c = B_T - V_T - 0.7$ . All parameters are given in millimag. The time axis gives days since 1989 January 0.

## Calibration Results

The computed parameters and their errors are shown in Figure 8.1, for two of the 16 possible combinations: vertical slits, lower branch, following field of view, for the  $B_T$  channel and  $V_T$  channel, respectively. Whereas the parameters depending on slit coordinate and colour showed no significant variations and no long-term drifts, the zero-point, or offset, exhibited a clear change with time. This effect was also present in the other 14 combinations not shown here. There was a monotonous change of roughly 55 millimag over the period between day 600 and day 1300, corresponding to a decrease in sensitivity of 5 per cent. The first three months of observations behaved differently in the two channels, without a continuous increase; this was possibly due to the many changes of instrument focus during this time. The offset also changed after three months of sun-pointing (the gap after day 1300) and again after a shorter gap near day 1470. All other parameters remained constant within their limits of uncertainty.

## Main Processing and Reprocessing Calibration

The motivation for distinguishing between these two processing chains in photometry was the usage of different single-slit response functions in the detection process (see Chapter 10). In the main processing, observations of bright stars were severely affected by the non-linearity of the photomultipliers at high count rates, yielding too faint magnitudes. During the reprocessing estimation the amplitudes for bright stars were obtained from the wings of the signal where the count rates were lower and the photomultipliers behaved linearly. As a consequence, observations of stars brighter than  $V_T = 3$  mag in the Tycho Catalogue and the Epoch Photometry Annex were taken from reprocessing photometry. Regarding the calibration parameters  $c_i$  there was no significant difference between main and reprocessing calibration. Thus, Figure 8.1 is not repeated for reprocessing.

---

## 8.3. Verification Methods

---

The present section deals with the comparison of the observed median and the ground-based standard magnitudes of the stars in the Tycho internal transit data base (TPOC, see Chapter 11). Overall properties of the published catalogues are discussed in Chapters 16 and 19.

Verification took place at different levels of processing, starting from immediate comparisons of observed magnitudes of standard stars with the standard star catalogue. More crucial comparisons were done at the level of the Tycho internal transit data base. This data base served as a basis to construct the Tycho Epoch Photometry Annex and Tycho Catalogue, as described in Chapter 11.

### Verification During Processing

As soon as the calibration parameters had been computed for a given photoset, they were applied to all observations of selected stars (the selection for this purpose being larger than the set of standard stars). The resulting calibrated transit data entered into

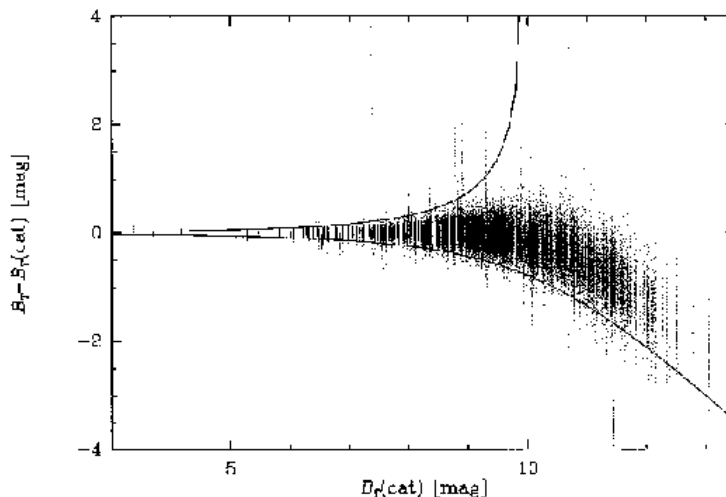


**Figure 8.2.** Reduced Tycho observations for 937 stars with ground-based magnitudes in a given sky region. Each point represents one observation and gives the difference between the reduced and ground-based magnitude for a single transit. Thus, transits for a given star show up on a line with constant ground-based  $B_T(\text{cat})$ . The solid curves indicate the  $3\sigma$  limits from photon noise for a background of 18 counts per sample as given by Equation 8.6.

a gradually increasing transit catalogue. This catalogue allowed a crucial external verification of the data. A completely independent calibration of the star mapper (including a different background and signal amplitude estimation) was carried out by the NDAC consortium. Calibrated magnitudes and error estimates were checked to be consistent between these two data streams. This was done for star mapper data from the start of the mission, using a sample of up to 30 000 stars.

### Effects of Jet Firings

Early investigations showed that the estimated signal amplitudes were affected by errors in the assumed instantaneous scan speed. For instance, an error of  $0.2 \text{ arcsec s}^{-1}$  could change the measured magnitude by about 0.010 mag. This led to the exclusion of all transits within about 2.1 s following a jet firing of the satellite attitude control system.

### Recalibration of Passbands

During the mission the Tycho spectral passbands were redetermined (see Chapter 13). This necessitated a revision of the standard star magnitudes, which in turn resulted in changes of the instrument calibration parameters. A direct comparison between calibrated transits from the old and the new system showed that only few of the calibration parameters had actually changed. In the  $B_T$  channel, the offset and colour term were affected, while in the  $V_T$  channel only the colour term had changed. This was consistent with the fact that mainly the  $B_T$  passband had been redefined. The change in the  $B_T$  offset was of the order of 20 millimag. It can directly be seen when comparing Figure 8.1(a) with Figure 1 in Großmann *et al.* (1995).

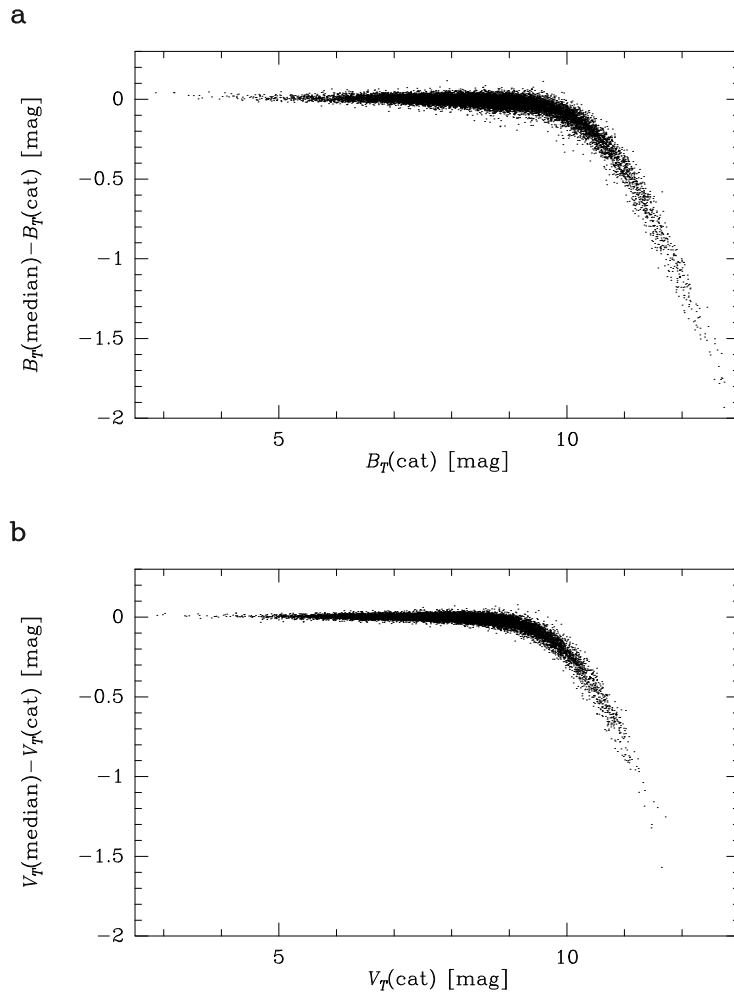


**Figure 8.3.** Calibrated Tycho observations of 17 683 standard stars distributed over the whole sky. Each point represents the median magnitude for one star. The figure shows the difference between the observed Tycho median magnitude and the ground-based magnitude: (a) for the  $B_T$  channel, and (b) for the  $V_T$  channel.

### Modifications of the Standard Star Sample

The redefinition of the passbands did not only lead to changed standard star magnitudes, but also to a change in the sample of standard stars. At the time of the change, existing satellite data could already be used to check the (supposedly single) standard stars for duplicity. In addition, results of an early calibration of 800 days of mission (Großmann *et al.* 1995) were used to cancel variable stars and possible misidentifications from the standard star sample.

## The Standard Stars: Catalogued and Observed Values

The original sample of about 30 000 stars with ground-based magnitudes contained many stars which were not usable for the calibration process (see Section 8.2). This is clearly demonstrated in Figure 8.2, showing about 100 000 single observations of 937 stars in a given sky region. While most observations are located within the  $3\sigma$  photon noise limit, several clearly fall outside. These observations either indicate variable stars, close doubles, or stars with an incorrect ground-based magnitude. Removing these stars restricted the sample to 17 683 stars. However, the sample actually used during main processing and reprocessing calibration was smaller still, because of the magnitude limits imposed in addition (see Section 8.2).

Figure 8.3 compares the calibrated Tycho magnitudes of the ‘cleaned’ 17 683 standard star sample with the catalogued  $B_T$  and  $V_T$  magnitudes. For each star the difference between the Tycho median magnitude and the ground-based magnitude is plotted. The strong bias for stars fainter than the 9.0 mag is due to the censoring (i.e. non-detection) of individual transits. It is the reason why standard stars fainter than 9.0 mag were excluded from the determination of calibration parameters, and why the usage of median magnitudes for the Tycho Catalogue was restricted to stars brighter than  $V_T = 8.0$  mag and  $B_T = 8.5$  mag. The fainter stars had to be subjected to the more sophisticated de-censoring treatment described in Chapter 9.

V. Großmann



## 9. DE-CENSORED MAGNITUDES OF FAINT STARS

*The Tycho Catalogue is dominated by stars too faint to be detected every time they were crossing the star mapper slit systems. This means that some of their transits got lost in the detector noise. Simple median magnitudes of detections consequently have a large bias, of 0.2 and 0.8 mag at  $V_T = 10$  and 11 mag. Therefore, the magnitudes of the faint stars have been derived not only from the detections, but taking into account the censored measurements. This procedure, called 'de-censoring', was used for computing the  $B_T$  and  $V_T$  magnitudes of about 1 018 000 stars. A comparison with ground-based photometric standard magnitudes showed that the bias was reduced to a value of 0.025 and 0.07 mag at  $V_T = 10$  and 11 mag, which is less than the standard errors. The magnitudes have been corrected for this systematic error, and it has been verified that the quoted standard errors are fairly realistic external errors.*

---

### 9.1. Introduction

---

The Tycho catalogue contains all the stars which received enough detections for the derivation of an astrometric solution with an acceptable accuracy. Among several conditions, a minimum number of 30 transits usable in astrometry was requested. Since this number is only about 25 per cent of the mean number of transits per star, the catalogue content is dominated by stars which are too faint to be detected each time they crossed the star mapper slit systems.

For these stars, the acquisition of a detection depends on two factors. The first is related to the circumstances of the transits; since the transits were detected only when the signal-to-noise ratio was larger than 1.5, the limit of detectability was shifted toward bright magnitudes when the background increased; moreover, the mean number of photons received from the star depends also on the slit system (vertical or inclined), the field (preceding or following), and so on. The second factor is a matter of chance; the actual number of photons counted when a star is crossing a slit system is approximately the mean value, but with statistical variations. When only the signals above a threshold are detected, the fainter signals are censored, and the remaining ones are on average brighter than the mean magnitude of the star. An estimation of this bias was derived from standard stars and is plotted in Figure 8.3(b) for the  $V_T$  magnitude. It appears

from this figure that all stars fainter than  $V_T = 10.5$  mag have a bias increasing with the true magnitudes in such a way that their measured magnitudes were in fact always about 10. Therefore, the bias cannot be determined from the mean measured magnitude alone.

The median magnitudes were kept for about 30 000 stars with  $V_T < 8$  mag and  $B_T < 8.5$  mag. The magnitude of the other stars were computed with a method taking into account the censored measurements. This method is presented hereafter. It is based on a statistical model that is described in Section 9.2. The verification of its validity and the derivation of some parameters is presented in Section 9.3. The complete procedure is explained in Section 9.4. The results and the correction of the remaining bias are presented in Section 9.5.

This chapter describes the de-censoring as it was actually carried out. The earlier brief descriptions in Section 1.6 and in Volume 1, Section 2.2 differ slightly.

---

## 9.2. The Statistical Model

---

Before retrieving information from non-detections, it is necessary to know how the measurements were done. The data acquisition was described previously in Chapters 4 and 8, but the process is too complicated to be taken completely into account. The statistical model is a simplified summary of the whole process, restricted to the main characteristics.

### General Outline and Detection Censoring

In the absence of any star, background photons were counted in both the  $B_T$  and  $V_T$  channels. The intensity of the background was estimated in each channel, each time the transit of a star was predicted. When a star was crossing a slit system of the star mapper, the increase of the photon count was estimated within an interval of 6.7 samples (1 sample = 1/600 s); 6.7 is expressed as 1/0.15 hereafter.

The total number of photons contributing to the detection of the star was then:  $N_{B_T+V_T} = n_{\text{back}_B} + n_{\text{back}_V} + n_B + n_V$ , where  $n_{\text{back}_B} + n_{\text{back}_V}$  photons were emitted by the background, and  $n_B + n_V$  photons were emitted by the star in the two channels.  $N_{B_T+V_T}$  obeys a Poisson distribution; this distribution depends only on one parameter, the mean value of  $N_{B_T+V_T}$ , denoted  $\langle N_{B_T+V_T} \rangle$  hereafter:

$$\langle N_{B_T+V_T} \rangle = \langle n_{\text{back}_B} \rangle + \langle n_{\text{back}_V} \rangle + \langle n_B \rangle + \langle n_V \rangle \quad [9.1]$$

$\langle n_{\text{back}_B} \rangle$  and  $\langle n_{\text{back}_V} \rangle$  were derived from the intensities of the background expressed in counts per sample.  $\langle n_B \rangle$  and  $\langle n_V \rangle$  are related to the actual magnitudes of the star,  $B_T$  and  $V_T$ , in the following equations:

$$\langle n_B \rangle = 10^{0.4(B_{\text{cal}} - B_T)} / 0.15 \quad [9.2]$$

$$\langle n_V \rangle = 10^{0.4(V_{\text{cal}} - V_T)} / 0.15 \quad [9.3]$$

where  $B_{\text{cal}}$  and  $V_{\text{cal}}$  are calibration terms representing the instrument sensitivity. These terms were called  $m_{\text{off}}$  in Chapter 8; their values are given in Table 8.1.

The detection of a stellar transit depended on its signal-to-noise ratio,  $SNR_{B_T+V_T}$ . The signal-to-noise ratio of a signal  $S$  is generally defined as  $SNR = S/\sigma_S$ , and for a Poisson distribution with the parameter  $\lambda$ ,  $\sigma_\lambda = \sqrt{\lambda}$ .  $SNR_{B_T+V_T}$  is then defined as:

$$SNR_{B_T+V_T} = \frac{N_{B_T+V_T} - \langle n_{\text{back}_B} \rangle - \langle n_{\text{back}_V} \rangle}{\sqrt{N_{B_T+V_T}}} \quad [9.4]$$

Thus, the statistical uncertainties of the two background contributions were neglected because they were formed as averages over long stretches of time. When  $SNR_{B_T+V_T}$  was larger than 1.5, the detection was recorded and the magnitudes of the stars were searched for in both channels. When  $SNR_{B_T+V_T}$  was below 1.5 the detection was censored, but, since the transit was predicted, the non-detection was recorded too; a non-detection consists essentially of the estimations of the background, and the calibration terms (or flags permitting their reconstruction).

### The Spurious Non-Detections

The non-detections were not all generated by transits below the detection threshold. The assignment of a detection to a given star depended on the following successive conditions:

- the epoch of the detection was close to the predicted transit time. The limit in time corresponded to an offset in position of 3 arcsec, but, on the other hand, the predicted transit times used in detection were inaccurate, since they were based on a preliminary determination of the attitude of the satellite;
- after the updating of the prediction using the final attitude determination, the distance between the star and the position of the slit was less than 0.6 arcsec. This value was derived from an histogram of the distances, in order to discard the false detections generated by random variations of the background (this selection is less critical in astrometry, where a limit of 1 arcsec was applied).

When the two conditions above were not satisfied, the actual detections of the stars were lost, but the transits were recorded as non-detections. These lost detections are referred to as ‘spurious non-detections’. The probability that a detection could be lost and changed into a spurious non-detection was included in the model as a constant parameter.

### The Magnitude Censoring

When a detection was obtained, the photon counts in the two channels were considered separately in order to determine the  $B_T$  and  $V_T$  magnitudes. Using the background level estimated by the detection process (see Chapters 2 and 4), one obtains:

$$B_{\text{meas}} = B_{\text{cal}} - 2.5 \log(N_B - \langle n_{\text{back}_B} \rangle) - 2.5 \log 0.15 \quad [9.5]$$

$$V_{\text{meas}} = V_{\text{cal}} - 2.5 \log(N_V - \langle n_{\text{back}_V} \rangle) - 2.5 \log 0.15 \quad [9.6]$$

where  $B_{\text{meas}}$  and  $V_{\text{meas}}$  are the measurements of  $B_T$  and  $V_T$ . In practice, however, the magnitudes were derived from a slightly different method, and measurements were obtained only when it was possible to fit the slit response function to the photon counts. As a consequence, the faintest measurements were censored. This second censoring is called the ‘magnitude censoring’ hereafter. It took effect below a threshold that had to

be determined. The  $B_T$  or  $V_T$  values which were not measured are flagged as such in the Tycho Epoch Photometry Annexes.

---

### 9.3. The Adaptation of the Model to the Actual Data

---

Since the model in the previous section is a simplification of the complexity of the processes involved in the photometric reduction, it was necessary to check that the data had the properties that were assumed. Moreover, two parameters still remained to be determined: the threshold of the magnitude censoring and the proportion of spurious non-detections.

In practice, several different versions of the model were used to compute de-censored magnitudes for about 1 018 000 stars of the Tycho catalogue. The parameters derived hereafter refer to the version used essentially for the 721 000 faintest stars. About 297 000 stars were treated with slightly different versions, but it was verified that the results were similar for the range of magnitudes where they were applied.

#### Correction of the Actual Measurements and Magnitude Censoring

The assumption that the cumulated photon counts obeyed a Poisson distribution with the parameter  $\langle N_{B_T+V_T} \rangle$  derived in Equations 9.1 to 9.3 was the keystone of the model. This hypothesis had to be checked, especially for faint stars, when the censoring was important. On the other hand, the distribution of  $N_{B_T+V_T}$  derived from the actual measurements cannot be directly compared with a Poissonian distribution, since it was biased as a result of the censoring. The following approach was then used to solve this problem: Only the  $B_T$  measurements of red standard stars were considered. Since these stars have  $B_T$  much fainter than  $V_T$ , their detections depended essentially on the photon counts in the  $V_T$  channel. Therefore, the statistics of the photon counts in  $B_T$  were not affected by the detection censoring, but only by the magnitude censoring (symmetrically, the  $V_T$  measurements of blue stars had the same property). The idea was then to check if the photon counts  $N_B$  obtained for a given  $\langle N_B \rangle$  obeyed a Poisson distribution with parameter  $\langle N_B \rangle$  as long as  $N_B$  is larger than a limit given by the magnitude censoring.

It appeared that the distribution of  $N_B$  contained an excess of measurements with large  $N_B$ . This was attributed to an overestimation of  $n_B$ , the number of photons received from the stars, or, in other words, to a non-linearity of the initial Tycho estimation process. Investigations were carried out in order to evaluate this bias. In practice, the amplitude of the signal,  $S_B$ , expressed in counts per sample, was considered instead of  $n_B$ ; they are equivalent, since  $S_B = 0.15 \times n_B$ . For each transit, the mean signal  $\langle S_B \rangle$  was derived from the real  $B_T$  magnitude and from the calibration terms according to Equation 9.2. At the same time, the estimated intensity of the background,  $\text{back}_B$ , expressed in counts per sample, was used instead of  $\langle n_{\text{back}_B} \rangle$ ; again,  $\text{back}_B = 0.15 \times \langle n_{\text{back}_B} \rangle$ . The measurements of several standard stars in narrow intervals of  $\text{back}_B$  and of  $\langle S_B \rangle$  were considered together, and the distributions of  $S_B$  actually obtained were compared to the theoretical distributions. An example of these comparisons is represented in Figure 9.1. Various thresholds in the signal-to-noise ratio in  $B_T$  were introduced, in order to take into account the magnitude censoring. It was found that the distribution of  $S_B$  is in agreement with the theoretical distribution when the following conditions are satisfied:

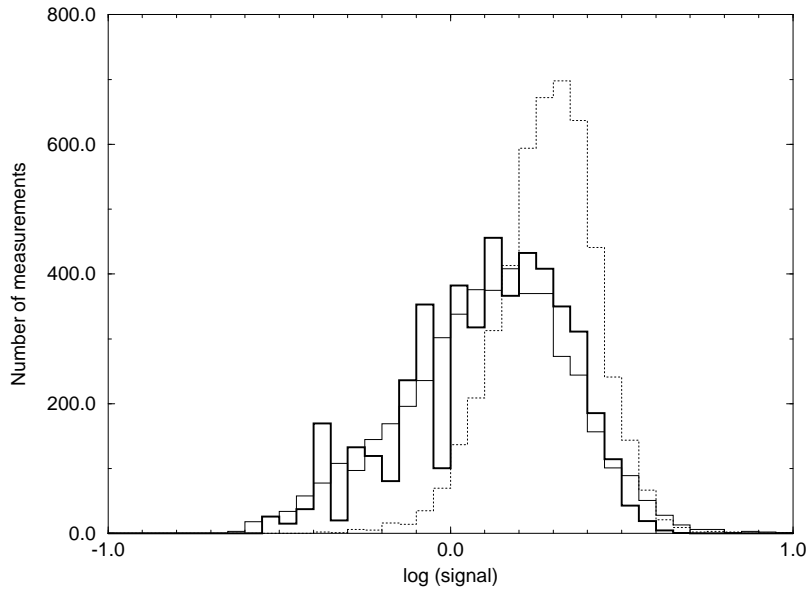


**Figure 9.1.** The distribution of the signals in  $B_T$ , derived from the measurements of the red standard stars with  $B_T - V_T > 0.7$  fulfilling the following conditions: transit of the inclined slit system,  $\langle S_B \rangle$  between 0.5 and 2 counts per sample, and  $\text{back}_B$  between 1 and 2 counts per sample. In order to take into account the magnitude censoring, the measurements with a signal-to-noise ratio  $\text{SNR}_B < 0.5$  are discarded. The dotted line refers to the signals estimated in the photometric reduction, and the thin solid line to the corrected signal. The distribution derived from the model is plotted as a thick line for comparison; it contains gaps and peaks because the total photon count in  $B_T$ ,  $N_B$ , was assumed to be an integer number.

- $S_B$  was corrected using a relation depending on its initial estimation, on the background, and on the slit system of the star mapper. The corrected  $S_B$  are given in Table 9.1. This correction was important for  $B_T$  fainter than about 11 mag, but it became negligible for brighter measurements;
- the corrected measurements of  $B_T$  with signal-to-noise ratios  $\text{SNR}_B < 0.5$  were discarded.

The measurements of the  $V_T$  magnitude should fit the model under the same conditions, because they were derived with the same algorithms as the measurements of  $B_T$ . The problems of the adequacy of the Poisson distribution and of the determination of the magnitude censoring were thus solved at the same time.

### Verification of the Detection Threshold

It was assumed in the model that the detection condition was  $\text{SNR}_{B_T+V_T} > 1.5$ , with  $\text{SNR}_{B_T+V_T}$  derived from Equation 9.4. Although the detection threshold  $\text{SNR} = 1.5$  was included in the detection process (see Chapter 6), the validity of this hypothesis needed to be confirmed, because the signal estimations used in the detection process were derived from a different algorithm to the estimations used in photometry. Therefore, the detections were not actually based on  $\text{SNR}_{B_T+V_T}$ , but on an estimation which is

**Table 9.1.** Calculation of the corrected signal from the initial estimation and from the background, according to the slit systems; signals and backgrounds are expressed in counts per sample.

Slits			Vertical	Inclined
$S < 2$	and	back < 2	$S \times (0.8 \ln(1 + S) - 0.23)$	$S \times (0.8 \ln(1 + S) - 0.2)$
		back $\in [2, 3[$	$S \times (0.9(\ln(1 + S))^{1.1} - 0.45)$	$S \times (0.8(\ln(1 + S))^{1.3} - 0.35)$
		back $\in [3, 4[$	$S \times (0.9(\ln(1 + S))^{1.1} - 0.59)$	$S \times (0.8(\ln(1 + S))^{1.2} - 0.43)$
		back $\in [4, 5[$	$S \times (0.9(\ln(1 + S))^{1.1} - 0.638)$	$S \times (0.8(\ln(1 + S))^{1.2} - 0.505)$
$S > 2$	or	back > 5	$S - 3 \times \text{back}^2 / (S + \text{back})^2$	$S - 2 \times \text{back}^2 / (S + \text{back})^2$

called  $SNR_{\text{det}}$  hereafter. For this reason, it is necessary to check that, after corrections of the signals  $S_B$  and  $S_V$ ,  $SNR_{B_T+V_T}$  is equivalent to  $SNR_{\text{det}}$ .

A random set of detections with  $SNR_{\text{det}}$  close to 1.5, and with available measurements of both  $B_T$  and  $V_T$  was considered. The signals  $S_B$  and  $S_V$  were derived from the measured magnitudes  $B_T$  and  $V_T$ , and they were corrected by means of Table 9.1.  $SNR_{B_T+V_T}$  were then calculated, and compared to  $SNR_{\text{det}}$ . It appeared that the median of  $SNR_{B_T+V_T}$  was close to the median  $SNR_{\text{det}}$ , but the scatter was rather large: for 70 per cent of the detections, the ratio  $SNR_{\text{det}}/SNR_{B_T+V_T}$  was between 0.8 and 1.6.

The detection condition  $SNR_{B_T+V_T} > 1.5$  was finally considered as valid, although it is only an approximation of the actual statistical properties of the data. In reality, some transits were detected although  $SNR_{B_T+V_T}$  was below the threshold, and some others were censored although they should have been detected.

### The Proportion of Spurious Non-Detections

The proportion of spurious non-detections was derived from bright photometric standard stars: it was found that about 6 per cent of the transits of bright stars resulted in non-detections, which were in fact lost detections. For both faint and bright stars, this percentage is also the proportion of spurious non-detections among all the transits that would have been detected if they were searched in the right place.

---

## 9.4. The De-Censoring Procedure

---

As a matter of taxonomy, according to the definitions reported by Kendall & Stuart (1961), the censoring in Tycho is a ‘censoring on the left of Type I’, since the measurements smaller than a threshold were lost. Various techniques for solving statistical problems involving missing data were developed during the last decades (Little & Rubin 1987). Some of them were successfully applied in astronomy (Feigelson & Nelson 1985, Isobe *et al.* 1986). However, the censoring of the Tycho data was rather unusual, since it came from two different origins: the detection censoring was related to the photon counts in the  $B_T$  and in the  $V_T$  channels considered together, but the magnitude censoring depended only on the photon counts in one channel. Moreover, the rate of spurious non-detections should also be taken into account. Therefore, the iteration

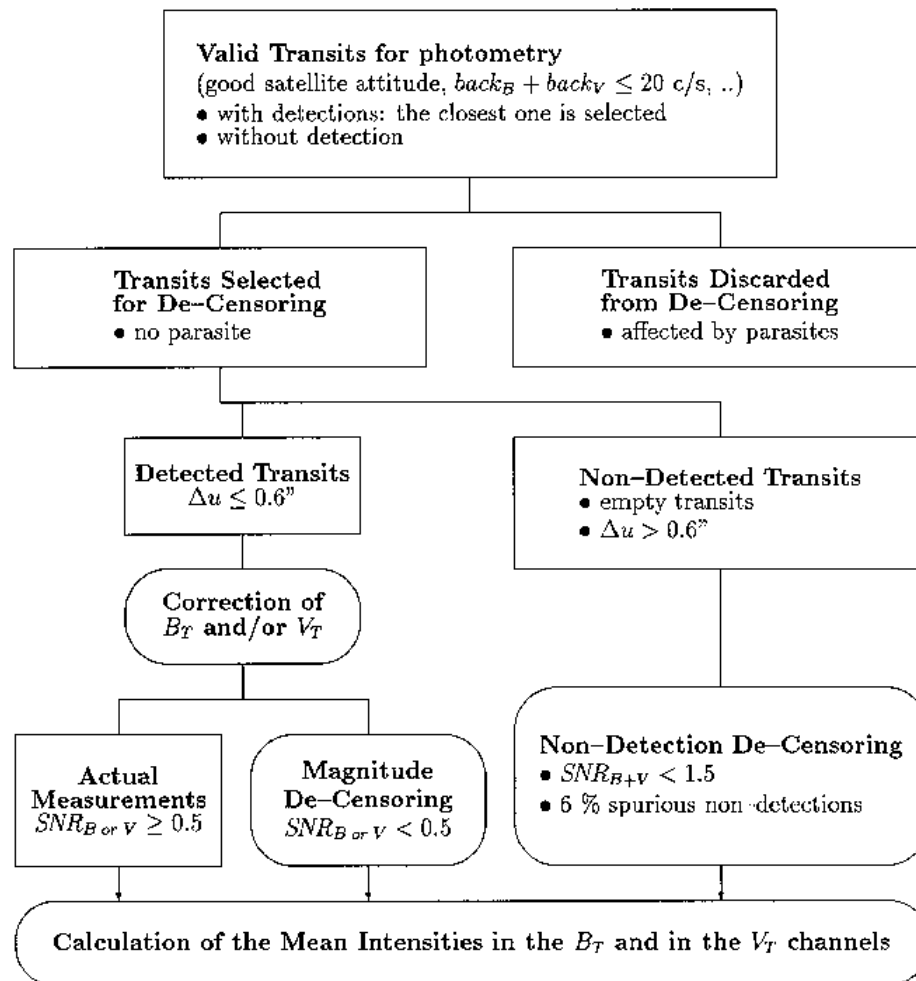


**Figure 9.2.** The overall organisation of de-censoring. The data and the condition of selection are indicated in rectangular boxes; the oval boxes represent the processes.

technique explained hereafter was preferred over the more sophisticated methods, such as ‘survival analysis’, presented in the papers mentioned above.

The basic principle of the calculation consisted of computing the mean intensity corresponding to each censored measurement, assuming the  $B_T$  and  $V_T$  magnitudes of the star were known. The mean intensities were related to the censored measurements, and new estimations of  $B_T$  and  $V_T$  were derived from all transits. The calculation was then repeated until it had converged. The different processes are explained hereafter, and the overall organisation is summarized in Figure 9.2.

### The Input Data

Every time a star of the catalogue crossed a slit system of the star mapper, the following data were recorded in the complete photometric observation catalogue (they are also given in the Tycho Epoch Photometry Annex for a selection of stars):

- a parasite flag, indicating when another star was crossing a slit system at the same time;

- the background in both channels  $\text{back}_B$  and  $\text{back}_V$ , expressed in counts per sample;
- a set of flags determining  $B_{\text{cal}}$  and  $V_{\text{cal}}$ , the calibration terms defined in Equations 9.2 and 9.3.
- when the transit was detected, the photometric reduction attempted to derive the measurements  $B_{\text{meas}}$  and  $V_{\text{meas}}$ .

The transits affected by parasites or with the total background  $\text{back}_B + \text{back}_V > 20$  counts per sample were not taken into account.

Each iteration was based on *a priori* values of the magnitudes,  $B_{\text{iter}}$  and  $V_{\text{iter}}$ . These values were assumed to be constant in time; as a consequence, the magnitudes derived from de-censoring are different from the median magnitudes when the stars are variable.

### The Weights of the Transits

The transits of each star were obtained with backgrounds and instrumental sensitivities varying from one transit to another. In order to base the calculation on the most reliable transits, weights were derived from the transit parameters and assigned to the transits in each channel. The weights were defined as the squares of the signal-to-noise ratios, assuming the magnitudes  $B_{\text{iter}}$  and  $V_{\text{iter}}$ ; for each channel, they were:

$$W_M = \frac{10^{0.8(M_{\text{cal}} - M_{\text{iter}})}}{0.15 \times (10^{0.4(M_{\text{cal}} - M_{\text{iter}})} + \text{back}_M)} \quad [9.7]$$

where  $M$  designates the  $B_T$  or the  $V_T$  channel. A couple of weights ( $W_B$ ,  $W_V$ ) was assigned to each transit used in the de-censoring, censored or not.

### The Treatment of the Actual Measurements

When a measurement of the magnitude was recorded, it was used to reproduce the original signal:

$$S_M = 10^{0.4(M_{\text{cal}} - M_{\text{meas}})} \quad [9.8]$$

The corrected signal,  $S'_M$ , was derived from the formulae in Table 9.1. The signal-to-noise ratio in the channel was then calculated from:

$$\text{SNR}_M = \frac{S'_M}{\sqrt{0.15 \times (S'_M + \text{back}_M)}} \quad [9.9]$$

When  $\text{SNR}_M$  was less than 0.5, the measurement of the magnitude was censored. Otherwise, the measured intensity of the star was derived by:

$$I_M = S'_M 10^{-0.4M_{\text{cal}}} \quad [9.10]$$

$I_M$  received the weight  $W_M$  calculated above and it was included in the calculation of the mean intensity of the star,  $\langle I_M \rangle$ , in Equation 9.18.

### The Censored Magnitudes

A magnitude measurement was censored when a transit was detected, but the photometric reduction failed to derive a measurement, or when the corrected signal provided

$SNR_M < 0.5$ . It was assumed that the censored magnitudes all satisfied this latter condition, and the upper limit of the total number of photons in the channel ‘ $M$ ’, called  $N_{M\text{sup}}$  was derived from the equation:

$$\frac{N_{M\text{sup}} - \text{back}_M/0.15}{\sqrt{N_{M\text{sup}}}} = 0.5 \quad [9.11]$$

On the other hand, the actual number of photons,  $N_M$ , obeyed a Poisson distribution with the parameter  $\langle N_M \rangle$ :

$$\langle N_M \rangle = 0.15 \times (10^{0.4(M_{\text{cal}} - M_{\text{iter}})} + \text{back}_M) \quad [9.12]$$

The average photon count when  $N_M < N_{M\text{sup}}$  was thus derived. The mean intensity corresponding to the censored magnitude was then:

$$I_M = (0.15 \times \langle N_{M; N_M < N_{M\text{sup}}} \rangle - \text{back}_M) \times 10^{-0.4M_{\text{cal}}} \quad [9.13]$$

$I_M$  then received the weight  $W_M$ , and it was taken into account in the calculation of the mean intensity of the star, as if it were derived from an actual measurement. This is the central idea of the de-censoring procedure.

### The Censored Detections

The calculation of mean intensities had to take into account the contribution of ‘censored detections’ when a predicted transit was not detected.

The censored detections were due to a total photon count in both channels,  $N_{B_T+V_T}$ , below an upper limit related to the detection condition in signal-to-noise ratio. This limit, referred to as  $N_{B_T+V_T\text{sup}}$ , was the solution of the equation:

$$\frac{N_{B_T+V_T\text{sup}} - (\text{back}_B + \text{back}_V)/0.15}{\sqrt{N_{B_T+V_T\text{sup}}}} = 1.5 \quad [9.14]$$

with  $N_{B_T+V_T} = N_B + N_V$ , where  $N_B$  and  $N_V$  obeyed Poisson distributions with the parameters  $\langle N_B \rangle$  and  $\langle N_V \rangle$  derived from Equation 9.12. The mean intensities  $I_{B\text{cen}}$  and  $I_{V\text{cen}}$  were computed from simulations of pairs  $(N_B, N_V)$ , taking into account only those such as  $N_B + N_V < N_{B_T+V_T\text{sup}}$  (in practice, only  $N_B < N_{B_T+V_T\text{sup}}$  and  $N_V < N_{B_T+V_T\text{sup}}$  were generated). The probability of getting a censored detection,  $P_{\text{cen}}$ , was calculated at the same time.

### Spurious Non-Detections

Since spurious non-detections were lost detections, they also contributed to the censored data. However, the censoring is then in the opposite sense, it being assumed that the transits would have been detected if they had been searched for at the correct place. For a lost detection, the mean intensities  $I_{B\text{lost}}$  and  $I_{V\text{lost}}$  could in principle be calculated analogously to  $I_{B\text{cen}}$  and  $I_{V\text{cen}}$ , but now assuming  $N_B + N_V > N_{B_T+V_T\text{sup}}$ . In practice, however,  $I_{B\text{lost}}$  and  $I_{V\text{lost}}$  were derived from the intensities due to censoring and from the probability of censoring with the equation:

$$I_{M\text{lost}} = \frac{I_{M\text{iter}} - P_{\text{cen}} I_{M\text{cen}}}{1 - P_{\text{cen}}} \quad [9.15]$$

where  $I_{M\text{iter}}$  was derived from the input magnitude assumed in the present iteration step:

$$I_{M\text{iter}} = 10^{-0.4M_{\text{iter}}} \quad [9.16]$$

### Merging the Censored Detections and the Spurious Non-Detections

It was assumed that, when the photon count was above the detection threshold, it was possible that the detection was lost, with the probability  $P_{\text{lost}} = 6$  per cent. The intensities corresponding to censoring and to a lost detection were then combined. Expressing  $I_{M_{\text{lost}}}$  as in Equation 9.15, the mean intensities for a transit without detection were finally:

$$I_M = \frac{P_{\text{lost}} I_{M_{\text{iter}}} + P_{\text{cen}} (1 - P_{\text{lost}}) I_{M_{\text{cen}}}}{P_{\text{cen}} + (1 - P_{\text{cen}}) P_{\text{lost}}} \quad [9.17]$$

$I_M$  then received the weight calculated in Equation 9.7.

### The Mean $B_T$ and $V_T$ Magnitudes and the Convergence Criterion

After the calculations above, all the transits selected in de-censoring received intensities in the  $B_T$  and in the  $V_T$  channel. The actual measurements were transformed to intensities by Equation 9.8, the correction in Table 9.1, and Equation 9.10. Mean intensities were related to the missing (censored) measurements censoring. The next process was then the derivation of the mean  $B_T$  and  $V_T$  magnitudes of the star for the iteration step.

In on-ground photometry, the mean magnitude of a star is computed as the average of the magnitude measurements. This method is used since the distribution of the logarithm of the photon counts obeys a Gaussian law, due to scintillation (Sterken & Manfroid 1992). This was not true for Tycho photometry, and the mean magnitudes were derived from the average intensities. For each channel, the average intensity of the star,  $\langle I_M \rangle$ , was computed from:

$$\langle I_M \rangle = \frac{\sum W_M I_M}{\sum W_M} \quad [9.18]$$

The magnitude was then:

$$M_{\text{sol}} = -2.5 \log \langle I_M \rangle \quad [9.19]$$

The input magnitude of the next iteration step depended on the direction of the shift of the solution,  $M_{\text{sol}}$ , from the input magnitude  $M_{\text{iter}}$ . When the shift was in the same direction as in the previous step, the new input  $M_{\text{iter}+1}$  was even farther from  $M_{\text{iter}}$  than  $M_{\text{sol}}$ . On the other hand, when  $M_{\text{sol}}$  was coming back toward the previous input magnitude,  $M_{\text{iter}-1}$ , then  $M_{\text{iter}+1}$  was exactly  $M_{\text{sol}}$ ; moreover, a convergence flag was then turned on, when the shift was less than 0.05 mag.

New iterations were computed as long as the convergence was not obtained in both channels. When one of the convergence flags was on, it was revisited after each iteration, and it was turned off when the new solution was farther than 0.05 mag from the magnitude obtained when it was turned on. When  $B_T$  and  $V_T$  had both converged, an ultimate iteration was still done, including the computation of the percentiles and the estimation of the errors.

## Computation of the Percentiles

The median and the 15th and 85th percentiles were computed for the measurements of  $V_T$ . This calculation was different from the calculation of the mean magnitudes in two aspects: no weights were assigned to the transits, and the censored or missing measurements were not changed in mean measurements, but in the distribution function of the magnitude. In practice, a histogram of the  $V_T$  magnitudes was calculated. The bin size of the histogram depended on the magnitude derived in the previous iteration. For stars fainter than 8.8 mag, it was:

$$\text{step} = \min(0.008 + 0.017 \times (V_T - 8.8)^2, 0.10) \quad [9.20]$$

Each actual measurement was simply counted in the corresponding bin. Each censored magnitude became a normalized distribution function which was integrated in the bins corresponding to magnitudes fainter than the measurement threshold. The treatment of the missing detections was more complicated, since the distributions were not restricted to magnitudes fainter than the detection threshold, due to the probability of missing detections. It was then necessary to calculate the distribution functions for the whole range of the histogram.

Each percentile was derived from the histogram of the magnitudes, using a linear interpolation on the bin where it was found.

The percentiles derived from de-censoring should be used with caution, since a basic hypothesis of de-censoring is that the stars are not variable. For this reason, they were included in the Tycho catalogue only when  $V_T$  was fainter than 9.5 mag. For stars brighter than this limit, the percentiles derived from the actual measurements were preferred, but a bias correction was applied.

## Estimation of the Errors

The errors of the magnitudes  $B_T$  and  $V_T$  of the stars were derived from estimations of the variances of the mean intensities  $\langle I_B \rangle$  and  $\langle I_V \rangle$ :

$$\text{var}(\langle I_M \rangle) = \frac{\sum W^2 \text{var}(I_M)}{(\sum W)^2} \quad [9.21]$$

The problem was then to calculate the variance of the intensity for each transit,  $\text{var}(I_M)$ . The calculation was easy for the actual measurements since:

$$I_M = (0.15N_M - \text{back}_M) \times 10^{-0.4M_{\text{cal}}} \quad [9.22]$$

and since the background was a constant determined for the transit, it appeared that:

$$\text{var}(I_M) = 0.15 \times (I_M 10^{-0.4M_{\text{cal}}} + \text{back}_M 10^{-0.8M_{\text{cal}}}) \quad [9.23]$$

where  $I_M$  is the corrected intensity calculated by Equation 9.10.

The variance of the mean intensity derived for a censored magnitude or for a missing detection was much more difficult to calculate. It depended on the accuracy of the assumed magnitude (but this is the very result that was searched), and also on the accuracy of the model. The difference between  $SNR_{B_T+V_T}$  and  $SNR_{\text{det}}$  was neglected in calculating  $I_B$  and  $I_V$ , but the effect of this simplification could not be ignored in the estimation of the variances. A problem this complicated cannot be solved analytically,

but only with simulations; unfortunately, this technique would have been too time-consuming to treat one million stars within the time limit. On the other hand, the errors of the magnitudes of the photometric standard stars were derived from the actual measurements only, and it appeared that they were reliable estimates. Therefore, the censored detections and the censored magnitudes were finally ignored in calculating Equation 9.21.

The standard deviation of the intensity,  $\sigma_{\langle I_M \rangle}$  was computed as  $\sqrt{\text{var}(\langle I_M \rangle)}$ , and the error of the magnitude ‘on the bright side’, called  $\sigma_M^-$ , was defined as the offset in magnitude when the intensity was increased by  $\sigma_{\langle I_M \rangle}$ :

$$\sigma_M^- = 2.5 \log \left( 1 + \frac{\sigma_{\langle I_M \rangle}}{\langle I_M \rangle} \right) \quad [9.24]$$

$\sigma_M^-$  is called the ‘error on the bright side’ since the probability that the actual magnitude is brighter than  $M - \sigma_M^-$  is 16 per cent. On the other hand, the ‘error on the faint side’ is the error corresponding to a  $1\sigma$  decrease of the intensity; it may be derived from  $\sigma_M^-$  with Equation 9.25:

$$\sigma_M^+ = -2.5 \log(2 - 10^{0.4\sigma_M^-}) \quad [9.25]$$

$\sigma_M^+$  is larger than  $\sigma_M^-$ , and it is impossible to derive when  $\sigma_M^- > 0.75$  mag. For this reason, only  $\sigma_{B_T}^-$  and  $\sigma_{V_T}^-$  were given in the Tycho Catalogue.

---

## 9.5. Verification of the Results of De-Censoring

---

### Bias of the De-censored Magnitudes

The differences between the de-censored magnitudes and those of standard stars are plotted in Figure 9.3 for the  $V_T$  magnitudes. The large bias toward bright magnitudes that was present in Figure 8.3(b) has disappeared, but a closer examination of this plot reveals that the de-censored magnitudes are about 0.06 mag too faint when  $V_T > 10.6$  mag. For the  $B_T$  channel, a 0.05 mag bias was also found around  $B_T = 11.4$  mag. These biases were determined as functions of the actual on-ground magnitudes, and were next converted into functions of the de-censored magnitudes. Since the number of standard stars was very small for  $V_T > 11$  mag and  $B_T > 11.8$  mag, the corrections are accurate only below these limits. They were added to the de-censored magnitudes, resulting in the final  $V_T$  and  $B_T$ . In Figure 9.4, the thick line represents the proportion of photometric standard stars with Tycho  $V_T$  fainter than on-ground  $V$  minus 50 per cent; it is always close to 0 per cent, confirming that the bias was properly corrected.

### Verification of the Error Estimates

If the computation of the errors was correct, the proportion of stars actually brighter than  $M - \sigma_M^-$  should be 16 per cent (again,  $M$  refers to the magnitude  $B_T$  or  $V_T$ ). On the other hand,  $\sigma_M^+$  should provide a 16 per cent proportion of stars actually fainter than  $M + \sigma_M^+$ . This was verified from the standard stars. In practice, the errors of the on-ground magnitudes must also be taken into account, and the differences between the Tycho magnitudes and the on-ground magnitudes were compared to the quadratic sums of the Tycho errors and of the on-ground errors. The results for  $V_T$  are presented in Figure 9.4. For  $V_T$  brighter than 9.5 mag, the proportion of stars outside the error

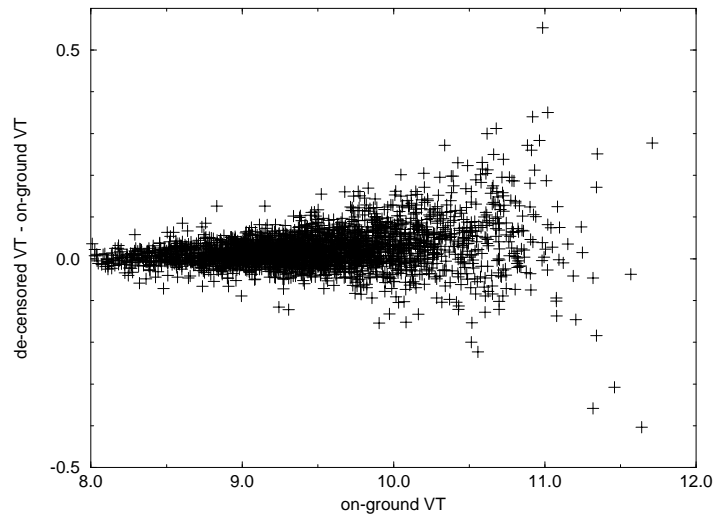


**Figure 9.3.** The slight remaining bias of the de-censored  $V_T$  magnitudes versus the true magnitudes of standard stars. This bias was corrected for the final Tycho magnitudes (see Figure 9.4).

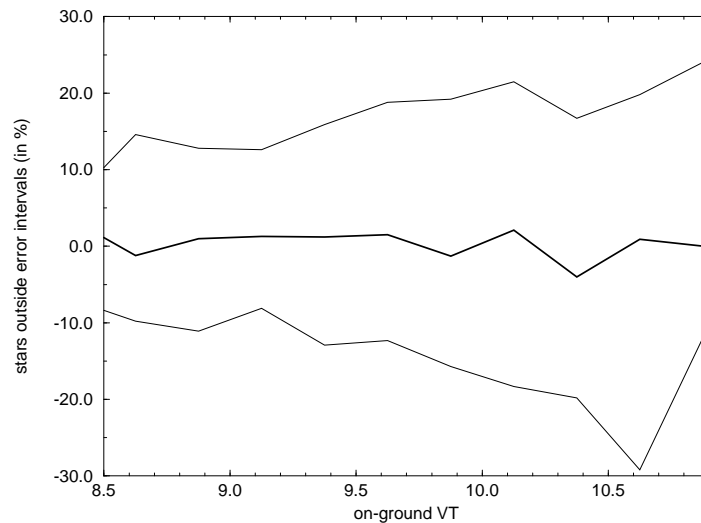


**Figure 9.4.** The proportions of stars outside the error intervals for  $V_T$ . The upper line is the proportion of photometric standard stars with Tycho magnitudes too faint at the  $1\sigma$  level when compared to on-ground magnitudes. The thick line is the excess of stars with Tycho magnitudes fainter than the on-ground magnitudes (see explanations in the text). The lower line is the proportion of photometric standard stars with Tycho magnitudes too bright at the  $1\sigma$  level; for readability of the figure, it is given as negative. Note that the figure thus contains the faint stars at the top. The proportions of stars outside the error interval appear too small when  $V_T$  is brighter than 9.5 mag, but this is due to overestimations of the errors of the on-ground magnitudes.

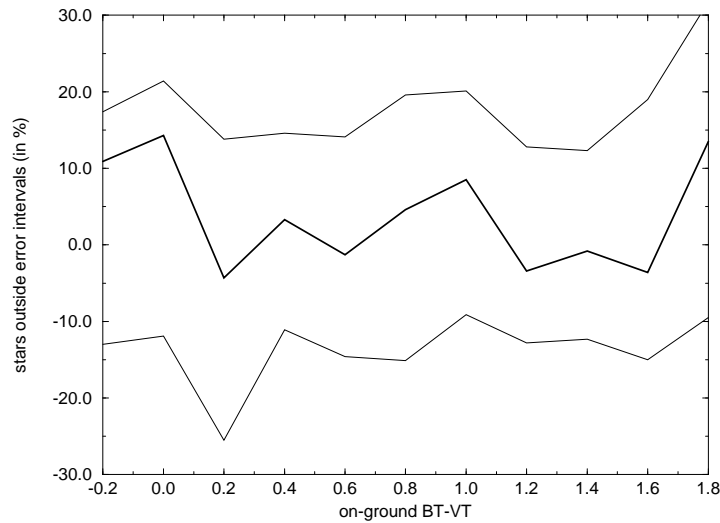


**Figure 9.5.** The proportions of stars outside the error intervals for  $B_T - V_T$  derived from the photometric standard stars fainter than  $B_T = 9.5$  magnitudes. The upper line is the proportion of stars with Tycho  $B_T - V_T$  too large (or too red) at the  $1\sigma$  level. The thick line is the excess of stars with Tycho  $B_T - V_T$  larger (or redder) than the corresponding on-ground value. The lower line is the proportion of stars with Tycho  $B_T - V_T$  too small (too blue) at the  $1\sigma$  level; for readability of the figure, it is given as negative. Note that the figure thus contains the red stars at the top.

intervals are even smaller than expected, suggesting that the Tycho errors could be overestimated. In fact, for so bright magnitudes, the on-ground errors are on average 3 times larger than the Tycho errors, and the overestimation concerns obviously the former rather than the latter. For  $V_T$  around 11 mag, the ratio of the errors is the opposite, and the agreement is acceptable.

The estimation of the error of  $B_T - V_T$  was also verified, as well as the absence of bias in the colour indices. Since a colour index corresponds to the ratio of two intensities, it is not straightforward to derive a standard deviation. The errors of  $B_T - V_T$  were derived from the 16 per cent and 84 per cent percentiles, which were calculated by assuming that the errors of  $\langle I_B \rangle$  and  $\langle I_V \rangle$  obeyed a Gaussian distribution in a good approximation. These percentiles were then calculated using the formulae:

$$\sigma_{B_T - V_T}^- = 2.5 \log \frac{c + t}{c - 1/t} \quad [9.26]$$

and

$$\sigma_{B_T - V_T}^+ = 2.5 \log \frac{c + 1/t}{c - t} \quad [9.27]$$

with  $c$  given by

$$c = \sqrt{\left(\frac{\langle I_B \rangle}{\sigma_{\langle I_B \rangle}}\right)^2 + \left(\frac{\langle I_V \rangle}{\sigma_{\langle I_V \rangle}}\right)^2} - 1 \quad [9.28]$$

and  $t$  given by

$$t = \frac{\sigma_{\langle I_B \rangle} \langle I_V \rangle}{\langle I_B \rangle \sigma_{\langle I_V \rangle}} \quad [9.29]$$

$\sigma_{B_T - V_T}^-$  is the error on the ‘blue side’ since the probability is 16 per cent that the actual  $B_T - V_T$  is less than the measured one minus  $\sigma_{B_T - V_T}^-$ . On the other hand,  $\sigma_{B_T - V_T}^+$  is the error on the ‘red side’. For simplicity, only the largest of the two was given in the Tycho

Catalogue. The proportions of stars outside the error interval given by Equations 9.26 and 9.27 were derived for both sides, from the photometric standard stars. Again, the errors of the on-ground magnitudes were taken into account. The proportion of stars with Tycho  $B_T - V_T$  larger than the corresponding on-ground value was also derived, in order to check that the Tycho colour indices were not biased. The results are shown in Figure 9.5. Apart from random variations due to the small number of standard stars (270 per bin on average, but only a few dozens at the extremities of the plot) the errors and the median look satisfactory.

J.-L. Halbwachs



## 10. REPROCESSING OF THE SATELLITE DATA

*The reprocessing of the Tycho data remedied some defects of the Tycho Input Catalogue and some defects of the main processing. For this purpose it repeated most processing steps, but for a much smaller number of objects. The use of improved software and of an update of (a part of) the input catalogue were the essential ingredients for the improvement over the main processing. All the raw data from the Tycho instrument were treated a second time, but no prediction updating and no star recognition processes were needed, because good on-ground attitude and a sufficiently precise star catalogue were used from the very start. The photometric and astrometric analysis for the reprocessing was performed independently from that for the main processing. The two separate data sets were then merged into the Tycho Catalogue, as described in Chapter 11.*

---

### 10.1. Introduction

---

The main processing of the Tycho raw data was a compromise between the wish to complete an output catalogue within a given (short) time and with the given resources of computing power and man power, while at the same time aiming for an optimum scientific exploitation of the data. Some of the drawbacks on data quality stemming from this compromise were eliminated for some groups of celestial objects by the reprocessing, as described in this chapter. Only after the start of the main mass processing did it become apparent that such a reprocessing for the most badly treated objects would be possible within the time frame and resources of the Tycho data analysis. Also, some of the defects needing improvement were discovered only at that stage. Thus, the reprocessing served a collection of different purposes. A special input catalogue, called Tycho Input Catalogue Update (TICU) was prepared. Its composition, reflecting the various specific purposes of the reprocessing, is described in Section 10.2. It had a total size of 306 766 entries, i.e. less than 10 per cent of the size of the Tycho Input Catalogue.

Special versions of the prediction, detection and transit identification software had to be written for the reprocessing, in order to avoid the prediction updating steps and to speed up and improve detection and transit identification. In contrast, the procedures used in the photometric and astrometric calibrations and reductions for the reprocessing

## TYCHO DATA FLOW - reprocessing

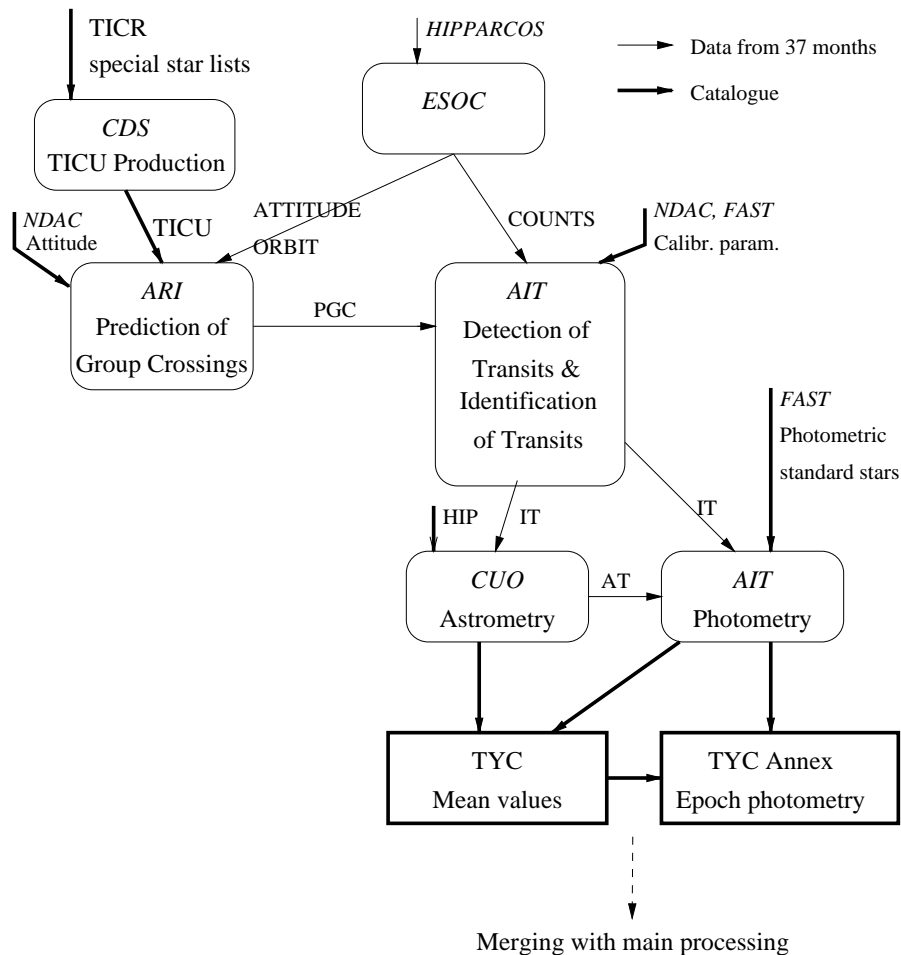


**Figure 10.1.** The data flow of the Tycho reprocessing. Explanation is given throughout Chapter 10. The abbreviations for the main institutes and data streams are the same as in Figure 1.2. TICU is the Tycho Input Catalogue Update, described in Section 10.2.

were the same as in the main processing. A special data stream was created for the solar system objects, which is described in Chapter 15.

The data flow in the Tycho reprocessing is sketched in Figure 10.1. It is simpler than that of the main processing. The individual steps and data streams are described in the following sections.

Originally, it was expected that the reprocessing results would be preferred over those from the main processing for a large fraction of the Tycho Input Catalogue Update objects. But later it was found that the reprocessing had some weaknesses, too. In the end, astrometric results from the reprocessing were included in the Tycho Catalogue for about 9000 stars, and photometric results for about 55 000 stars. This choice, and the reasons for it, are described in Chapter 11.

---

## 10.2. The Tycho Input Catalogue Update

---

The Tycho Input Catalogue Update served the same purpose for the reprocessing as the Tycho Input Catalogue did for the main processing. It contained eight different groups of stars, reflecting the different purposes of the reprocessing. They are described in this subsection. The eight groups of stars partly overlap, so that the sum of their sizes is larger than the total size of the Tycho Input Catalogue Update quoted previously.

### Companion Stars

The search for companion stars (Section 5.4) yielded slightly more than 100 000 non-redundant objects which were between 3 and 20 arcsec from their 'parent' Tycho Input Catalogue position. They were all included in the Tycho Input Catalogue Update, because some transits for them might have been lost in the main processing. The reason for this is that transits with signal-to-noise ratios below 1.8 were not searched for beyond 6 arcsec from the Tycho Input Catalogue position (see Section 2.4). Almost all transits with offsets between 6 and 20 arcsec were outside the original Predicted Group Crossing interval, and were lost when the signal-to-noise ratio was below 1.8. In other words, the inclusion of the distant companion stars into the reprocessing improved their detection threshold.

### Serendipity Stars

All the 57 933 serendipity stars (see Section 5.5) were included in the Tycho Input Catalogue Update, for the same reason as the distant companion stars. The improvement of the signal-to-noise limit for the accepted transits, from 3.5 to 1.8 in this case, was even more important for these stars than for the companions.

There was a second reason to include the serendipity stars. Prediction is strictly valid at the Tycho Input Catalogue position only. Using the predicted group crossings for the interpretation of transits at other positions meant an implicit extrapolation of the attitude. The limited precision of the scan speed led to a loss of precision with increasing distance from the Tycho Input Catalogue position. Furthermore, no attitude extrapolation at all was possible across attitude control jet firings. This subject, and its consequences for the serendipity search, were already discussed in Section 5.5.

### Stars with Duplicate Tycho Input Catalogue Identifications

Due to a trivial error, the Tycho Input Catalogue contained 61 pairs of stars with identical TICID1 and TICID2 (see Table 3.1) identification numbers. These 122 stars could not be treated in the main processing, since their predictions and detections were inseparably mixed in the various Tycho data streams. They were included in the Tycho Input Catalogue Update with new, unambiguous identification numbers.

## **Stars with High Proper Motions**

Another trivial error in the production of the Tycho Input Catalogue led to incorrect input positions for about 2000 stars with high proper motions. Most of them were found by the recognition process in spite of this. But for some of them, a significant improvement could nevertheless be expected from the reprocessing. Thus, a selection of about 350 stars was included into the Tycho Input Catalogue Update, either because the correct position lay far from the Tycho Input Catalogue position, or else because the Tycho Input Catalogue Revision did not contain a good solution at all.

## **Double Stars**

Two groups of stars were included into the Tycho Input Catalogue Update in order to subject them to the special double star treatment described in Chapter 14. The first, containing about 14 000 objects, was selected by cross-identifying the Tycho Input Catalogue Revision with the Catalogue of the Components of Double and Multiple Stars (CCDM, Dommanget 1989a), the Washington Catalogue of Visual Double Stars (WDS, Worley & Douglass 1984) and the catalogue of Coureau (1990). The second, containing roughly 8 000 objects, was a list of stars without previously known duplicity, but which had been discovered (or at least suspected) to be double in the course of the Tycho main processing. Entries for this list arose in the detection of transits, as well as in the astrometry processing. More details are given in Chapter 14.

## **Standard Stars**

The astrometric and photometric standard stars used in the main processing had to be included into the Tycho Input Catalogue Update in order to do the instrument calibrations for the reprocessing in the same way as for the main processing. A separate calibration was necessary because the modifications in the detection of transits (see Section 10.5) necessarily led to differing calibration parameters. In addition, an independent calibration should give confidence in the correctness of the results. The list of standards thus included into the Tycho Input Catalogue Update had about 60 000 entries. Whenever possible, the astrometric data from the Tycho Input Catalogue Revision (but only for close companions) were used instead of the Tycho Input Catalogue data for the standard stars.

## **Bright Stars**

Finally, all Tycho Input Catalogue objects brighter than magnitude 9, but having no counterpart in the previously discussed stellar groups were added to the Tycho Input Catalogue Update. There were two reasons for doing so. First, all bright stars should receive the photometric improvement due to the refined detection and estimation of transits in the reprocessing (see Section 10.5). Second, the bright stars were needed to perform the parasite recording, i.e. the flagging of (potentially) disturbed transits. This set increased the size of the Tycho Input Catalogue Update by about 70 000 objects. All bright Tycho Input Catalogue entries having a close companion counterpart in the Tycho Input Catalogue Revision within 3 arcsec were entered into the Tycho Input Catalogue Update with the improved data from the Tycho Input Catalogue Revision, all others with their original Tycho Input Catalogue data.

## **Cross-Identification Files**

Some of the Tycho Input Catalogue Update entries had to be renumbered, in order to avoid confusion, and in order to accommodate the several companions that occasionally had arisen under the same Tycho Input Catalogue identification number. Cross-identification files between the Tycho Input Catalogue Revision and the Tycho Input Catalogue Update, and between the Tycho Input Catalogue and the Tycho Input Catalogue Update were produced to keep track of the identities and correspondences.

---

### **10.3. Prediction of Group Crossings**

---

Special prediction software was set up for the reprocessing. The basic algorithm of the prediction process was the same as in the main processing (Chapter 4). In particular, reprocessing prediction used the Tycho Input Catalogue Update in the same way as the prediction process of the main processing had used the Tycho Input Catalogue. The big difference was the usage of on-ground attitude instead of on-board attitude. This, in combination with the much more precise stellar input data provided by the Tycho Input Catalogue Update (as compared to the Tycho Input Catalogue), made the prediction updating steps unnecessary.

Despite the basic similarity, the reprocessing prediction software differed from the original prediction software in many respects. The on-ground attitude files did not provide all the information contained in the telemetry tapes. Therefore the data interfaces between the various Tycho processing steps had to be slightly modified for the reprocessing. Furthermore, some information which was added to the data flow in the prediction updating steps of the main processing, had to be inserted at the (first) prediction step of reprocessing. In addition, the prediction of group crossings for solar system objects was included in the reprocessing (see Section 10.4).

Prediction for the main processing was fairly slow, for two reasons. First, it was a heavy computation process. The computing time was reduced by a factor of 10 in the reprocessing, because it is almost exactly proportional to the number of objects in the input catalogue. Second, the handling of 1400 telemetry tapes was very time-consuming at the Heidelberg computing centre. This was avoided in the reprocessing by eliminating the telemetry tapes altogether. For this purpose, the European Space Operations Centre on request provided cumulated Data Catalogue and Orbit files, covering the whole Hipparcos mission in a very compact form.

All this made reprocessing prediction very quick. After some trial runs, the final processing commenced in September 1994. Within five weeks, 80 per cent of the mission had been processed. The reprocessing prediction was completed in November 1994.

The reprocessing prediction software was also used for prediction redoing (see last paragraphs of Section 4.1), however it used the Tycho Input Catalogue as input instead of the Tycho Input Catalogue Update.

---

## 10.4. Prediction for Solar System Objects

---

The prediction process had to treat 59 solar system objects (Chapter 4). Due to a software error, this had not been done satisfactorily in the main processing. Therefore the solar system objects were treated again in the Tycho reprocessing. Only data from the reprocessing were used for the published Tycho observations of solar system objects.

### The Object List

The object list included the major planets Venus, Mars, Jupiter, Saturn, Uranus, Neptune, the five moons: Io, Ganymede, Callisto, Europa, Titan, and finally the 48 brightest minor planets. The list of minor planets was deliberately extended beyond the expected brightness limit of Tycho in order to be sure that no useful object would be missed (in analogy to the 3 million Tycho Input Catalogue for stars, where only 1 million Tycho stars could actually be expected).

The planets with large angular diameters, namely Venus, Mars, Jupiter and Saturn, were included in the list for technical reasons only. Tycho could not be expected to yield useful astrometric or photometric data for them. Their inclusion was necessary to give warnings that these very bright objects were crossing the star mapper slits, temporarily drowning any other object crossing at about the same time. Even Uranus, Neptune and the Galilean moons were expected to be too extended for correct photometric measurements through the 0.9 arcsec wide star mapper slits. But astrometry of interesting precision could be hoped for. All minor planets, on the other hand, were small enough to be measured without problems.

### Inclusion into the Prediction Algorithm

The solar system objects could not be treated in the same way as the stars, because they cannot be assigned to one of the 'regions' on the sky which were used to organize the Tycho Input Catalogue access (see Section 4.1). They were treated quite separately, therefore, in the prediction software. About once per mission day, a subset of the 59 objects was selected for actual treatment. The main criterion was that the ephemeris position be within about 2 degrees from the instantaneous scanning great circle of the satellite. In addition, a minor planet was included in the prediction process only if its ephemeris predicted it to be brighter than  $V = 11.8$  mag, i.e. the same magnitude limit as for the stellar Tycho Input Catalogue objects was used here. An enlarged analogue of the 'scanning pentagon' of Figures 4.1 and 4.2 (taking the daily motion of a planetary object into account) was used to further restrict the list. Due to these measures, the computing time needed for ephemeris access and apparent positions computations of planetary objects was only 1 to 2 per cent of the total time needed for reprocessing prediction.

Within each attitude time interval (see Section 4.1), satellitocentric apparent positions were computed for the selected objects from the respective ephemerides. Predicted group crossings were then calculated as for the stars. Different sorts of ephemerides were available for the three groups of solar system objects. The numerical representation

as well as the astronomical meaning of the data given in the ephemerides were different for each group. Their usage for the prediction process is briefly described hereafter.

### **Ephemerides and Apparent Positions for the Major Planets**

The Development Ephemeris, DE200, of the Jet Propulsion Laboratory was used for the major planets (including Earth). It gives barycentric cartesian location and velocity vectors  $X_{\text{obj}}$  and  $V_{\text{obj}}$  in the J2000 equatorial coordinate system (nominally). These vectors are represented by Chebyshev polynomials as a function of Barycentric Coordinate Time (BCT). In order to derive apparent positions for the objects from these data, one has to compute:

- the light-travel time from object to satellite  $t = |X_{\text{sat}} - X_{\text{obj}}|/c$ , where  $X_{\text{sat}}$  is the barycentric satellite location, and  $c$  is the velocity of light;
- the barycentric location vector of the object, corrected for the light-travel time,  $Y_{\text{obj}} = (X_{\text{obj}} - V_{\text{obj}})t$ ;
- the geometric position of the object with respect to the satellite, i.e.  $Y_{\text{obj}} - X_{\text{sat}}$ , normalized to unity;
- the aberration correction to this geometric position, using the barycentric velocity vector of Hipparcos.

This procedure implied two approximations which were, however, of no noticeable astrometric effect: the second step ignored the acceleration of the object in its orbit, while the transformation from geometric to apparent position (last step) ignores the relativistic light deflection by the Sun and the Earth.

### **Ephemerides and Apparent Positions for the Moons**

Ephemerides were made available by J. Arlot of Bureau des Longitudes, especially for the purpose of Hipparcos data reductions. They give the geocentric position offsets between a moon and its parent planet as offsets in right ascension and declination (J2000), represented by Fourier coefficients as a function of Terrestrial Time (TT). In order to derive apparent positions for the objects from these data, one has to:

- compute the satellitocentric apparent position of the parent planet, as above;
- transform this to right ascension and declination;
- add the right ascension and declination offset derived from the moon's ephemeris.

This procedure implied a number of approximations: (1) the differential parallax between parent planet and moon due to the line-of-sight component of the planet-moon location vector was ignored (this vector could not be inferred from the available ephemeris data). The effect was largest for Callisto, where it could reach 40 mas at maximum; (2) the differential light-travel time was ignored for the same reason. Again, the effect was largest for Callisto, where it could be of the order of 10 mas at maximum; (3) due to the 'daily' parallax of the Hipparcos satellite (13 arcsec at the distance of Jupiter) the difference in location between planet and moon translates into different right ascension and declination offsets if viewed from the Earth or from the satellite (the effect is small); (4) the same applied for aberration. The effect again is small.

## Ephemerides and Apparent Positions for the Minor Planets

Ephemerides were provided by A. Bec-Borsenberger of Bureau des Longitudes. They gave geocentric astrometric positions of the objects in the form of ecliptic longitudes and latitudes (J2000). In addition, the geocentric distance and magnitude were given. All four quantities were represented by Chebyshev polynomials as functions of Terrestrial Time (TT). In order to derive apparent positions from these data, one had to:

- compute the geocentric location vector of the minor planet from the Chebyshev representation of longitude, latitude and distance (note that this was already light-time corrected, since the input was an astrometric position);
- subtract the geocentric satellite location vector to get the geometric position of the object with respect to the satellite;
- apply the aberration correction due to the barycentric velocity of Hipparcos.

This procedure was approximate in practically every aspect, but it was computationally simple and accurate enough.

---

### 10.5. Detection of Transits

---

The reprocessing detection process was carried out in the same way as described in Section 4.3, except for one difference: the amplitude estimation for very bright stars was carried out using the wings of the signal, as for these stars the centre of the signal was disturbed by non-linearity in the response (saturation) of the photomultipliers. To do this, special single-slit response functions had to be constructed because those used for the main processing covered only a width of 3.8 arcsec. The new single-slit response functions were constructed at Tübingen, using individually selected transits of bright stars ( $2 < m < 5$  mag). They were applied to transits with a signal-to-noise ratio above 250.

---

### 10.6. Identification of Transits

---

With the omission of the prediction updating steps in the reprocessing, transit identification lost two of its major tasks, namely to introduce an improved star catalogue and improved attitude into the Tycho data reduction chain. Nevertheless a sort of transit identification was necessary, for three remaining purposes: the addition of identity probabilities, the format changes necessary to transform raw transits into identified transits, and the parasite recording. This 'abridged transit identification' was performed in parallel with the reprocessing detection in a single process, and no major changes were needed in the detection and transit identification programs. A control program made calls to the detection and transit identification software in alternation. The absence of a prediction updating-3 data stream as input for transit identification was compensated by a simple intermediate program converting the reprocessing Predicted Group Crossing data to pseudo-updating data before the runs of the transit identification program. As a consequence, the raw transit files, which had been the main output of the detection

and input of the transit identification process, were only temporary files in reprocessing. They were deleted immediately after treatment by transit identification and not stored on magnetic tapes. The combination of the two logical processing steps into a single program is indicated in Figure 10.1.

The parasite recording in the abridged transit identification was done with the same algorithm as for the main processing. Nevertheless the outcome was different, since the Tycho Input Catalogue Update was by definition (see Section 10.2) complete down to magnitude 9 only. In the main processing, all parasites down to Tycho Input Catalogue Revision magnitude 10.5 had been recorded.

---

## 10.7. Verification Methods

---

Testing and verification for the reprocessing was very similar to that of the main processing. At a very late stage, a minute but systematic astrometric defect of the reprocessing data was discovered in the calibration parameters, as described in Chapter 7. The precise cause of the defect could not be found within the available time, but it was definitely due to an error of the reprocessing prediction software.

Ironically, the error did not damage the redoing data, which had been produced with the same prediction software before the problem became known. In redoing, the defect was (unknowingly) repaired by the prediction updating step. When the defect was recognized in the reprocessing data, it was too late for an updating step there. Thus, an empirical correction was applied to the astrometric parameters, as described in Chapter 11.

U. Bastian, K. Wagner



## 11. PRODUCTION OF THE TYCHO CATALOGUE

*The principal stages of the Tycho Catalogue production are outlined. The chapter is divided into three parts: the astrometric part, production of the Tycho Epoch Photometry Annex, and production of photometric mean values. The astrometric analysis was decisive in the determination of the stellar contents of the Tycho Catalogue, the quality of solutions, merging criteria etc. The Tycho Catalogue of mean values was constructed in the course of astrometric adjustments and transformations of the calculated data, while the photometric data were computed in a separate process.*

---

### 11.1. Production of the Astrometric Catalogue

---

The routine astrometric reductions were carried out as a series of iterative updates of a working catalogue, called the Star Constants Catalogue (SCC). In the main processing the Star Constants Catalogue contained more than 1 200 000 entries, including all the TICR (Tycho Input Catalogue Revision) entries and hexagon points (see Section 7.4); it contained some auxiliary information and the following data:

1. Identification number from the input catalogue.
2. Coordinates from the input catalogue.
3. Combined  $T$  magnitude from the input catalogue.
4. Accumulated number of accepted observations.
5. Current Cholesky triangle matrix of 15 elements and the right-hand part.
6. Current solution for astrometric parameters.
7. Condition number of solution.
8. Square norm of residual vector.
9. Corrections to astrometric parameters.
10. Corrections to the tangential coordinates 'H30 - TICR' (where H30 was the preliminary 30-month Hipparcos Catalogue) for monitor stars only.
11. HIP identification number for monitor stars.

The data from the input catalogue (items 1 to 3) stayed unchanged. The proper motions and parallaxes of the input catalogue were not present in the Star Constants Catalogue, but in annexes to TICR. These values were exactly the same as those used in the prediction of transit times. The data of items 4 to 8 were updated with an observation equation for a given star when an observation of this star was encountered and had been accepted for the astrometric solution. The number of accepted observations  $N_{\text{astrom}}$  then increased by 1, the Cholesky factor and the right-hand part were updated by Givens

rotations, and the condition number was updated. The square norm of the residual vector  $\rho$  was increased by the newly calculated residual:

$$\|\rho\|^2 = \sum_{n=1}^{N_{\text{astrom}}} (\Delta u / \sigma_{u,n})^2 \quad [11.1]$$

Solving for astrometric parameters each time a new observation was obtained, was superfluous but it cost relatively little in computing time when compared with the time spent on disk input/output operations.

The corrections to astrometric parameters (item 9) were updated after each complete iteration for all but the monitor stars, which were a subset of the Hipparcos intermediate 30-month catalogue ‘H30’ (see Section 7.2). For the 105 000 monitor stars only the corrections to tangential coordinates were updated, while the relevant fields for proper motion and parallax contained differences ‘H30 – TCR’, calculated once and forever as soon as the preliminary 30-month Hipparcos Catalogue H30 had become available from NDAC. The corrections to positions were however stored separately (item 10). This introduced an important difference between the monitor stars and the rest: For an ordinary star, the corrections to the proper motion and parallax were updated as many times as the number of iterations (5 in the main processing and 3 in the reprocessing). For a monitor star, however, these corrections have effectively been updated only once, when the final parameters were derived. This most probably accounts for a difference in precision between the positions and the other parameters in the Tycho Catalogue, when compared with the Hipparcos Catalogue. This is described in Chapter 18.

When all observations were reduced and the final solution was achieved, the 5 astrometric parameters were derived from the input catalogue data, the current solution and the previously accumulated corrections. At this stage, the on-ground proper motions and parallaxes had to be taken into account again. Finally, several distinct transformations had to be carried out on data in the Star Constants Catalogue.

- the final astrometric parameters were computed by adding the final solution and the accumulated corrections to the input catalogue values. For positions the final equatorial coordinates were derived from the local plane (tangential) coordinates and the input catalogue positions by Equation 1.2.23 of Volume 1;
- the Cholesky triangle matrix was transformed into a covariance matrix, and the formal errors of the solution were derived;
- the formal errors in the Star Constants Catalogue were multiplied by the standard error of unit weight  $\sigma_{\text{u.w.}}$ , that is:

$$\sigma_{\text{u.w.}} = \sqrt{\|\rho\|^2 / (N_{\text{astrom}} - 5)}. \quad [11.2]$$

This factor was usually slightly larger than 1.0, but could be much larger for very disturbed stars, double stars and entirely false stars. The resulting internal standard errors are discussed in Chapter 18;

- the position and proper motion, and the covariance matrix were transformed from the epoch of Tycho Input Catalogue J1990.0 to the standard Hipparcos-Tycho Catalogue epoch J1991.25. The covariance matrix was transformed by the simplified treatment in Section 1.5.4 of Volume 1. The position and proper motion were transformed rigorously as described in Section 1.5.5 of Volume 1, assuming  $V_R = 0$  since the radial velocity was always unknown;
- auxiliary parameters of the solution, e.g. the signal-to-noise ratio  $F_s$ , were calculated.

---

## 11.2. Merging

---

The two runs of Tycho data reductions, the main processing and the reprocessing, were quite independent of each other, and the merging of the two resulting catalogues is described here. The reductions were based on two different input catalogues (TICR and TICU) with different stellar contents, and the positions for common stars could also disagree. The two data reductions were implemented separately, and some of the principal stages were significantly updated for the reprocessing, e.g. the prediction. A few off-line tasks were accomplished in the course of reprocessing, such as close double star treatment and astrometry and photometry of solar system objects.

As an intermediate astrometric result of the two processing runs, two Star Constants Catalogues were constructed, called respectively SCC and SCU. The structure of the catalogues was similar, as described in the previous section. They were transformed into so-called CUO\_CAT provisional catalogues, namely CUO\_CAT\_f for the main processing and CUO\_CAT\_u for the reprocessing, containing 1 150 157 and 289 158 entries respectively.

The general strategy of ‘merging’ for a star contained in both catalogues was strictly to take only one of the alternative solutions; a combination or a mixture of the data from the two sources was never allowed. A cross-identification list of common stars in TICR and TICU (see Section 10.2) was used to infer the identity of stars since many of them had received different identification numbers in TICU. A sorted *ad hoc* lookup table was produced, based on this list, to facilitate quick and automatic identification of stars. The list contained, however, a few errors of the two following kinds:

- stars supposed to be identical but having considerably different positions;
- stars not given in the cross-identity list but being in fact identical.

The latter kind of inconsistencies was taken care of in a series of redundancy analyses. The former inconsistency was resolved by way of position comparison for supposedly identical stars in the two solutions. The stars were accepted as identical if the positions agreed within 1 arcsec, otherwise both stars were kept in the merged catalogue CUO\_CAT\_1, representing possibly a double or multiple system. In fact, only 57 such pairs were found.

All entries of very low astrometric quality in both catalogues were rejected at this stage of catalogue construction. Since too many stars should not be rejected before a more careful analysis was undertaken, a rather loose criterion was adopted to define a low astrometric quality. A solution was considered to be of no value for further processing if the number of accepted transits was below 25. The total set of stars in the two catalogues could be divided into 3 groups:

- approximately 207 000 stars in common between the two solutions;
- 943 000 stars represented only in the main processing;
- 82 000 stars given only in the reprocessing.

The corresponding numbers of low-quality stars were 46 000, 21 000 and 78 000. The large fraction of low-quality solutions in the reprocessing was related to the so-called

serendipity stars, the vast majority of which were proved to be non-existing stars, false entries. It should be noted that many of the 21 000 bad stars in the second group were later reintroduced in the final catalogue, but without astrometric solution, for the sake of their photometry.

The remaining 926 000 stars of reasonable quality in the two last groups were all adopted for CUO\_CAT\_1. The 161 000 stars with redundant solutions of the first group required a careful consideration. At this stage, a proper choice had to be made between the two alternative solutions.

It had become clear in the course of practical work and by some provisional checks that the astrometric quality of the reprocessing was inferior to the main processing. The lower quality was so conspicuous that even the error model for single observation had to be adjusted. The variance of the transit time, given by Equation 7.6, was modified to:

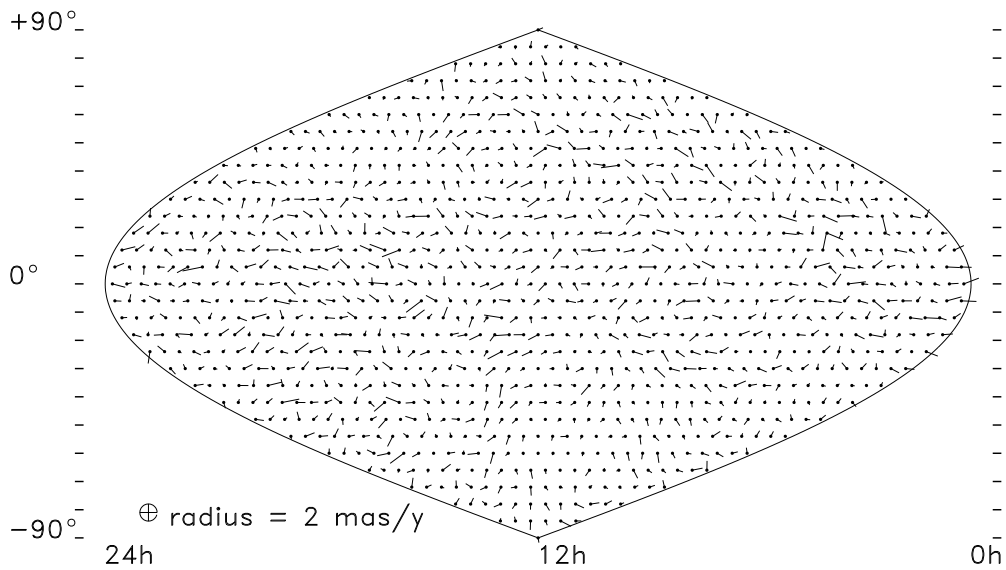
$$\sigma^2 = \sigma_{\text{ph}}^2(A, B) + (\sigma_{\text{att.1}} + \sigma_{\text{att.2}})^2 \quad [11.3]$$

where  $\sigma_{\text{ph}}^2(A, B)$  is a theoretically derived variance due to photon noise, as a function of the amplitude  $A$  and the background  $B$ , and  $\sigma_{\text{att.2}}$  is an empirical correction to the previously estimated attitude error  $\sigma_{\text{att.1}}$ . The total attitude error in the brackets was typically 7 mas and 30 mas in the main processing for vertical and inclined slits, respectively. These values were larger during the reprocessing, and also varied from 12 to 18 mas and from 30 to 37 mas, respectively, at different intervals of the mission. The increase of the quadratic term affected particularly the overall precision of the 5 astrometric parameters for bright stars (brighter than 9 mag), as was shown by comparison with provisional main mission data. For the brightest stars the deterioration of precision was a factor of 1.5 in positions, 2.3 in proper motions and 2.0 in parallaxes.

A small but quite obvious increase of systematic errors was also found in the reprocessing solution by comparison with provisional main mission results. In parallaxes, for example, a negative bias of  $-2.5$  mas was found, meaning that the reprocessing parallaxes were in general 2.5 mas too small. The largest errors appeared however in proper motions. Zonal mean differences of proper motions ‘Tycho – Hipparcos’ are shown in Figure 11.1 for the main processing (upper plot) and for the reprocessing (lower). The zonal errors of proper motions in the main processing are typically below 2 mas/year, while in the reprocessing a value of 5 mas/year is quite frequent and a smooth geometrical pattern is clearly seen. This pattern becomes even more pronounced when differences ‘main processing – reprocessing’ are plotted (Figure 11.3, upper plot).

The poor performance of the reprocessing astrometry for both accidental and systematic errors is believed to be caused by an unknown error in the prediction software used for reprocessing. The error was ‘minor’ in the sense that it could not be visible in the rather rough checks like the ‘cloud plots’ (Section 4.5) at the early stages of the data processing. It was decided not to make further efforts to locate the error or repeat the data reprocessing, lest an inevitable delay of the Tycho catalogue release should result. This decision was also facilitated by the possibility of diminishing the zonal systematic errors by means of the spherical functions technique described in the following section. Still, the reprocessing solution had to be downweighted in the merging, because the updated error model could perhaps not properly describe the remaining systematic part of the errors. Therefore, a reprocessing solution (u) was preferred instead of the main processing solution (f) only when  $s_{\text{max}}^f/s_{\text{max}}^u > 1.15$ , where  $s_{\text{max}} = \max\{\sigma_i, i = 1, 2, \dots, 5\}$ . Only some 9000 reprocessing solutions survived this strict selection. They belong

## Mean difference in pm (T-H), Main proc.



## Mean difference in pm (T-H), Reproc.

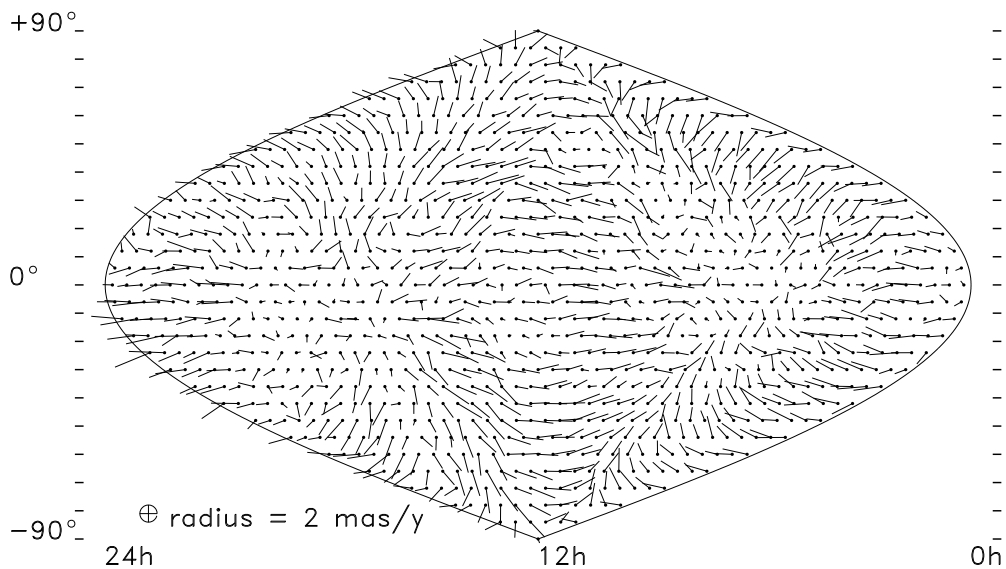


**Figure 11.1.** Sky projection of differences 'Tycho - Hipparcos' in proper motions for the main processing solution (upper plot) and the reprocessing (lower). The length of a vector shows the value of the difference in mas/year, and the azimuthal angle indicates its position angle on the sky. The plots are cosine sky projections, in equatorial coordinates, with a cell size of  $6^\circ \times 6^\circ$ .

typically to stars of high astrometric quality with perhaps much improved initial positions in TICU.

About 1 070 000 stars were contained in CUO\_CAT\_1, more than 98 per cent of which had been taken from the main processing. They were subject to several distinct procedures, such as systematic corrections, redundancy analyses, removal of false entries, etc., thus completing the astrometric catalogue production.

---

### 11.3. Completing Steps of the Catalogue Production

---

The fraction of stars in CUO\_CAT\_1 with solutions from the reprocessing, however small it was, had to be corrected for systematic differences in all five astrometric parameters. Since the final main mission astrometry was not available at that time, the reprocessing part was simply adjusted to the main processing part, leaving the task of final systematic correction, including rotations, to the very end of the catalogue production.

#### Correction of Systematic Differences ‘Reprocessing – Main Processing’

A rather conventional technique of spherical functions representation was used to carry out this task. The original method applied to astrometry was proposed by Brosche (1966), and further developed by several other authors. The differences in astrometric parameters were represented by the expansion:

$$\Delta a_i = \sum_{j=0}^J c_j^i Y_j(\alpha, \delta) + \epsilon \quad [11.4]$$

where  $Y_j$  are spherical orthogonal functions,  $\Delta a_i = (\Delta\alpha \cos \delta, \Delta\delta, \Delta\pi, \Delta\mu_\alpha \cos \delta, \Delta\mu_\delta)$  are the astrometric parameter corrections, and  $\epsilon$  is the random component of the differences. The spherical harmonics  $Y_j$  are orthogonal for different  $j$ , and they can be normalized as:

$$\int_0^{2\pi} \cos \delta \, d\alpha \int_{-\pi}^{\pi} Y_j(\alpha, \delta) Y_l(\alpha, \delta) \, d\delta = \delta_{jl} \quad [11.5]$$

where  $\delta_{jl}$  is the Kronecker symbol. The spherical harmonics are related to associated Legendre polynomials by the equation:

$$\begin{aligned} Y_{nms} &= R_{nm} P_{nm}(\cos \delta) \sin m\alpha & \text{or} \\ Y_{nmc} &= R_{nm} P_{nm}(\cos \delta) \cos m\alpha \end{aligned} \quad [11.6]$$

where:

$$\begin{aligned} R_{nm} &= \sqrt{\frac{(2n+1) 2(n-m)!}{4\pi (n+m)}} & m \neq 0 \\ &= \sqrt{\frac{1}{4\pi}} & m = 0 \end{aligned} \quad [11.7]$$

the index  $m = 0, 1, \dots, n$ , and  $n = 0, 1, \dots, N$ . The index  $j$  counts all different spherical orthogonal functions from 0 to  $J = (N+1)^2$ . An easy way to compute the associated Legendre polynomials is to use the following expression (Press *et al.* 1986):

$$P_{mm}(\cos \delta) = (2m-1)!! \cos^m \delta \quad [11.8]$$

and the recurrences:

$$\begin{aligned} P_{(m+1)m} &= \sin \delta (2m+1) P_{mm} \\ (n-m) P_{nm} &= \sin \delta (2n-1) P_{(n-1)m} - (n+m-1) P_{(n-2)m} \end{aligned} \quad [11.9]$$

Equation 11.4 could not be directly used for the whole set of stars in a simple way. Apart from the necessity of re-normalising the basic functions due to the uneven distribution of Tycho stars over the sky, any attempt to introduce statistical weights for individual stars would require also a re-orthogonalisation. In principle, this could be achieved by Gram-Schmidt orthogonalisation, with computational difficulties. A new approach was used instead, in order to avoid weighting of individual stars. The sky was divided into a number of cells of  $6^\circ \times 6^\circ$  size. Weighted mean differences of the astrometric parameters of stars within each cell were computed and assigned to a reference point in the centre of the cell. The statistical weights of the reference points were fairly uniform and could therefore be neglected in the following computations. The orthogonality and normalisation of the basic functions were proven to hold within the relative precision of  $10^{-4}$  over the set of the reference points by direct calculation. The expansion corresponding to Equation 11.4 was sought then for the reference points, disregarding individual stars. The method is fast and convenient for big catalogues. It is quite justified for the determination of large-scale systematic distortions.

For each astrometric parameter, 81 terms of Equation 11.4 ( $N = 8$ ) were calculated. As expected, the largest terms were found in proper motion differences, i.e. in  $\Delta\mu_\alpha \cos \delta$ :  $-3.55 Y_{11s}$  mas/year, and in  $\Delta\mu_\delta$ :  $2.10 Y_{21s}$  mas/year, where  $Y_{11s} = \sqrt{0.75/\pi} \cos \delta \sin \alpha$  and  $Y_{21s} = \sqrt{1.25/\pi} \cos \delta \sin \delta \sin \alpha$ . The standard errors of the coefficients  $c_j^i$  were typically 0.05 to 1.00 mas/(year). The dominating term for parallax was  $1.37 Y_{00c}$  mas, where  $Y_{00c} = \sqrt{0.25/\pi}$ .

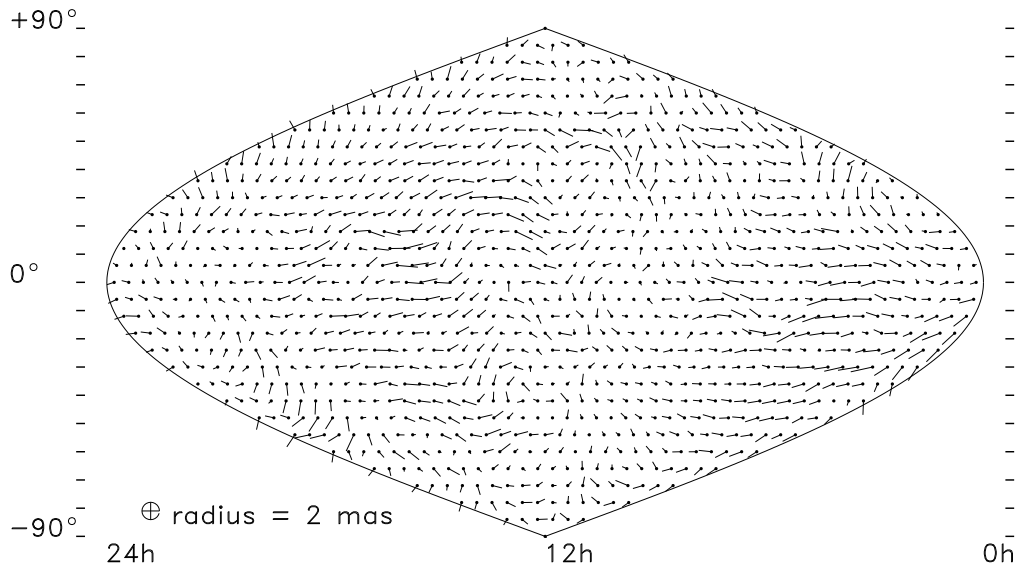
Before deriving a spherical function representation, it had to be ensured that the rotation (relative orientation) between coordinate systems or the spin between proper motion systems is negligibly small. Alternatively, a method exists to derive the rotation and the spin, when statistically significant, by means of a spherical function representation, where they appear at certain terms (Vityazev 1994). A more traditional way of rotation and spin determination was chosen, since no computational limitation was experienced for the rather small number of stars (about 200 000). The rotation and spin turned out to be very small, as expected.

The resulting systematic corrections were applied individually to each of the reprocessing stars in CUO\_CAT\_1. The vector plots in Figures 11.2 and 11.3 show the great improvement of the reprocessing solution after this correction. All smooth variations of both position and proper motion differences were removed by spherical harmonics, leaving only some small-scale disturbances. The negative bias of reprocessing parallaxes also disappeared. The result seems satisfactory enough to consider the merged catalogue as a uniform astrometric solution, called CUO\_CAT\_2.

### Redundancy Analysis #1

Due to imperfections of the input catalogue and some errors in the TCR-TICU cross-identification list a small number of stars could appear two or even three times, under different identification numbers, in CUO\_CAT\_2. Such redundancies had to be eliminated. The astrometric solutions could of course be different for redundant entries. An entry was considered to be redundant if the position at J1991.25 was within 1 arcsec of

## Mean difference in pos (F-U)



## Mean difference in pos (F-U), after correction

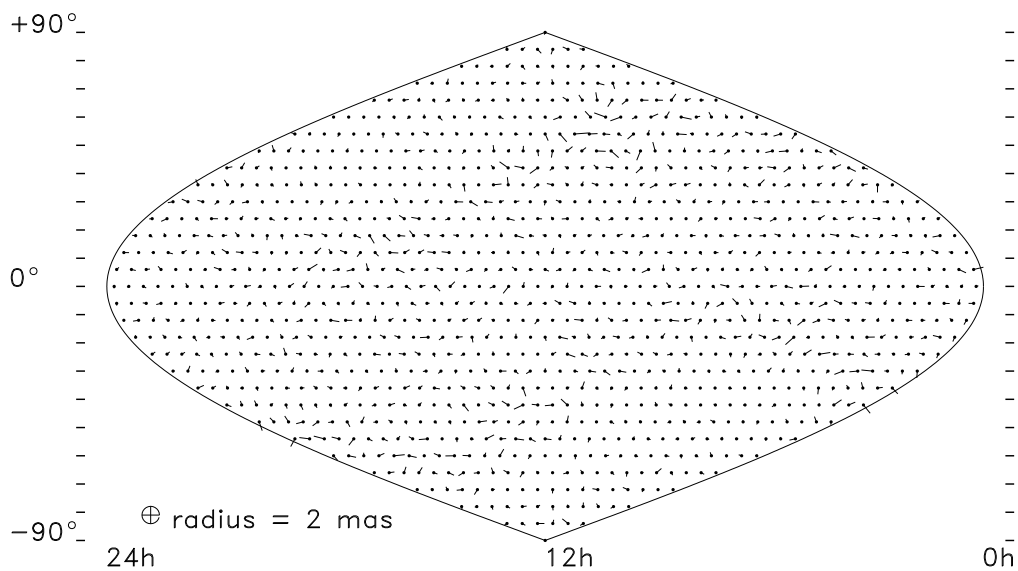
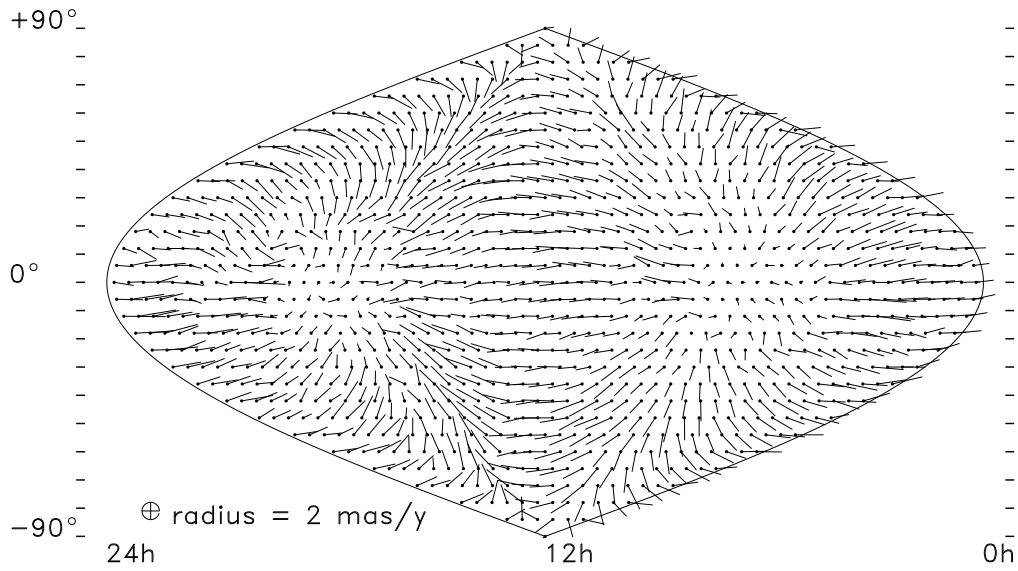


**Figure 11.2.** Sky projection of differences 'Main processing – Reprocessing' in positions. The length of a vector shows the value of the difference in mas, and the direction indicates its position angle on the sky. Cosine sky projection in equatorial coordinates, cell size  $6^\circ \times 6^\circ$ .

## Mean difference in pm (F-U)



## Mean difference in pm (F-U), after correction

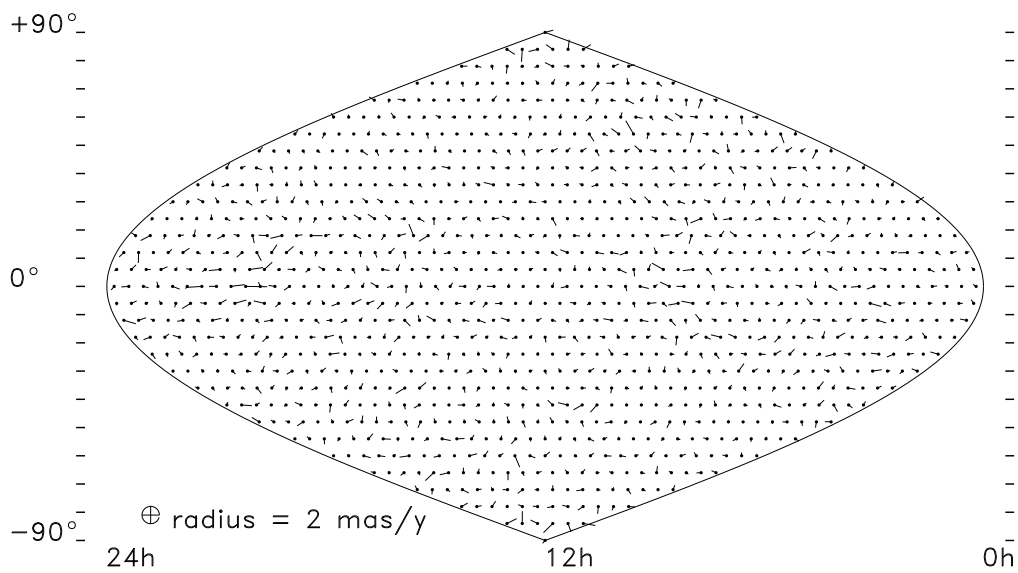


**Figure 11.3.** The same as Figure 11.2, but for proper motions.

another entry. That was the only criterion of redundancy adopted, reliable photometric data not yet being available. The limit of 1 arcsec was approximately the angular resolution of the Tycho instrument, being at the same time at least an order of magnitude larger than the expected error of positions. 1348 pairs of redundancies were found, some of them triple.

Selection of stars in the redundant pairs to be retained in the catalogue was made according to the following rules, in order of decreasing priority:

- if two stars in a pair have solutions from different sources (main processing and reprocessing) then the main processing solution is preferred, unless  $s_{\max}^f/s_{\max}^u > 1.15$  (see Section 11.2);
- if two stars in a pair belong to different quality classes then the star of higher quality is preferred;
- the solution with highest  $F_s$  is preferred.

Some 792 redundant entries were discarded in this analysis, the rest was referred to as the CUO\_CAT\_3 catalogue.

### Discarding Artefacts and Side Lobes

At this stage, the catalogue still contained quite a few spurious entries, i.e. non-existing stars. Two kinds of spurious entries could be distinguished, depending on their origin:

- intrinsic artefacts of the Tycho Input Catalogue;
- false components introduced by the recognition processing (see Chapter 5), usually closer than 20 arcsec to a bright real star.

The former kind were mostly identified with bright galaxies and planetary nebulae, confused in the Guide Star Catalog with stars, and stars with unknown or erroneous proper motions. The latter comprised chiefly so-called side lobes, i.e. parasitic signals due to interference of photon counts from different slits of the star mapper. Side lobes appeared at certain distances from sufficiently bright stars, and their presence is clearly seen in a pair statistics like that in Figure 16.16 where peaks at 5.6 and 11.3 arcsec are visible.

There was no certain criterion to distinguish false entries, due to a random excess of counted photons, from entries due to real stars. Only rather general statistical characteristics, available in the catalogue, could be used in practice, allowing few real stars to be lost, but never reaching a complete cleanness. With respect to side lobes, a satisfactory pair statistics was achieved only after some 23 600 components of multiple entries having quality flags  $Q$  above 5 had been discarded.

The intrinsic artefacts of the input catalogue were more difficult to recognize. It was noticed, however, that a specific group of so-called ‘COMPI 10’ entries was especially abundant with them. The ‘COMPI 10’ stars were included in TICR at positions where the Tycho Input Catalogue had a rather bright object which was, surprisingly, not found in the Tycho recognition processing. This fact was already a hint that there might be no star at the place, or it might be an extended object. A dedicated study revealed that only about 30 per cent of ‘COMPI 10’ stars were true. In the study, a total of 29 such objects were identified in a collection of 31 photographic prints, 55 arcmin in diameter,

obtained with the Danish 1.5 m telescope at La Silla around 1990 for another purpose. The sample was classified into galaxies (8), false stars (11), and true stars (10) by visual inspection. Even true stars might, however, be too faint for Tycho to contain other than spurious information. Since detected transits at galaxies and at empty spots do not concentrate towards the estimated position, the signal-to-noise ratio  $F_s$  is always small. It was therefore decided to discard 23 100 'COMPI 10' stars with  $Q$  above 6 ( $F_s < 5$ ).

Such rejections and cleaning procedures resulted in a series of catalogues, up to CUO\_CAT\_6.

### **Additions to the Catalogue and Redundancy Analysis #2**

A few special groups of stars were included in the catalogue after dedicated treatments and analyses. Firstly, the result of double star reduction in astrometry (Section 14.4) was merged with the catalogue. There were two kinds of output from that reduction:

- 517 stars failed to be resolved into separate entries, but were found to be missing in the catalogue, at the same time. Such lost stars were mainly caused by the parasite recording, which rejected too many proper transits, when TICR contained a few (often false) nearby components;
- 1657 pairs of resolved double stars, to be merged with the catalogue.

Among the 3314 resolved components, 2232 had already been present in the catalogue. These were basically components successfully resolved by the recognition processing. A decision was taken to prefer always the solution from the double star reduction, since a much more careful selection of transits had been made, where the misleading parasite recording did not affect the result. The merging was carried out in a second redundancy analysis.

Secondly, 33 567 low quality stars ( $Q = 9$  in Field T40, see Volume 1, Section 2.2) mainly in clusters or other dense regions were inserted in the catalogue. These stars had previously been rejected, but were re-introduced with the positions of TICR, without proper motions and parallaxes, because they could be of interest for photometry. Only 13 077 of them survived the following rejection and cleaning procedures, and some of them may still be false.

Finally, a dozen serendipity stars were re-introduced after a dedicated study at Strasbourg, based on inspection of Digital Sky Survey maps. The resulting catalogue CUO\_CAT\_11 contained 1 074 030 stars.

### **Redundancy Analysis #3**

A search for internal redundancies was repeated because of the recent additions. The same limit on distance of 1 arcsec was adopted. 9593 pairs of redundancies were found, with at least one of the components being a  $Q = 9$  star. As a result, 9530 entries were deleted.

### **Rotation and Systematic Corrections**

The rotation and spin between the current Tycho and the final Hipparcos coordinate and proper motion systems were determined and corrected in Tycho as soon as a nearly

complete version of the Hipparcos Catalogue became available. Just over 96 000 single reference stars, common to Tycho and Hipparcos and for which the relevant astrometric parameters in the two catalogues agreed within  $3\sigma$ , were selected. Each star provided two equations for the rotation, and another two for the spin, as described in Section 1.5.7 of Volume 1. The equations were solved by the least-squares method iteratively, adjusting each time the selection of stars.

The astrometric Tycho processing was tied to a preliminary coordinate system, N18 (see Volume 3, Chapter 11), which was consistent with the first version of attitude parameters, used throughout the data reduction, and supplied with a consistent main mission astrometric solution, based on 18 months of the mission. The rotation between this system and the final ICRS system was found to be  $(+40.04, +41.54, -67.60) \pm 0.01$  mas. The spin between the two proper motion systems was, as expected, much smaller, only about 1 mas/year.

After the rotations had been determined and applied to all positions and proper motions in TYC, large-scale zonal errors were corrected. The same technique of spherical harmonics (Section 11.2) was used again. The set of data was reduced by means of computing weighted mean differences in cells of  $6^\circ \times 6^\circ$ , and then 81 coefficients  $c_j$  of Equation 11.4 were determined for each astrometric parameter. The appearance of the differences is shown in Figures 11.4 before and after the corrections. It is clearly seen how the spherical functions remove extended features like the broad ‘streams’ in position in Figure 11.4(a), the upper plot. The degree of improvement can be expressed through median absolute differences over the sample of cells. The values were, before and after the correction respectively 1.25 and 0.83 mas for positions, 1.22 and 0.93 mas/year for proper motions and 0.64 and 0.57 mas for parallaxes. It was concluded that the systematic errors of the Tycho Catalogue with respect to the Hipparcos Catalogue are within 1 mas(/year), when the weighted mean differences are considered.

The systematic differences Tycho–Hipparcos are most probably due to systematic errors in the preliminary N18-NDAC attitude used in the final Tycho processing. The N18 catalogue was based on an early sphere solution in which some distortions due to the Hipparcos Input Catalogue still remained. These distortions could only partly be compensated by the instrument calibration parameters because the latter represented an average of about 10 satellite revolutions, rather than being related to zones on the sky. The remaining zonal errors thus provide an indirect view of the intricate influence of the attitude errors on the distortions of resulting astrometric parameters.

### **Cross-Identification and Merging with the Hipparcos Catalogue**

Ideally, the cross-identification of stars in the Tycho and Hipparcos Catalogues with a limit of 1 arcsec on the position difference should be straightforward and unambiguous due to the following circumstances:

- the combined formal error of a position is at least ten times smaller than the limit of 1 arcsec;
- Tycho astrometry never resolves components of double stars closer than 1 arcsec to each other.

For the vast majority of stars this criterion of identity was in fact sufficient and ample. Only a handful of stars required special consideration. In some cases positions in the Tycho and Hipparcos Catalogues disagreed by more than 1 arcsec, but the identity of

## Mean difference in pos (T-H)

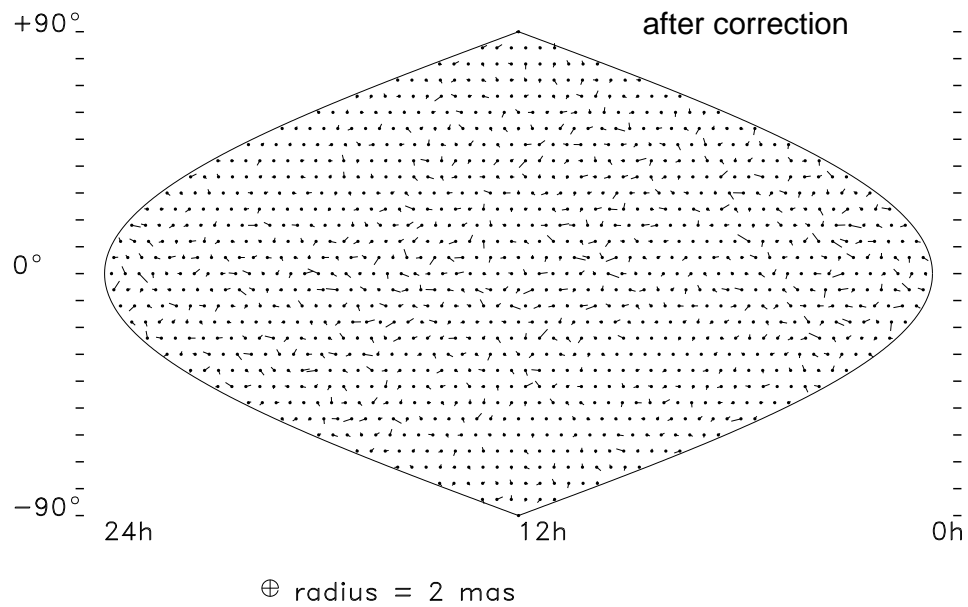
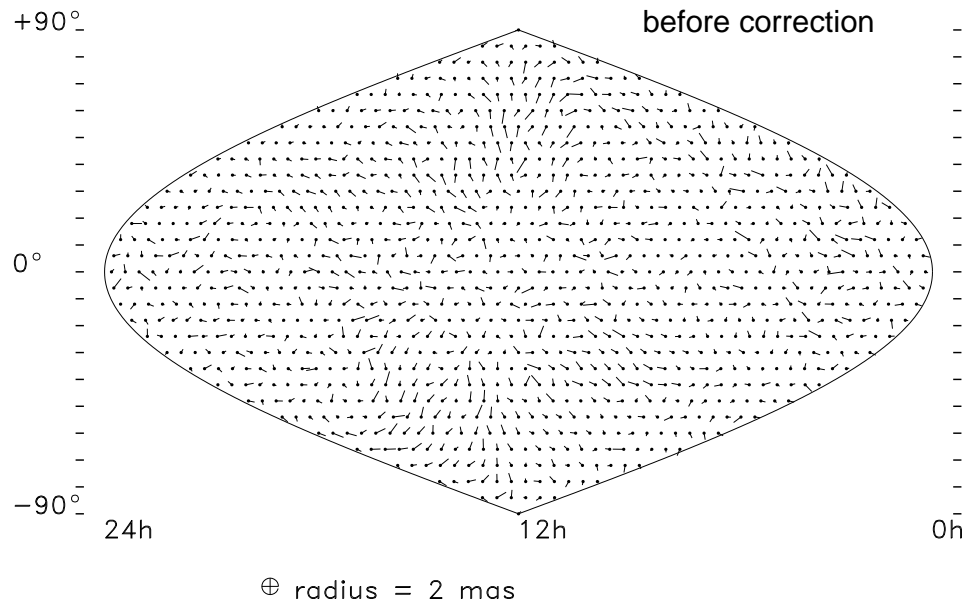


**Figure 11.4 (a)** Sky projection of differences 'Tycho - Hipparcos' in positions. The length of a vector shows the value of the difference in mas, and the azimuthal angle indicates its position angle on the sky. Cosine sky projection in equatorial coordinates, cell size  $6^\circ \times 6^\circ$ .

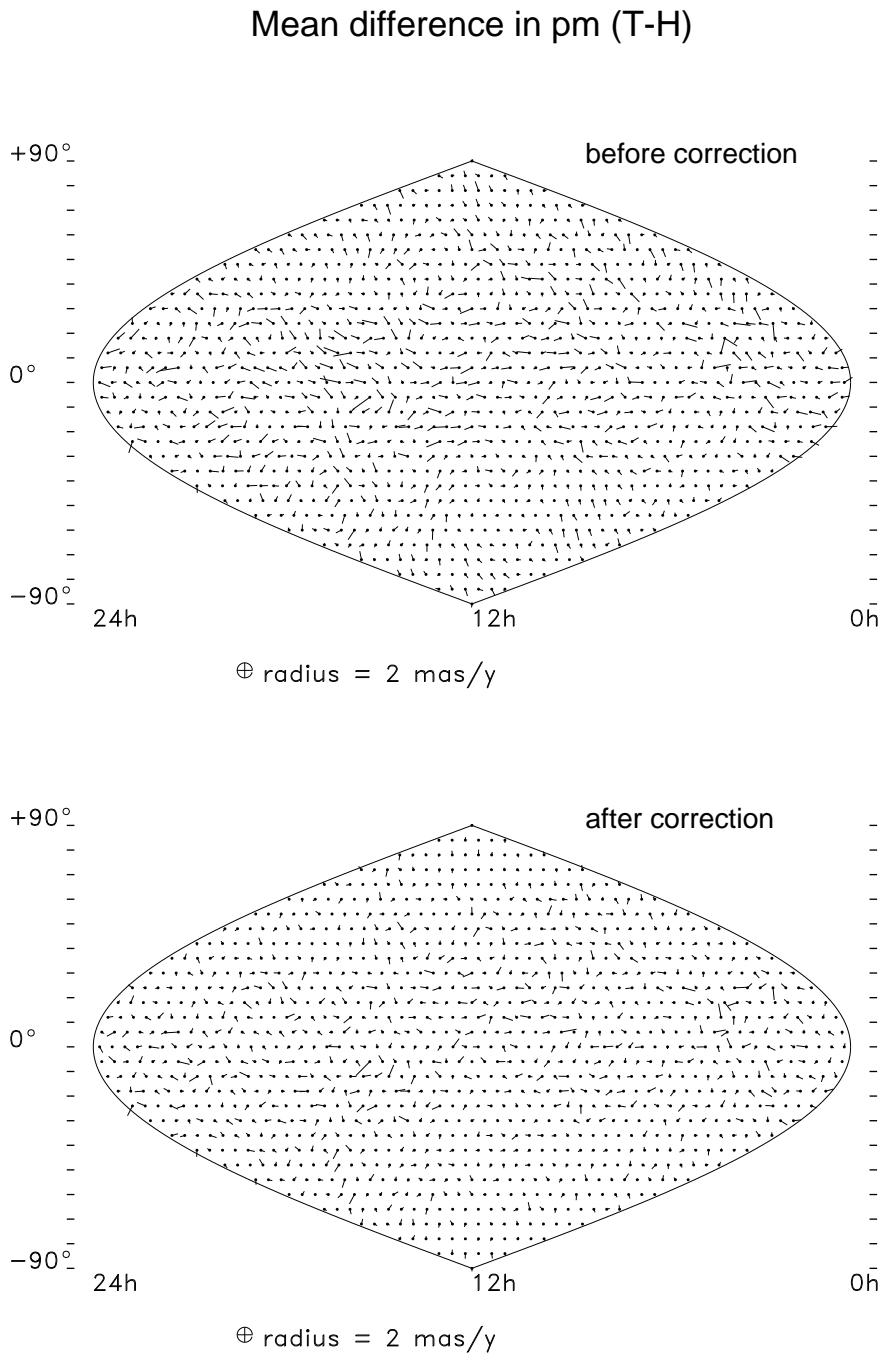


**Figure 11.4 (b)** Sky projection of differences 'Tycho - Hipparcos' in proper motions. The length of a vector shows the value of the difference in mas, and the azimuthal angle indicates its position angle on the sky. Cosine sky projection in equatorial coordinates, cell size  $6^\circ \times 6^\circ$ .

## Mean difference in parallax (T-H)

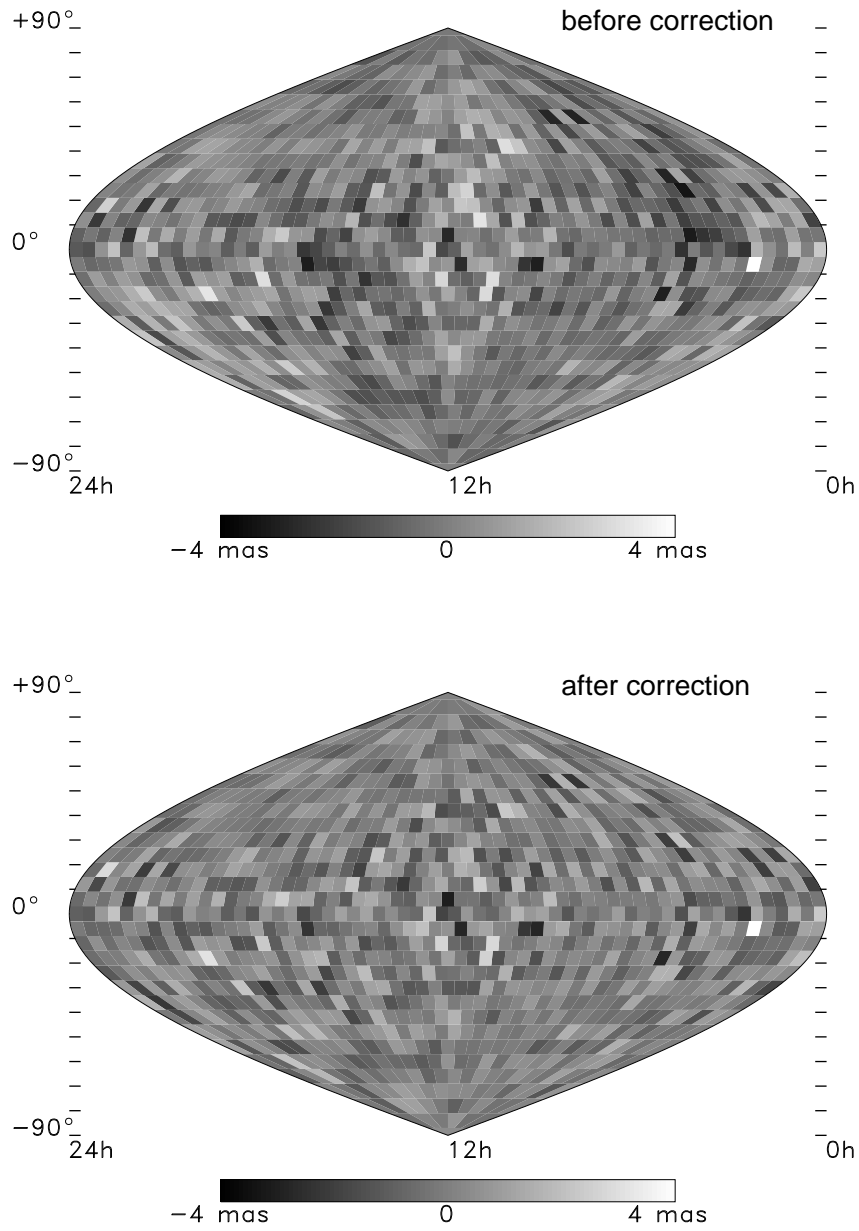


**Figure 11.4 (c)** Sky projection of differences 'Tycho - Hipparcos' in parallaxes. Cosine sky projection in equatorial coordinates, cell size  $6^\circ \times 6^\circ$ .

the entries was quite clear. These were the cases of so-called grid-step errors in the Hipparcos Catalogue, where a position could be wrong by a multiple of 1.2 arcsec. In order to get rid of most uncertainties clearly due to the grid-step error, the limit was extended up to 2.0 arcsec for 57 entries.

Finally, 102 096 main Hipparcos Catalogue entries and 20 892 components of the Double and Multiple Star Annex C were cross-matched and merged in the Tycho Catalogue. 2887 Hipparcos stars and 3694 components were not found in the Tycho Catalogue and were added for the sake of completeness. Less than 20 of these can still be due to grid step errors (see Chapter 18). This constituted the ‘maximum’ catalogue CUO\_CAT\_19, from which entries could only be deleted.

### Refinement of the Catalogue

A few further attempts were made to refine the catalogue as soon as provisional  $B_T$  and  $V_T$  magnitudes had become available for most of the stars. Some 13 000 entries were gradually deleted after dedicated analyses of the stellar contents, involving available photometric data, pair statistics and comparison with the Guide Star Catalog (GSC):

- 783 entries with  $Q = 9$  for which the photometric reduction did not converge to a definite result;
- 11 700 entries of low quality which were in disagreement with GSC. About 10 000 of them were  $Q = 9$  stars with a difference in position between the Tycho Catalogue (TYC) and GSC larger than 3 arcsec, and with  $V_T > 9$  mag. Another 1700 stars of  $Q = 5 - 8$  were rejected if the difference in positions was larger than 1.5 arcsec and/or the difference in magnitudes was larger than 1.5 mag, and the star was in a pair with another TYC star, closer than 36 arcsec. This rejection was based on the finding that for bright double stars GSC provided very often the position of a photocentre, or of a spike, which resulted in a TYC solution of low quality with  $V_T \simeq 11$  mag. The criteria that were used for rejection were shown to be reliable through visual inspection of a large number of maps, obtained with the Digital Sky Survey. This rejection also improved the appearance of pair statistics;
- a handful of stars of  $Q = 7 - 9$  were removed from the catalogue, if they appeared in close pairs with Hipparcos stars, and the Hipparcos entries did not bear any indication of duplicity.

These rejections and other minor improvements led to the catalogue CUO\_CAT\_25, which was transformed into the Tycho Catalogue format, supplemented with magnitudes and other photometric data, and with subsidiary information, such as proximity flags, notes, etc.

---

## 11.4. Production of the Tycho Epoch Photometry

---

Tycho photometry for individual transits is contained in the Tycho Epoch Photometry Annexes, divided into two parts, A and B. The smaller one (TEPA A) includes transit data for 34 446 stars and is delivered on the ASCII CD-ROM set along with the main Hipparcos and Tycho catalogues. The larger one (TEPA B) will be available from CDS,

Strasbourg, and provides epoch photometry for 481 553 stars, including all TEPA A stars.

The final internal data base and the derived catalogues were sorted according to star number (i.e. to the TYC identifier) and the transits belonging to one star were sorted in time. However, the starting point was a data base in the chronological observing sequence of stars as specified by the scanning law of the satellite, comprising 432 million transits of 1 208 168 stars in the TCR catalogue (main processing) plus 103 million transits of 306 766 stars in the TICU catalogue (reprocessing).

Thus, more than 500 million transits had to be sorted according to star number and the time. This huge process was split into several steps as shown in Figure 11.5. The figure also illustrates the calibration process and the construction of the photometric mean catalogues preceding the production of the final Tycho Catalogue. Figure 11.5 shows only the part of the TDAC data flow related to photometry and catalogue production. A comprehensive overview of the data flow is given in Chapters 1 and 12.

The main features of Figure 11.5, as discussed below, are:

- physical sorting;
- calibration and reduction to the Tycho photometric system;
- assignment of astrometric information to single transits;
- computation of photometric mean values;
- construction of the Tycho Epoch Photometry Annex.

Other points to be mentioned are the computation of Barycentric Julian Date and the selection of stars for TEPA A and TEPA B. The latter process is described in Section 2.6 of Volume 1. The selection between photometric data from the main processing and reprocessing is discussed in Section 11.5.

All data base names and processes appearing in Figure 11.5 are abbreviated throughout the remaining part of this chapter as follows:

Transit data:

PGCU	Predicted Group Crossings Update
ITDB	Identified Transits Data Base
TPOC	Tycho Photometric Observation Catalogue
TPOC1/2	different stages of sorting in the TPOC
AT files	All-Transits files: containing astrometric residuals for single transits
TPOC A/B	the TPOC subsets (still binary) preceding the Tycho Epoch Photometry Annex files TEPA A and TEPA B

Star catalogues:

TPMC	Tycho Photometric Mean Catalogue
TYC(internal)	A complete Tycho Catalogue containing additional information for each star.

## Physical Sorting

Due to the huge amount of data the sorting according to star number and the sorting of the transits according to time was split into several steps. The boxes at the right in Figure 11.5 give the physical sorting status (together with some other information) of each transit data base.

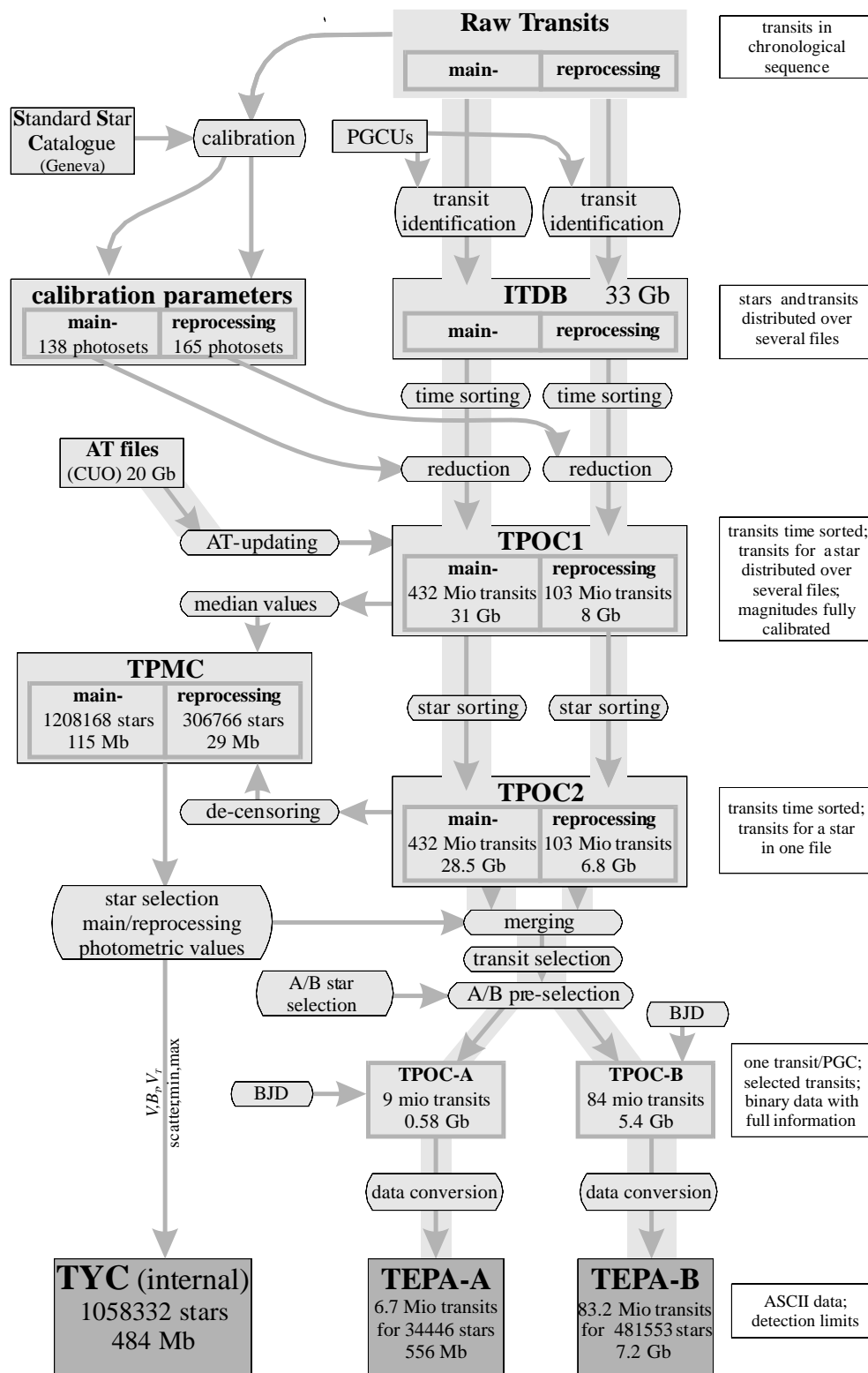


**Figure 11.5.** Data flow for the production of Tycho epoch photometry. Shaded rectangular boxes show data bases while rounded boxes show programs. To the right the main properties of each data base is given. Abbreviations are explained in the text.

Starting from the 'raw transits' data stream, the 'transit identification' process led to a data base (the ITDB) with transit data of one star distributed over many disk files and even the single transits distributed inside one file (though logically connected by means of pointers).

The next step, resulting in TPOC1, sorted all stars according to their Tycho Input Catalogue number and all the transits for each star according to time. But stars and transits were still distributed over many disk files. During this step the still growing ITDB and the TPOC1 co-existed.

Production of the TPOC2, completely sorted according to star number and time, had to wait until the ITDB and TPOC1 were completed. The TPOC2 contained all stars and their time-sorted transits in several physical files, each covering 80 Guide Star Catalog regions, i.e. 122 files covering the whole sky in the main processing and (due to a special numbering) 157 files in the reprocessing.

### **Calibration and Reduction to the Tycho Photometric System**

The time-dependent calibration was carried out with the raw transits as input data, using the Geneva Standard Star Catalogue as a reference system (see upper left part of Figure 11.5). The calibration was done separately for the main processing and reprocessing (details can be found in Chapter 8), giving time intervals of varying length (between 3.4 and 18.0 days) with constant calibration parameters, called 'photosets'. The reduction to the Tycho photometric system was done at the stage of TPOC1 construction for each single transit, with 138 photosets covering the whole mission (165 photosets for reprocessing).

### **Assignment of Astrometric Information to Single Transits**

Because there may be several detections inside one 'predicted group crossing' interval (see Section 2.6) it was necessary to select the correct one. Given only photometric information this would have been easy only for bright stars, but quite unreliable for faint stars. The only method to identify 'correct' transits unambiguously is to use the information obtained from astrometric processing, i.e. the astrometric residual of a transit  $\Delta u$  and its expected standard error  $\sigma_u$ . Due to their importance both values are also given for each single transit in the Tycho Epoch Photometry Annex.

Therefore, astrometric information for single detections for both the main and the reprocessing (available from CUO as 'AT-files') was assigned to detections in TPOC1 by the process 'AT-updating'.

### **Computation of Photometric Mean Values**

For all stars the median values and percentiles were computed and stored in the TPMC together with the de-censored magnitudes for stars fainter than 5 mag. The de-censoring work on TPOC2 was the most time consuming single process in Figure 11.5.

Both de-censoring and median computations used the astrometric information, but only de-censoring checked for parasites (i.e. possible disturbances of transits by other stars giving too bright magnitudes). The storage of both median and de-censoring values in

the TPMC enabled the necessary comparison of the different methods, and it allowed postponement of the decision on the actual limit for the usage of medians as late as just before the final Tycho Catalogue production. The actual limits to use median values and the decision process selecting between main and reprocessing data are described in Section 11.5.

### Construction of the Tycho Epoch Photometry Annex

While the TPOC2 data base contained *all* transits measured with the Tycho experiment and in both main and reprocessing, the final catalogue should contain only valid transits:

- there should be only one detection per ‘predicted group crossing’ interval. If more than one detection was found, the transit with smallest  $|\Delta u|$  was chosen;
- the added background in the  $B_T$  and the  $V_T$  channel was required to be below 100 counts per sample;
- the  $z$  coordinate had to fulfil the condition  $|z| < 1195$  arcsec, i.e. transits near to the slit edges were ignored;
- for the inclined slits, transits within 10 arcsec of the apex were omitted too;
- transits close to jet-firings controlling the attitude of the satellite were ignored.

This ‘transit selection’ in combination with the ‘A/B star selection’ led to the construction of the immediate predecessor catalogues to the Tycho Epoch Photometry Annexes, i.e. to the TPOC A/B data bases. The merging selected the data from either the main or the reprocessing, as described in the next section. Thus, TPOC A/B contained only one solution for a given star.

In the ‘data conversion’ process the binary TPOC data were rewritten to the ASCII format described in Section 2.6 (Volume 1), and detection limits for not-measured magnitudes were computed, as described in Section 16.4. Furthermore, the star content was reduced to exactly those stars with the Field T50 = A/B flag (see Volume 1, Section 2.2) set in the Tycho Catalogue, (this is the reason for the lower number of transits in Tycho Epoch Photometry Annexes as compared to TPOC A/B, see Figure 11.5).

---

## 11.5. Photometric Part of the Tycho Catalogue

---

The photometric ‘mean’ values in the Tycho Catalogue were extracted from the two Tycho Photometric Mean Catalogues (TPMC), the one based on the TICR, thus containing mean values from main processing data, the other one based on TICU, containing results from reprocessing data (as described in the preceding section). Both catalogues contained ‘mean’ data and percentiles derived from median computations and from de-censoring for each star.

For all stars brighter than  $B_T = 8.5$  mag and  $V_T = 8.0$  mag the mean magnitudes given in the Tycho Catalogue are median values. Down to these magnitude limits there were almost no censored transits, and the median and de-censored magnitudes agreed within 0.005 mag, i.e. within the calibration uncertainties. The number of stars with median magnitudes given is thus only 29 524.

Regarding photometry, the major difference between the main processing and the reprocessing was the usage of different single-slit response functions (see Section 8.3). The reprocessing gave better estimates of signal amplitudes for the very bright stars because estimation was done in the wings of the signal. Thus, 129 stars brighter than  $V_T = 3$  mag have reprocessing median magnitudes.

While 1687 stars were available only in the reprocessing, for 133 469 stars a decision had to be made from which processing the mean values and transit data should be taken. The main principle during ‘star selection’ (see Figure 11.5) was to retain a maximum of information, i.e. to prefer that processing which yielded ‘mean’ magnitudes in both channels. Because this was the case for most stars, in a second step that processing providing most accepted transits was chosen if the number of accepted transits differed by more than 10 per cent in de-censoring and 20 per cent in median computations. If not, the astrometrically selected processing was chosen for this star. Thus, the processing yielding the maximum number of accepted transits was chosen for 53 620 stars (out of 103 220) with de-censored magnitudes and 1072 stars (out of 27 099) with median magnitudes.

While the flag in Field T36 of the Tycho Catalogue (see Volume 1, Section 2.2) indicates whether median or de-censored magnitudes are given, the selection whether mean values were derived from main or reprocessing data can only be found in the star header flags in the Tycho Epoch Photometry Annexes.

### **Remarks on Uncertain or Missing Tycho Magnitudes**

The flag in Field T57 of the Tycho Catalogue was set equal to ‘M’ for about 20 000 stars which were suspected to have very uncertain magnitudes, mostly because of a standard error larger than 0.3 mag (see Volume 1, Section 2.2 for details).

This flag was also set in cases where the number of photometric transits  $N_{\text{photom}}$  was less than 16 since it was realized that some magnitudes with very few transits were wrong especially for faint stars. The minimum number of transits for an accepted astrometric solution was however always equal to 30. The flag was set to ‘M’ for this reason and in a few other cases when  $V_T$  was outside the interval of the 15th and 85th percentiles. In these altogether 896 cases the approximate  $T$ -magnitude from the astrometric processing was given, i.e., flag ‘T’ in Fields T36 and T7, and no  $B_T$ ,  $B_T - V_T$  or percentiles were given. The photometry of all these stars may be studied in detail by means of the Tycho Epoch Photometry Annex B, and the deviation may then sometimes be found to be caused by intrinsic stellar variability.

If  $B_T$  or  $V_T$  magnitudes fainter than 15.0 mag were computed by the de-censoring analysis the values were replaced by blanks in the main Tycho Catalogue because these faint magnitudes were considered to be unrealistic, see Volume 1, Section 2.2, Fields T32–39 for details.

For such reasons a total of 8753 entries contain no value of the colour index  $B_T - V_T$ , including the 6301 stars with data only from the Hipparcos Catalogue (see Volume 1, Section 2.2, Fields T37–38).



## 12. TYCHO PROCESSING SUMMARY

*An overview of the actual data processing in the Tycho project and the size of the various data streams is given. Compared to the overview of the Tycho processing given in Chapter 2, this chapter puts the emphasis on the technical structuring of the data reduction chain, rather than on its scientific logic.*

---

### 12.1. Introduction

---

As already described in Chapter 2, the TDAC processing scheme was a very complex data reduction pipeline with large amounts of data flowing through the different stages. Figure 12.1 shows an overview of the complete processing scheme of the main processing (left) and the reprocessing (right). The main purpose of this figure is to provide a different overview of the Tycho data reduction than was given in the Figures 1.2 and 10.1. The figure consists of two principal sorts of objects:

- boxes with embedded texts, indicating the institutes and the types of processes carried out;
- arrows with associated texts, indicating the type and volume of data transferred between the processing steps.

All the processes internal to TDAC are marked by boxes having the same size; smaller boxes indicate auxiliary data provided by institutions from outside TDAC, e.g. the Standard Star Catalogue (SSC) from Geneva. The arrows indicate the direction of data delivery, their width give a hint of the relative amount of data. Approximate numbers for the data volume are given with most of the arrows. The abbreviations present in the figure are those used throughout this volume. Some of those considered most important, sparsely used or particularly confusing because of the existence of a number of similar ones are briefly explained in the lower part of the figure.

Figure 12.1 emphasizes the actual data flow and the technical structuring of the data reduction chain, while Figures 1.2 and 10.1 put more emphasis on the scientific logic. The figure also shows more clearly the dependencies between the different stages and major blocks, like the main processing, reprocessing and the catalogue production.

Since most of the arrows in Figure 12.1 denote physical data interfaces (i.e. mostly 160-Megabyte half-inch magnetic tapes delivered by surface mail), it is obvious that the definition and proper application of these interfaces played a key role within TDAC. In fact, the consumption of time per tape and disk input/output processes, rather than

the actual processing of the data, has been the main bottleneck within TDAC. The process with the highest data turnover from and to other processes was the detection and estimation step in the main processing. More than half of the computing time and power in this step was used to maintain the input/output from and to tapes.

---

## 12.2. Raw Data and Pre-Reduction

---

The main entry point of the reduction scheme was the delivery of the telemetry tapes from the European Space Operations Centre to TDAC. Two identical copies of these tapes were sent in batches of about one month of real satellite time to Astronomisches Rechen-Institut, Heidelberg, and Astronomisches Institut, Tübingen. The attitude, satellite status and orbit data were used at Heidelberg, the housekeeping and raw photon counts (Tycho data stream) were used at Tübingen.

Figure 12.1 is divided into two big data reduction chains, namely the main processing and reprocessing. Each of the two chains is also divided into two major blocks, although less obviously. They are separated by the arrows labelled 'ITDB'. The two reduction blocks above the 'ITDB' arrows (i.e. the upper left and upper right portions of the figure) form the pre-reduction of the raw data. Their results are the two identified transit data bases (ITDB), one for the main processing and one for the reprocessing, respectively.

### The Pre-Reduction Block for the Main Processing

The pre-reduction block for the main processing (upper left) consisted of eight different processing steps distributed between the participating institutes. Much of the complexity of this first block stems from the need to distribute the huge amount of data and processing requirements of the Tycho project over several institutes (this statement has to be understood in view of the computer technology affordable at the time of project initiation, i.e. about 1985). There were also scientific reasons for the complex structure, signified by the intermediate processes recognition, prediction updating and transit identification, which were described in Chapter 2.

Some software tools could be used for several processing steps. This is indicated by using a single box in the case of prediction updating where the independent processes 'updating-2' and 'updating-3' have been carried out by essentially the same software. Some of the logical processing steps were integrated into a single technical process or at least lined up to build a processing pipeline. This is indicated in the figure by the boxes containing two or three different processes.

### The Pre-Reduction Block for the Reprocessing

Most of the resources used in reprocessing were imported from the main processing and adopted or expanded to the special needs. The reprocessing scheme looks much more straight-forward, because there was no need to carry out the recognition and updating steps, as explained in Chapters 2 and 10.



The box containing the three processes: detection, transit identification, and photometric reduction indicates the processing pipeline established at Tübingen in order to reduce input/output from and to tape.

---

### 12.3. Sorting and Catalogue Preparation

---

There is another, somewhat hidden, division in Figure 12.1, namely between the transit (time) and the star (coordinate) domain of the TDAC data flow. This division is not particularly relevant in terms of astronomy, but it implied a very demanding data reorganisation, consisting mainly of a large degree of re-sorting. This reorganisation is indicated by the small gap between the upper and the lower part of Figure 12.1, connected only by the arrows labelled ITDB.

The thin diagonal arrows running towards the astrometric calibration box represent a reformatted version of the ITDB, also of 30 Gigabytes, delivered from Tübingen to Copenhagen. Due to the rather different output requirements of the astrometric and photometric branches of the Tycho data reduction, the sorting took place at very different stages of the processing. Astrometry was an iterative process where the astrometric parameters of the stars (and their errors) were consecutively updated as new observations were treated. Thus the individual observations were used during the first processing steps only. Photometry, on the other hand, was supposed to produce the Tycho Photometric Annexes, containing individual observations for selected groups of stars. Thus the photometry process had to keep on-line most of the information belonging to the individual transits. The ITDB was a strictly time-sorted data base of transit records, but it already contained a pointer structure for every star, tying together all its transits. The physical sorting of the records took place within the box labelled 'TPOC Production'. This box actually represents a complex processing scheme, which is detailed in Chapter 11 (see Figure 11.5).

#### All-Transits Updating

The arrows labelled 'AT' (All-Transits), leading from the boxes 'Astrometric Calibration' to the photometry blocks should be discussed here because they are mentioned only briefly in Sections 7.4 and 11.4.

Astrometric residuals are the most reliable means to decide whether a transit is true or false or parasitic. The de-censored magnitudes and all transits contained in the Tycho Epoch Photometry Annexes should thus be based on a transit data base selected by astrometric criteria. Moreover, the separately derived photometric and astrometric values in the final catalogue should be based on a common set of transits (the transits actually used by Tycho photometry and astrometry are subsets of such a common set, but not necessarily exactly identical). Since astrometry was carried out at Copenhagen and photometry at Tübingen, a special data stream was created to tell photometry which transits had been used by astrometry for the derivation of the astrometric parameters for each star. This data stream was called AT ('All-Transits') since it contained almost all transits, not only the accepted ones. Each transit was accompanied by flags and quantities indicating the acceptance level, and the reasons for rejection, if any.

This data stream was quite different from all the others defined within TDAC, because it was designed more than five years after the other ones, using hardware and software tools which had become available in the meantime. It contained floating point values and flags originating in a certain hardware architecture. Moreover the data was compressed and archived using the standard ZIP tool, version 2.0.1, available on a wide variety of computing platforms. The data were sent on the small EXA-byte tapes, each containing more than ten times as much data as the 160-Megabytes magnetic tapes used in all other TDAC data exchange. The advantages of this procedure were obvious:

- the compression resulted in a very small number of tapes, and thus facilitated the possibility of running a huge stretch of data from a single tape without human interaction;
- a single ZIP archive file contained a large number of data files, thus the data handling was much easier;
- there was no need to write dedicated input/output routines in order to code/decode the data (the transition from the IEEE format to the VAX format was carried out using available standard routines).

The all-transits updating was a big processing step since it was necessary to identify every record contained in the all-transits files with exactly one record in the Tycho Photometric Observation Catalogue, and to rewrite the identified transit records in the Tycho Photometric Observation Catalogue, updated with some of the all-transits information.

---

#### **12.4. Catalogue Production**

---

The actual production of the catalogue was separated from the other steps, because the data contained in the final catalogue were merged from a number of different sources and the format of the catalogues is quite different from what was used inside TDAC. In Figure 12.1 the complex processes of Tycho Catalogue and Photometry Annex production are merged into a single box each. The individual processing steps belonging to them are detailed in Chapter 11.

A. Wicenec



## 13. PHOTOMETRIC STANDARD STARS

*A catalogue of photometric standard stars, carrying  $B_T$  and  $V_T$  magnitudes predicted from ground-based measurements in various photometric systems, was used for the photometric calibration of the Tycho instrument.*

---

### 13.1. The Preliminary Standard Star Catalogue

---

Before the launch of Hipparcos a program for the collection of ground-based photometric data for the mission was set up, mainly at Geneva and Lausanne (see Grenon *et al.* 1992). This program included the compilation of existing data as well as new measurements. The resulting big collection of data in a broad variety of photometric systems (UBV, uvby, Geneva, Walraven, VRI, etc.) was checked, cross-identified and homogenized as far as possible. Transformation formulae from these ground-based photometric systems to the expected photometric passbands ( $B_T$ ,  $V_T$  and  $H_p$ ) of the Hipparcos satellite were derived, using the pre-launch calibration data of the various detectors. The transformations were then used to compute predicted magnitudes for as many stars as possible in the expected photometric bands.

The stars with the most reliable and precise data were selected from catalogues of photometric standard stars for the in-orbit calibration of the Hipparcos and Tycho photometry. The actual use of the resulting Tycho photometric standard star catalogue in the data reductions was described in Chapters 8 and 9.

A total of 267 016 ground-based measurements was transformed to  $B_T$  and  $B_T - V_T$ . 1200 stars with unreasonable or discordant colours and magnitudes were rejected. Candidate standards were selected among the remaining 99 000 stars according to the following criteria:

- mean error of predicted  $V_T$  smaller than 0.035 mag;
- mean error of predicted  $B_T - V_T$  smaller than 0.020 mag;
- at least two independent ground-based measurements.

These three criteria defined the first-priority candidates. The selection was relaxed to only the last of the criteria, i.e. at least two independent measurements, for an additional list of second-priority candidates.

The full list of 99 000 stars, with about 25 000 candidate standards was cross-identified with the Tycho Input Catalogue at Strasbourg. This resulted in about 65 000 matches,

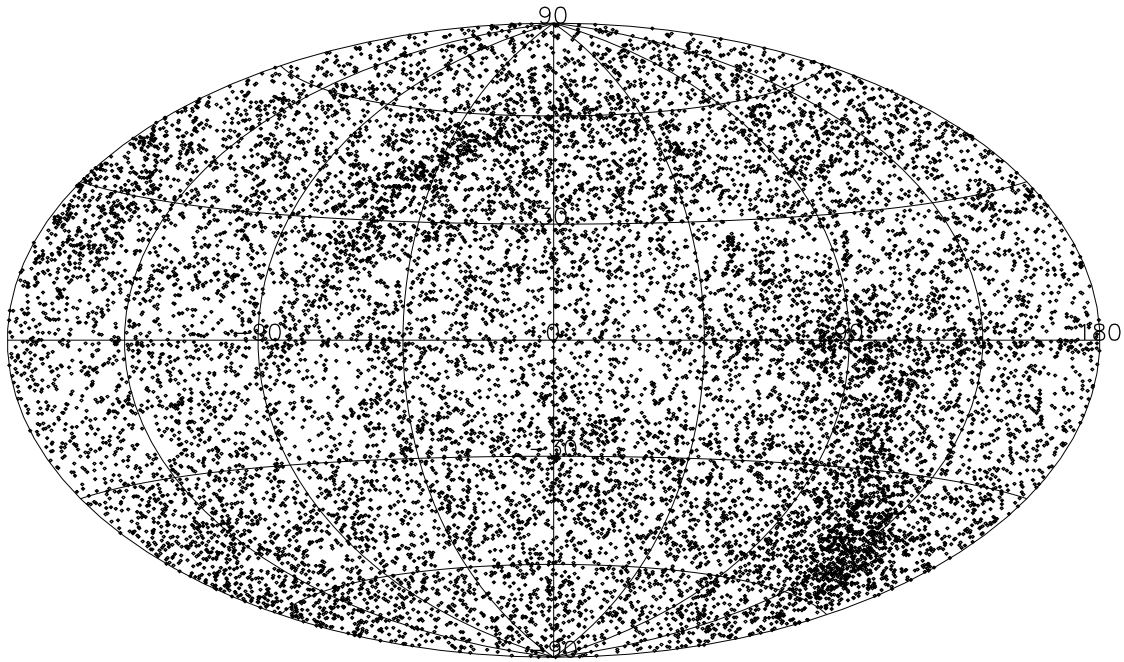


**Figure 13.1.** The celestial distribution of the 13 600 stars of the revised photometric standard star catalogue which were actually used in the reprocessing calibration (equatorial coordinates, north up, right ascension increasing to the right, vernal equinox in the center). Areas of enhanced density are the galactic plane, the north and south galactic pole regions, several star clusters, and a particularly well-observed Milky Way region around  $\delta = -50^\circ$ .

including 23 502 candidates. This list was further reduced by eliminating known double stars (and a few known variables), and by excluding all stars fainter than 9 mag or brighter than 4.5 mag (for reasons explained in Chapter 8). The magnitude selection was done separately for the two spectral passbands.

In the end, slightly less than 10 000 stars were actually used for the Tycho photometric calibration, both in  $B_T$  and  $V_T$ . The selection still included a few stars with erroneous predicted magnitudes, and even a few variables, as can be seen from the outliers in Figure 8.2.

---

## 13.2. The Revised Standard Star Catalogue

---

The catalogue of photometric standards was revised during the mission, both in its stellar content and in the magnitudes for the individual stars. There were essentially four reasons for the revision:

- previously unknown duplicity was detected for quite a number of the standard stars from the comparison of the Hipparcos main grid ‘ac’ and ‘dc’ magnitudes (see Volume 3, Chapter 14);
- preliminary reductions of the star mapper photometric data showed that some of the predicted  $B_T$  and  $V_T$  magnitudes were incorrect;

- the preliminary photometric calibration of the star mapper yielded significant colour coefficients (index 4 in Table 8.2), indicating that the actual photometric passbands of the Tycho instrument deviated slightly from the pre-launch expectations;
- additional ground-based photometric data were included to increase the number of candidate standards.

The third of these reasons led to a re-determination of the Tycho passbands. New transformation formulae from ground-based photometric systems to predicted  $B_T$  and  $V_T$  magnitudes were derived, and used to define revised standard star magnitudes. The changes in the Tycho photometry caused by the revision were moderate: the zero-point calibration coefficient (index 1 in Table 8.2) changed by about 20 millimag for the  $B_T$  channel, and by only a few millimag for the  $V_T$  channel. The colour coefficients changed by 15–25 millimag per mag (depending on the slit group and field of view) for both channels. The change in the colour terms implied a shift of the effective wavelengths of the order of a few nanometers.

The revised catalogue contained 29 000 candidate standards. After the elimination of doubles and the reduction of the magnitude range (4.5 to 9 mag, as before), 13 600 standard stars suited for the Tycho photometric calibration remained. These were used for the reprocessing calibration. Their distribution on the celestial sphere is shown in Figure 13.1. The main processing calibration could use only 10 000 of them, for purely technical reasons, originating in the data flow organisation.

U. Bastian, V. Großmann



## 14. SPECIAL TREATMENT OF DOUBLE AND MULTIPLE SYSTEMS

*Stars with separations closer than 3 arcsec were usually not separated in the star recognition process (as described in Chapter 5). The limit of resolution was mainly determined by the slit width of 0.9 arcsec, and not by the much smaller optical resolution of the telescope. In the reprocessing, a particular effort was made to apply an adequate treatment to known double stars and suspected double stars. The close double stars were eventually detected in two different ways, depending on their separations. Between 1.5 and 3 arcsec, both components could be detected separately, and the individual positions could be derived. When the separations were between 0.4 and 1.5 arcsec, the duplicity was detected on the basis of a correlation between the measured magnitude and the position angle of the star mapper slits on the sky.*

---

### 14.1. Introduction

---

The observation of components of double and multiple systems was already treated in Chapter 5. All stars closer than 6 arcsec to the entries of the Tycho Input Catalogue were searched in the star recognition process. The components were numbered in sequence of magnitude, with the brightest coming first. Then the selection area was extended from 6 to 20 arcsec in radius for the search of the so-called ‘wide companions’. These processes ran satisfactorily for finding components brighter than  $T = 10.5$  mag and with separations between 3 and 20 arcsec (see Section 5.7). Positions and photometry were derived for these stars as for single stars, and they were included in the Tycho Input Catalogue Revision.

A separation limit of 3 arcsec is large compared to the diffraction limit of the Hipparcos telescope. With an aperture of 29 cm, and an effective wavelength (in the  $V_T$  filter) of 532 nm, the radius of the first dark diffraction ring is only 0.38 arcsec. The wide separation threshold in Tycho was indeed not determined by the optics of the telescope but by the detection and star recognition processes. The detection algorithm was optimized for faint stars in order to obtain a catalogue containing as many stars as possible. A model curve corresponding to a single star was fitted to the photon counts (see Sections 4.3 and 4.4). Since the path of a star across each slit of the star mapper is 0.9 arcsec long, the components of double stars were distinguished only when the projection of the separation vector along the scan direction was about twice as large.

In practice, stars as close as 1.2 arcsec were sometimes separated, but the components were safely distinguished only when the projected separation was larger than 2 arcsec. As explained in Section 5.7, a limit of 2 arcsec in the detection process corresponds to a separation limit of 3 arcsec in the star recognition process because detections collected at different scan directions are necessary for finding a star.

Close double stars with separations of less than 3 arcsec were treated in dedicated processes. The components with separations between 1.5 and 3 arcsec were distinguished on the basis of double detections. Stars closer than 1.5 arcsec were also found since their detections have statistical properties different from those of single stars.

The close double star processing consisted of several tasks, shown in Figure 14.1. The processing was controlled by two object lists called 'stars flagged in reprocessing' and 'stars brighter than  $V_T = 10.5$  mag', respectively (the second row of boxes in Figure 14.1).

The former object list formed part of the Tycho Input Catalogue Update, the input catalogue for the reprocessing (see Section 10.2). The selection was based on the double stars already known (Section 14.2), but also on a search for possible double stars performed at roughly midway through the mission (Section 14.3). New candidate double stars emerged from an analysis of the raw photon counts, and from the residuals of a preliminary astrometric reduction. All these possible double stars received two sorts of special treatment in the reprocessing, in order to confirm their duplicity. These treatments were supplements to the astrometric analysis (Section 14.4) and to the detection process (Section 14.5).

The second star list, essentially the brighter half of all Tycho stars, was submitted to a special photometric analysis (Section 14.6). It was based on the fact that the detection algorithm provided a signal with a larger amplitude when the components of a double star were aligned on the slits of the star mapper than when they were perpendicular to the slits. As a consequence, duplicity mimicked variability. However, double stars could be distinguished from true variable stars since their brightness was correlated with the position angle of the slits.

---

## 14.2. Close Double Stars from Catalogues

---

The first source of close double stars to be selected for the reprocessing was constituted by the ground-based catalogues of visual double or multiple stars. The double stars relevant for Tycho were selected and cross-matched with the Tycho Input Catalogue Revision. Systems with separations larger than 3 arcsec were ignored, since it was assumed that they had been properly separated in the Tycho Input Catalogue Revision. Components closer than the diffraction limit were also ignored. The list was thus restricted to separations between 0.35 arcsec and 3 arcsec.

From the statistics of the Tycho Input Catalogue Revision it was clear that the fraction of stars represented in the Tycho Catalogue would drop rapidly for combined  $T$  magnitudes between 10.7 and 12 mag. For that reason, only double stars with both components brighter than 12 mag were selected. Moreover, whenever the components were too close to be separated, the contribution of the secondary to the total luminosity was required to be above a certain level, i.e. to make it detectable in the raw Tycho signal. Double

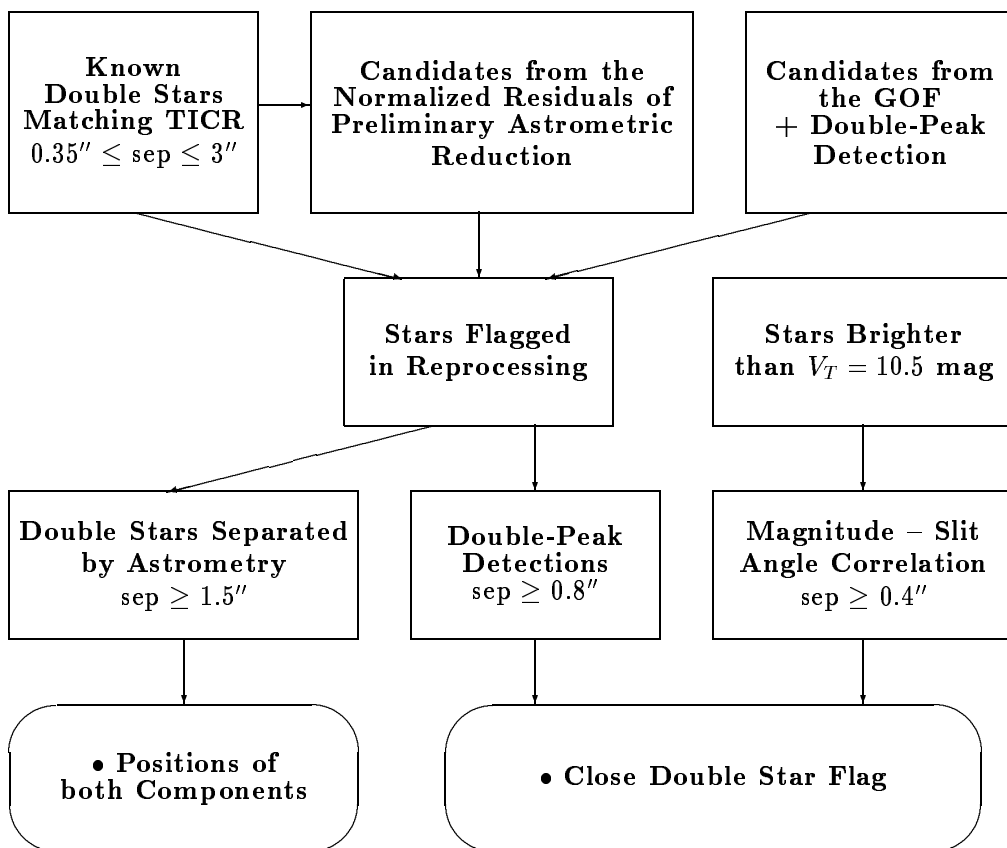


**Figure 14.1.** The data flow in close double star processing. The rounded boxes refer to the results in the final Tycho Catalogue. TICR is the Tycho Input Catalogue Revision; GOF = goodness-of-fit.

stars with magnitude differences larger than 3 mag and separations less than 1.5 arcsec were discarded.

## Catalogues

The known visual systems were found in three different sources. Most important was the Washington Double Star Catalogue ('WDS', Worley & Douglass 1984). The WDS is virtually complete for stars with separations larger than about 1 arcsec, but some new double stars closer than this limit have been discovered since its publication. Apart from incompleteness, another drawback of the WDS is the very poor accuracy of the coordinates: they are provided with last digits corresponding to  $0.1^m$  for right ascension, and 1 arcmin for declination.

The second source was a part of the Catalogue of Components of Double and Multiple Stars ('CCDM', Dommanget 1983, 1989b), which was published as an Annex of the Hipparcos Input Catalogue (Turon *et al.* 1992, 1993). This catalogue provides positions with an accuracy of some arcsec, which is much better than the WDS.

Third, the Catalogue de 2550 Etoiles Doubles COU ('COU', Coureau 1990) includes several hundred double stars of the northern hemisphere which were discovered by Paul Coureau after the publication of the WDS. In addition it provides recent measurements of the relative positions of components for many of the stars in the WDS. The accuracy of coordinates is the same as in the WDS.

The numbers of double stars satisfying the selection criteria among the WDS, the CCDM, and the COU were 13 826, 3569, and 1394 respectively, but several systems were in duplicate or even in triplicate, since the three catalogues are overlapping (hereafter, a 'double star' is a primary component and a fainter star; a close system of  $N$  stars is considered as  $N - 1$  double stars). The WDS and the COU were merged, and the entries also in CCDM were discarded, since CCDM provides better coordinates than the two other catalogues. For the remaining stars in the merged WDS+COU file, accurate positions were searched in the catalogue of Positions and Proper Motions, or 'PPM' (Röser & Bastian 1991; Bastian *et al.* 1993). The cross-matching with PPM was done in order to increase the probability of selecting the correct double stars afterwards. Whenever a case appeared to be ambiguous, two entries for the double star list were constructed, one from the PPM and one from the WDS+COU file. Finally three lists were obtained: 6980 entries with coordinates from WDS or COU, 4423 entries with coordinates from PPM, and 3569 entries from CCDM.

### **Cross-Matching the Double Stars with the Tycho Input Catalogue Revision**

The positions of double stars from the catalogues were compared with the positions of stars in the Tycho Input Catalogue Revision and a cross-matching was performed. Different selection rules were used, depending on the accuracy of the positions of the double stars.

For the double stars with coordinates from WDS or COU, matching stars were requested to be closer than 3 arcmin and the magnitudes of the primary components to differ by less than 2 mag from the magnitude in the Tycho Input Catalogue Revision. When several stars of the Tycho Input Catalogue Revision satisfied these criteria, a priority selection algorithm was applied. The stars closer than 3 arcsec to the original positions in the Tycho Input Catalogue were selected first, since the stars with large offsets in position were assumed to be false stars (see Chapter 5). When no star satisfied this condition, the stars found at more than 3 arcsec were considered. When no stars at all had been found in the star recognition process, then the stars brighter than 10.725 mag in the original Tycho Input Catalogue that were kept in the Revision were also taken into account. This selection provided a total of 6127 stars from the Tycho Input Catalogue Revision, which matched 5405 objects from the ground-based double star catalogues.

The double stars with coordinates from PPM were selected according to the following rule. Stars in the Tycho Input Catalogue Revision closer than 3 arcsec to the PPM positions were considered, and up to three stars were selected: the closest star, the closest star actually found in the star recognition process, and the brightest star found in the star recognition process. 4405 stars from the Tycho Input Catalogue Revision were thus associated with 4356 double stars with PPM coordinates.

The double stars with coordinates from CCDM were cross-matched using a rule similar to that for PPM coordinates. Since the positions in the CCDM are less accurate than those in the PPM, the selection distance was 20 arcsec instead of 3 arcsec, however.

**Table 14.1.** Origin of the coordinates of double stars matching the Tycho Input Catalogue Revision, split into classes of separation. The numbers of double stars in the ‘Merged’ line are different from the sums of the columns since some double stars are common to the PPM and the WDS+COU list.

Separations	0.35" – 1"	1" – 2"	2" – 3"	Sum
CCDM	1581	1189	770	3540
PPM	2156	1416	784	4356
WDS+COU	2250	1674	1481	5405
Merged	5965	4255	3014	13234

3768 stars from the Tycho Input Catalogue Revision were thus associated with 3540 double stars.

In the end a total of 14 237 Tycho Input Catalogue Revision stars had been associated with 13 234 double stars in the WDS+COU and in the PPM lists. The origins of cross-matching and statistics of the separations between the components are presented in Table 14.1. These stars were flagged and added to the Tycho Input Catalogue Update, described in Section 10.2.

---

### 14.3. Candidate Double Stars from Tycho Observations

---

#### Preliminary Selection from Detection

Double stars closer than about 2 arcsec were usually not separated by the detection algorithm. However, systems with separations of about 1 arcsec still generated transits with the profiles of the four photon peaks differing from those of a single star. This showed up as a ‘bad’ value of some goodness-of-fit parameter derived in the detection process while fitting slit response functions to the observed photon counts. This property was used as a first step in selecting candidate double stars from the photon counts. As a preparation for this step, the mean goodness-of-fit values and their standard deviations were calculated for different bins of  $T$  magnitudes, for photon counts in the  $B_T$ ,  $V_T$  and  $T$  bands. The mean values together with the standard deviations were used in a goodness-of-fit check implemented in the transit identification program. For each detection, the appropriate mean goodness-of-fit was derived from the  $B_T$ ,  $V_T$  and  $T$  magnitudes. A detection was flagged when its actual goodness-of-fit value differed by more than one standard deviation from the mean values. The detections were assigned to a star in the Tycho Input Catalogue Revision when they were less than 1.4 arcsec from the corresponding predicted group crossing. This procedure was applied to a part of the mission corresponding to 247 full days of observation, between 22 April 1990 and 3 March 1991.

The second step in selecting candidate double stars from the Tycho observations was a ‘double-peak test’ applied to the photon counts of the transits flagged by the above goodness-of-fit test. The photon counts in the  $T$  band were read and folded with the non-linear 4-peak filter. Then a single-star profile was fitted to the folded counts, the initial values for transit time and signal amplitude of the peak being set to the maximum count rate in a 4-sample interval centered on the transit time derived by routine detection and estimation. If the fit was successful, the resulting profile was subtracted from the

count rates and a second maximum was searched inside a 20-sample interval (i.e. 5.625 arcsec) centered on the initial transit time. If a second maximum was found, the corresponding starting values were set and a double-star profile was fitted to the initial folded data.

The test was considered to be successful if the signal-to-noise ratios of both peaks were larger than 1.5, if the separation of the peaks was between 0.45 and 2.8 arcsec, and if the secondary peak could not be attributed to another star of the Tycho Input Catalogue Revision. The whole procedure (goodness-of-fit test plus double-peak test) resulted in the flagging of 0.9 per cent of all transits. In order to keep a reasonable number of candidate double stars, all stars having less than 4 transits successfully tested with the double-peak fit were discarded.

For the remaining stars on the list, it was checked whether the double-peak separation was correlated with the slit angle. The stars with the best correlation were selected, aiming at a number of about 10 000. A list of 8687 stars was finally obtained, including 1608 stars matching the list of known double stars.

### **Preliminary Selection from the First Iteration of Astrometric Reduction**

Another selection of candidate double stars was performed on the principle that the (unresolved) detections of double stars should be more widely scattered around the positions derived in astrometric reduction than those of single stars. The parameter describing this statistical property was the normalized residual from the astrometric adjustment, defined as:

$$R = \sqrt{\frac{\|\rho\|^2}{N_{obs} - 2}} \quad [14.1]$$

where  $\rho$  is the normalized residual vector of the individual observed transit times (see Equation 11.1), and  $N_{obs}$  is the number of observations.

A first iteration of the Tycho astrometric reduction process was run on the first 17 months of the mission, and the normalised residuals were derived. It appeared that many stars found in the star recognition process at more than 3 arcsec from positions in the original Tycho Input Catalogue had large  $R$ , since they were in fact false stars. These stars were discarded from the search for double stars, as were also the stars having a companion closer than 10 arcsec.

The selection criterion for candidate double stars depended on  $R$  and on the  $T$  magnitude. It was tuned by considering the stars matching known doubles among the stars with large  $R$ . Only pairs with separation between 0.8 and 2 arcsec, and with a difference of magnitudes  $\Delta m$  less than 1 mag were taken into account, since they were the easiest to detect. It was assumed that all double stars brighter than  $T = 7$  were known. Their intrinsic proportion among stars was thus derived from counts in the Tycho Input Catalogue; the result was 0.78 per cent. Considering, on one hand, the number of stars in the Tycho Input Catalogue Revision, and, on the other hand, the known double stars, completeness coefficients were derived for magnitude bins, and the proportions of stars that should be double were calculated for different intervals of  $R$  and  $T$ . The selection threshold of candidate double stars was set in order to get an estimated proportion of true double stars (known or not) of at least 20 per cent among the selected stars. All stars fainter than 10 mag were discarded by this criterion, and 1217 stars were finally selected, including 420 stars matching the double stars from catalogues.

When the known double stars from catalogues (Section 14.2) were discarded from the count, the selection from detection and from astrometry finally provided 7846 new candidate double stars. They were added to the 14 237 known doubles, the combined list of 22 083 stars was flagged in the Tycho Input Catalogue Update, in order to be submitted to dedicated double-star treatment during the reprocessing, as described in the next two sections.

---

#### 14.4. Astrometric Reduction of Close Double Stars in Reprocessing

---

##### Solving Astrometric Observation Equations for Selected Double Stars

This section describes the dedicated treatment for known or suspected close doubles that was performed in the course of the astrometry processing at Copenhagen.

All detections assigned to a star flagged for double-star treatment in the Tycho Input Catalogue Update (see Sections 14.2 and 14.3) were collected in an *ad hoc* ‘Catalogue of Observation Equations of Close Doubles’ (OECD), containing all necessary information for the analysis. During generation of the OECD, there was no rejection of detections due to the usual astrometric criteria (see Chapter 7). In particular, detections with large residuals or large normalized residuals were not rejected, for obvious reasons. Thus, detections as far as 5 arcsec (the limit set up by transit identification) from the specified position in the input catalogue were available. Parasite recording (see Section 7.2, Figure 7.1) was also ignored, otherwise a lot of useful observations would have been lost as disturbed by parasites when both components of a double star had been detected in the recognition process and had obtained separate entries in the Tycho Input Catalogue Revision.

The OECD contained all parameters of the original observation equations (see Equation 7.7), plus the  $B_T$  and  $V_T$  amplitudes and the background values in the  $B_T$  and  $V_T$  passbands. These photometric quantities were needed to compute median  $B_T$  and  $V_T$  magnitudes of resolved components, corrected for the photometric bias at faint magnitudes due to the detectability threshold. The resulting  $B_T$  and  $V_T$  magnitudes were included in the Tycho Catalogue, along with the astrometric parameters. The photometric treatment was somewhat simplified and less precise compared to the routine photometry for the Tycho Catalogue, however.

Detections assigned to a selected double star were processed with an algorithm divided into a few steps. First, an astrometric solution for a ‘central’ component was attempted. To start an iterative process, all detections with residuals (observed minus predicted) smaller than 1.1 arcsec in absolute value were chosen, and a starting estimate of the position was calculated by the least-squares method. This solution was used later on as a first approximation. The median magnitude  $T_m$  of the central component was also estimated from the set of detections used in the adjustment. This quantity was used at subsequent iterations for the selection of detections in the following way. All detections with magnitudes more than 1 mag from  $T_m$  were excluded from the analysis, whatever their astrometric residual. This allowed the diminution to some extent of the influence of disturbing parasitic transits, and the improvement of the assignment of detections, provided the two components were of considerably different magnitudes.

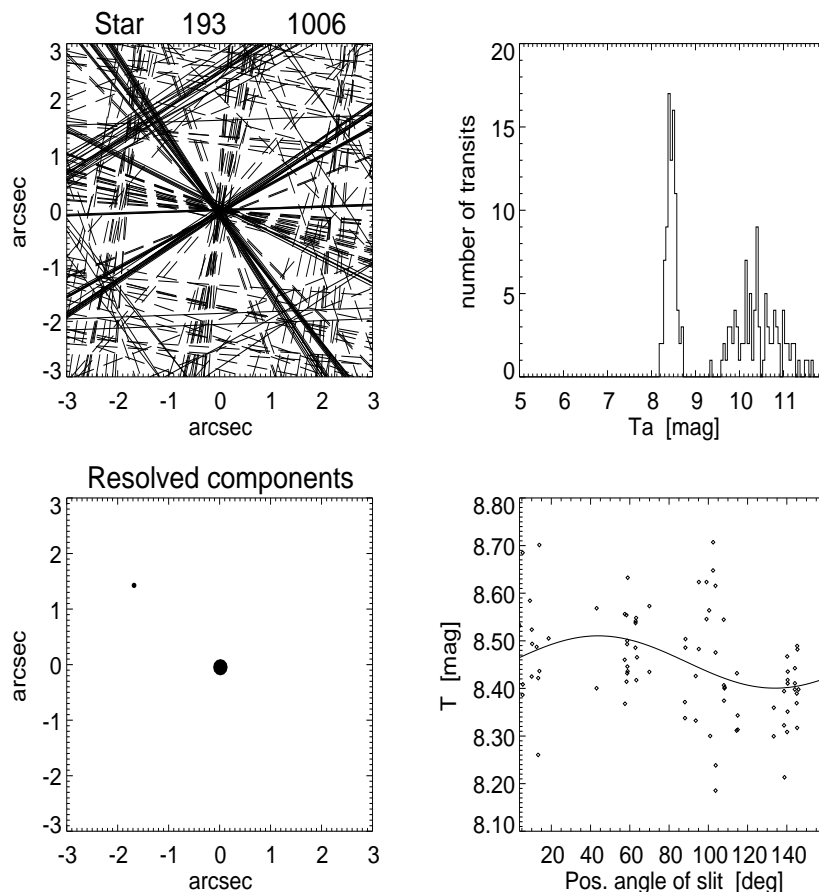


**Figure 14.2.** Double star analysis in astrometry. Top left: detection line map, solid lines belong to transits of the vertical slit; top right: distribution of magnitudes  $T_a$ , derived directly from the amplitudes of each detection; lower left: resolved components, size of circles correspond to estimated  $T_m$  magnitude; lower right:  $T_a$  as function of position angle of the detection line. The first harmonic fitting curve is shown as a solid line.

The astrometric residuals were used as additional selection criterion in the course of subsequent iterations. A detection was accepted if its residual was smaller than  $3\sigma_u$ , where  $\sigma_u$  is the expected standard deviation for this detection, as calculated in the routine processing and written into the Catalogue of Observation Equations of Close Doubles. In order to compute the residuals, the position obtained at the previous iteration was used. Hence, the iterated position could drift from one iteration to the next, and the selection of observations was repeated among the whole set of detections. The  $T_m$  value was updated every time. There were six such iterations, excluding the startup described in the previous paragraph.

Corrections to the tangential coordinates of the central component were calculated in this way. All observations assigned to the central component in the last iteration were left out of the analysis, in order to facilitate the subsequent detection of secondaries, typically fainter components. In this respect, the method resembled a cleaning algorithm of image processing.

In general, Tycho astrometry was unable to determine proper motions and parallaxes for resolved components of close double systems individually. Thus the on-ground proper

motions had to be used in the calculation of the mean positions at the Tycho Catalogue standard epoch J1991.25.

### Solving Secondary Components

The search for and solution of secondary components proceeded in two steps. In the first step the detections assigned to the central component were subjected to a special photometric analysis. It was aimed at finding the position angle of a secondary component in the vicinity of the first one. It exploited the simple fact that the amplitude of a detection depended on the difference between the position angle of the star mapper slits and the axis of the double star. If the slit crossed both stars at the same time, the amplitude was larger, and, vice versa; the minimum amplitude was expected when the slit was perpendicular to the axis of the double. The minimum of the function  $T_a(p)$ , where  $p$  is the position angle of the slit, indicated the direction towards the secondary component, modulo  $\pi$ . In order to determine this minimum safely, a harmonic analysis of the magnitudes:

$$T_i = a_0 + a_1 \cos(2p_i) + b_1 \sin(2p_i) \quad [14.2]$$

was performed, where  $p_i$  is the position angle of the slit at the moment of the  $i$ -th observation,  $T_i$  is the magnitude of the  $i$ -th observation, and  $i = 1, 2, \dots, M$ . Equations 14.2 were solved for the coefficients  $a_0$ ,  $a_1$  and  $b_1$  by the least-squares method. Then the full amplitude of the modulation curve was  $A_T = 2\sqrt{a_1^2 + b_1^2}$ , and the phase  $\phi = \arctan(a_1, b_1)/2$  determined the possible direction  $p_s$  to the secondary component.

The larger the amplitude  $A_T$ , the more confidence existed in the presence of that secondary. The formal criterion was the signal-to-noise ratio for the amplitude:

$$F_T = A_T / \sigma(A_T) \quad [14.3]$$

This number was important for the flagging of suspected unresolved double stars described in Section 14.6, but in the context of the present section, the search for secondary components was undertaken no matter what the  $F_T$  value was.

Having determined the possible position angle  $p_s$  of the suspected double star, two starting points were placed in the two opposite directions  $p_s$  and  $p_s + \pi$  at distances of 1.9 arcsec from the central component, and an astrometric solution was attempted for both of them, in the same way as described above for the central component. The only difference was that for the iterations the threshold value of residuals was set to  $4\sigma_u$  instead of  $3\sigma_u$ , in order to take into account the possible disturbing influence of the central component. Other directions were not examined, which avoided a lot of false detections of faint stars caused by the data noise. In fact, a secondary component could not be found in the rare cases when the analysis of  $T_a(p)$  had given a position angle  $p_s$  wrong by more than about 30 degrees. This could happen basically for two reasons: (i) unrecorded parasitic transits survived the filtering on  $T_a$  and were accepted for the central component, and (ii) the central component was a variable star and the time-variations of its magnitude were correlated with the position angle of the slits by chance.

A number of separate components (maximum 3) could indeed be detected as a result of this treatment. Their equatorial coordinates  $\alpha$  and  $\delta$  were derived from the known tangential coordinates and the input catalogue position.  $B_a$  and  $V_a$  magnitudes were calculated for all detected components with a simplified photometric calibration procedure. These magnitudes were forwarded for inclusion in the Tycho Catalogue. The

final decision on whether a newly-found component was to be used as an additional star in the Tycho Catalogue was made after a redundancy analysis of all astrometric results.

### Performance of the Method

The reprocessing list of 22 083 known or suspected close double stars contained more than 2000 stars having a preliminary double-star solution by NDAC derived from measurements of the Hipparcos main instrument. These were used to assess the success of the above-described double star processing. The preliminary NDAC solutions for double stars provided separations and position angles rather than coordinates of components. Consequently only relative positions of the components could be compared. Generally, the accuracy of the NDAC solution was better than that of Tycho by almost one order of magnitude. It could therefore be assumed that any difference in relative positions of the components was due to the inaccuracy of the Tycho solution.

It happened quite often that the algorithm described above gave two resolved companions located in approximately opposite directions relative to the central one. Since triple stars are fairly improbable with this limiting magnitude, one of the companions was almost surely false. Such false stars were due to a side effect of the filtering of the raw data in the detection process. Any fairly bright star generated a 'blind area' around itself of about 1.4 arcsec radius, where detections were extremely scarce, while the probability of a detection was enhanced by the filtering at distances from 1.4 to 2.8 arcsec. On a detection line map (e.g. Figure 14.2) the star is surrounded by a cloud of transits, mostly false by nature. Occasionally, dense concentrations of false detections are interpreted as a faint companion star.

The problem was therefore to distinguish between real and false resolved companions (the latter are called 'ghosts' in the following discussion). From the sample of NDAC double stars it was concluded that a resolved companion is most probably true if the difference of separations  $\rho_{\text{TYC}} - \rho_{\text{HIP}}$  fell into the interval  $[-0.34, 0.26]$  arcsec and position angle  $\text{PA}_{\text{TYC}} - \text{PA}_{\text{HIP}}$  was in the interval  $[-23, +23]$  degrees. The real distribution of the true companions is much narrower, as shown in Figure 14.3. The full width at half maximum of the distribution is 0.07 arcsec for separations and  $3^\circ$  for position angles. Figure 14.3 (centre left) represents the separations of all 817 pairs resolved by Tycho versus the NDAC separations. The cloud of ghosts (diamonds) is concentrated around  $\rho_{\text{TYC}} \simeq 2.5$  arcsec, as expected. It was found that the magnitudes of the ghosts were typically fainter than 10.7 mag, but a fair number of true companions as faint as that were also detected.

The signal-to-noise ratio  $F_s$ , defined in Section 7.4, proved to be highly efficient in separating false and real stars. Figure 14.3 (centre right) shows the  $F_s$  distributions of the 152 ghosts and 665 true companions. Choosing a limit of 4.4 on  $F_s$  would provide a clear distinction between true and false stars. With this limit, only 2 of the 152 ghosts in the figure remain, which were in fact badly solved real stars, and 638 of the 665 true companions survived.

The 0.1, 0.5 and 0.9 quantiles of the  $\rho_{\text{TYC}} - \rho_{\text{HIP}}$  distribution as a function of the true separation are shown in Figure 14.3 (lower left). There is a strong bias of Tycho separations, appearing also in Figure 14.3 (top left). It was caused by the adopted detection filtering, devised for single symmetric star images in the raw photon counts. When a star image was highly asymmetric due to the presence of a nearby companion, the symmetric detection filter gave a transit time shifted towards the companion, i.e.

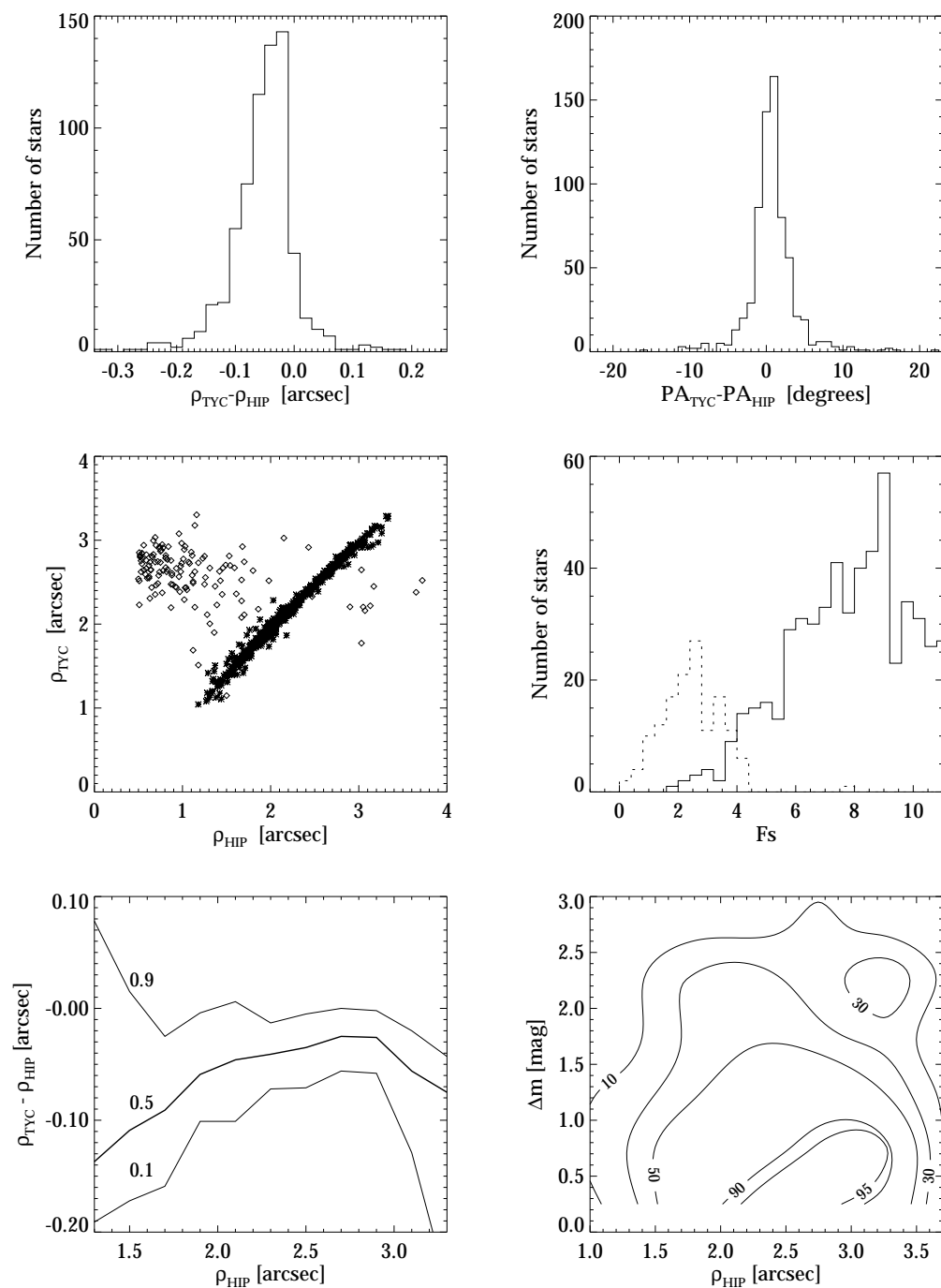


**Figure 14.3.** Performance of the method to resolve close double stars: The two upper plots show distributions of successfully resolved stars versus ‘Tycho – Hipparcos’ differences in separations and position angles; centre left: Tycho separations versus Hipparcos separations for ghosts (diamonds) and true components of double stars (asterisks); centre right: distributions of ghosts (dashed line) and true stars (full drawn line) versus  $F_s$  value; lower left: quantiles of the distribution of resolved stars versus difference in separations, as a function of NDAC separation; lower right: percentage of successfully resolved double stars as a function of separation and difference of components in magnitude, shown as a contour map.

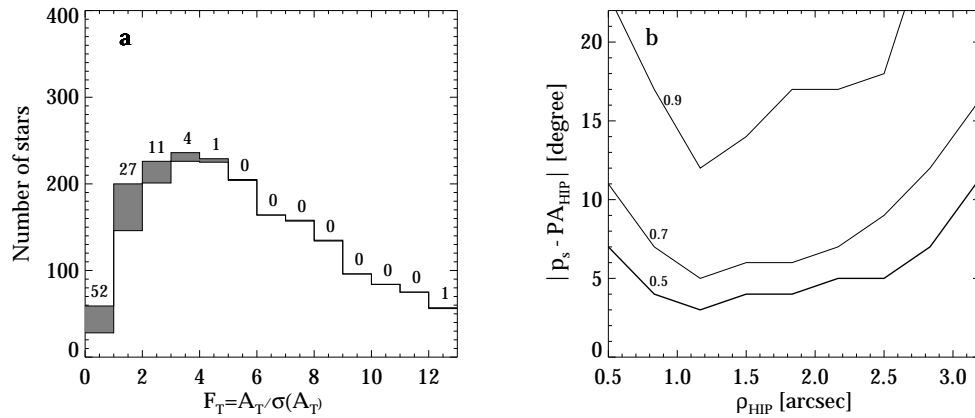


**Figure 14.4.** Performance of the photometric method for determining the position angle of close double stars: (a) distribution of 2000 double stars in common with the Tycho Catalogue versus the signal-to-noise ratio  $F_T$  from Equation 14.3. The blank area under the histogram indicates the distribution of successful determinations, while the shaded area represents the number of wrong estimations. The percentage of the latter are given at the top of each bin; (b) quantiles of the distribution of  $|p_s - PA_{HIP}|$  versus the separation for all the 2000 NDAC stars observed by Tycho. The slightly thicker line gives the 0.5 quantile, i.e. the median.

too small separations were obtained. The dependence of the bias on the separation can also be qualitatively understood in this way. In principle, the Tycho separations could have been corrected by means of the available Hipparcos data, but a correction to the absolute positions of each component given in the Tycho Catalogue was not known. The bias therefore had to remain uncorrected in the Tycho Catalogue. Thus, the resolved double stars in the Tycho Catalogue are corrupted by the strong systematic error shown in Figure 14.3. They are therefore not recommended for use as astrometric reference stars.

The best performance of the method was achieved at separations from 2.3 to 2.9 arcsec. The performance depended also on the magnitude difference between the two components. Figure 14.3 (lower right) covers the whole set of 3308 NDAC double stars. The percentage of successful Tycho solutions is shown as a contour map, depending on the true separation and the difference in magnitude as found in the NDAC solution. Nearly all components of equal magnitudes with separations from 2.2 to 3.2 arcsec were correctly resolved, while double stars with  $\Delta m > 3$  mag turned out to be beyond the capability of Tycho.

Altogether, some 1657 non-redundant pairs were resolved and included in the Tycho Catalogue.

The performance of the photometric method of position angle determination, described in the previous subsection, could also be determined from the NDAC double star sample. The  $p_s$  values were directly compared with the NDAC position angles. The distribution of  $|p_s - PA_{HIP}|$  in Figure 14.4(b) shows a good performance of the method for separations from 1.0 to 2.5 arcsec, and reasonable results were obtained for smaller separations, down to 0.5 arcsec. This high degree of success prompted the large-scale search for unknown double stars described in Section 14.6.

The distribution of the 2000 stars from the NDAC list in Figure 14.4(a) shows that the majority of doubles have signal-to-noise ratio  $F_T$  above 3. The blank part of the histogram corresponds to correctly determined position angles, i.e. when the  $p_s$  value falls within  $\pm 25$  degrees of the correct angle. The shaded part represents the numbers of outliers, while the numbers at the top of each bin give the percentage of wrong determinations. It appears that the method performs well when  $F_T > 3$ , where less than about 4 per cent of wrong estimations can be expected. A number, though very small, of wrong estimations at high  $F_T$  values could be caused by true photometric variability of some double stars.

---

### 14.5. Double-Peak Detection in Reprocessing

---

For all transits of each known or suspected double star the raw photon count rates in a 200-sample interval, centred on the predicted transit times, were extracted into a separate file in the detection reprocessing at Tübingen (Chapter 10). This was done for the whole mission. The file was submitted to a special double-peak fitting and double star solving procedure which will be briefly described in the following.

The double-peak fit described in Section 14.3, was applied to the photon counts, but with several important differences: data from the entire mission (rather than 247 days) were used, double-peak distances up to 4.2 arcsec were accepted, and no test was carried out to check whether the secondary peak could be attributed to an unrelated ('parasitic') star.

Even for a true double star a proportion of transits yielding perfect single-star detections had to be expected, namely whenever the two stars were aligned parallel to the star mapper slits, i.e. when the position angles of the slits  $\theta_s$  and that of the double star  $\theta_d$  were the same. But double peaks were detectable when  $\theta_s$  was sufficiently different from  $\theta_d$ . The error-free double-peak distance is always given by

$$\rho_s = \rho |\sin(\theta_s - \theta_d)| \quad [14.4]$$

where  $\rho$  is the true separation of the double star. Fitting this relation to the actually measured double-peak distances, the separations and position angles of the suspected doubles were calculated. The double-peak fit gave individual amplitudes which were converted to magnitudes by a rough preliminary calibration formula. Thus the position angles could be derived without the uncertainty of  $\pm\pi$  mentioned in Section 14.4.

Formal fits were obtained for almost all of the 22 083 candidate double stars. But it was clear that many of these results were spurious, i.e. created by pure chance from a random combination of noise peaks. Selection criteria were developed, therefore, in order to suppress the spurious cases. They were based on the goodness-of-fit of the parameter adjustment using Equation 14.4, on the number of successful double-peak fits agreeing with Equation 14.4, and on the ratio between this number and the total number of successful double-peak fits. An additional criterion discarded all cases with high magnitude differences and small separations. The thresholds for these criteria were fixed by a comparison with the 2357 preliminary NDAC solutions already mentioned in Section 14.4. The aim was to minimize the number of 'false' solutions. A solution was assumed to be false if it had a separation difference of more than 0.2 arcsec or a position angle difference of more than  $20^\circ$  to the NDAC solution.

Two sets of thresholds were defined. Applying the first set led to a set of double stars with an error rate of false solutions clearly below 0.5 per cent. These stars were flagged 'D' (double) in Field T49 (Section 2.2, Volume 1) of the Tycho Catalogue. The median absolute differences between such solutions and the NDAC reference were 0.026 arcsec in separation and  $1.1^\circ$  in position angle.

The second set of thresholds aimed at an error rate of 5 per cent. Stars satisfying it were flagged 's' (suspected) in Field T49, unless the photometric method of double star search (see Section 14.6) confirmed the duplicity. Applying the two sets of thresholds to all 22 083 candidate stars led to 3239 'D' and 2650 's' stars.

The method described above was most efficient for separations between 1 and 3 arcsec. According to the NDAC comparison set, nearly all stars were correctly resolved in this range if their magnitude difference  $\Delta m$  was below 1.5 mag. But at least 40 per cent of the candidates were correctly resolved down to separations of 0.6 arcsec (at  $\Delta m = 0$  mag) or 1.2 arcsec (at  $\Delta m = 1.2$  mag).

---

### 14.6. Photometric Duplicity Search

---

As explained in Section 14.4, the observed magnitude for each transit of a close double star depended on the orientation of the system relative to the slits of the star mapper. A large-scale photometric search for duplicity based on this phenomenon was applied to the roughly 480 000 Tycho stars with  $V_T < 10.5$  mag, i.e. roughly the brighter half of all stars observed by Tycho. The results of this investigation were used to flag stars in the Tycho Catalogue (Field T49) accordingly. Again, as for the results of the preceding section, certain and less significant cases of duplicity were distinguished in the flagging. In addition, the flags were devised to indicate whether no photometric search for duplicity was performed (about 570 000 stars) or whether no signs of duplicity were found in spite of the search (450 000 stars). The photometric search added about 5200 stars flagged 'D', i.e. fairly certain doubles, to the 3200 already found by the method of the previous section. This investigation was performed at Tübingen in the framework of the main photometric reductions.

J.-L. Halbwachs, V.V. Makarov, K. Wagner

## 15. SPECIAL ASTROMETRY AND PHOTOMETRY OF SOLAR SYSTEM OBJECTS

*Solar system objects were observed by the star mapper if they were sufficiently bright and sufficiently small in angular size. This resulted in a list of positional observations by Tycho of 5 minor planets, 3 satellites and 2 major planets, and their estimated  $B_T$  and  $V_T$  magnitudes. The adaptation of the reduction algorithms for the planetary objects is outlined in this chapter, and the reduction of pairs of successive observations on the inclined and vertical slits to obtain two-dimensional positions on the sky is presented. The precision and accuracy of the Tycho results are discussed in a comparison with Hipparcos and ground-based observations.*

---

### 15.1. General Overview of Planetary Data Treatment

---

The proper acquisition and reduction of Tycho observations of planets was recognized as an important task for the Tycho Consortium. Although the precision of these observations is moderate compared to the Hipparcos main mission data (see Volume 3, Chapter 15), Tycho astrometry and photometry have some advantages which made it a worthwhile task. Each passage of a planet across the inclined, and then the vertical slits of the star mapper provides a nearly simultaneous determination of the position of the object in two dimensions in the tangential plane, while the main grid position determination is always one-dimensional, see Section 2.7.2 of Volume 1. Regarding astrometry of planets, observations on the inclined slits become particularly interesting since measurements only along the scanning direction, as obtained by the main grid and the vertical slits of the star mapper, cannot provide the ecliptic longitudes of objects in the ecliptic zone nearly as accurately as the latitudes, due to the features of the scanning law. The width of the star mapper slits in the scan direction is significantly larger than that of the main grid, allowing four planets and satellites of larger angular size to be observed (Uranus, Neptune, Ganymede and Callisto). Last but not least, the two-dimensional position determinations are supplemented by simultaneous photometric observations in the  $B_T$  and  $V_T$  passbands for all but the largest planets.

Since rapidly moving planets could not be treated with the same model of five astrometric parameters as ordinary programme stars, several major changes had to be made in some of the principal stages of the data processing. The prediction of transit times was designed and implemented specially for planetary objects, as described in Section 10.4. The resulting Predicted Group Crossings were merged in chronological sequence with

the predictions for programme stars, constituting the input for the detection and transit identification procedures, including parasite recording. These latter did not distinguish between planets and stars and remained unchanged. In the identified transit data stream the transits of planets could be recognized easily by special object designations resembling Tycho Input Catalogue identification numbers (see Chapter 3), but having zeroes in the place of the Guide Star Catalog region numbers. The format and the structure of the data were exactly the same otherwise.

In the astrometric reduction, the existing routine procedures of the Tycho data processing were retained whenever possible. For that reason a dummy entry was created for each planetary object in the Star Constants Catalogue for reprocessing. The five astrometric parameter updates (Section 11.1) were kept null throughout the processing. In this way, the transits of planets could be drawn through the same stages of the main astrometric reductions, including filtering of low-quality observations, correction of residuals transit times for calibration parameters, astrometric updates (always zero in this case), etc.

At the point where the observation equation was calculated, a few input data parameters and computed terms were written in a special 'planet observations' file. One record of this file corresponded to one detected transit of a planet. Each record contained the following data:

- the object's identification number;
- the predicted transit time in the Terrestrial Time (TT) scale;
- the first two coefficients of the observational equation (Equation 15.1);
- the corrected astrometric residual in arcsec;
- the astrometric weight of the observation, corresponding to  $\sigma_u$  in arcsec;
- the signal amplitude in the  $B_T$  and  $V_T$  passbands;
- slit group flags;
- All-Transits (AT) flags (see Sections 7.4, 11.4 and 12.3), related to the astrometric quality of the observation;
- the position angle of the scan direction,  $\theta$ .

The planet observations file was not self-contained since only a correction to the ephemerides position could be directly derived from its contents, but not the observed position itself. The complete planet observations file was therefore returned to the prediction processing site in Heidelberg, to be supplemented with the predicted apparent positions. The actual time of observation instead of the predicted transit time was also computed, taking into account once again the actual spin velocity of the satellite. This modified planet observations file was a self-contained set of information for the final determination of equatorial coordinates, standard errors and other relevant data, as described in more detail in the next section. The final coordinates are independent of the ephemerides used in prediction.

The observed  $B_T$  and  $V_T$  magnitudes were calculated directly from the amplitudes in the planet observations file by a simplified calibration procedure. The user should be aware of systematic errors of these magnitudes for objects with angular diameters which are not small compared to the slit width. For such objects a dedicated study is required, taking into account the single-slit response functions (Section 1.5), the Tycho estimation process (Section 4.4) and the phase and limb darkening of the object.

---

## 15.2. Reduction of Planet Observations

---

The primary astrometric information about the position of a given object is contained in the transit time. The transit time  $\tau$  is the moment, derived in the detection and estimation process (Chapter 4), when the object crosses the fiducial line of the slit group. By definition, the projected along-scan distance  $u(t)$  of the object from the slit group is zero at the transit time,  $u(\tau) = 0$ . In all Tycho data reductions, the observed transit time  $\tau$  was compared with the predicted time of group crossing  $\tau_{\text{calc}}$ , calculated from a suitable ephemeris, the current grid calibration parameters and satellite attitude at the calculated time of transit  $\tau_{\text{calc}}$ . It follows that the observed difference in along-scan distance is  $\Delta u = u_{\text{obs}} - u_{\text{calc}} = -v_{\text{scan}}(\tau_{\text{obs}} - \tau_{\text{calc}})$ , (Equation 7.5).

The observation equation for a star crossing one slit group is given by Equation 7.4. When adjusted to a planet, crossing one slit group, the equation is simpler since only  $(\Delta\alpha, \Delta\delta)$  are unknowns. It is noted that the instrumental calibration terms, great-circle zero point corrections and correction for the movement in the  $z$  direction have been subtracted in the right-hand part of the equation, in the same way as for ordinary stars.

We define the calculated position of the planet at the inclined slit at the calculated time of transit  $t_1$  ( $t_1; \alpha_1, \delta_1$ ) and similarly ( $t_2; \alpha_2, \delta_2$ ) for the following vertical slit group. The resulting two observation equations in general form are:

$$\frac{\partial u}{\partial \alpha^*} \Delta \alpha^* + \frac{\partial u}{\partial \delta} \Delta \delta + \text{noise} = \Delta u \quad [15.1]$$

where  $\Delta \alpha^* = \Delta \alpha \cos \delta$ . Assuming that the ephemeris used by prediction is sufficiently accurate for the calculation of the planet motion during the short interval  $t_2 - t_1$ , one can rewrite the observational equations in the following form:

$$\begin{aligned} A_1 \Delta \alpha_{2^*} + B_1 \Delta \delta_2 &= \Delta u_1 \\ A_2 \Delta \alpha_{2^*} + B_2 \Delta \delta_2 &= \Delta u_2 \end{aligned} \quad [15.2]$$

for a pair of sequential observations on the inclined and vertical slits (called an elementary observation hereafter), where  $\Delta \alpha_{2^*}$  and  $\Delta \delta_2$  are unknown corrections to the equatorial coordinates of the planet at the calculated epoch  $t_2$ , which are chosen arbitrarily as the reference epoch of the elementary observation. The right-hand parts are the observed and corrected along-scan distances. The coefficients can be written for the inclined slit as:

$$\begin{aligned} A_1 &= \frac{\partial u_1}{\partial \alpha^*} = \sin \theta - \text{sign}(z) \cos \theta \\ B_1 &= \frac{\partial u_1}{\partial \delta} = \cos \theta + \text{sign}(z) \sin \theta \end{aligned} \quad [15.3]$$

and for the vertical slit as:

$$\begin{aligned} A_2 &= \sin \theta \\ B_2 &= \cos \theta \end{aligned} \quad [15.4]$$

where  $\theta$  is the position angle of the  $w$  axis (see Figure 15.1),  $\text{sign}(z)$  is the sign of the  $z$  coordinate ( $-1$  for the lower branch of inclined slits and  $+1$  for the upper).

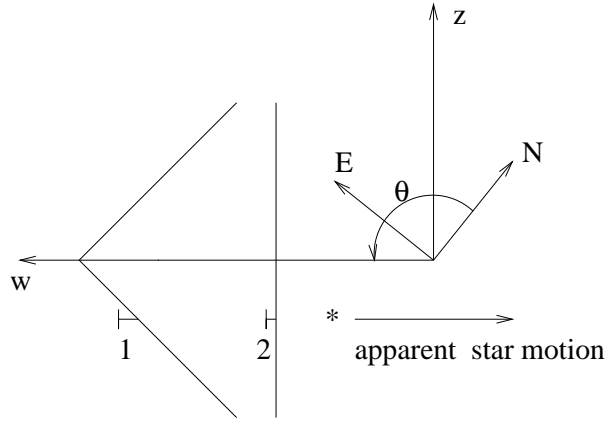


**Figure 15.1.** The star mapper coordinate system ( $w, z$ ). The position angle  $\theta$  from prediction is illustrated for a given direction of north. The observations  $\Delta u_1$  and  $\Delta u_2$  are indicated at 1 and 2.

Then, directly from Equations 15.2:

$$\begin{aligned}\Delta\alpha_{2*} &= \text{sign}(z)(B_1\Delta u_2 - B_2\Delta u_1) \\ \Delta\delta_2 &= -\text{sign}(z)(A_1\Delta u_2 - A_2\Delta u_1)\end{aligned}\quad [15.5]$$

The variances in equatorial coordinates can be obtained from the above formulae:

$$\sigma_{\alpha_*}^2 = B_1^2\sigma_2^2 + B_2^2\sigma_1^2 \quad [15.6a]$$

$$\sigma_\delta^2 = A_1^2\sigma_2^2 + A_2^2\sigma_1^2 \quad [15.6b]$$

where the standard deviations  $\sigma_1$  and  $\sigma_2$  are given in the planet observations file.

Finally, it should be noted that the derived corrections to the coordinate components in general are not statistically independent. The covariance is:

$$\begin{aligned}C(\alpha_*, \delta) &= -A_2B_2\sigma_1^2 - A_1B_1\sigma_2^2 \\ &= -\sigma_1^2 \cos \theta \sin \theta + \sigma_2^2 \text{sign}(z)(\cos^2 \theta - \sin^2 \theta)\end{aligned}\quad [15.7]$$

The correlation coefficient is calculated as:

$$\rho_{\alpha_*}^\delta = \frac{C(\alpha_*, \delta)}{\sigma_{\alpha_*}\sigma_\delta} \quad [15.8]$$

Each published elementary astrometric observation is completely described by the derived position  $(\alpha_{\text{obs}}, \delta_{\text{obs}})$ , the epoch  $t_2$ , standard errors  $\sigma_{\alpha_*}$  and  $\sigma_\delta$  and correlation  $\rho_{\alpha_*}^\delta$ . In addition, the position angle  $\theta$ , slit flag  $\text{sign}(z)$  and standard errors  $\sigma_1$  and  $\sigma_2$  are given to enable future systematic corrections of the data.

---

### 15.3. Accuracy and Precision

---

A full comparison of Tycho astrometric data for solar system objects with on-ground observations of the same epoch is given below. It is noted that the results are quite compatible in that the Tycho accuracy is close to or slightly better than that achieved in the best on-ground observations at the Bordeaux and Carlsberg meridian circles. The Tycho observations are complementary since they cover periods around the quadratures while meridian circle observations are obtained around opposition.

At the same time, as can be seen from Figures 15.2–15.9, the real uncertainty of Tycho observations, reflected in the scatter, is significantly larger than the formal standard errors (error bars). A few features of the astrometric reduction as well as the intrinsic characteristics of the objects explain this discrepancy.

The images of planets are broader and more flat at the tops than the diffraction limited images of stars. But the formal errors were still derived by means of the same error model (Makarov & Høg 1995) which is adequate for stellar images only. This especially concerns Uranus, Neptune and the two Jovian satellites. In fact, the error model is not applicable to extended objects at all. The differences in the error bars are due to variations of the detected amplitude or sky background but the broadening of the image gives the larger effect. Accidental proximity of parasitic stars also disturbs observations, as mentioned in Section 2.7 of Volume 1, but for the 10 rather bright objects the effect is relatively moderate. We conclude that the standard errors  $\sigma_1$ ,  $\sigma_2$ ,  $\sigma_{\alpha^*}$  and  $\sigma_\delta$  given among the published data can serve only as approximate indicators of the observation quality. In particular, the error ellipse described in Section 2.7 cannot be regarded as an estimation of a certain confidence range in the sense usually attributed to it (see e.g. Press *et al.* 1986, Section 14.5).

As far as systematic errors are concerned, it is noted that the positions are strictly tied to the ICRS system, and large-scale distortions of the Tycho coordinate system are estimated to be as small as 1 mas. Yet, there are much larger intrinsic systematic errors in the data due to physical and geometrical phase effects, i.e. phase, shape or albedo corrections are not taken into account. It is possible to apply this correction afterwards in the case of Tycho, and here follows a general description of how it might be achieved. A discussion of these effects is given by Lindegren (1977) for observations with a slit micrometer on a meridian circle, very similar to the Tycho instrument. The method was applied to observations by Lindegren & Høg (1977). As applied to the Tycho observations the method translates into a series of numerical simulations.

For any given observation of a planet, two two-dimensional images can be simulated, one image as a star-like source, and another as a disk with realistic phase, shape and albedo. These two images should be transformed into simulated Tycho counts by integration in the along-slit direction, convolution with the slit response function (Figure 1.3) and discretisation of the resulting 4 profiles into 0.281 arcsec bins, which is a sufficiently accurate approximation for the purpose. To do these computations, the position angle  $\theta$  and the inclined slit flag  $\text{sign}(z)$  should be used. The next step would be to apply the detection Q-filter to the 4 digitized profiles, that is explicitly  $[1, 1, 1, 0, -1, -1, -1]$  (see Section 4.3). Following the steps of the detection processing, the transit time is derived from the filtered counts by simple linear interpolation between two adjacent counts where the value changes from negative to positive. Then the whole procedure of coordinate determination should be repeated, as described in the previous section, taking the differences in transit times instead of the residuals  $\Delta u_1$  and  $\Delta u_2$  for inclined and vertical slit crossings, respectively. The resulting  $\Delta\alpha^*$  and  $\Delta\delta$  are the required systematic corrections to the observed equatorial coordinates. In principle the same simulations could be used to correct the  $B_T$  and  $V_T$  magnitudes.

To assess the validity of astrometry for the solar system objects, the Tycho positions were compared to other observations and to calculated positions from the ephemerides. A first comparison was made between the Hipparcos and the Tycho positions for the 6 solar system objects which are in common with the two catalogues (five minor planets and the planetary satellite S VI-Titan). As the transits across the star mapper and the main grid

occurred almost simultaneously, a direct comparison between the Tycho and Hipparcos observations could be achieved. The Tycho positions were transformed into a one-dimensional abscissa and were corrected for the epoch offset between the observations ( $\simeq 11$  s), assuming a constant velocity  $dv/dt$  calculated from the ephemeris. The residual  $\Delta v$ , i.e. the difference between the Tycho and Hipparcos abscissa on a great circle, is given by (see Section 2.7 of Volume 1):

$$\Delta v = v^{\text{Tycho}} - v^{\text{Hip}} \simeq (\sin \theta \quad \cos \theta) \begin{pmatrix} (\alpha - \alpha_0) \cos \delta \\ \delta - \delta_0 \end{pmatrix} + (t_{\text{Hip}} - t_{\text{Tycho}}) dv/dt \quad [15.9]$$

where  $\theta$  is the position angle of the FAST or NDAC reference great circle,  $(\alpha, \delta)$  are the equatorial coordinates from Tycho at epoch  $t_{\text{Tycho}}$ , and  $(\alpha_0, \delta_0)$  is the reference position of the Hipparcos solar system objects catalogue at epoch  $t_{\text{Hip}}$ . The normalized difference is derived from the approximation:

$$\sigma_{\Delta v} \simeq [(\sin \theta \sigma_{\alpha^*})^2 + (\cos \theta \sigma_{\delta})^2 + \sin 2\theta \rho_{\alpha^* \delta} \sigma_{\alpha^*} \sigma_{\delta}]^{1/2} \quad [15.10]$$

since the variance of the Hipparcos measurements can be neglected here.

The one-dimensional differences are shown for all objects in common as a function of epoch on top of Figure 15.2(a); the lower panel shows an histogram of the normalized difference with the theoretical Gaussian of same mean and variance as the data sample. Similar graphs are obtained for each object at the top of Figures 15.3 to 15.8. Figure 15.2(b) and Figures 15.3 to 15.9 show the residuals  $\Delta \alpha \cos \delta$  and  $\Delta \delta$  between the observed and calculated astrometric positions obtained for each Tycho solar system object. These are given together with the residuals provided by L.V. Morrison for the Carlsberg instrument observations, and residuals obtained by M. Rapaport at the Bordeaux Observatory. The ephemerides of the minor planets were computed according to the osculating elements set of the ‘Ephemerides of minor planets for the year 1996’ (Batrakov *et al.* 1995). The ephemerides of the major planets are given by DE200 except for S VI-Titan where they are calculated from the DE403 solution. The ephemerides of the Galilean satellites are taken from the G5 theory of Arlot (1982), the ephemerides for S VI-Titan are taken from the theory of Dourneau (1993) for Tycho and the more recent theory TASS1.6 of Vienne & Duriez (1995) for the Bordeaux observations.

The scatter on the residuals for the major planets is greater than expected from the formal error on a single observation; it is however stressed that all positions for any solar system object refer to the combination of the slits group crossing positions without any correction for photocentre offset due to phase effect. The systematic offset on the residuals in right ascension for the major planet is in agreement with the ground-based observations and known to be mainly due to the DE200 ephemeris.

E. Høg, D. Hestroffer, V.V. Makarov

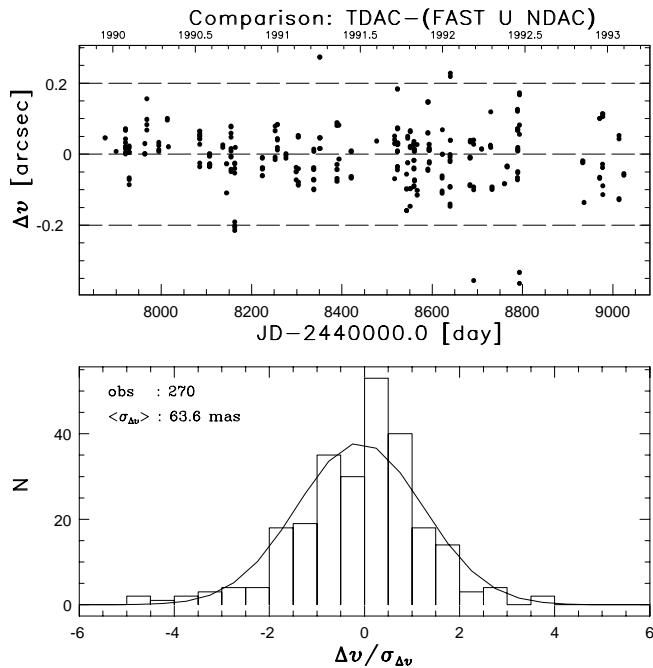


**Figure 15.2(a).** Comparison between Tycho and Hipparcos abscissae for five minor planets and S VI-Titan. The one-dimensional differences are given as a function of epoch in the top panel. The lower panel gives the distribution in units of the scatter, the number of observations and the mean standard deviation  $\langle \sigma_{\Delta V} \rangle$ .

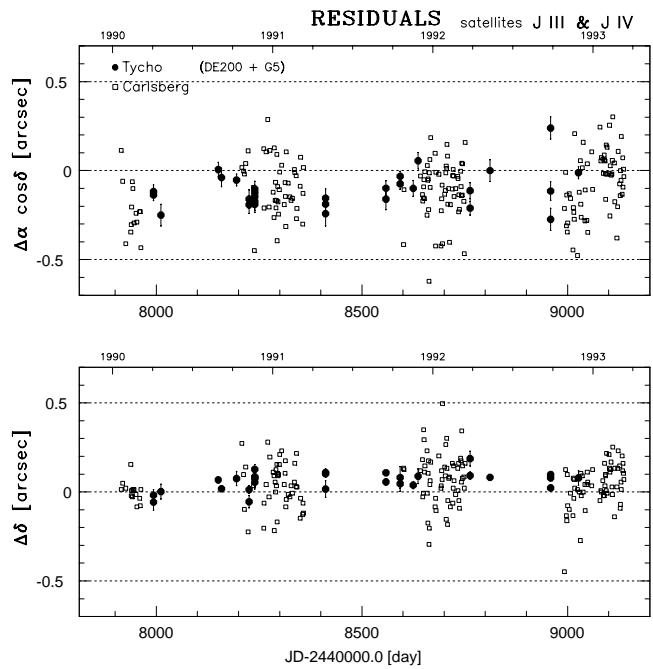


**Figure 15.2(b).** Residuals for Tycho observations of the Galilean satellites J III-Ganymede and J IV-Callisto, together with residuals obtained from Carlsberg instrument observations.

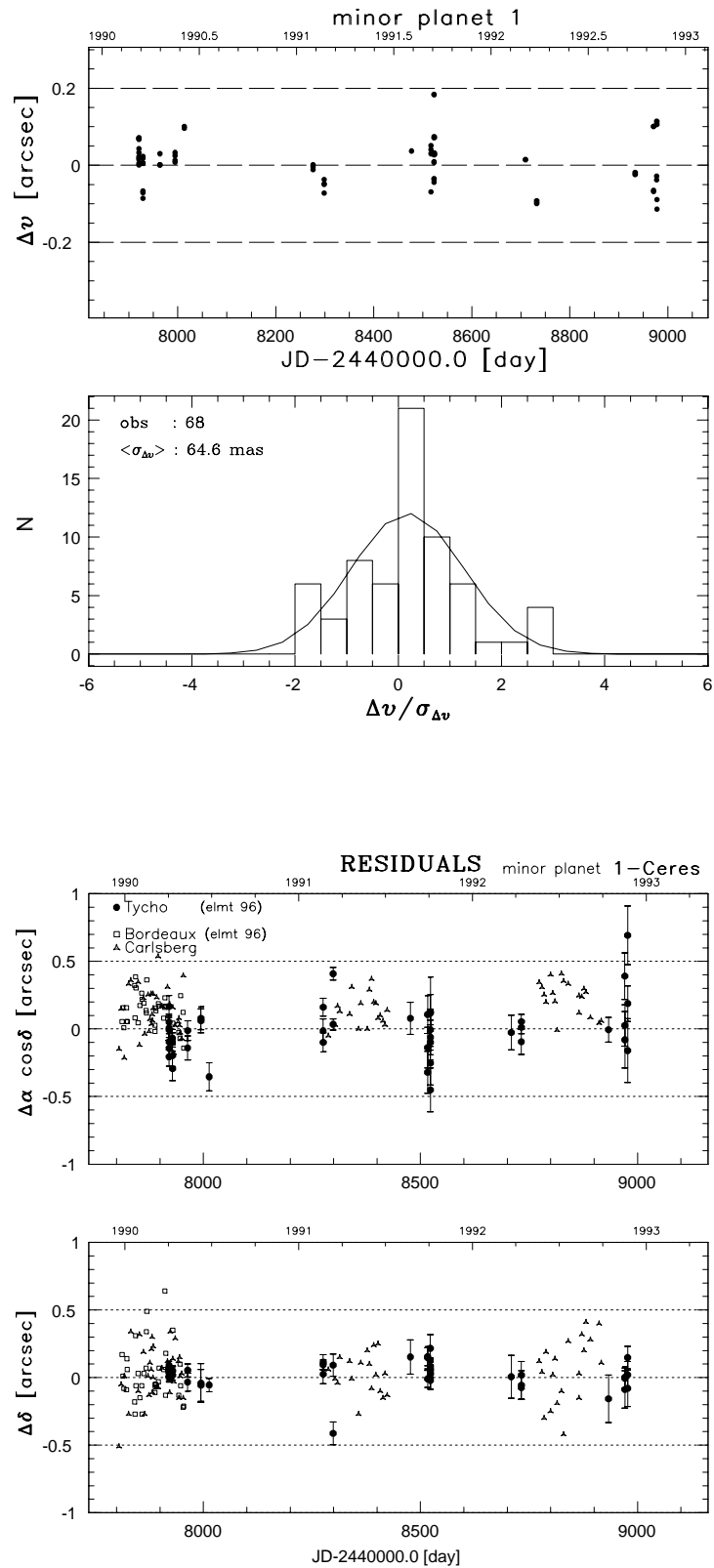


**Figure 15.3.** Residuals for Tycho observations of (1) Ceres together with residuals obtained from ground-based observations (lower), and residuals with respect to Hipparcos results (upper). The Bordeaux and Carlsberg data and residuals were provided by M. Rapaport and L. V. Morrison.

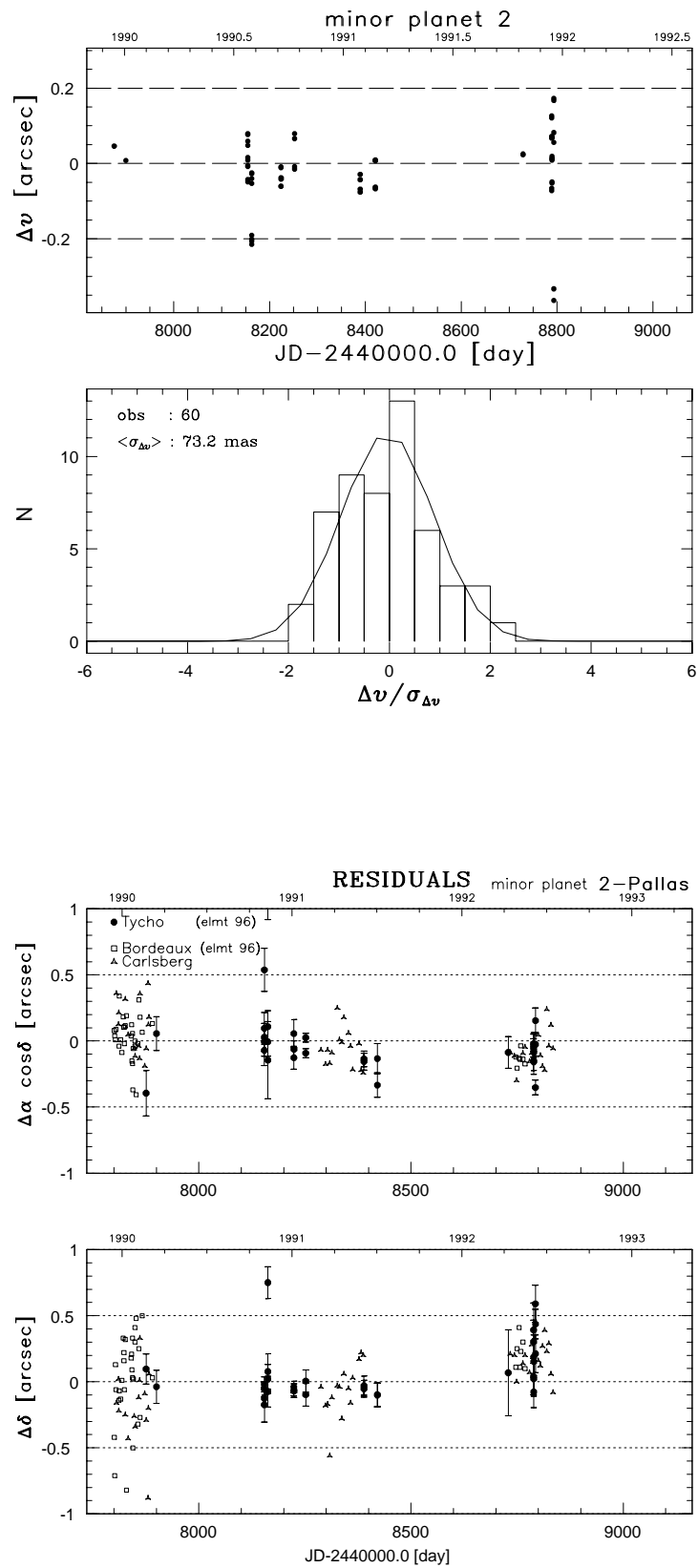
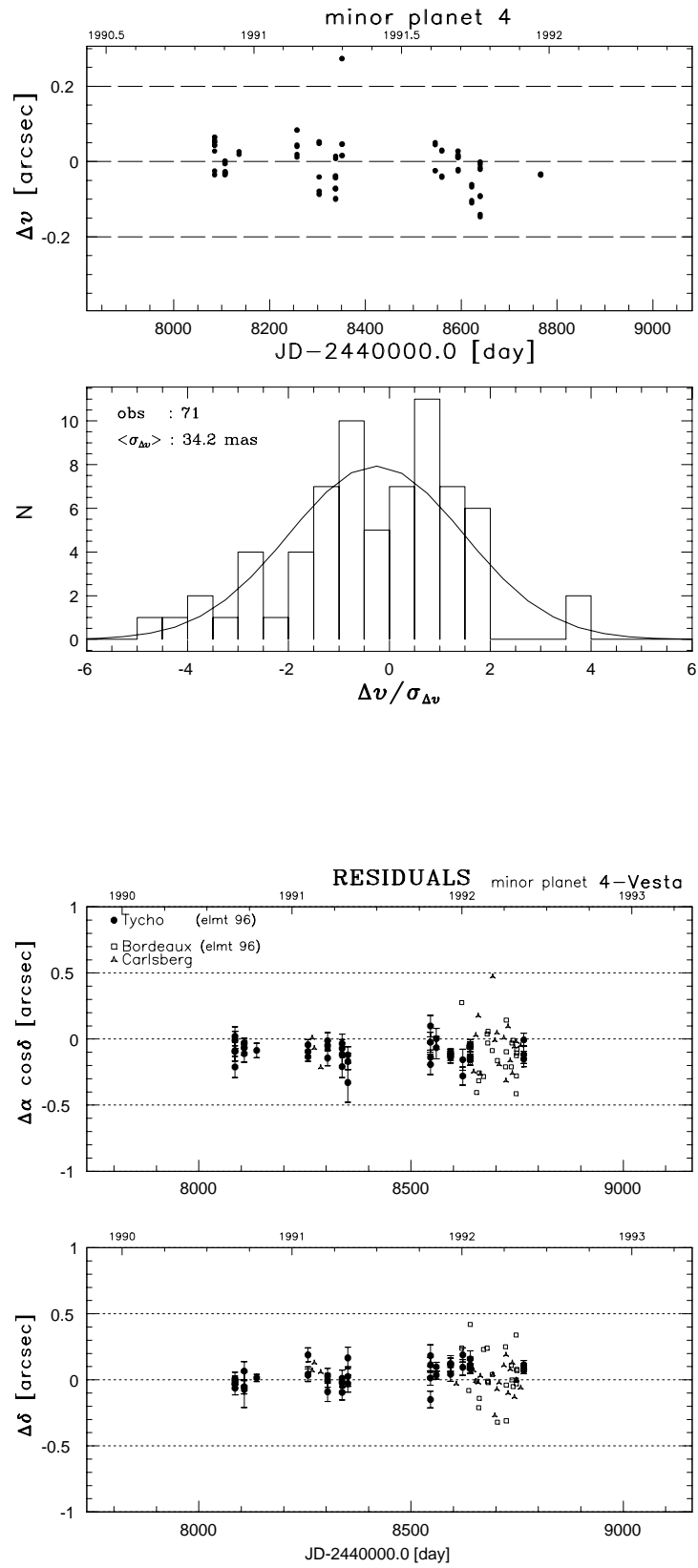


Figure 15.4. Same as Figure 15.3 for (2) Pallas.



**Figure 15.5.** Same as Figure 15.3 for (4) Vesta.

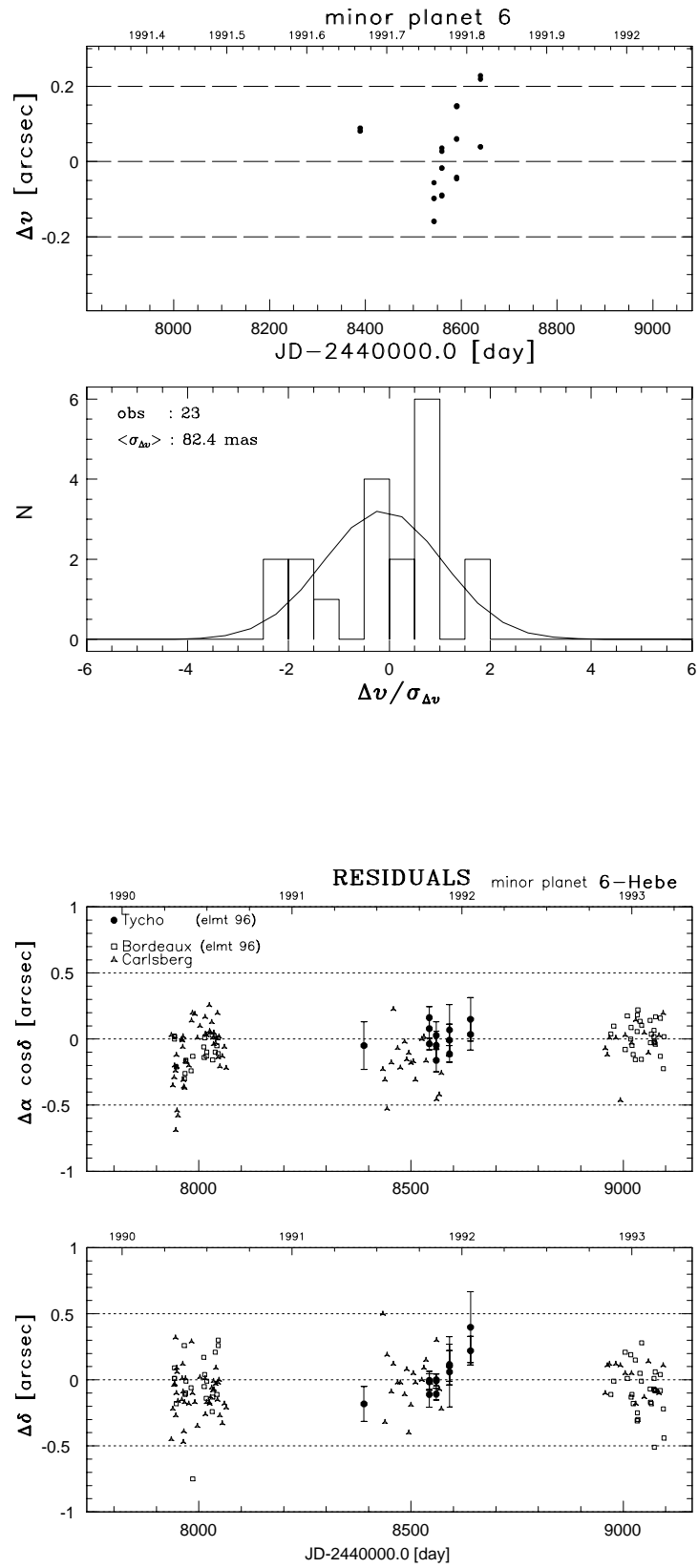
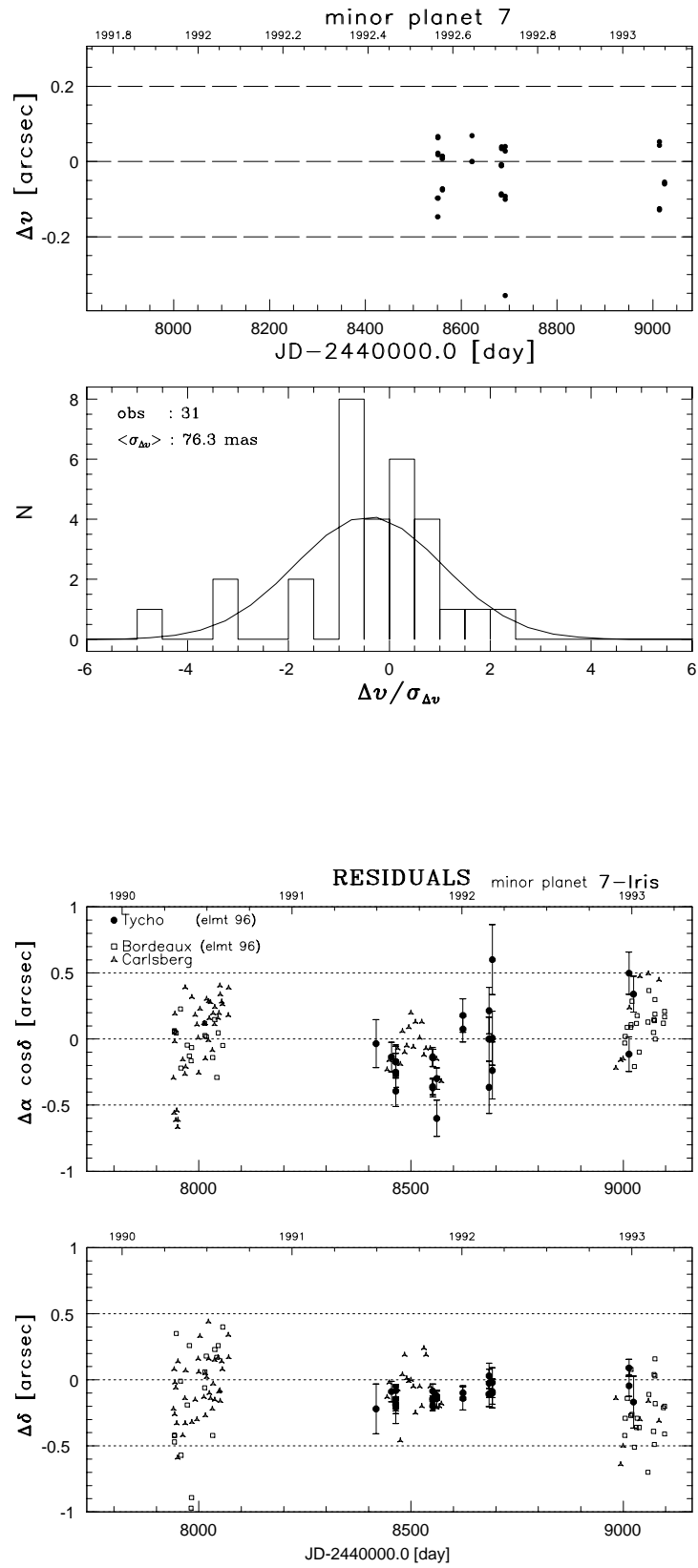


Figure 15.6. Same as Figure 15.3 for (6) Hebe.



**Figure 15.7.** Same as Figure 15.3 for (7) Iris.

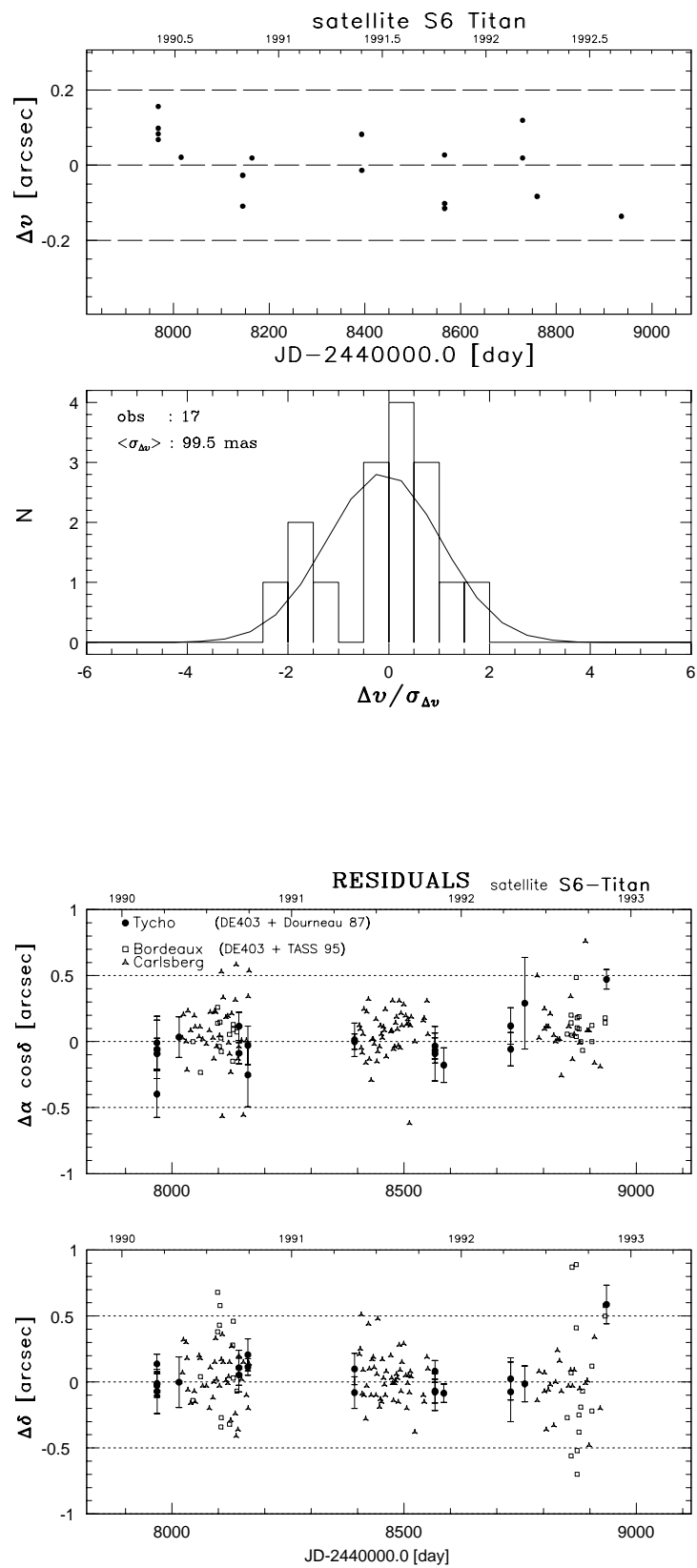
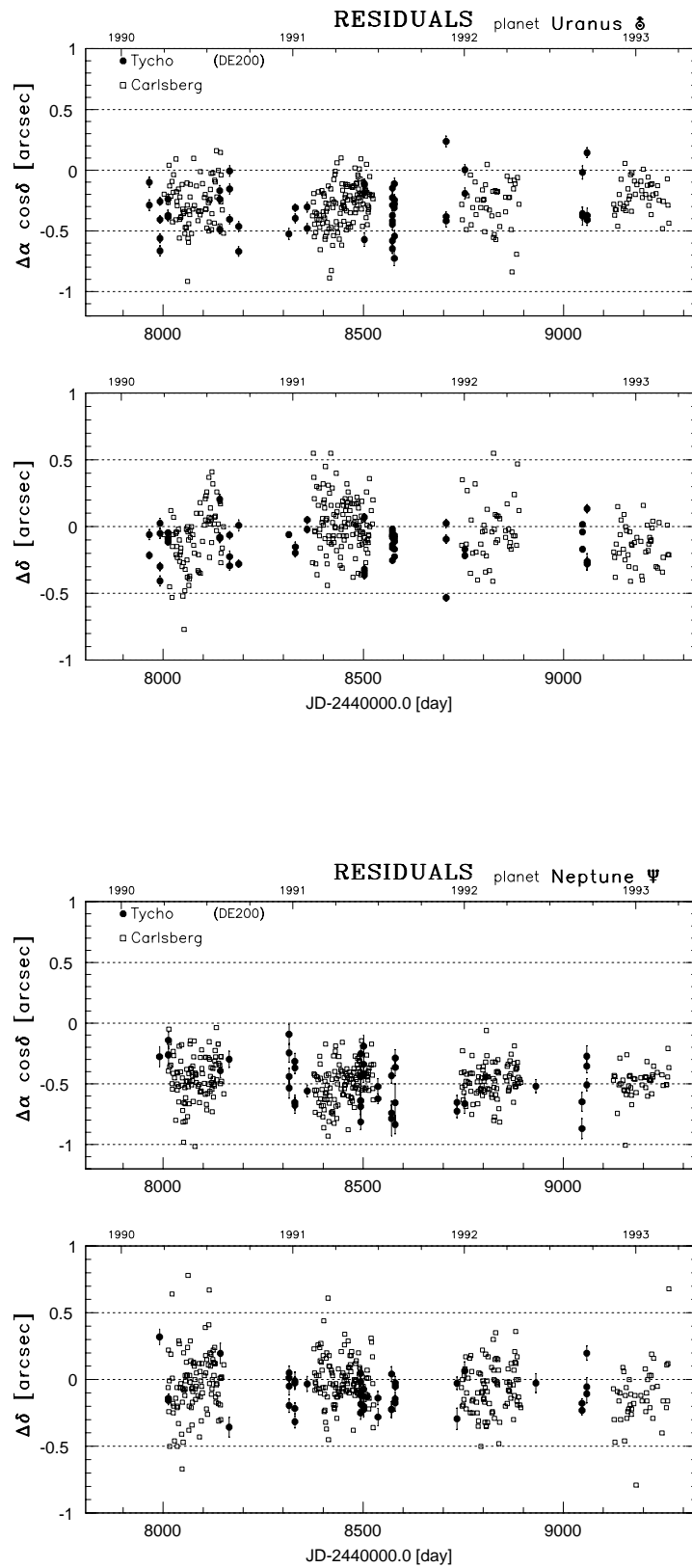


Figure 15.8. Same as Figure 15.3 for the Saturnian satellite S VI-Titan.



**Figure 15.9.** Residuals for Tycho observations of Uranus and Neptune, together with residuals obtained from Carlsberg instrument observations. The calculated positions are taken from the DE200 ephemeris solution.

## 16. CONTENTS OF THE TYCHO CATALOGUE

*An overview of the Tycho Catalogue contents is given in the first section, followed by detailed descriptions, tables and plots related to the astrometric and photometric contents, mainly derived from internal analysis of the catalogue. Comparisons with other catalogues are given in Chapter 18.*

---

### 16.1. Overview of the Tycho Catalogue

---

This section gives a general overview of the Tycho Catalogue. A detailed description of each field of the catalogue files may be found in Volume 1, Section 2.2 and Section 2.6.

The Tycho Catalogue, and its photometric annex, referred to as the Tycho Epoch Photometry Annex, is an observational catalogue. It contains data derived exclusively from the Hipparcos satellite's star mapper observations, with the exception of certain cross-identifications.

The Tycho Catalogue provides positions and two-colour photometry (in  $B_T$  and  $V_T$ ) for more than one million stars brighter than  $V_T = 11.5$  mag. The median standard error is 25 mas in position and 0.10 mag in the  $B_T - V_T$  colour index. These values apply at the median magnitude  $V_T = 10.5$  mag for stars of median colour index  $B_T - V_T \simeq 0.7$  mag. Parallaxes and proper motions were also derived, although the individual values are generally of limited significance. Table 16.1 presents the number of stars and the standard errors of the results as a function of  $V_T$ . The catalogue is more than 99 per cent complete down to  $V_T \simeq 10$  mag, the incompleteness mainly occurring in dense fields.

The Tycho Catalogue contains entries for 1 058 332 stars and resolved components of multiple systems of which 1 052 031 entries (stars) were observed by Tycho and the remaining 6301 entries are those stars from the Hipparcos Catalogue and Part C of the Double and Multiple Systems Annex that were not observed by Tycho. These 6301 so-called HIP-only stars are included for the convenience of the user, but the entries are merely pointers to the Hipparcos Catalogue where the complete records must be sought. The HIP-only stars are typically stars too faint for the star mapper and components of double stars not resolved by Tycho, but also some bright stars were missed because of crowding or non-linearity of the detectors. With the HIP-only stars included, only some 120 stars from the Catalogue of Positions and Proper Motions (PPM) brighter than 9 mag are missing in the Tycho Catalogue, see Chapter 17.

**Table 16.1.** The table gives the number of stars in the Tycho Catalogue (TYC) and the number of Tycho catalogue stars not included in the Hipparcos Catalogue (HIP), along with the corresponding median standard errors for stars within the given intervals of  $V_T$  magnitude (the column 'All' also including entries for which  $V_T$  is not available). Systematic errors in astrometry are less than 1 mas and 1 mas/yr, although the external standard errors (the true accuracies) may be 50 per cent larger than the quoted standard errors for faint stars. In photometry, systematic errors may reach the level of the quoted standard errors for faint stars. The photometry for about 20 000 stars is considered to be uncertain, for example when the standard errors are larger than 0.3 mag.

Interval of $V_T$	<6.0	6-7.0	7-8.0	8-9.0	9-10.0	10-11.0	>11.0	All	<9.0
Median $V_T$ , mag	5.38	6.63	7.62	8.62	9.61	10.58	11.19	10.47	8.33
$N$ (TYC)	4553	9550	27750	78029	211107	515029	205934	1052031	119882
$N$ (not in HIP)	4	55	3485	36511	182773	506720	205275	934901	40055
Median standard errors in astrometry (mas):									
Position (J1991.25)	1.8	2.6	4.0	6.7	12.9	27.2	39.2	24.6	5.6
Parallax	2.5	3.6	5.3	8.6	16.4	34.3	49.6	31.2	7.2
Proper motion/yr	2.3	3.3	5.0	8.3	16.0	33.5	48.6	30.2	7.0
Median standard errors in photometry (mag):									
$B_T$	0.003	0.006	0.010	0.018	0.036	0.084	0.128	0.074	0.014
$V_T$	0.003	0.005	0.008	0.014	0.027	0.064	0.122	0.057	0.012
$B_T - V_T$	0.005	0.008	0.014	0.024	0.049	0.117	0.200	0.104	0.019
$B - V$	0.004	0.007	0.012	0.020	0.041	0.098	0.171	0.087	0.017

The Tycho Catalogue gives a massive supplement to the Hipparcos Catalogue for the fainter stars and also an important complement for the brighter stars. The catalogue contains 40 000 stars brighter than  $V_T = 9$  mag which are not in the Hipparcos Catalogue. For these stars the median precision is 7 mas in position, parallax and annual proper motion and 0.019 mag in  $B_T - V_T$ . Double stars with separations larger than 2 arcsec and with moderate magnitude differences could usually be resolved.

The reduced data comprise two parts. The main catalogue (the Tycho Catalogue, or TYC) contains the astrometric and summary photometric data for each star. The Tycho Epoch Photometry Annex (described in Section 16.4 and in Volume 1, Section 2.6) contains the summary photometric data for all stars, along with all the individual photometric observations for a subset of stars observed with sufficiently high signal-to-noise ratio and believed to be of particular interest. The main catalogue also provides quality indicators and flags giving warnings about stars unsuited as reference stars, flags indicating duplicity, flags stating the methods used in deriving astrometry and photometry etc. Full details are given in Volume 1, Section 2.2.

---

## 16.2. Astrometric Content

---

This section presents an overview of the astrometric contents of the Tycho Catalogue. Table 16.2 shows the median standard errors of position, parallax and annual proper motion for various intervals of  $V_T$  magnitude.

For stars brighter than  $V_T = 5.0$  mag the positional error from Tycho is of similar quality as the Hipparcos positional error. It increases with magnitude, reaching about 60 mas

**Table 16.2.** Median standard errors of astrometric parameters versus magnitude: position component at the mean epoch J1991.25, parallax, and proper motion component.  $N$  is the number of stars in each interval, the 0.5 mag bins being centred on the given  $V_T$ . The standard errors for annual proper motion and parallax appear to be about 25 per cent higher than for position. The errors of position and proper motion components in right ascension and declination are respectively about 5 per cent higher and 5 per cent lower than the errors in the table. Systematic errors are less than 1 mas.

$V_T$ mag	N	$\sigma_{\text{pos}}$ mas	N	$\sigma_{\text{par}}$ mas	$\sigma_{\text{pm}}$ mas/yr
≤5.0	1447	1.5	1428	2.0	1.9
≤9.0	119348	5.6	118304	7.2	6.8
All	1038946	24.4	1035439	30.8	29.8
0.5	5	1.9	5	2.7	2.4
1.0	6	2.5	6	3.0	3.0
1.5	12	1.5	12	2.2	2.0
2.0	38	1.4	36	2.0	1.6
2.5	45	1.2	44	1.9	1.6
3.0	90	1.5	90	2.0	2.0
3.5	140	1.5	138	2.0	1.8
4.0	266	1.4	262	2.0	1.8
4.5	484	1.5	478	2.2	1.9
5.0	863	1.6	851	2.2	2.0
5.5	1477	1.8	1455	2.5	2.2
6.0	2564	2.0	2536	3.0	2.7
6.5	4614	2.5	4560	3.4	3.0
7.0	7798	3.0	7722	4.1	3.8
7.5	13299	3.8	13169	5.1	4.8
8.0	22591	4.8	22413	6.2	6.0
8.5	37729	6.3	37426	8.2	7.8
9.0	62478	8.7	61929	11.1	10.8
9.5	102221	12.2	100993	15.4	15.1
10.0	166009	17.8	165139	22.5	21.9
10.5	261412	26.2	261385	33.2	32.4
11.0	283126	34.7	283112	43.7	42.7
11.5	69016	41.5	69016	52.4	51.2
12.0	2499	52.5	2499	66.2	66.5
12.5	138	64.0	137	77.3	84.8
13.0	16	64.5	16	74.6	75.2
13.5	6	62.4	6	77.2	82.6
14.0	4	60.2	4	70.8	71.2

for the faintest stars, which is still very good compared to ground-based results. The density of Tycho stars on the sky is shown in Figure 16.1. Values range from 5 to 156 stars per square degree, the highest values occurring in the galactic plane and the lowest in the dust clouds in Ophiuchus. The limiting magnitude is not the same all over the sky, as shown in Figure 16.4 and 16.5. Therefore the plot in Figure 16.1 does not give a correct picture of the true distribution of all stars brighter than a given limiting magnitude. A more correct picture is given in Figure 16.2 showing only the just above

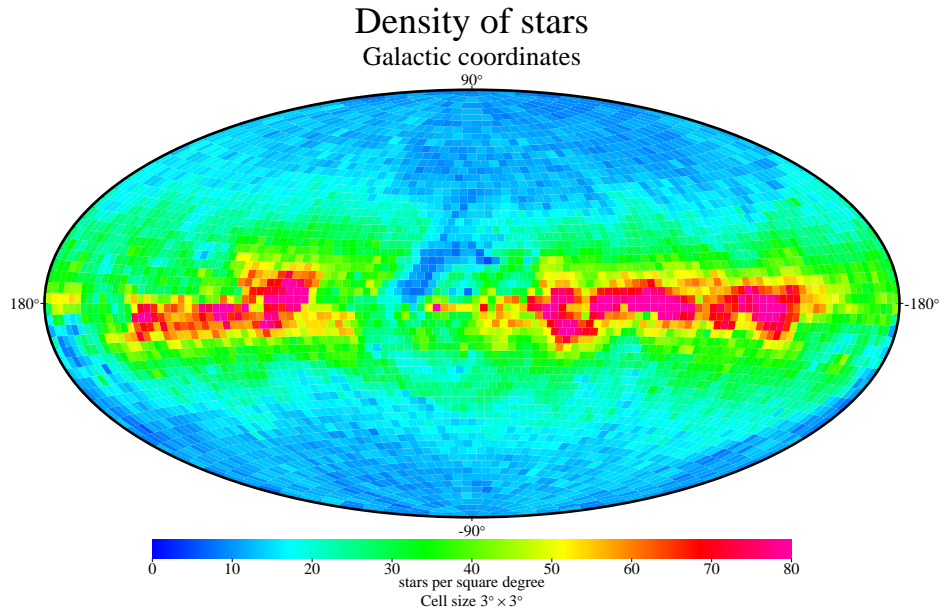


**Figure 16.1.** The number of stars per square degree in galactic coordinates. The actual range of values is from 5 to 156.

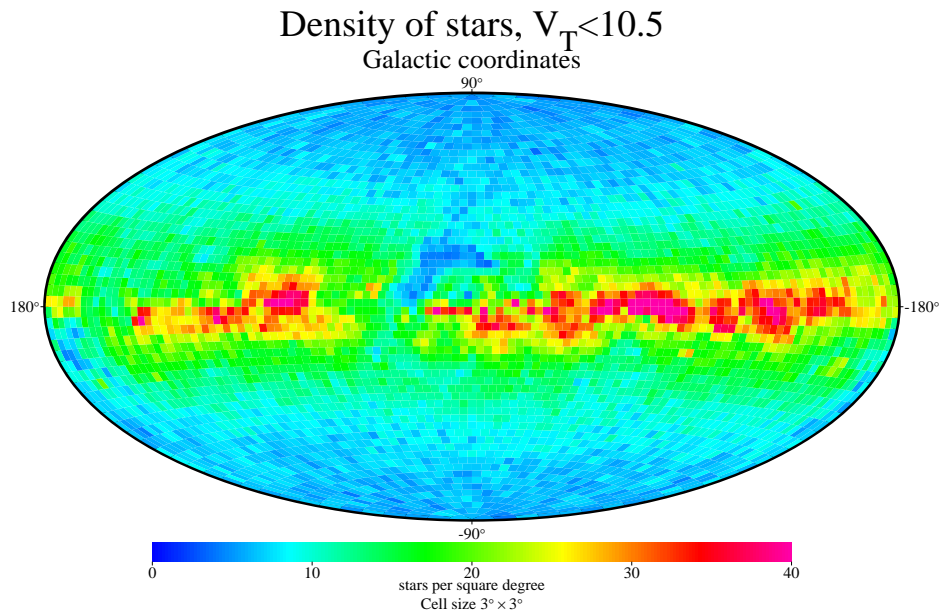


**Figure 16.2.** Distribution of the brighter half of the stars. With a limit of  $V_T = 10.5$  mag the Tycho catalogue is almost complete and the true distribution of stars brighter than this magnitude is evident. The actual range of values is from 3 to 82.



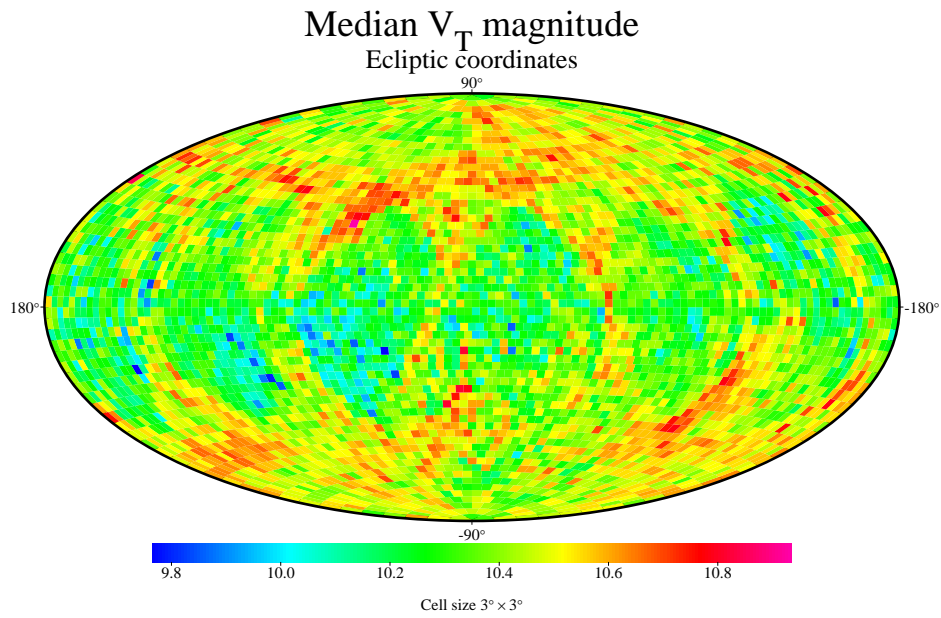


**Figure 16.4.** The median  $V_T$  magnitude plotted in ecliptic coordinates.

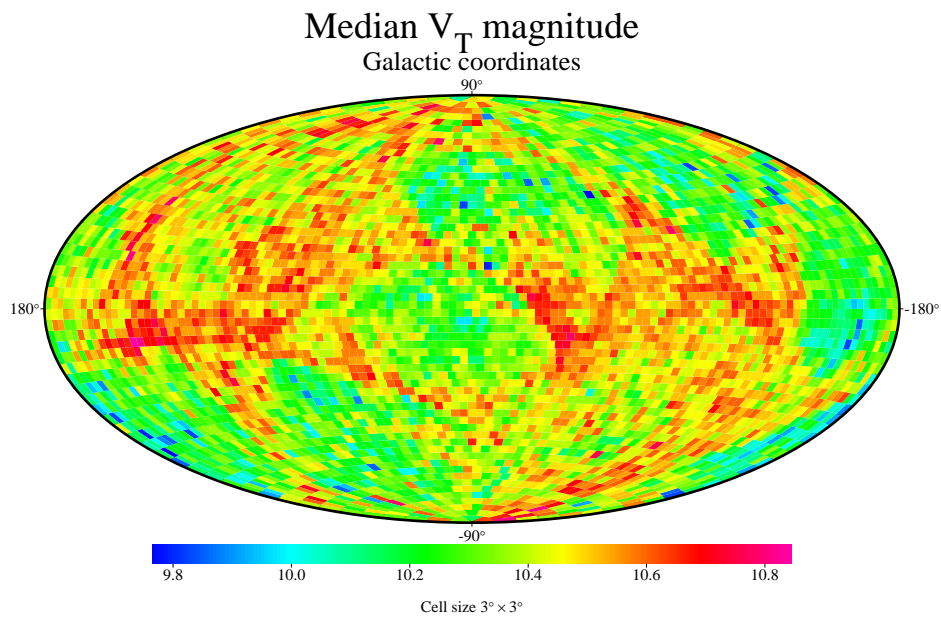


**Figure 16.5.** The median  $V_T$  magnitude plotted in galactic coordinates.

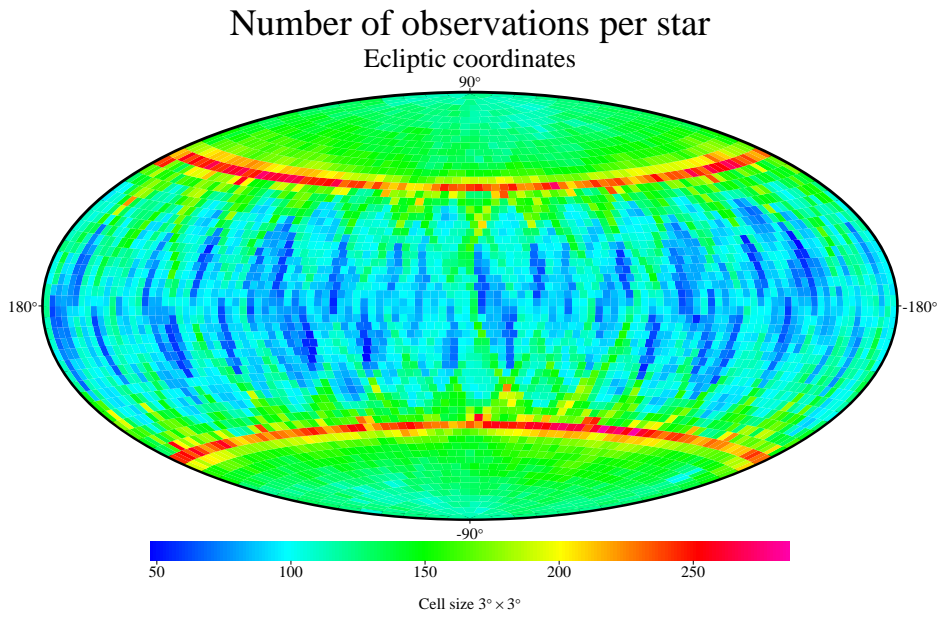


**Figure 16.6.** The median number of astrometric observations. The scanning law for the satellite produces maxima at ecliptic latitude  $\pm 47^\circ$ .

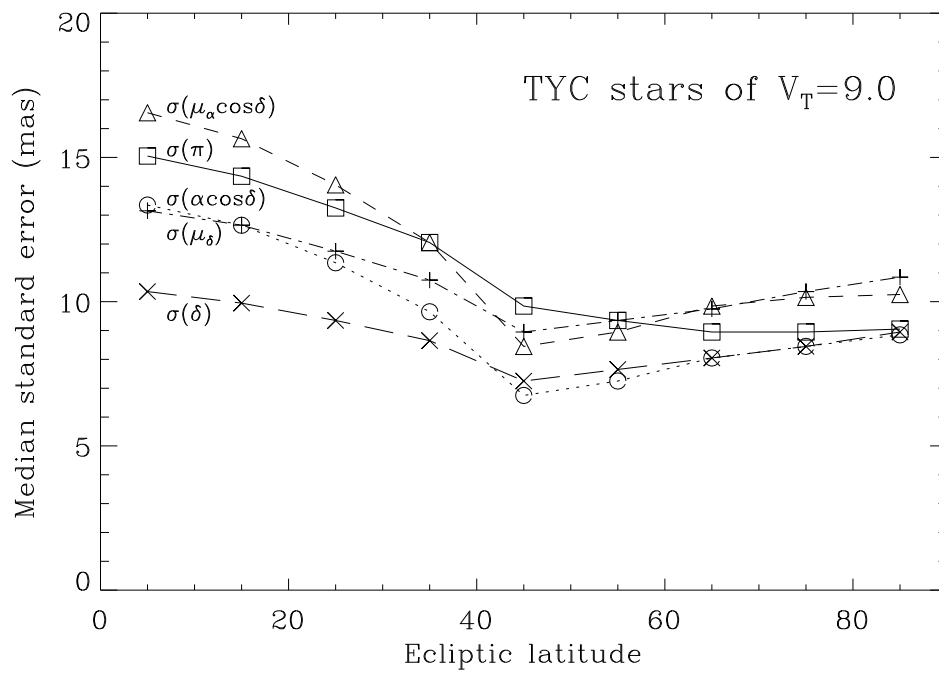


**Figure 16.7.** The standard error of the astrometric parameters as a function of ecliptic latitude.

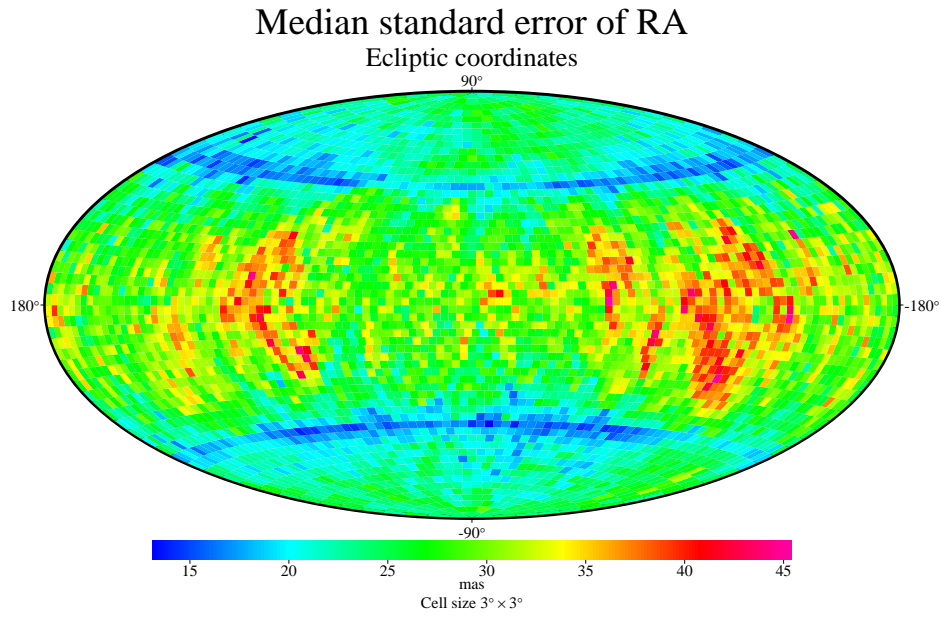


**Figure 16.8.** The median standard error of right ascension (in ecliptic coordinates).

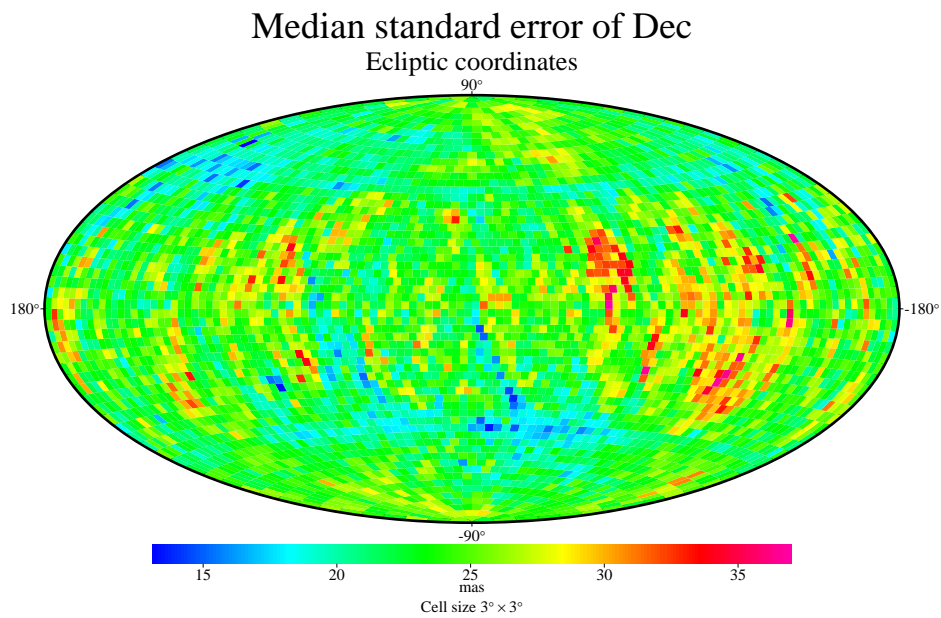


**Figure 16.9.** The median standard error of declination (ecliptic coordinates).

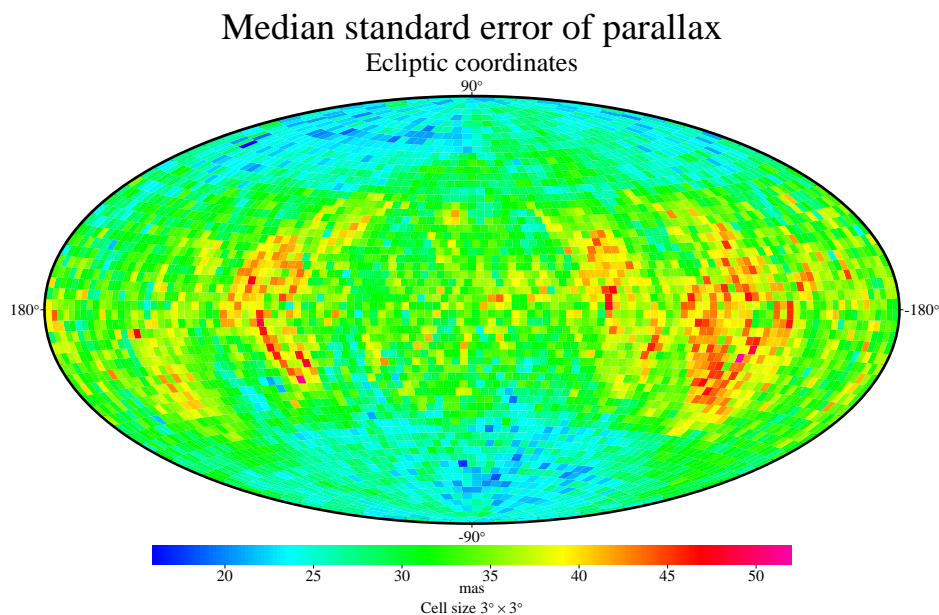


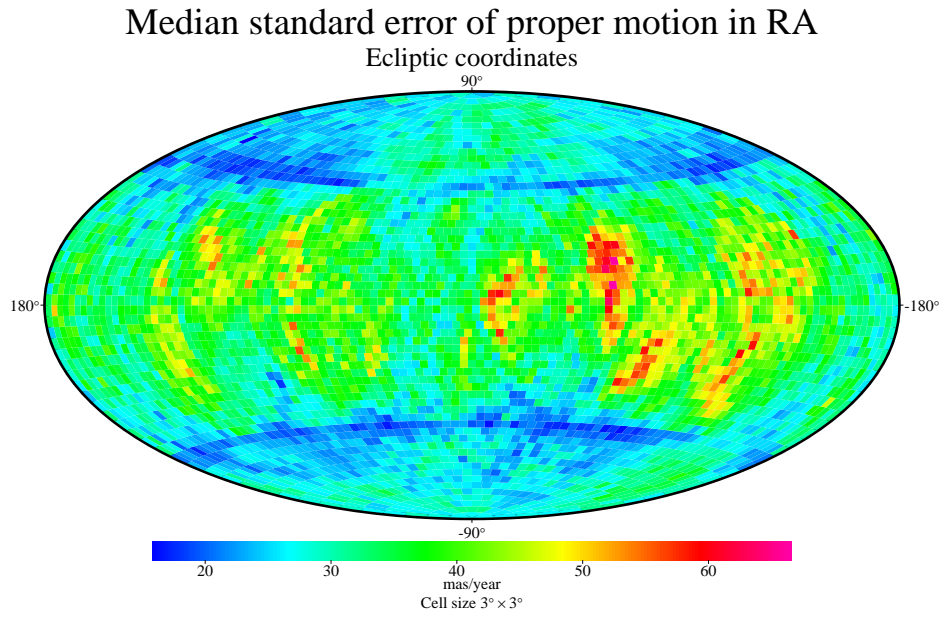
**Figure 16.10.** The median standard error of the parallax (in ecliptic coordinates).

**$F_s$ , F2 and correlation coefficients:** Figure 16.13 shows  $F_s$  which is a measure of the signal-to-noise ratio, see Section 7.4. It is based on the assumption that detections within 0.7 arcsec of the mean position represent signal detections plus background detections, whereas detections between 0.7 and 1.4 arcsec represent background only. Usually images are sharp on a low rate of background detections, giving  $F_s$  values which are the square root of the number of transits used. Figure 16.13 is therefore very similar in appearance to Figure 16.6.

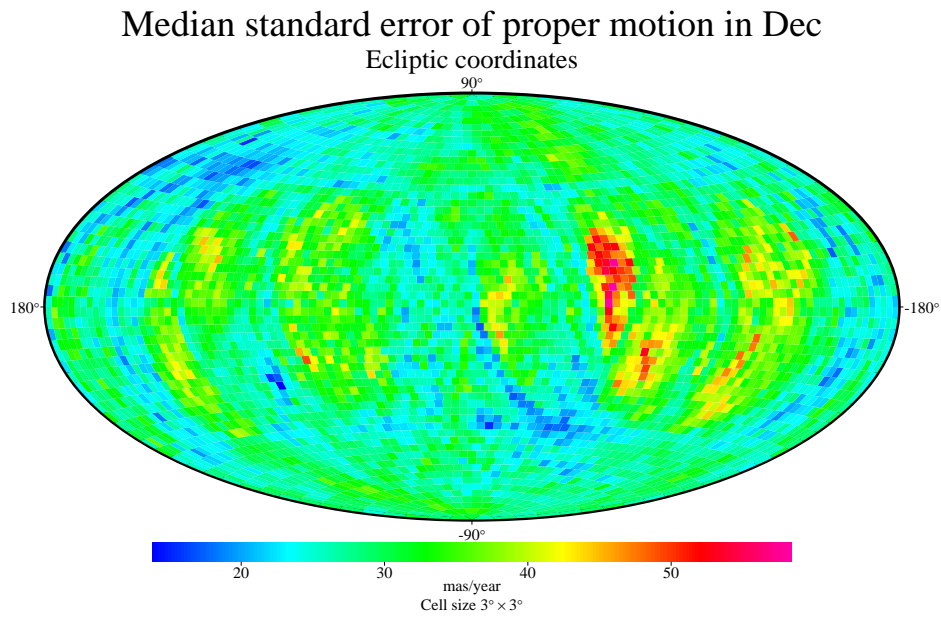
Figure 16.14 shows F2, the so-called goodness-of-fit parameter. The idea was to check whether the scatter of the residuals, after fitting the five parameters, corresponded to the expected scatter. If this expected scatter can be realistically computed, F2 should have a mean value of 0.0 and a standard deviation of 1.0 (see Field H30 in Section 2.1 of Volume 1). A value of 3.0 represents a rather too poor fit and  $-3.0$  a rather too good fit. The computed values of F2 do not live up to these expectations, probably because too small a scatter was predicted for the faint stars. F2 was therefore not used in the production of the Tycho Catalogue and the values should be used with much care.

Figure 16.15 shows the distribution of the correlation coefficients for the five astrometric parameters. With the exception of panels (d) and (h), all coefficients have their maximum about 0.0 and a half-width at half maximum about 0.2. The dominance of negative values in panels (d) and (h) merely tells that the mean observational epoch is somewhat later than the catalogue epoch (J1991.25) (see Equation 1.2.6 and 1.2.8 of Volume 1).

**Pair statistics:** If stars were uniformly distributed on the sky, the number of stars within some distance from a particular star should be proportional to the area within that distance, i.e. to the square of the distance for small distances. The number of stars per interval of distance is then proportional to the distance. This is also true when the density of stars on the sky is constant within small areas (1 arcmin in radius, say) although it is variable when distances of several degrees are considered. Figure 16.16 shows the distribution of distances between pairs of Tycho stars (excluding HIP-only



**Figure 16.11.** The median standard error of annual proper motion in right ascension.



**Figure 16.12.** The median standard error of annual proper motion in declination.

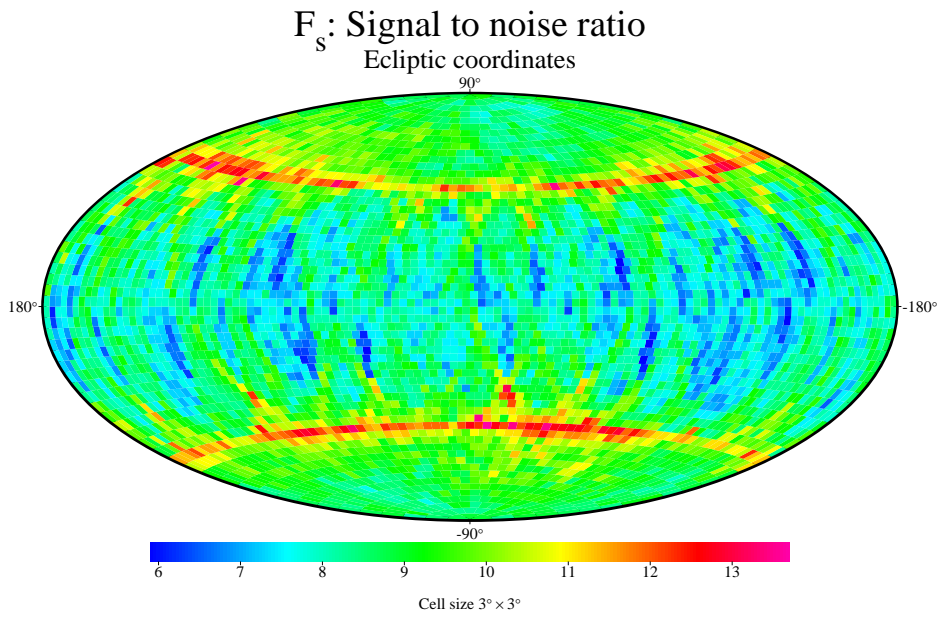


**Figure 16.13.** The median value of the signal-to-noise ratio,  $F_s$ . When the rate of background detections is low,  $F_s$  is the square root of the number of astrometric observations.

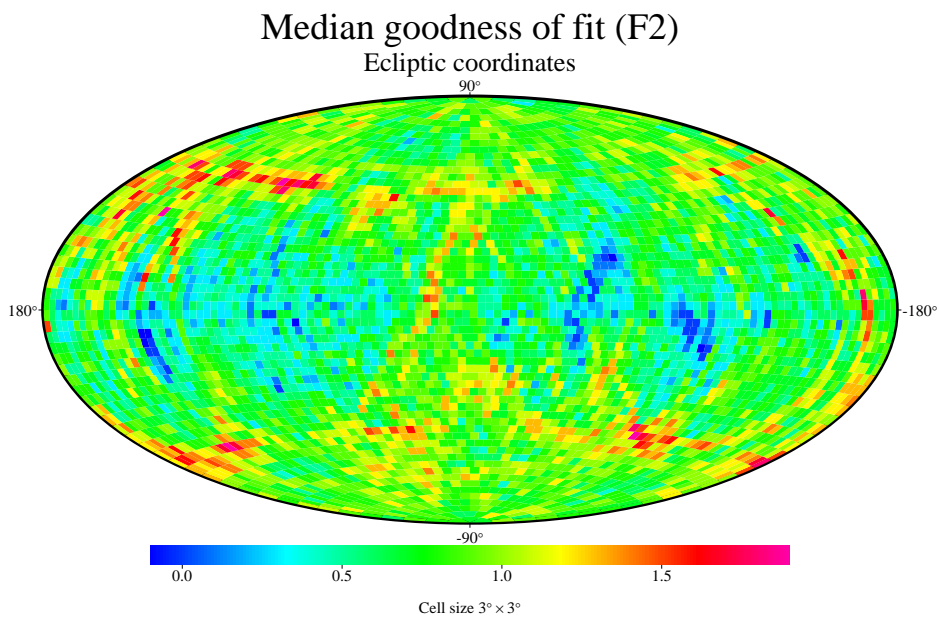


**Figure 16.14.** Plot of the goodness-of-fit,  $F_2$

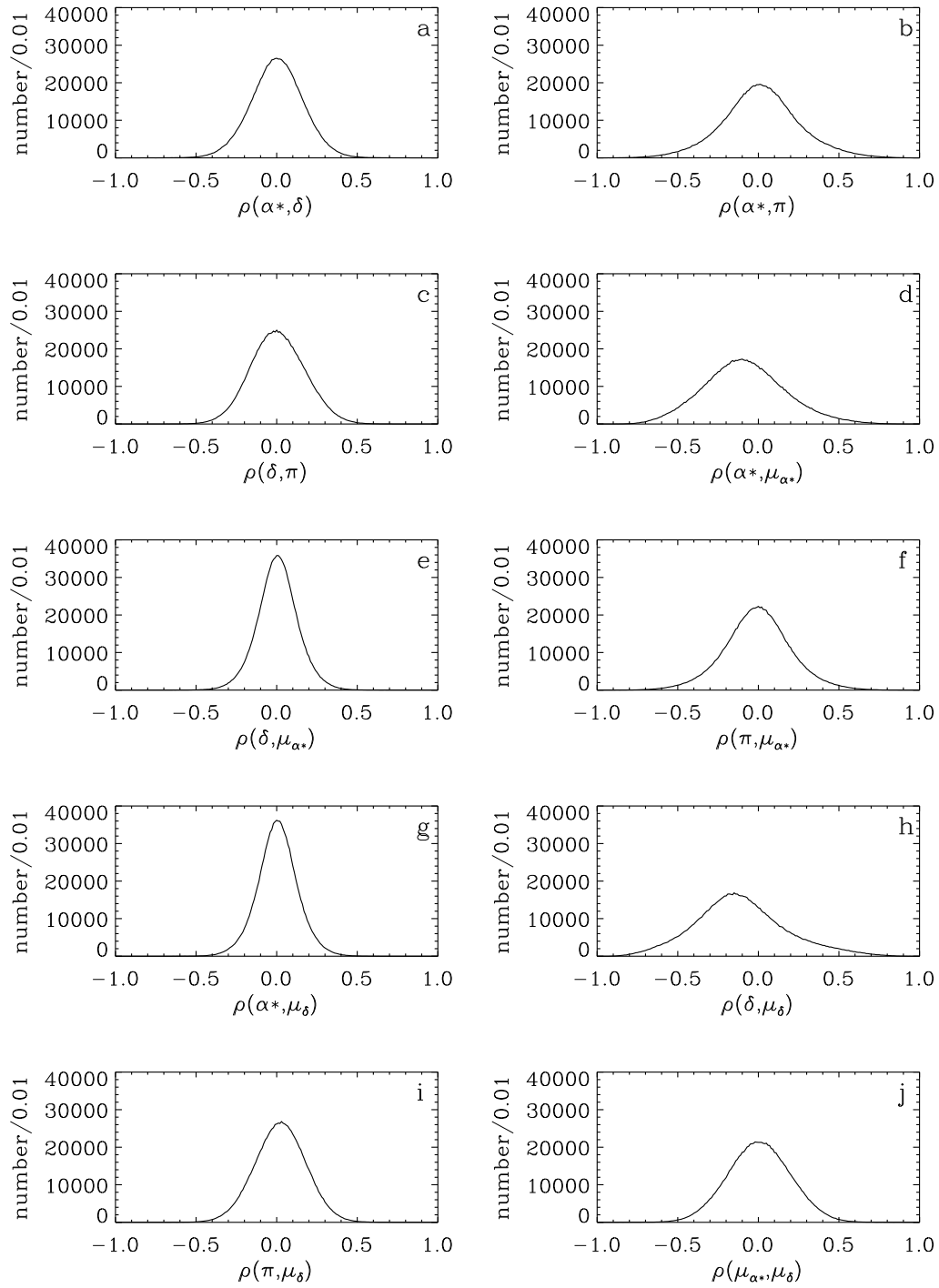


**Figure 16.15.** The distribution of the correlation coefficients for the five astrometric parameters.

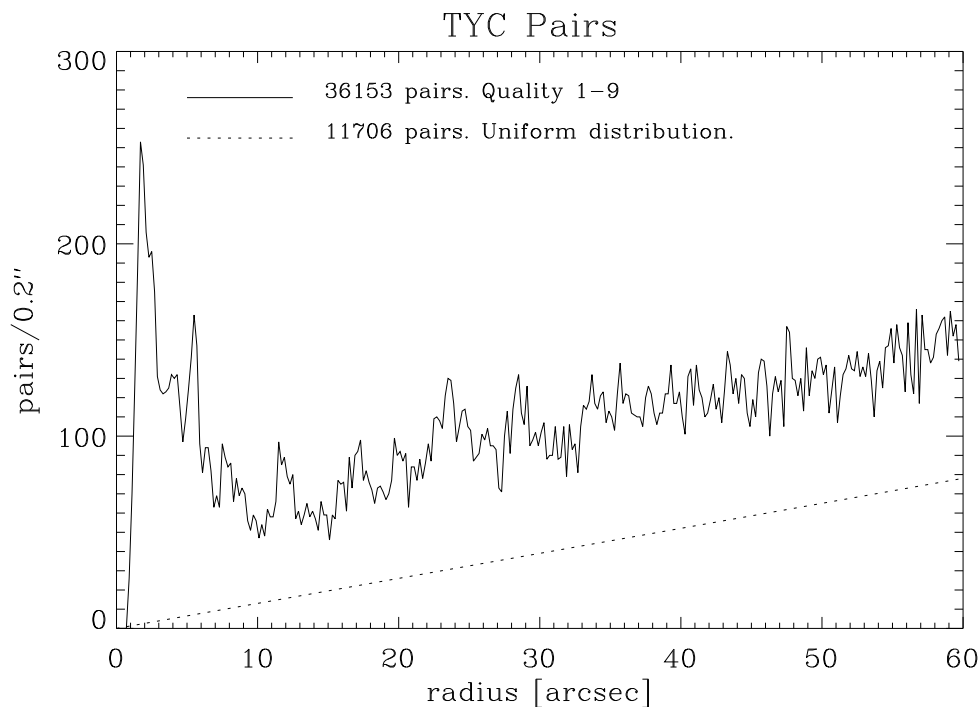


**Figure 16.16.** Distribution of distances between all pairs of Tycho Catalogue stars. For comparison the distribution for a uniformly populated sky is also given. The peaks at 5.6, 11.3, 17, 23, 29 and 34 arcsec are due to side lobes.

stars). Resolved double stars produce a peak at 2 arcsec separation. There are, however, other peaks of a less innocent nature, i.e. the peaks at 5.6, 11.3, 17, 23, 29 and 34 arcsec. These distances correspond to the side lobes of the response function of the slits, as discussed in Section 4.3. A star may give rise to false detections at these distances or make true detections brighter when another star is crossing the slit system at the same time.

It is estimated from Figure 16.16 that a few hundred stars that are either false or actually too faint for Tycho detection, have found their way into the final catalogue, due to side lobes. For the same reason, the brightness of the double star components was overestimated as explained in Section 19.5. The question of false stars is discussed further in Chapter 17.

**Parallaxes:** The individual parallaxes in the Tycho Catalogue are generally of low significance. Figure 16.17(a) shows the distribution of measured parallaxes. The negative wing contains 44 per cent of the stars. The overall median value is 4.0 mas, see Figure 16.18 which shows the median parallax across the sky. Figure 16.17(b) shows the distribution of the parallax divided by its standard error. Because the true parallaxes are generally much smaller than the error, we would expect an almost normal distribution. The dashed curve is a Gaussian distribution centred at 0.2 and with a standard deviation of 1.33. This suggests that the internal standard error should be increased some 30 per cent to produce the external standard error. The external errors of the Tycho Catalogue are discussed further in Chapter 18.

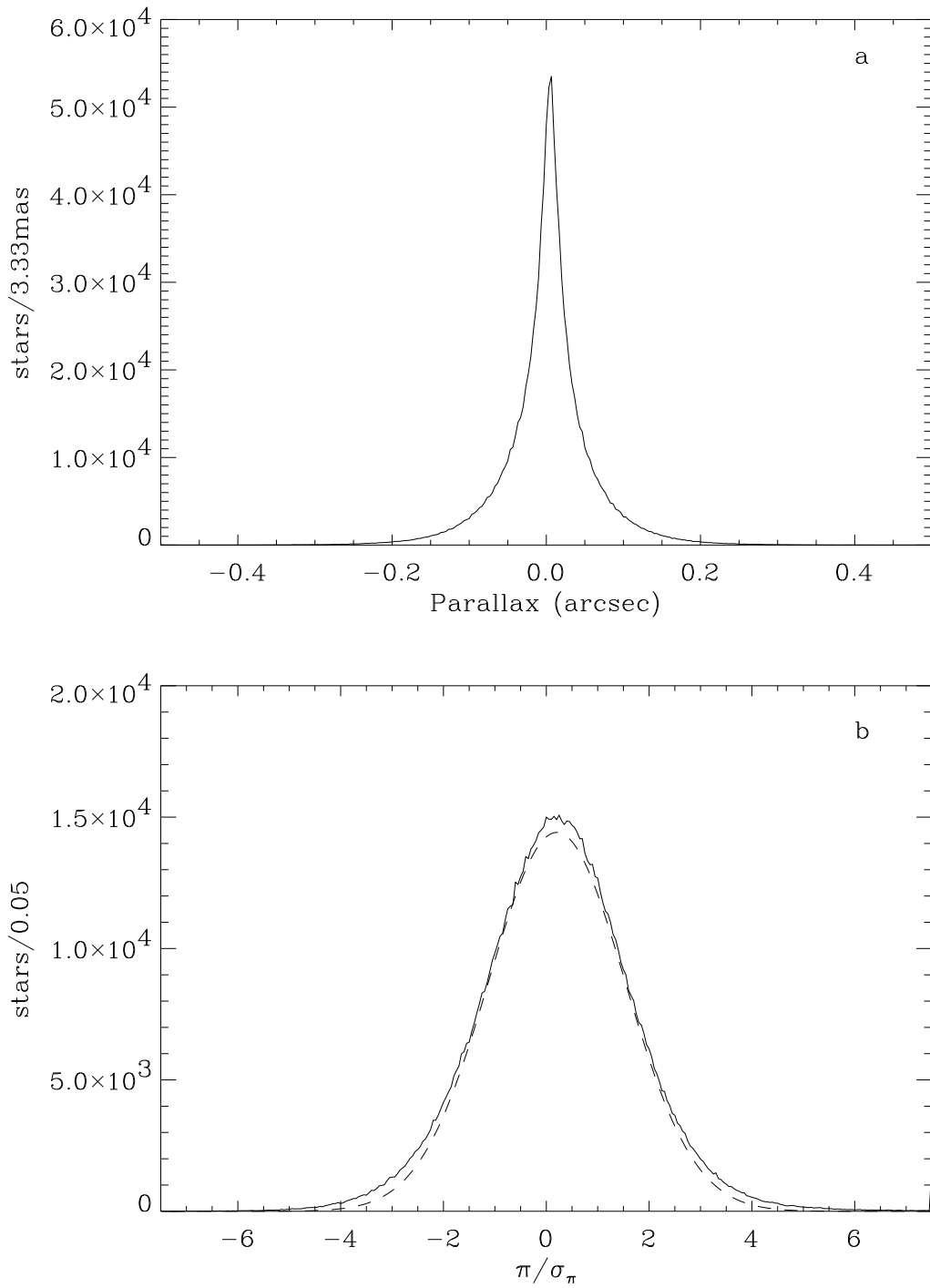


**Figure 16.17.** Distribution of parallaxes and their significance. The dashed curve is a Gaussian fit with standard deviation 1.3.

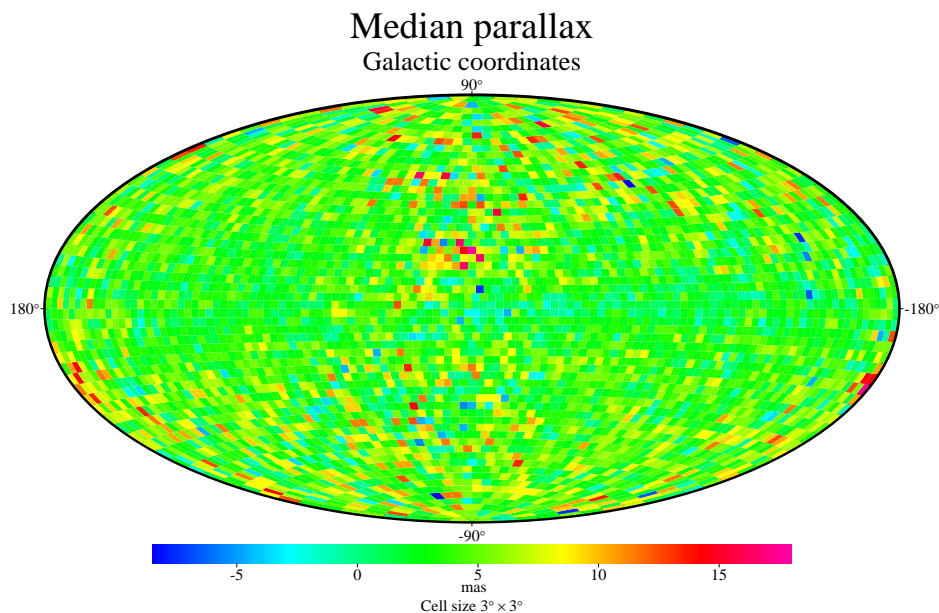


**Figure 16.18.** The median parallax. The overall median is 4 mas. Towards the Hyades ( $l = 180^\circ$ ,  $b = -20^\circ$ ) and the dust clouds in Ophiuchus ( $l = 0^\circ$ ,  $b = 20^\circ$ ) the median parallax is much higher.

---

### 16.3. Photometric Content

---

The Tycho Catalogue contains photometric data for both the southern and the northern sky obtained with a single instrument. The two colour bands  $B_T$  and  $V_T$  define a new independent system providing mean magnitudes for 1 047 132 stars. An additional 4647 stars obtained photometric values from a special treatment in the astrometric reductions, e.g. the double stars (see Section 14.4).

Table 16.3 summarizes median standard errors for all stars with  $B_T$  or  $V_T$  values in the Tycho Catalogue including the approximate magnitudes obtained during astrometric processing. The  $\sigma_{B_T-V_T}$  depends on magnitude, but also on the colour itself. Values for  $\sigma_{B_T-V_T}$  as a function of  $V_T$  and  $B_T - V_T$  are given for non-variable stars in Table 16.5, i.e. for photometric standard stars.

The approximate magnitudes for about 4600 stars, mainly from the astrometry processing, were only given a simple calibration. For the remaining part of this section, only stars with fully calibrated magnitudes are discussed, i.e. the 1 050 000 stars with median or de-censored magnitudes derived from single transits calibrated in the  $B_T$  and  $V_T$  system as described in Chapter 8. The distribution of the fully calibrated magnitudes is shown in Figure 16.19. Technically, these magnitudes are for the stars in the Tycho Catalogue defined by Field T36 (Section 2.2, Volume 1) equal to 'M' or 'N', indicating that the magnitude is a median magnitude ('M') for bright stars ( $B_T < 8.5$  mag and  $V_T < 8.0$  mag) or a de-censored magnitude ('N'). While median magnitude determination took into account only the detected observations, the de-censoring process also accounted for the non-detections (this is described in detail in Chapter 9). Table 16.4 gives some important numbers for fully calibrated stars.

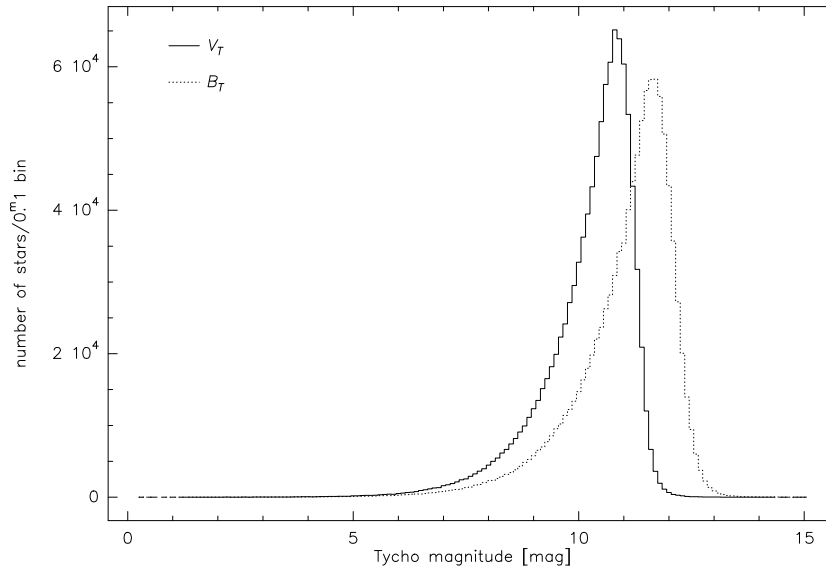
**Table 16.3.** Median standard error of mean magnitude and colour index versus magnitude.  $N$  is the number of stars in each interval, the 0.5 mag bins being centred on the given  $V_T$ .  $\sigma_{B_T}$  is given as a function of  $B_T$ , while  $\sigma_{V_T}$  and  $\sigma_{B_T-V_T}$  are given as functions of  $V_T$ . Systematic errors are much smaller, except for the faintest stars.

$B_T$ mag	N	$\sigma_{B_T}$ mag	$V_T$ mag	N	$\sigma_{V_T}$ mag	$V_T$ mag	N	$\sigma_{B_T-V_T}$ mag
≤5.0	919	0.003	≤5.0	1455	0.003	≤5.0	1451	0.003
≤9.0	58763	0.009	≤9.0	119878	0.012	≤9.0	119748	0.016
All	1050525	0.073	All	1051923	0.057	All	1049579	0.087
0.5	4	0.012	0.5	5	0.010	0.5	5	0.014
1.0	4	0.012	1.0	6	0.010	1.0	6	0.014
1.5	15	0.007	1.5	12	0.007	1.5	12	0.010
2.0	19	0.004	2.0	38	0.004	2.0	36	0.004
2.5	38	0.003	2.5	47	0.003	2.5	47	0.004
3.0	57	0.003	3.0	90	0.002	3.0	90	0.003
3.5	79	0.003	3.5	143	0.002	3.5	142	0.003
4.0	183	0.003	4.0	268	0.002	4.0	268	0.003
4.5	298	0.003	4.5	484	0.003	4.5	484	0.003
5.0	521	0.003	5.0	871	0.003	5.0	870	0.004
5.5	919	0.003	5.5	1490	0.003	5.5	1489	0.004
6.0	1416	0.003	6.0	2582	0.004	6.0	2578	0.005
6.5	2435	0.004	6.5	4647	0.005	6.5	4644	0.007
7.0	4092	0.005	7.0	7861	0.006	7.0	7857	0.009
7.5	6722	0.007	7.5	13381	0.008	7.5	13375	0.011
8.0	11146	0.009	8.0	22691	0.010	8.0	22681	0.014
8.5	17801	0.011	8.5	37864	0.013	8.5	37800	0.019
9.0	29686	0.014	9.0	62629	0.018	9.0	62558	0.027
9.5	47949	0.019	9.5	102441	0.026	9.5	102313	0.039
10.0	75708	0.026	10.0	166222	0.038	10.0	165927	0.058
10.5	120981	0.039	10.5	261852	0.060	10.5	261142	0.091
11.0	184604	0.058	11.0	286408	0.095	11.0	285919	0.137
11.5	273399	0.092	11.5	74953	0.151	11.5	74758	0.205
12.0	212866	0.145	12.0	4357	0.308	12.0	4227	0.440
12.5	53225	0.232	12.5	458	0.602	12.5	334	1.039
13.0	5455	0.401	13.0	78	0.900	13.0	17	1.879
13.5	682	0.680	13.5	25	1.601	13.5	0	–
14.0	144	1.042	14.0	12	1.887	14.0	0	–
14.5	61	1.495	14.5	4	2.412	14.5	0	–
15.0	16	1.881	15.0	4	2.670	15.0	0	–

Despite the different origin of magnitudes (using median and de-censored values) there are no discontinuities in the catalogue at  $V_T = 8$  mag or at  $B_T = 8.5$  mag. This results from the fact that bright stars had no censored observations. The difference between median and de-censored magnitudes is less than 0.005 mag at this magnitude and therefore below the calibration uncertainty. An artifact of different de-censoring processing schemes is however noticeable for the  $B_T$  channel in Figure 16.19: at  $B_T = 10.95$  mag the distribution in this Tycho channel has a not quite uniform slope; this is however only

**Table 16.4.** Numbers for fully calibrated stars.

	number of stars
$B_T$ and $V_T$ given	1047132
only $V_T$ given	173
only $B_T$ given	79
median magnitudes	29524
de-censored magnitudes	1017860

**Figure 16.19.** Distribution of all stars with at least one fully calibrated Tycho magnitude binned to 0.100 mag.

a minor effect. Thus, the  $B_T$  and  $V_T$  magnitudes can be treated as uniform entities and are simply referred to as mean magnitudes in the following sections.

Using these mean magnitudes, the colour-magnitude diagram in Figure 16.20 was constructed for all stars in the Tycho Catalogue with  $B_T$  and  $V_T$  magnitudes. Clearly visible is the completeness and the detection limit for a given Tycho colour. The large errors for very faint and very red stars (see Tables 16.3 and 16.5) are clearly visible. A remarkable feature of this diagram is the concentration of the stars in four vertical bands of constant colour. This is not an artifact, but reflects intrinsic structure of the Hertzsprung-Russell diagram, i.e. of the stellar population within a few hundred parsec.

**Photometric precision over the whole sky:** The standard error in  $V_T$ , depending on position in the sky, is shown in Figure 16.21 for all stars (upper panel) and in three magnitude ranges. Shown in a logarithmic colour-scale is the average  $\sigma_{V_T}$  as a function of the equatorial coordinates. The lowest average errors are achieved about  $45^\circ$  above and below the ecliptic plane. Stars located in these bands obtained the most observations due to the scanning law, as discussed in Section 16.2. As shown below, the number of observations is the main parameter for the precision of the mean magnitude. The effect of the scanning law is clearly seen in all but the faintest magnitude range with a low number of stars. Clearly visible with an increased average  $\sigma_{V_T}$  in all magnitude ranges is the Galactic centre region ( $\alpha, \delta: 266^\circ, -29^\circ$ ) and the region near  $\eta$  Carinae ( $\alpha, \delta:$

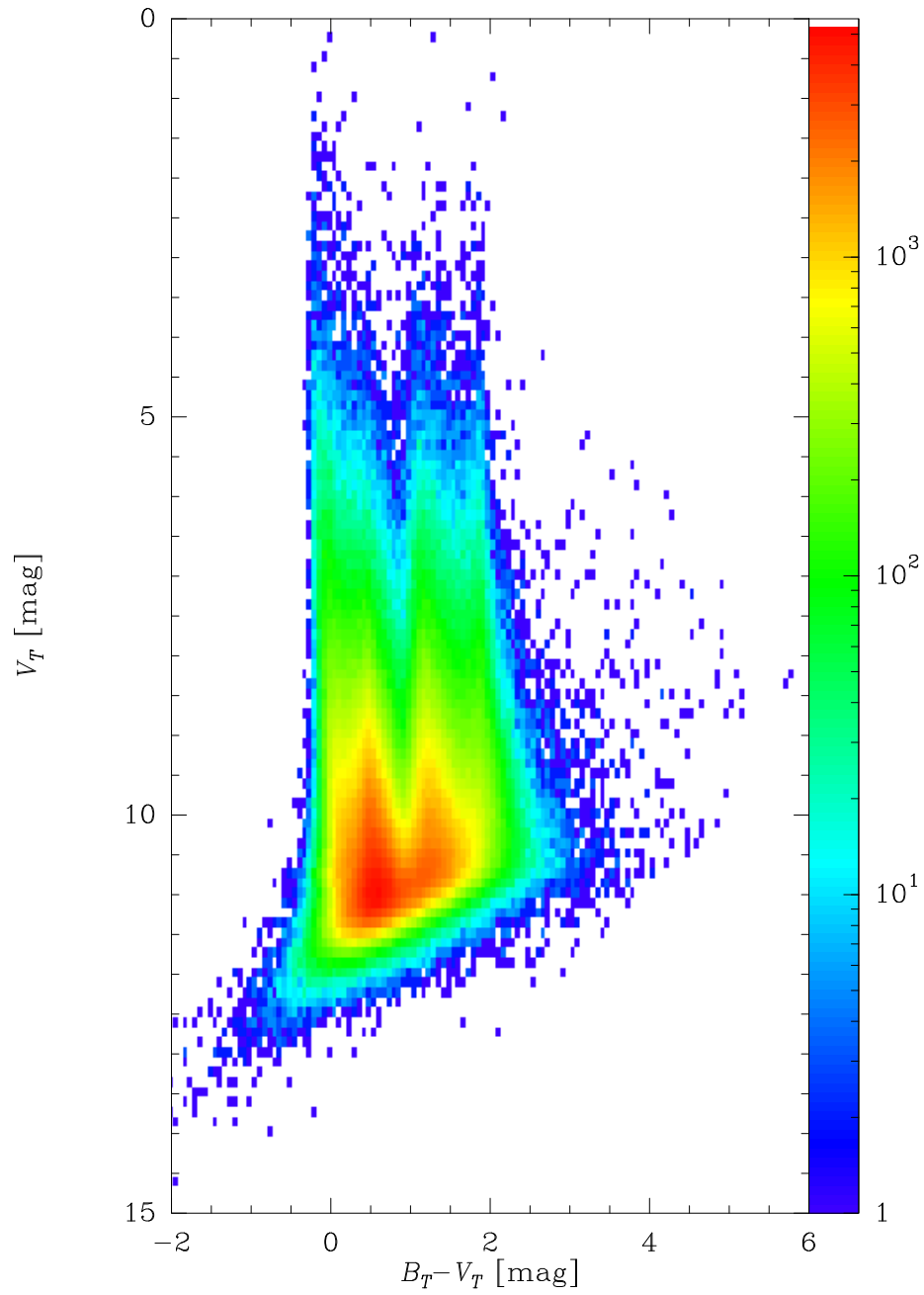


**Figure 16.20.** Colour magnitude diagram for all stars with  $B_T$  and  $V_T$  magnitudes. The logarithmic colour scale shows the number of stars in bins of 0.0625 mag in  $B_T - V_T$  and 0.125 mag in  $V_T$ .

**Table 16.5.**  $\sigma_{B_T-V_T}$  for three colour ranges as a function of  $V_T$  derived for non-variable stars with  $N_{\text{photom}}$  from 80 to 160 photometrically valid transits.  $n$  is the number of stars.

$B_T - V_T$		[-0.2,0.2]		[0.5,0.9]		[1.4,2.0]	
$V_T$ [mag]	n	$\sigma_{B_T-V_T}$ [millimag]	n	$\sigma_{B_T-V_T}$ [millimag]	n	$\sigma_{B_T-V_T}$ [millimag]	
5	95	3	24	4	20	5	
6	411	5	133	6	208	8	
7	952	8	722	10	255	13	
8	1217	13	2522	15	224	22	
9	600	21	1258	27	153	43	
10	86	44	552	54	100	120	
11	17	90	73	121	36	263	

160°, -60°). Higher than average errors in dense regions can be understood from the fact that many more parasite transits (i.e. transits with magnitude estimates disturbed by other stars) had to be rejected in de-censoring.

### Non-variable Stars: Precision of Mean Magnitudes in the Tycho Catalogue

The following paragraphs discuss the precision of magnitudes given in the Tycho Catalogue for non-variable stars (i.e. the 17 863 photometric standard stars described in Chapter 8), allowing an estimation of the overall precision as a function of several parameters in the Tycho observations for definitively constant stars.

**Precision depending on the number of observations:** A crucial parameter for the precision of a magnitude is the number of observations used to derive the  $B_T$  or  $V_T$  magnitude. Given in the Tycho Catalogue is the number of photometrically valid transits,  $N_{\text{photom}}$  (Field T43, Section 2.2 of Volume 1) which is also used to show the corresponding dependency of  $\sigma_{V_T}$  for two magnitude ranges in Figure 16.22. It should be noted that  $N_{\text{photom}}$  counts the number of detections in the case of a median, i.e. for the bright stars in Figure 16.22, but the sum of detections and non-detections in the case of a de-censored magnitude. In addition to this, a different background limit was applied in the de-censoring analysis and observations affected by parasites were rejected. For this reason and because other selection criteria were adopted in the astrometric reduction,  $N_{\text{photom}}$  cannot easily be compared with  $N_{\text{astrom}}$  which gives the number of transits retained in the astrometric adjustment (Field T29), see Figure 16.6.

**Precision depending on colour:** Besides the number of photometrically valid transits, another important parameter for the achieved precision of  $B_T - V_T$  at a given magnitude is the colour of the star. Table 16.5 gives  $\sigma_{B_T-V_T}$  for three different colour ranges as a function of  $V_T$ . The highest values occur for red stars, because the photon noise is larger in the  $B_T$  channel at a given  $V_T$  for large  $B_T - V_T$ .

### Colour of Stars on the Sky

Figure 16.23 shows the median Johnson  $B - V$  on the sky for Tycho stars. With a limiting magnitude of  $V_T = 11$  mag, the stars must generally be assumed to be within some 100–250 pc and the plot shows many features of the Galactic vicinity. About

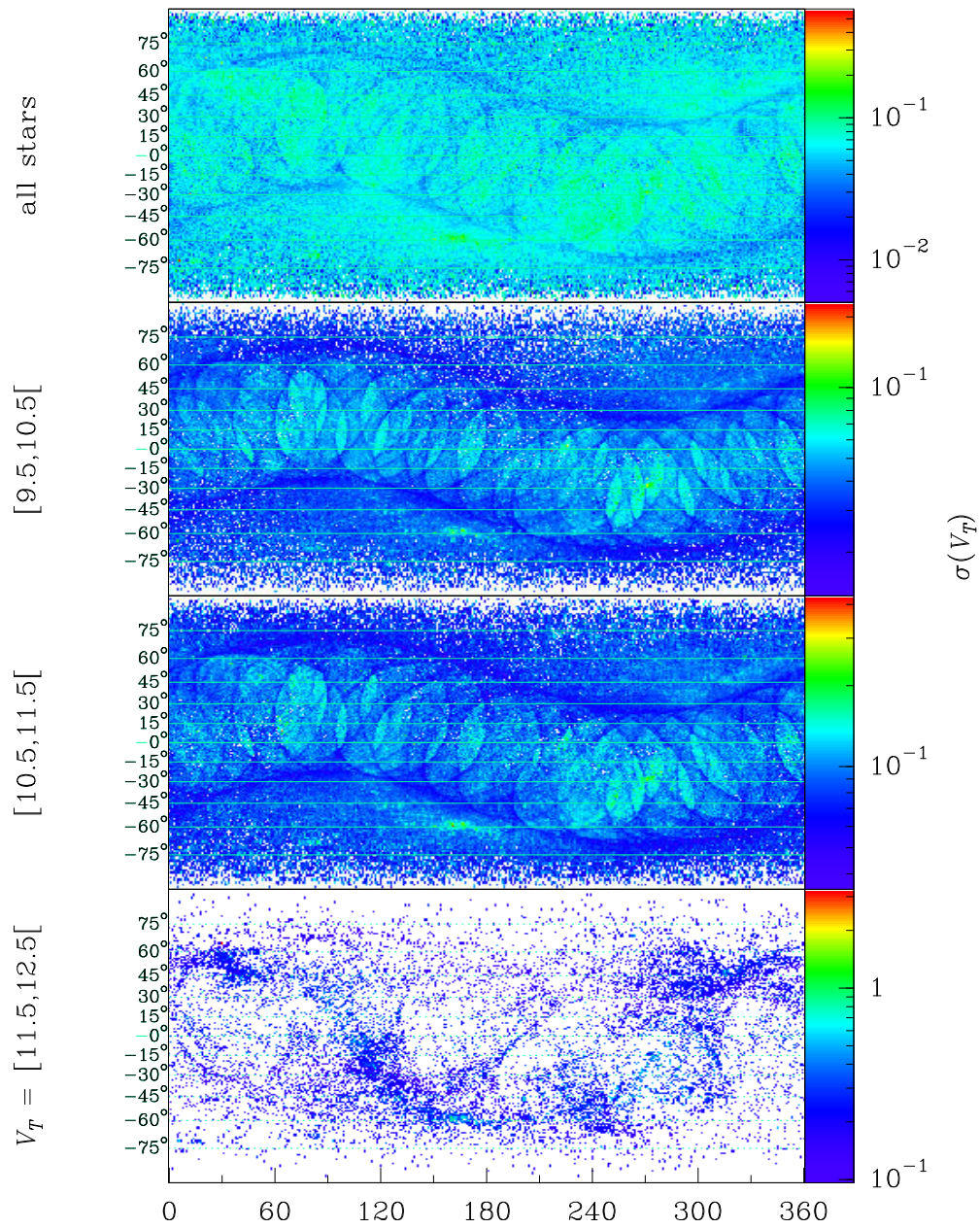


**Figure 16.21.** Average errors  $\sigma_{V_T}$  as a function of equatorial coordinates for all stars (upper panel) and stars in three  $V_T$  magnitudes ranges, from top to bottom:  $V_T = 9.5$  to  $10.5$  mag (338 227 stars),  $10.5$  to  $11.5$  mag (490 549 stars) and  $11.5$  to  $12.5$  mag (20 167 stars). The logarithmic colour scale shows the average  $\sigma_{V_T}$  with a resolution of 1 degree in right ascension.

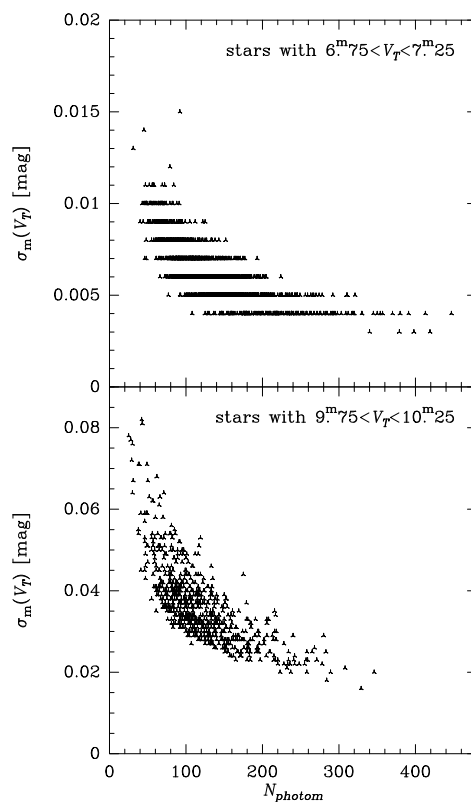


**Figure 16.22.** The error of the Tycho  $V_T$  magnitudes as a function of the number of observations  $N_{\text{photom}}$  given in the Tycho Catalogue for non-variable stars in two magnitude ranges (upper) 6.75 to 7.25 mag (1668 stars) and (lower) 9.75 to 10.25 mag (669 stars).

$30^\circ$  from the Galactic centre the dust complexes in Ophiuchus and Scorpius cause red giants or strongly reddened stars to dominate. In general, early types are in the majority, mainly because the catalogue is magnitude limited, causing the upper part of the Hertzsprung-Russell diagram to be over-represented. This is especially clear in the third quadrant of longitude ( $l \in [180^\circ, 270^\circ]$ ) where the picture is less affected by interstellar absorption.

---

#### 16.4. The Tycho Epoch Photometry Annex

---

The Tycho Epoch Photometry Annex (TEPA) contains individual transit data of selected stars and is divided into two parts. The smaller part, TEPA A, is delivered on CD-ROM as an ASCII file and comprises transits for 34 446 stars while the larger data base, TEPA B, contains transit data for 481 553 stars (including all TEPA A stars) and is made available through the Centre de Données astronomiques de Strasbourg. While TEPA A is formed by several peculiar groups of stars (and 5165 photometric standard stars for comparison) TEPA B gives mainly the 480 000 brightest stars. The exact criteria used to select stars for the Tycho Epoch Photometry Annex can be found in Volume 1, Section 2.6. Table 16.6 shows some statistics of stars and transits. The categories of stars do not, however, correspond strictly to the selection criteria but to the flags in the header record given for each star in the Tycho Epoch Photometry Annex (see



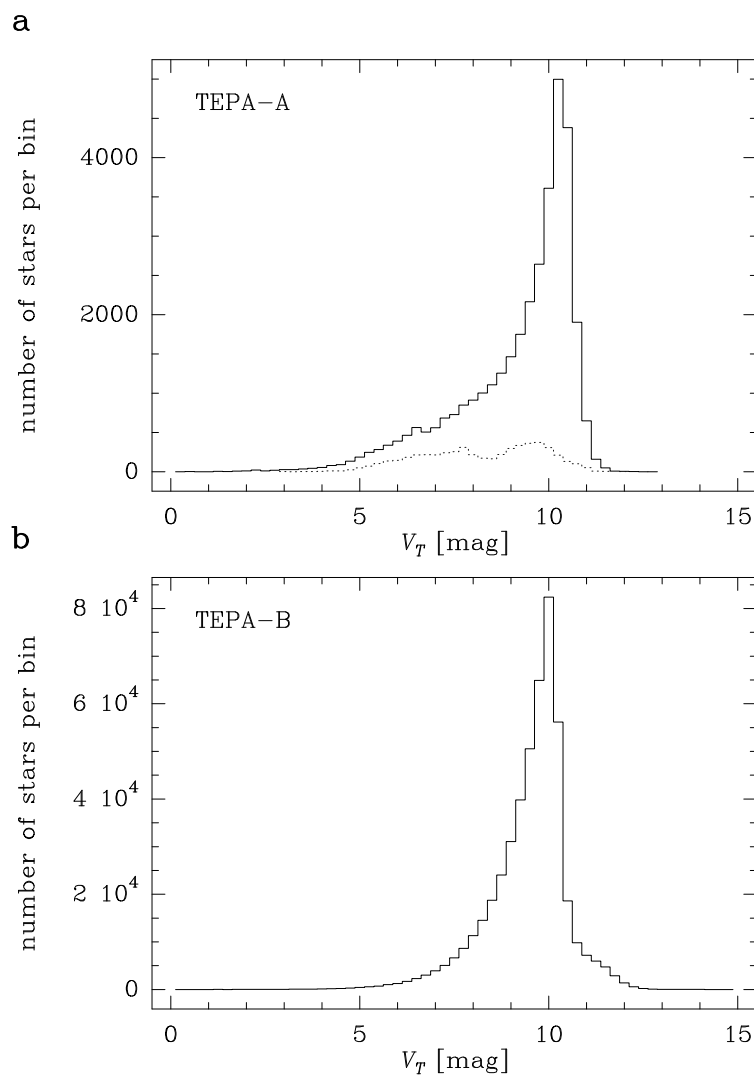


**Figure 16.24.** Distribution of all stars in (a) the Tycho Epoch Photometry Annex A and (b) the Tycho Epoch Photometry Annex B, binned to 0.25 mag. The dashed line in (a) shows the number of standard stars (see Table 16.6).

Table 2.6.1 in Volume 1 for a description of the star header record), i.e. to information given in Fields TH15 and TH16.

More specifically, the rows in Table 16.6 are described as follows:

- standard stars: gives the number of stars which were assumed constant at the beginning of the calibration process. The number given refers to Field TH16 (flag 1) marking standard stars for photometric calibration in reprocessing. After processing and variability analysis, 584 of these stars in the Tycho Epoch Photometry Annex B and 199 in Annex A were found to be flagged as variable or suspected variable in the General Catalogue of Variable Stars/New Catalogue of Suspected Variable Stars (GCVS/NSV) or from Hipparcos or Tycho variability analysis (see Section 19.2 for further discussion);

- standard stars (subset): gives only those stars used during main processing. This star sample is fully included within the sample of standard stars for reprocessing. The reason that the number of standard stars was lower for main processing is merely technical (and due to the transit data available for calibration). Therefore, the larger sample of stars marked by Field TH16 (flag 1) should be used if the Tycho Epoch Photometry Annex is searched for standard stars;
- reprocessing reduction: states that the transits for this star and the photometric quantities given in the Tycho Catalogue originate from the reprocessing data stream using reprocessing calibration (Section 11.4). This does not necessarily mean, however, that astrometric values were derived using reprocessing data (see Section 11.2);
- approximate magnitudes: means that the star did not obtain its photometric values from fully calibrated transit data, but from a dedicated treatment in the astrometric reductions applied, e.g. to double stars. Magnitudes of these stars were not derived using de-censoring and are systematically too bright (by up to 1 mag for a star of 11 mag);
- about 11–12 per cent of all transits in the Tycho Epoch Photometry Annex are found to be empty, i.e. the star was not detected in the added photon counts of the  $B_T$  and  $V_T$  channels. The detection limits  $B_{\text{det}}$  and  $V_{\text{det}}$  which are given in the Tycho Epoch Photometry Annex instead of  $B_T$  and  $V_T$  for empty transits were calculated assuming a signal-to-noise ratio of 1.5. When the star was detected in one channel, however, the detection limit given for the other channel was computed assuming a signal-to-noise ratio of 2.5. The entries ‘ $B_{\text{det}}$  given’ and ‘ $V_{\text{det}}$  given’ give the number of transits for the latter case.

The magnitudes of stars in the Tycho Epoch Photometry Annex A range from  $V_T = -0.6$  mag to 12.7 mag as can be seen from Figure 16.24 (and up to 15 mag in Annex B) with Canopus (TYC 8534–2277–1) being the brightest star included. The mean  $V_T$  magnitudes and the percentiles given in the star header are strictly the same as those in the Tycho Catalogue with the exception that percentiles in the Tycho Catalogue are replaced by blanks when fainter than 15.0 mag. Values for  $B_T$  percentiles and the number of measured transits for each channel are only given in the Tycho Epoch Photometry Annex.

### Number of Transits and Transit Selection

The mean number of transits given per star is 197 in the Tycho Epoch Photometry Annex A and 173 in Annex B. The minimum number is 28 and the maximum is 611. Only ‘valid’ transits are included, which might be either detections or non-detections. The number of measurements per star is given in the header record for both the  $B_T$  and the  $V_T$  channel. This number decreases for fainter stars. Non-detections may however also occur for bright stars (the 6 per cent ‘spurious non-detections’ discussed in Section 2.2 of Volume 1). The detection limits given for  $B_T$  and  $V_T$  are then meaningless. A ‘valid’ transit may even be a transit which was never used in photometry because of the criteria imposed during de-censoring or median computations.

## 17. VERIFICATION OF THE TYCHO CATALOGUE: STELLAR CONTENT

*In this chapter, the stellar content of the Tycho Catalogue is analyzed. Comparisons are made with major reference catalogues: the Hipparcos main catalogue, the Catalogue of Positions and Proper Motions (PPM), the Guide Star Catalog, etc. It is shown that the Tycho Catalogue can be considered a nearly complete star survey up to a magnitude limit of  $V_T = 10.5$  mag. Missing stars are listed, and cross-identifications are discussed.*

---

### 17.1. Introduction

---

In general terms, the Tycho Catalogue can be described as a survey of stars brighter than 11.0 mag. In practice, this means that the Tycho Catalogue contains about 99.9 per cent of the stars brighter than  $V = 10.0$  mag, and a large fraction of the stars in the range 10.0 to 11.5 mag. The completeness ratio drops, at the faint end, from more than 90 per cent at  $V = 10.5$  mag, to roughly 65 per cent at 11.0 mag and 10 per cent at 11.5 mag (see Figure 17.1). Among the 120 000 stars brighter than 9.0 mag in the Catalogue of Positions and Proper Motions (PPM), about 120 are missing in the Tycho Catalogue, i.e. 0.10 per cent. In this chapter the limits and characteristics of the survey are examined in more detail.

---

### 17.2. Completeness of the Tycho Catalogue at the Bright End

---

A few very bright stars, e.g. Sirius, were not observable by the star mapper. The dynamic range of the star mapper detector resulted in a non-linearity at the brightest magnitudes. Stars in very dense clusters and other dense fields could not be observed by Tycho, thus leaving the Tycho Catalogue incomplete in such regions. However, stars contained in the Hipparcos Catalogue and not observed by the Tycho star mapper have been added, for completeness, in the Tycho Catalogue and flagged accordingly. As a consequence, one can expect to have a complete catalogue at the bright end. There are some exceptions, setting aside the photometric variability, and the specific case of very close binaries. For instance, during the preparation of the Millennium Star Atlas the exercised eyes of Sky & Telescope experts discovered a missing star near Alcyone. Of a triangle of three stars near Alcyone, one is missing from the Tycho Catalogue: SAO 76188 (HD 23608). This star was also actually missing from the Guide Star

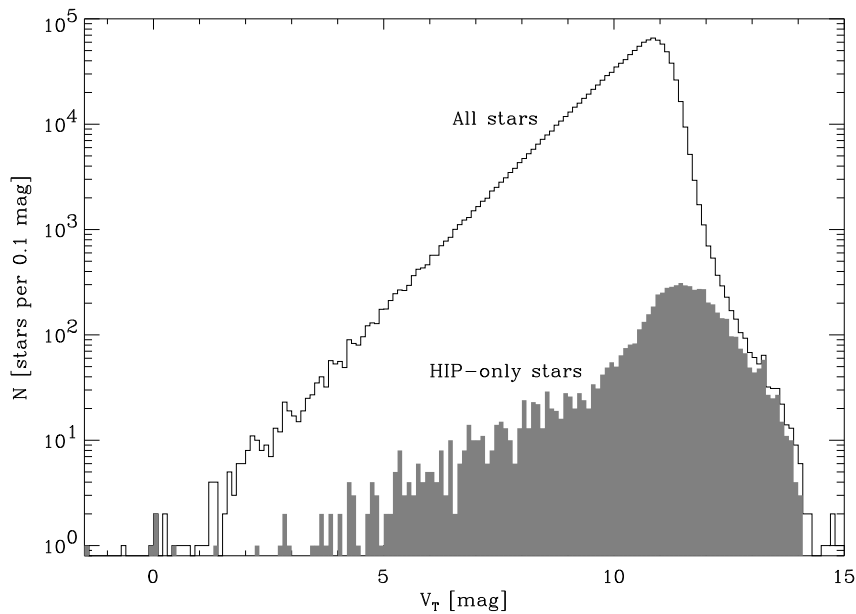


**Figure 17.1** Histogram of Tycho stars as a function of  $V_T$  magnitude. For 1 per cent of the stars another magnitude had to be used.

Catalog Version 1.0 but had been introduced into the Tycho Input Catalogue (and later on into Version 1.1 of the Guide Star Catalog) from the SIMBAD/INCA Data Bases. Although present in the Tycho Input Catalogue Revision (TICR), this star failed to be included in the final Tycho Catalogue, due to an insufficient number of transits not affected by parasites (see Section 7.2). The Hipparcos Catalogue does not contain the star, which would otherwise have been included as a ‘HIP-only’ entry.

A reasonably complete list of such bright missing stars can be derived from comparisons with ground-based catalogues. Stars in the Catalogue of Positions and Proper Motions (PPM), including the Bright Star Supplement, of magnitude 9.0 or brighter were sought in the Tycho Catalogue. Among a total of 143 490 stars, no Tycho Catalogue star was found within 3.0 arcsec in 137 cases. A closer examination showed that at least 117 stars are not in the Tycho Catalogue. These stars are listed in Table 17.1. In 103 cases there is not even a Tycho Catalogue star within 30 arcsec of the PPM position. In the 14 remaining cases there is a Tycho star at some distance, but it is very unlikely to be the PPM star. One of the missing stars, PPM 122593, is in fact HIP 31067. It has no astrometric solution in the Hipparcos main catalogue, but the result of a new astrometric solution is given in the notes.

Out of the 137 PPM stars, 20 are not clearly missing in the Tycho Catalogue. There is rather an inconsistency. Except for PPM 215592, all 20 stars seem to be in the Hipparcos Catalogue. These 20 stars are listed in Table 17.2. In 14 cases the PPM entry gives the position of the photocentre of Tycho double stars with separations 6.6–10 arcsec. The remaining six cases require individual remarks. PPM 323067 is flagged in the Catalogue of Positions and Proper Motions as ‘double’ and as a ‘problem case’. In SAO, in the Hipparcos Input Catalogue and on the Digitized Sky Survey it is much fainter than 9.0 mag, more like 10.5 mag. The other five PPM stars are at distances 3.1–3.8 arcsec from a Tycho star. They are all double stars with separations 5–16 arcsec and both components are in the Tycho Catalogue, but with different positions from the PPM Catalogue. The relative positions (position angle and separation) of these stars in the

CCDM are in good agreement with the Tycho positions. Therefore, the inconsistencies are probably due to errors in the PPM Catalogue. PPM 331230 is even a high proper motion star and part of an orbiting pair. It should finally be noted that the bright supplement to the PPM Catalogue (PPM numbers 400nnn) gives only approximate positions. It is concluded that among the stars of the PPM Catalogue brighter than 9 mag, only 117 are missing in the Tycho Catalogue, providing a completeness of 99.9 per cent.

### **Status of Bright Stars Absent from the Tycho Catalogue**

The status has been checked of stars brighter than 9.0, present in the Hubble Space Telescope Guide Star Catalog (GSC), and therefore in the Tycho Input Catalogue (TIC), but which are not in the Tycho Catalogue. There are 2028 such stars in the northern sky ( $V \leq 9.0$  mag), i.e. 1.5 per cent of the Tycho Input Catalogue in this magnitude range. There are 4635 such stars in the southern sky ( $B \leq 9.0$  mag; no  $V$  available). As explained below, most of these 'stars' are false Guide Star Catalog entries.

Such stars have been checked in two sample areas of  $6^\circ$  radius, one in the South and one in the North, using the Centre de Données astronomiques data bases: SIMBAD and ALADIN. In the South, from a test on 31 objects, 70 per cent are galaxies or nebulae and 30 per cent are redundancies. For the galaxies and nebulae the 'stellar' magnitude given by the Guide Star Catalog was too bright because these are extended objects. The redundancies occur when the same bright star appears on two plates with a position difference slightly too large for automatic identification. In the North, from a test on 15 objects, 50 per cent are redundancies, 25 per cent are galaxies/nebulae or false stars, most often flagged in the Guide Star Catalog with 'nonstar' class and 25 per cent are double systems. For these doubles the median position given by the Guide Star Catalog has not been confirmed by Tycho. Therefore the Tycho Catalogue obtained 'new' entries, carrying a new identification number.

All these features of the Guide Star Catalog were already known, and some of them have been corrected in later versions of the Guide Star Catalog. The comparison with the Tycho Catalogue provided useful tools for wiping out these defects from the Guide Star Catalog.

### **Does the Tycho Catalogue Include False Bright Stars?**

We have considered all Tycho Catalogue entries with  $V_T \leq 7.0$  mag and no Hipparcos Catalogue (HIP) identifier, as potential candidates for being 'false stars'. There are only 59 such entries:

- for one star (TYC 5619-1257-1 = HIP 78727) the Hipparcos Catalogue cross-identification was omitted in the Tycho Catalogue because of missing Hipparcos astrometry;
- 23 stars are components of a double or multiple system: the Hipparcos Catalogue number was assigned to (one of) the other component(s) of the system, but not to this one. An example is TYC 1800-2201-1 = HD 23629; HIP 17702 is assigned to HD 23630;

**Table 17.1.** Bright stars from the Catalogue of Positions and Proper Motions (PPM) which are missing in the Tycho Catalogue (117 cases).

PPM	m	RA Dec h m deg	pm " yr <sup>-1</sup>	HD	SAO	Other Name	Simbad type stat	Comments
A neighbouring star is present in the Tycho Catalogue within 30 arcsec; 14 cases:								
14174	8.0	03 16 +60	0.00	20053	23908		*i2	4049-1502-1 at 7.1 arcsec
187290	9.0	04 45 -03	0.01		131463		*	
122176	9.0	06 15 +10	0.01	43231	95453		*i2	735-863-1 at 5.4 arcsec
96101	8.7	06 31 +21	0.01	45900			*i2	1340-1326-1 at 8.1 arcsec
251060	8.3	06 49 -24	0.03	49892	172384		*i2	
253068	8.2	07 44 -24	0.83				?	Sim-
191001	8.6	08 07 -03	0.04	67324	135523		*	
222919	7.0	10 24 -18	0.02	90255	155965		V*	PN NGC 3242
400169	7.2	12 06 +68	0.00				D/M	ADS 8419 DS
359380	8.6	12 23 -62	0.02	107862	251882		*i2	
400197	7.4	14 50 -67	0.01			AV Cir	Cep	
294473	8.9	15 57 -31	0.01		207167		*i2	
322113	8.7	16 44 -42	0.06	150674	227139		*i2	
234740	8.4	18 34 -14	0.01	171333	161630		*i2	
No Tycho star within 30 arcsec; 103 cases:								
182211	7.3	00 24 -09	0.00	1987	128740	S Cet	Mira	
701131	8.4	01 06 -01	0.01	6592		Z Cet	Mira	
367685	8.5	02 29 -70	0.03	15919			*	
367701	8.3	02 32 -70	0.02	16242	255896		*	
353126	8.1	02 46 -68	0.01	17646			*	
212820	8.9	03 23 -10	0.01	21040	148931		*i2	
92883	8.9	03 47 +24	0.04	23608	76188		*i2	Cl: Pleiades
186599	8.9	04 09 -09	0.04	26316	130990		*	
186800	8.9	04 19 -02	0.04	27450	131117		*i2	
214263	8.7	04 23 -14	0.02	27913	149601		*	
187096	8.9	04 34 -02	0.02		131327		*	
280771	8.9	04 51 -34	0.08		195366		*	
187717	8.6	05 06 -09	0.01	33009	131781		*	
187853	8.9	05 15 -07	0.01				IRS	
47921	8.3	05 16 +46	0.06		40184		*i2	
248729	8.5	05 18 -25	0.02	34691	170292		*	
248800	8.7	05 21 -24	0.01	35164	170354		*i2	
354812	9.0	05 31 -61	0.01	37049	249301		*	
702316	9.0	05 35 -05	0.00			V1230 Ori	*iCl	Cl: NGC 1977
216476	7.1	05 56 -11	0.05	40120	150958		*	
216908	8.5	06 15 -11	0.02	43345	151269		*	
217036	8.6	06 20 -10	0.01	44258	151371		*	
189105	8.6	06 22 -04	0.01	44678	133186		*	
335155	9.0	06 24 -52	0.01		234486		*	
335172	8.5	06 25 -52	0.03	45634	234497		*	
335182	8.9	06 26 -52	0.06		234507		*	
122593	7.6	06 31 +16	0.05	45951	95765		*i2	
122609	8.5	06 31 +17	0.02	258878	95781	OW Gem	V*	
217355	8.6	06 33 -11	0.04	46564	151640		*	
217462	9.0	06 38 -13	0.02	47437	151732		*	
217467	8.8	06 38 -13	0.06	47496			*i2	

Table 17.1. (Continued).

PPM	m	RA Dec h m deg	pm " yr <sup>-1</sup>	HD	SAO	Other Name	Simbad type stat	Comments
251001	8.5	06 47 -20	0.02	49372	172328		*iCl	Cl: NGC 2287
283329	8.2	06 57 -31	0.02	51824	197403		*	
151884	9.0	07 04 +01	0.01	53391	114885		*	
151890	8.1	07 05 +00	0.01	53451	114891		2/M	
190469	9.0	07 37 -08	0.01	61177	134908		*i2	
703729	8.7	07 39 -00	0.01				?	Sim- IRAS 07369-0025??
714833	9.0	08 02 -13	0.01	66245		DX Pup	SRP	
312671	9.0	08 09 -47	0.00		219512		*	
784704	9.0	08 21 -76	0.03	71793		R Cha	Mira	
254377	8.7	08 22 -22	0.03	70712	175701		*	
220070	8.6	08 24 -11	0.01	70973	154216		*	
31719	8.5	08 31 +54	0.03	71677	26882		*	
220932	8.8	09 00 -17	0.01				?	Sim-
221044	8.8	09 05 -14	0.01	78031	154897		*	
192098	8.9	09 10 -08	0.03	78953	136643		*	
178057	9.0	10 01 -00	0.08	86842	137292		*	
315052	9.0	10 09 -43	0.00	88172	221806		*	
357865	8.6	10 14 -69	0.01				*	CPD-69 1182
288139	8.7	10 48 -31	0.02		201771		*	
288154	8.8	10 49 -30	0.02	93769	201783		*	
193935	8.6	10 55 -06	0.03	94636	94636		*	
194314	8.7	11 17 -07	0.07	98104	138108		*i2	
400161	3.8	11 18 +31	0.73	98230J		ξ UMa	V* *i2	
225140	8.8	11 56 -14	0.02	103696	156998		*	
260462	9.0	12 32 -25	0.10	109107	180874		*	
260514	8.9	12 34 -27	0.05	109393	180916		*	
226058	8.9	12 35 -18	0.01			U Crv	Mira	
360021	8.9	13 18 -67	0.01				*	
291948	8.2	13 53 -35	0.00	120987E	204956		*i2	
779714	8.3	13 54 -60	0.02	121022			*	
780093	9.0	14 37 -61	0.01				?	Sim-
229250	8.2	14 45 -18	0.02	129943	158786		*	
320305	7.7	15 10 -41	0.02	134267	225503		*i2	
293749	8.7	15 21 -36	0.04		206551		*	
294637	8.8	16 05 -31	0.02	144074	207312		*	
322370	7.9	16 54 -41	0.00	152314	227400		V*	Cl: NGC 6231
232686	9.0	17 09 -12	0.02				*	BD-12 4677
80006	8.5	17 11 +33	0.01	155591	65852		*	
296915	9.0	17 52 -34	0.01	320764	209380		*iCl	Cl: NGC 6475
749152	7.8	17 53 -34	0.01	162630			Sp2	
749154	9.0	17 53 -34	0.01				?	Sim- Cl: NGC 6475
749156	8.4	17 53 -34	0.01	162656			Sp2	Cl: NGC 6475
296958	6.5	17 53 -34	0.01	162678	209425		*iCl	Cl: NGC 6475
749167	8.6	17 54 -34	0.01				?	Sim- Cl NGC 6475 region
749169	8.9	17 54 -34	0.01	320859			*iCl	Cl: NGC 6475
296971	7.7	17 54 -34	0.01	162781	209435		*iCl	Cl: NGC 6475
297080	8.2	17 58 -36	0.06	163651	209543		*i2	

Table 17.1. (Continued).

PPM	m	RA Dec h m deg	pm " yr <sup>-1</sup>	HD	SAO	Other Name	Simbad type stat	Comments
297133	8.5	18 01 -30	0.02	164199	209601		*i2	
267782	7.5	18 03 -24	0.01	164816	186207		*iCl	Cl: NGC 6530
267805	8.9	18 04 -24	0.04	164948	186226		*iCl	Cl: NGC 6530
233999	8.6	18 05 -11	0.01	165148	161051		*	
268081	8.6	18 13 -28	0.01	166855	186494		*i2	
325276	9.0	19 37 -46	0.01	184558	184558		*	
764510	8.8	19 44 -41	0.01	186087		TV Sgr	Mira	
83501	8.5	19 45 +35	0.00		68812		*i2	
325713	8.9	20 00 -41	0.02	189119	229972		*	
237205	9.0	20 17 -12	0.01		163421		*i2	
348543	8.9	20 26 -56	0.02		246577		*	
86047	5.2	21 06 +38	5.26	201091	70919	V1803 Cyg	V* *i2	
238481	9.0	21 10 -16	0.01	358906	164193	Z Cap	Mira	
272333	8.9	21 19 -21	0.04	202841	190226		*	
301543	8.6	21 33 -30	0.03	204987	213085		*	
301657	8.9	21 39 -33	0.02	205890	213169		*	
301662	9.0	21 39 -33	0.01		213174		*	
205591	8.8	21 46 -06	0.01	207091	145655		*i2	
205592	8.4	21 46 -06	0.02	207092	145656		*i2	
273214	9.0	21 59 -25	0.10	208850	190801		*	
375228	9.0	22 03 -74	0.00	208833	257994		*	
722964	8.6	22 05 -13	0.05				?	Sim-
722977	8.6	22 07 -13	0.03				?	Sim-
327932	9.0	22 08 -44	0.04		230995		*	
329803	8.7	23 56 -49	0.00	224269	248066	R Phe	Mira	

## Abbreviations used in the tables

Alg	Eclipsing binary of Algol type
Cep	Classical Cepheid variable Star
D/M	Double or multiple star
HPM	High proper-motion Star
IRS	Infra-Red source
Mira	Variable Star of Mira Cet type
PN	Planetary Nebula
Sim-	Object was not present in Simbad
Sp2	Spectroscopic binary
SRP	Semi-regular pulsating Star
V*	Variable Star
*	Star
*i2	Star in double system
*iCl	Star in Cluster
?	No Simbad classification is available

**Table 17.2.** Bright stars from the Catalogue of Positions and Proper Motions (PPM) which are inconsistent with the Tycho Catalogue (20 cases).

PPM	m	RA Dec	pm	HD	SAO	Other	Simbad	Comments
		h m deg	" yr <sup>-1</sup>			Name	type stat	
Stars present in the Tycho Catalogue or error in the PPM Catalogue; 6 cases:								
331230	5.3	01 39 -56	0.34	10360			HPM *i2	8478-1394-2 at 3.8 arcsec
129400	7.3	12 51 +19	0.20	111845	100307		*i2	1452-906-1 at 3.1 arcsec
400211	7.2	15 55 -02	0.11				?	5023-464-1 at 3.6 arcsec
323067	6.3	17 31 -46	0.03		228073		*i2	faint star ?
236293	6.7	19 39 -16	0.07	185344	162853		*i2	6303-2842-1 at 3.3 arcsec
63460	8.2	22 49 +40	0.08	216122	52401		*i2	3218-1759-1 at 3.3 arcsec
PPM gives the photocentre position of two Tycho stars; 14 cases:								
244506	6.4	01 59 -22	0.09	12180	167451	AA Cet	V* *i2	6430-2303-1 at 3.7 arcsec
215592	8.6	05 19 -10	0.06	34750	150333		*i2	5335-1378-1 at 4.5 arcsec
309786	6.2	05 31 -42	0.04	36648	217374		*i2	7604-684-1 at 3.4 arcsec
283868	5.9	07 22 -35	0.07	58038	197907		*i2	7116-2739-1 at 3.4 arcsec
284007	5.4	07 28 -31	0.05	59499J			D/M	7104-3987-1 at 4.2 arcsec
286548	5.1	09 30 -31	0.07	82383J		$\zeta^1$ Ant	D/M	7158-2544-1 at 4.0 arcsec
286658	7.1	09 36 -31	0.04	83231	200538		*i2	7167-716-1 at 3.5 arcsec
259116	5.8	11 32 -29	0.12	100287	179968	17 Crt A	*i2	6663-1171-1 at 3.2 arcsec
400179	7.5	12 45 -75	0.04				*i2	9413-2768-1 at 3.8 arcsec
294448	5.4	15 56 -33	0.09	142629	207144	$\xi^1$ Lup	*i2	7337-1460-1 at 4.2 arcsec
294532	8.1	16 00 -36	0.06	143215	207220		*i2	7341-1239-1 at 3.2 arcsec
294737	5.6	16 09 -32	0.04	144927	207396		*i2	7334-2610-1 at 3.8 arcsec
400246	7.3	18 43 -52	0.00	172494B			*i2	8758-2848-1 at 3.3 arcsec
374833	7.1	20 58 -70	0.04	199005	257869	KZ Pav	Alg *i2	9325-1020-2 at 3.1 arcsec

- 4 stars are (according to SIMBAD/INCA Data Bases) fainter than the formal survey limit, and thus they were not included in the Hipparcos Catalogue. An example is: TYC 736-1489-1 = HD 45047;  $V_T = 6.9$  mag, but  $V(\text{SIMBAD}) = 7.5$  mag;
- 30 stars, a little brighter than the limit of the survey, were not, for various reasons, selected in the Hipparcos Input Catalogue. An example is TYC 1472-1427-1 = HD 124953;  $V_T = 6.0$  mag;  $V(\text{SIMBAD}) = 6.0$  mag;
- 1 false star (with appropriate flags, including astrometric quality,  $Q = 9$ ) was found at 26 arcsec from a very bright star and at the exact location of a much fainter Tycho Input Catalogue entry. This object is TYC 6842-1291-1;  $V_T = 6.4$  mag.

In a second step, stars in the range 7.0 to 8.0 mag were also considered, which are neither in the Hipparcos Catalogue nor in the HD Catalogue. As HD is expected to be complete at least to 8.0 mag, this criterion was used to look for potentially false stars in the Tycho Catalogue for this magnitude range. There are 76 such entries in the Tycho Catalogue:

- 42 had a PPM or other identification. Their magnitude in SIMBAD is compatible with  $V_T$ : thus there is confidence that they are real stars. The fact that the HD

number is missing can be generally explained by a multiple system or by a failed cross-identification in case of PPM/SIMBAD discrepancy;

- 34 remaining stars were searched in the Guide Star Catalog and on the SIMBAD and ALADIN sky images:
  - 9 have a faint Guide Star Catalog magnitude (in the range 11–12 mag) while  $V_T \simeq 8 - 9$  mag. They have an astrometric quality  $Q = 9$ ; they are most probably false stars, generally generated by transits from a nearby bright star. ALADIN confirms their faint Guide Star Catalog magnitude;
  - 2 are typical wide companions, real components of double systems, but not recorded in the HD Catalogue: TYC 5961–3346–1 and 8317–1714–1. For the first object, located in the cluster NGC 2287, one can see close by on the digitized sky image two stars of magnitude  $\simeq 10.0$  mag not catalogued in the Guide Star Catalog (because of overlapping spikes) and also missed by Tycho. These stars were probably already beyond the limits of the Tycho serendipity mode;
  - a problem occurred with a double system, where Tycho contains:
 

6510-569-1	$V_T = 7.5$ mag	CCDM = A	quality = 9
6510-569-2		CCDM = B	HIP-only star
6510-2299-1	$V_T = 7.6$ mag		quality = 9

at a place where there is actually, on the sky, a double system with a bright star ( $V = 7.5$  mag) and a fainter one ( $V = 11.2$  mag; the Catalogue of Components of Double and Multiple Stars (CCDM) = B star). Tycho reduction did not perform well here: if the quality flag is neglected two bright stars are found, while only one is actually there. If the quality flag is taken into account, no bright star remains;
  - the remaining 20 entries are confirmed stars, not recorded in the HD Catalogue for various reasons.

In conclusion, bright Tycho entries, provided they are flagged with an astrometric quality better than 9, proved to be of very high reliability.

---

### 17.3. Completeness of the Tycho Catalogue at the Faint End

---

A histogram of all stars in the Tycho Catalogue as a function of  $V_T$  magnitude is given in Figure 17.1. For 1 per cent of the stars another magnitude was used because no  $V_T$  was available. The slope indicates that the completeness ratio stays constant until  $V_T = 10.0 - 10.5$  mag. From the comparison with bright PPM stars we found a completeness ratio of 99.9 per cent at  $V_T = 9$  mag. After  $V_T = 10$  mag, the number of HIP-only stars begins to rise more steeply and we might expect a decline in the completeness ratio to begin there. Extrapolating the distribution in Figure 17.1, the completeness ratio is estimated to at least 90 per cent at  $V_T = 10.5$  mag, 65 per cent at 11 mag and 10 per cent at 11.5 mag. In order to avoid a bias in  $B_T - V_T$  colour index (see Figure 16.20), it is recommended to select stars on the basis of the  $T$  magnitude, which may be derived with the approximate formula:  $T = (B_T + V_T)/2$ . The completeness ratios are then 90 per cent at  $T = 10.8$  mag, 65 per cent at  $T = 11.5$  mag and 10 per cent at  $T = 11.8$  mag.

**Table 17.3.** The quality distribution of ‘new Tycho Catalogue entries’ (see text).

Quality	Number
1	8
2	41
3	349
4	627
5	14
6	12
7	112
8	161

The Tycho Catalogue includes, on the distribution tail, stars as faint as  $V = 12.0$  mag. The analysis of a statistical sample (with  $V_T$  in the range 11.0–12.1 mag) confirmed that these are appropriate entries in the Tycho Catalogue. There are a few thousand stars in the Tycho Catalogue fainter than 12.0 mag, but these magnitudes are quite uncertain, see Table 16.3.

### Additional Tycho Catalogue Entries

From the whole Tycho Catalogue 1584 entries carry a new Guide Star Catalog number, not already present in the Tycho Input Catalogue; they are mainly Tycho serendipity entries and wide companions; see Chapter 5. The Tycho Input Catalogue already contained additional stars with respect to the Guide Star Catalog Version 1.0; see Chapter 3.

Out of these 1584 entries, 260 are ‘HIP-only stars’ in the final Tycho Catalogue and are not considered in the following. Thus there are 1324 ‘new Tycho Catalogue entries’ in terms of the Guide Star Catalog/Tycho Input Catalogue identifications.

The quality distribution for these entries is given in Table 17.3.

A random sample of 30 stars was also analyzed:

- 13 (43 per cent) are rather bright stars for which the position has been substantially revised, so that the former Guide Star Catalog number could not be kept, at least from our automatic procedure. Some high proper motion stars may also fall into this category. An example (one of the brightest) is TYC 6445–990–1, which is the new number of GSC 6445 986 ( $V_T = 3.97$  mag). Ideally the original Guide Star Catalog number could have been kept, but this would have meant a careful assessment of each entry which would have delayed the catalogue production;
- 14 (47 per cent) are components of double systems for which the Guide Star Catalog gives the position of the photocentre, while the Tycho Catalogue gives the position of (at least one of) the individual components. An example is: TYC 6085–1618–1 and –1619–1 (GSC 6085 94);
- 3 (10 per cent) are ‘serendipity’ or ‘wide companion’ entries. It has already been shown by Egret *et al.* (1992) why the Guide Star Catalog missed such entries (confusion with spikes or halos of bright stars, etc.). An example is TYC 8317–1714–1, which is new. The companion star 8317–1709 was in the Guide Star Catalog, from the INCA Data Base.

---

#### 17.4. Cross References

---

The Tycho Catalogue gives cross-identifications to the Hipparcos Catalogue (HIP), the Catalogue of Positions and Proper Motions (PPM), the HD Catalogue, the DM Catalogues (partly) and it flags stars from the General Catalogue of Variable Stars (GCVS) and the New Catalogue of Suspected Variable Stars (NSV). Except for the Hipparcos Catalogue and the PPM Catalogue, these catalogues are of poor astrometric quality. For a catalogue the size of the Tycho Catalogue, it is therefore not always possible to provide fully correct and consistent identifications. Even for the Hipparcos Catalogue and the PPM Catalogue there were many non-trivial cases. The Hipparcos Catalogue also provides (in the machine readable version) references to the HD and DM Catalogues, and the critical user of the Tycho Catalogue may take advantage of this in order to detect possible mis-identifications for Hipparcos stars in the Tycho Catalogue. It is also advisable to check the notes of the Hipparcos Catalogue. These notes may give corrections to the identifications of some stars in the Hipparcos Input Catalogue, and such stars are likely also to have a wrong identification or a wrong flag in the Tycho Catalogue.

An example of a partly mis-identified star is GQ Ori (TYC 734-627-1). This Cepheid is the southern component of a visual double with separation 31 arcsec and both components around 9 mag. In the discovery paper (Kukarkin & Kurochkin 1947), it was erroneously identified with HD 42532 (TYC 734-1163-1) situated 5 arcmin away. HD 42532 was therefore included in the Hipparcos Catalogue (HIP 29386), flagged as known variable in the Tycho Catalogue and included in the Tycho Epoch Photometry Annex A. The true GQ Ori is in Annex B, it is not flagged as known variable and was not included in the Hipparcos Catalogue. To make things worse, the HD numbers of TYC 734-627-1 and its companion (TYC 734-2337-1) have been confused in the Tycho Catalogue, as they are in the Catalogue of Positions and Proper Motions (PPM). They should have been HD 253058 for TYC 734-627-1 and HD 253057 for the companion.

---

#### 17.5. Concluding Remarks

---

The analysis of the stellar contents of the Tycho Catalogue, summarized in this chapter, shows that the Tycho Catalogue presents unique characteristics making it the first reference survey of the one million brightest stars in the sky. The catalogue will, for this reason, be a very important tool for supporting cross-identification with other catalogues, surveys or wide-field images obtained from ground- or space-based telescopes, in the optical as well as in other wavelength ranges.

D. Egret, C. Fabricius

## 18. VERIFICATION OF THE TYCHO CATALOGUE: ASTROMETRY

*The Tycho astrometry of stars is verified through comparisons with the Hipparcos Catalogue and the Catalogue of Positions and Proper Motions (PPM). Systematic errors are negligible, of the order 1 mas and 1 mas/yr. The external standard errors, on the other hand, exceed the formal standard errors given in the Tycho Catalogue for stars fainter than  $V_T \simeq 9.5$  mag; at  $V_T = 10.5$  mag by a factor 1.5. Observations of solar system objects are compared with Hipparcos and ground-based results in Chapter 15.*

---

### 18.1. Astrometric Standard Errors

---

Internal and external standard errors for the Tycho Catalogue are discussed in this section. There are two kinds of internal standard errors: the ‘internal formal’ standard error which is derived from the diagonal elements of the covariance matrix of the least-squares solution, and the ‘internal corrected’ standard error which is obtained from the internal formal standard error by multiplication with the unit-weight error, derived from the residuals, see Section 11.1. Finally, the ‘external’ standard error can only be estimated by comparison with other catalogues of compatible or superior quality.

In this terminology all standard errors given for photometry and astrometry of the individual stars in the Hipparcos and Tycho Catalogues are internal corrected standard errors, except for the astrometric values in the Hipparcos Catalogue where internal formal standard errors are given. The background for the choice of internal corrected standard errors for the astrometric quantities in the Tycho Catalogue shall be given.

The internal formal standard errors for a given set of accepted observations depend only on the way the weighting of individual observation equations has been done, see Section 7.1. The weights of observations in the Tycho reduction were inversely proportional to the square of the expected standard error of the transit time  $\sigma_u$  (also called the *a priori* error) in Equation 7.6. The latter comprised the photon-statistical error  $\sigma_\tau$ , which was calculated as a function of only the estimated amplitude and background for a given transit, based on an advanced theory of Maximum Likelihood (ML) estimator for the astrometric location problem by Yoshizawa *et al.* (1985). It had been proven in the same paper by numerical simulations, that the non-linear ML technique and the linear digital filtering technique, which was in fact used in the Tycho reduction algorithms, had very

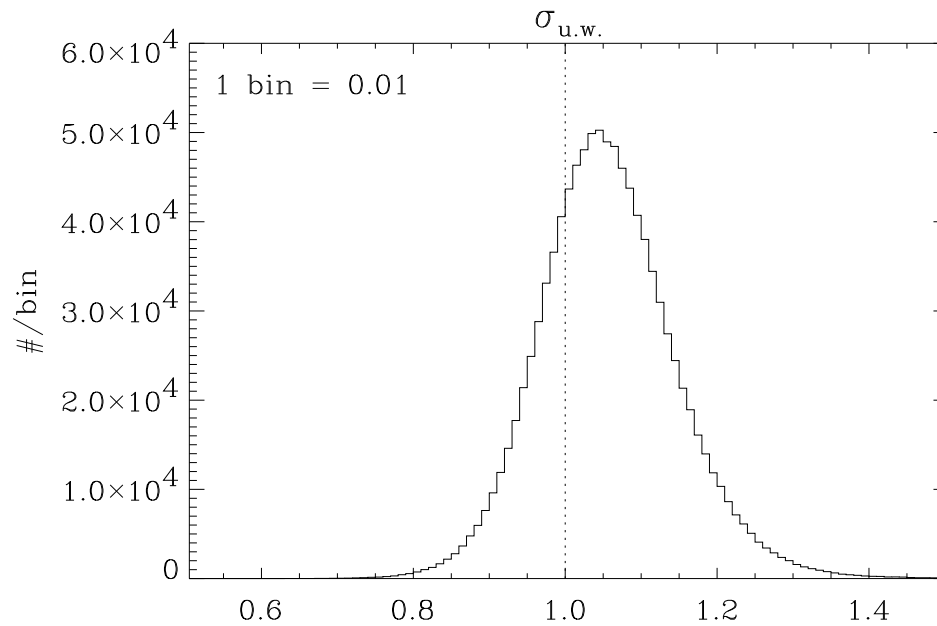


**Figure 18.1.** Distribution of the unit-weight error for the stars in the Tycho Catalogue.

similar performances at magnitudes up to 10. It should be noted that the Tycho filtering (see Chapter 2) was in fact non-linear only in the presence of spikes or if bright stars disturbed each other. Otherwise it was linear and thus ensured the quick processing.

At fainter magnitudes than 10, however, the difference between the two methods could be significant, but the results of the simulations were rather uncertain. For the lack of something better, the strictly theoretical expression of the Maximum Likelihood estimator was used as *a priori* errors. It was checked several times in the course of the data reduction, that the error model provided a quite reliable result for stars brighter than 10 mag, while for the fainter majority of stars the observed scatter of transit times typically exceeded the *a priori* error. This can be seen in Figure 18.1, where the unit-weight error distribution is shown for the stars in the Tycho Catalogue. The distribution is centered at 1.05, meaning that the formal error was typically 5 per cent smaller than the observed scatter. If such formal errors were used as standard errors in the Tycho Catalogue, as was done in the Hipparcos Catalogue, then the final precision of the astrometric parameters would have been systematically overestimated by merely 5 per cent on average, but it could be larger than 20 per cent for many stars (Figure 18.1).

There are several reasons for the deviation of the unit-weight error,  $\sigma_{u.w.}$ , from unity. First, it is expected on theoretical grounds that the Maximum Likelihood estimator theory does not apply well to extremely faint signals, which correspond to about magnitude 11 for Tycho. Even if it did, the linear filtering in detection could have performed in a different way at faint magnitudes, yielding a slightly worse estimation. Second, there were some features of the Tycho astrometric observations, which could not be properly accounted for by a simple and practical error model. The disturbing influence of unrecorded parasitic signals was perhaps especially strong on faint target stars. Besides, this influence could be different for different stars, depending on the neighbourhood, possible duplicity, etc. This was a good reason to choose the correction of the standard error by  $\sigma_{u.w.}$  for each star individually, as stated in Section 11.1, rather than trying

to find an empirical error model, fitting the real uncertainties of observations at faint magnitudes.

The unit-weight error can be calculated for every star in the Tycho Catalogue, given a goodness-of-fit ( $F2$ ) value, by means of the equation referred to in Volume 1, Section 2.2 (Field T30). A few stars have no  $F2$  value and are excluded from this discussion. The bias of the  $\sigma_{u.w.}$  distribution is correlated with various quality measures in the Tycho Catalogue. For instance, the mean  $\sigma_{u.w.}$  for non-recommended astrometric stars (Field T10 = 'X') is 1.11, but it is as small as 1.04 for the recommended reference stars. There is also a systematic variation of this statistics with  $V_T$  magnitude, see Figure 18.2. The unit-weight error appears to depend on the number of astrometric observations,  $N_{astrom}$ , for stars brighter than  $V_T = 10.0$  mag, but not for fainter stars. The reason for the dependence might be that a relatively smaller number of observations for a bright star will remain when a larger than average number of observations are rejected due to parasitic transits, e.g. from the other component in a double star. It is noted that there are 84 000 stars in the Tycho Catalogue with  $N_{astrom} < 70$ , and about 16 000 of them are brighter than 10.0 mag. A representative histogram of  $N_{astrom}$  is given in Figure 7.6(d).

Since the unit-weight error is generally not larger than 1.10, it is concluded that the internal model of statistical weights was satisfactory. It will, however, appear from the following analysis of external errors of the Tycho Catalogue, that although the correction has in general increased the standard errors in the catalogue, and for faint stars particularly so, it was not sufficient to provide a quite correct measure of astrometric accuracy, at faint magnitudes.

The ratio of external standard errors to internal corrected standard errors is satisfactory, about 1.1 for the five astrometric parameters for stars with  $V_T < 10$  mag. It is about 1.5 at the median magnitude  $V_T = 10.5$  mag for positions (Figure 18.4), for proper motions (Figures 18.8(d) and 18.8(e)), and for parallaxes (Figure 18.9). The ratio increases to 1.8 at  $V_T = 11.0$  mag, and the main reason is probably the rejection of outliers (Chapter 7) which is quite significant at faint magnitudes.

---

## 18.2. Comparison with the Main Hipparcos Catalogue

---

The Hipparcos Catalogue has been used for deriving calibration parameters for the Tycho Catalogue and for defining the system of Tycho positions, parallaxes and proper motions. This section and Section 18.3 show to which extent the Hipparcos and Tycho systems agree and to which extent the error estimates in the Tycho Catalogue are realistic. In Sections 18.3–18.5 properties of positions, proper motions and parallaxes will be treated separately.

Figure 18.3 shows sky plots of the median residuals, 'Hipparcos–Tycho', in cells of  $15^\circ \times 15^\circ$ . Residuals were computed at the Tycho mean observational epoch for the 68 103 recommended reference stars in common and brighter than  $V_T = 9$  mag. Each cell therefore represents about 370 stars. The values are close to zero, as expected, with a cell-to-cell scatter of 0.3 mas for positional coordinates, 0.4 mas for parallax and 0.7 and 0.4 mas/yr for the two proper motion components. With 370 stars in each cell and median standard errors of 5–7 mas for the Tycho Catalogue stars a cell-to-cell scatter of 0.3 mas is expected. Except for the proper motion in right ascension, this is very close

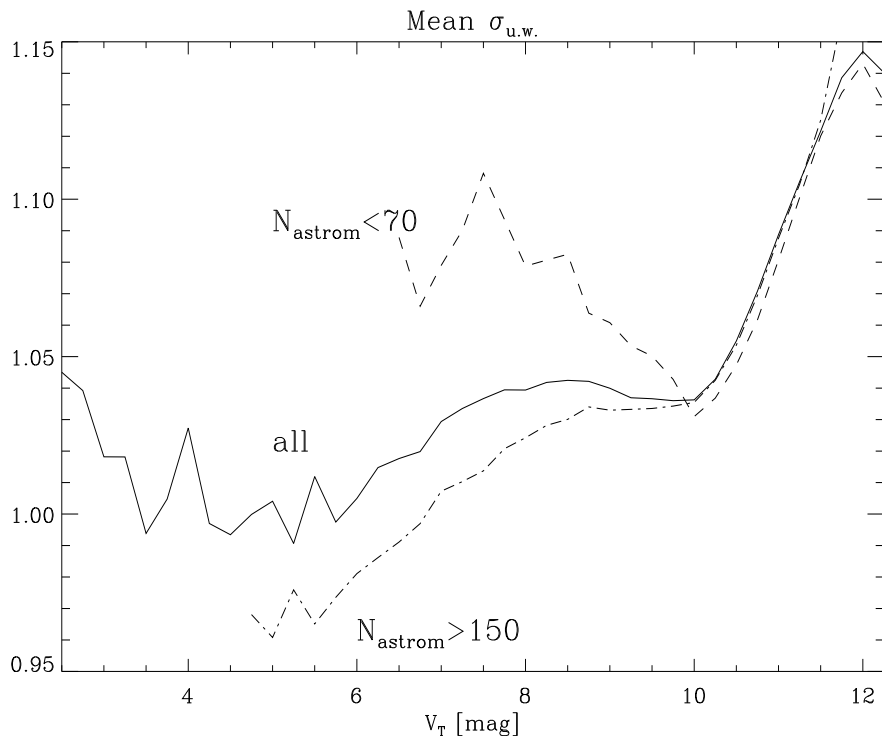


**Figure 18.2.** Mean unit-weight error,  $\sigma_{u.w.}$ , versus  $V_T$  magnitude for all stars in the Tycho Catalogue, and for stars with  $N_{astrom}$  greater than 150 and smaller than 70, as indicated in the plot.

to the actual values. We may therefore conclude that the Tycho system is practically identical to the Hipparcos system on a  $15^\circ$  scale.

In order to estimate the reliability of the internal standard errors given in the Tycho Catalogue, the residuals ‘Hipparcos–Tycho’ discussed above were also measured in units of the internal standard error of ‘Hipparcos–Tycho’. Ideally, the distribution of this quantity should have a median of 0 and the 16th and 84th percentiles at  $-1$  and  $+1$ , respectively. Figure 18.4 shows half the difference between the 84th and 16th percentiles as a function of  $V_T$ , the sample of stars having been extended also to include the fainter stars. This half difference can be understood as a robust estimate of the ratio between the external and the internal errors. Any deviation from the expected value of  $+1$  can be attributed to the Tycho Catalogue because the errors of the Hipparcos Catalogue are negligible in this comparison, except for the brightest stars.

For the positional coordinates, the ratio between the external error and the internal standard error lies at 1.05 for stars brighter than  $V_T = 9.25$  mag; it then rises rapidly for fainter stars, reaching 1.5 at  $V_T = 10.5$  mag (the median magnitude for Tycho) and 1.8 at  $V_T = 11$  mag. For parallax and proper motion the ratio stays close to 1.0 for all magnitudes. There is, however, strong evidence that the external errors in parallax and proper motion for non-Hipparcos stars follow if not the same then at least a similar pattern as the right ascension and declination. The difference between Hipparcos and non-Hipparcos stars arises because Hipparcos parallaxes and proper motions were used as starting values in each iteration of the astrometric reductions as explained in Section 11.1. The properties of non-Hipparcos stars are discussed further in Sections 18.3 and 18.6.

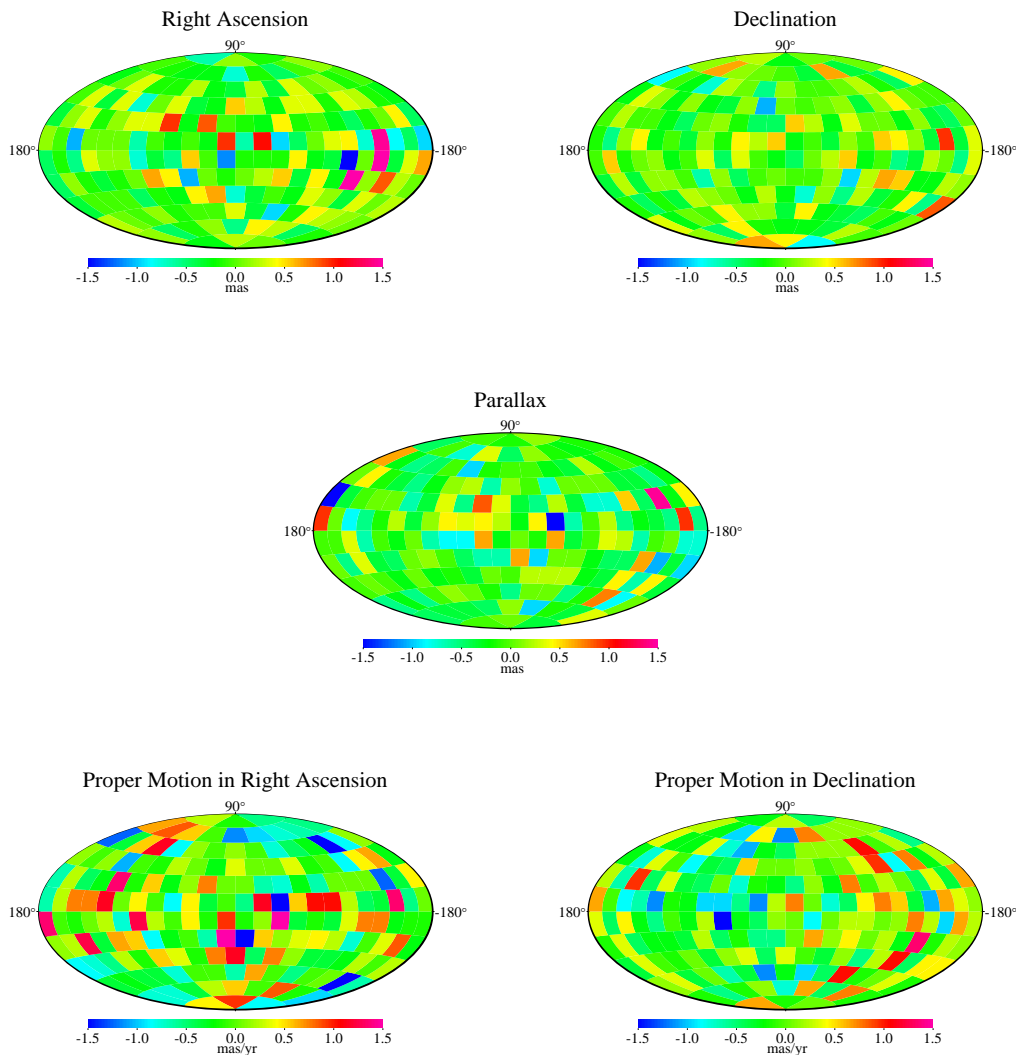


**Figure 18.3.** Median differences, 'Hipparcos–Tycho', in equatorial coordinates for recommended astrometric reference stars brighter than  $V_T = 9$  mag. The cell size is  $15^\circ \times 15^\circ$ .

The cross-identification between the Hipparcos and Tycho Catalogues was generally simple with more than 110 000 stars identified closer than 100 mas from the Hipparcos position. A general identification limit of 1 arcsec was adopted, but in a few cases identity was accepted at distances up to 1.8 arcsec. In such cases either Tycho or Hipparcos must be in error, or a photocentre of a double star system was cross-identified with a resolved component. Double stars are often resolved in the Hipparcos Catalogue but not in the Tycho Catalogue. Figure 18.5 shows the tail of the distribution of distances between the Hipparcos and Tycho positions for cross-identified catalogue entries of quality  $Q = 1 - 8$  stars (see Table 7.1). Double stars are only included in the plot if resolved in both catalogues. This means that 97 665 single stars and 13 072 components of double stars are included. The tails beyond 200 mas, shown in the figure, contain only 95 (0.1 per cent) and 253 (1.9 per cent) stars, respectively. The double star distribution is somewhat broader than for single stars as could be expected. More significant, though very small, is the peak with 40 stars at 1.25 arcsec. Errors in the Tycho treatment of double stars

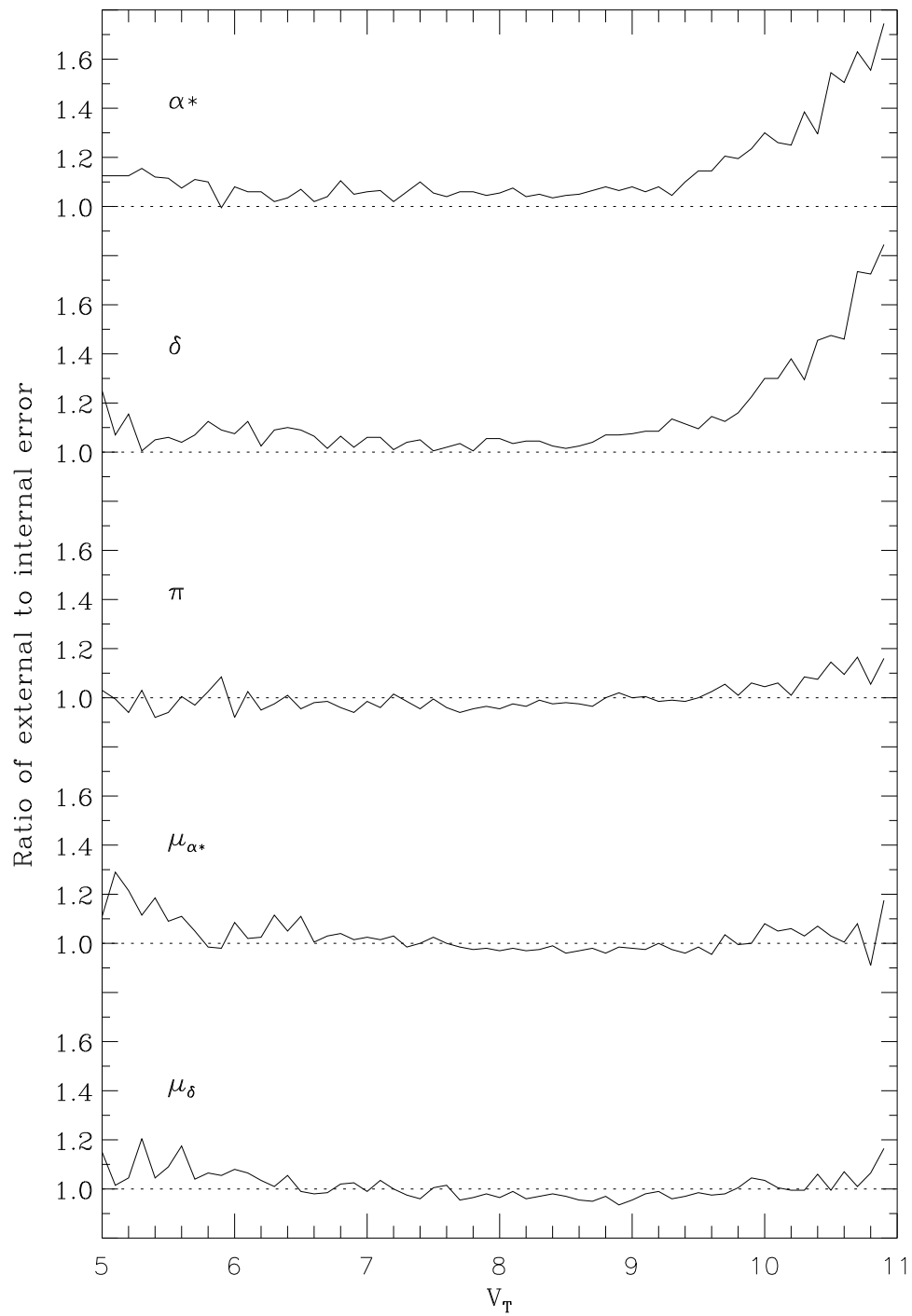


**Figure 18.4.** The ratio of external error to internal standard error for the Tycho Catalogue derived from a comparison with Hipparcos values. The absence of a rise for parallax and proper motion for stars fainter than 9 mag only applies to Hipparcos stars, as explained in the text.

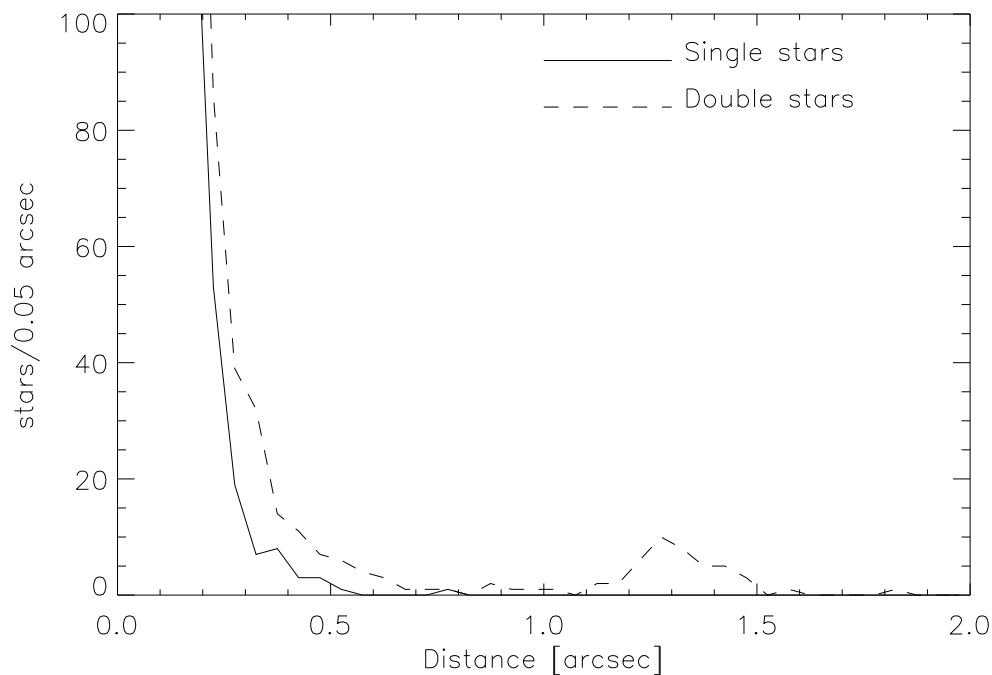


**Figure 18.5.** Tail of the distribution of distances between Hipparcos and Tycho positions for cross-identified single stars and resolved components. See the text for further explanation.

can certainly not be excluded, but the prime suspect is in fact Hipparcos. The grid used in the main mission has a period of 1.21 arcsec. This means that the abscissa derived in a particular transit is only known modulo 1.21 arcsec. A subtle combination of input catalogue error, dominating scan directions and configuration of the double or multiple system, can result in such grid-step errors finding their way to the final catalogue. In the Hipparcos Catalogue, the quality of the solution is normally quite low in these cases, with standard errors in the range 4–120 mas for 78 per cent of the stars.

In the Hipparcos main mission, the instantaneous field of view has a diameter of 38 arcsec. All stars within this field contribute to the signal and will ideally be resolved in the double star treatment. We therefore do not expect to find Tycho stars near Hipparcos stars, unless the Tycho star is also a Hipparcos star. The stars that we do find lead us to suspect errors either in the Tycho Catalogue or in the Hipparcos Catalogue. Figure 18.6 shows the distribution of distances between Tycho stars not cross-identified in the Hipparcos Catalogue and Hipparcos stars not cross-identified in the Tycho Catalogue. The question is, if some of these pairs are artefacts caused by large errors in Hipparcos or Tycho. There are 64 pairs involving 59 quality  $Q = 1-8$  Tycho stars and 58 pairs involving quality  $Q = 9$  stars. Also plotted are the positions corresponding to grid-step errors in Hipparcos and side lobes in Tycho.

There are no pairs with small separations simply because such pairs are cross-identified. In Figure 18.6(a), representing the good Tycho positions, there is a strong correlation between the distribution of pairs and the likely error-induced distances for distances up

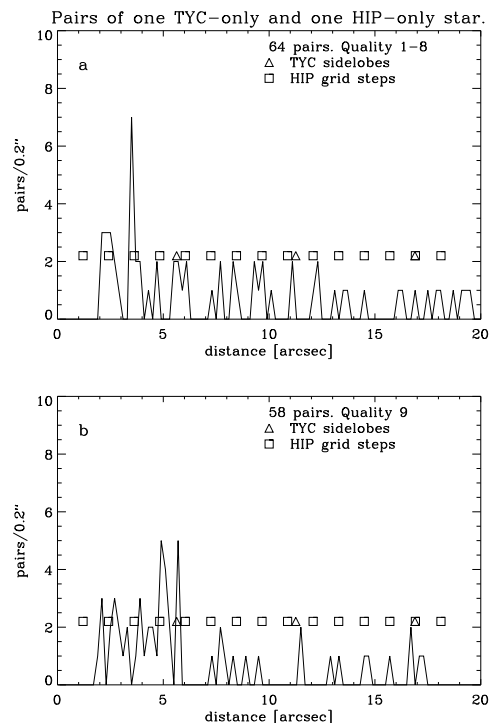


**Figure 18.6.** Distribution of the distances between entries in the Tycho and Hipparcos Catalogues with no cross-identification, called respectively TYC-only and HIP-only stars. The distances introduced by typical error sources are marked. (a) pairs with quality  $Q = 1 - 8$ ; (b) pairs with  $Q = 9$ .

to 6–7 arcsec, whereas the correlation is rather weak at higher distances. These quality  $Q = 1-8$  stars all belong to double or multiple systems, a fact leaving open the possibility that both Tycho and Hipparcos are correct albeit incomplete, but also the possibility that errors have indeed been introduced. In Figure 18.6(b), representing the low quality Tycho stars, the correlation is weak at all distances. The quality  $Q = 9$  stars are, by definition, of low quality so these 58 pairs are probably dominated by errors in Tycho.

---

### 18.3. Comparison with the PPM Catalogue

---

A comparison with positions in the Catalogue of Positions and Proper Motions (PPM) (Röser & Bastian 1991; Bastian *et al.* 1993) is of limited value for the verification of the Tycho Catalogue. For the proper motions, however, a comparison is useful because the PPM proper motions have standard errors of only 4 mas/yr, compared to typically 30 mas/yr for the Tycho Catalogue.

An investigation of the PPM (Fabricius 1993), based on recent ground-based observations, has shown a magnitude equation in PPM and the comparison was therefore carried out for bright and faint stars separately. Figure 18.7 shows a comparison, ‘TYC–PPM’, for the four available astrometric parameters. There are indeed some striking differences between the stars brighter than  $B_T = 10$  mag and the fainter stars. In right ascension, differences are prominent for faint stars around declination  $20^\circ$  at right ascension 0–10 hours. In declination there are interesting features for faint stars around declination

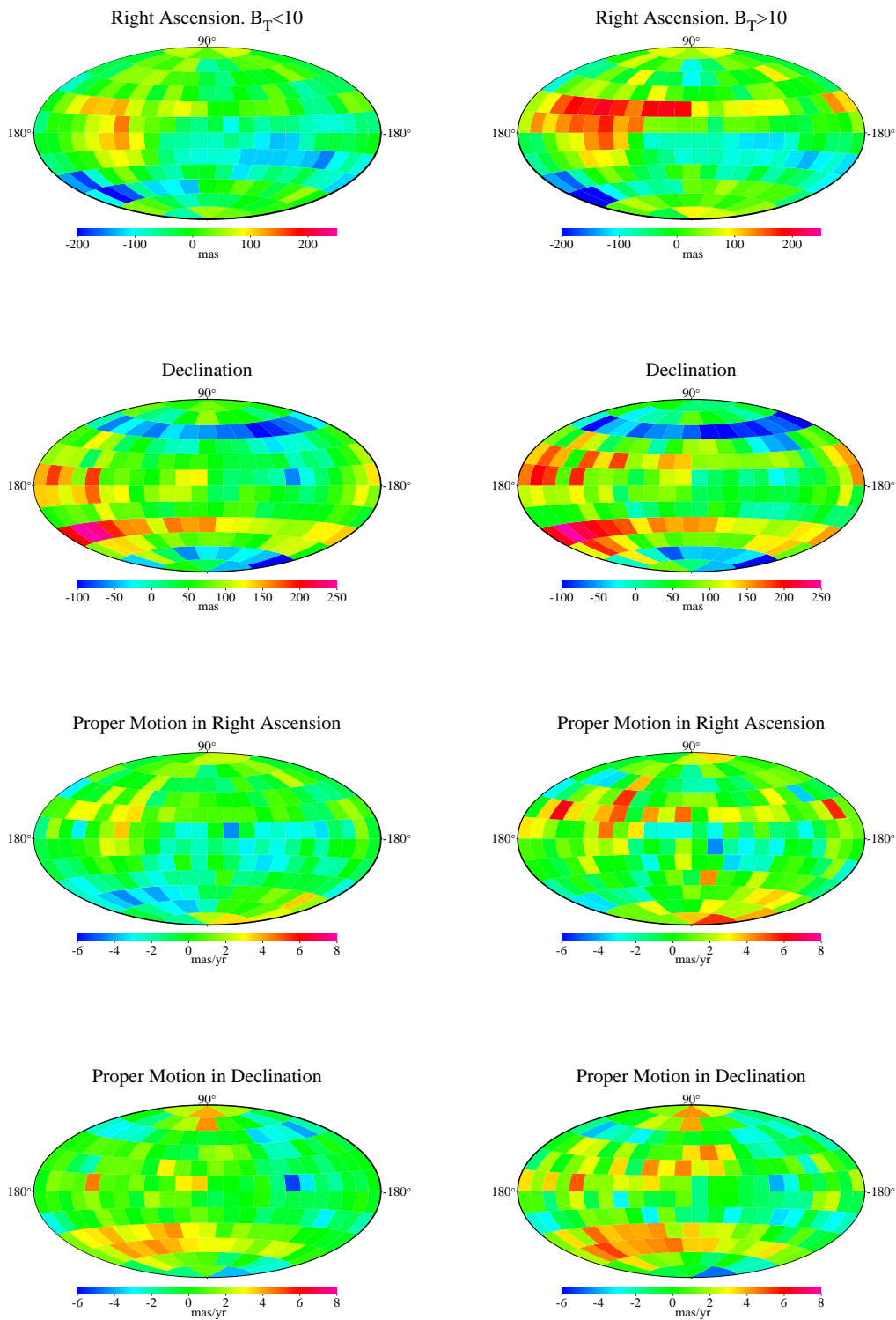


**Figure 18.7.** ‘TYC–PPM’ in equatorial coordinates, where TYC is the Tycho Catalogue and PPM is the Catalogue of Positions and Proper Motions. The four figures to the left show the median difference for the 134 760 stars brighter than  $B_T = 10$  mag and the four figures to the right show the median difference for the 276 737 stars fainter than  $B_T = 10$  mag. The cell size is  $15^\circ \times 15^\circ$ .

20° and 50°. In position the cell-to-cell scatter is around 70 mas, giving the order of magnitude of the systematic differences between PPM and ICRS. For proper motion the cell-to-cell scatter is around 2 mas/yr and values rarely exceed  $\pm 5$  mas/yr. This is the same order as the internal standard error of the PPM Catalogue, and well below the internal standard error of the Tycho Catalogue proper motions for stars fainter than  $V_T \simeq 9$  mag. It is therefore meaningful to make a comparison between the two catalogues for the proper motions of faint stars, without applying systematic corrections.

Figure 18.8 shows a comparison between proper motions in the PPM Catalogue and in the Tycho Catalogue. Figure 18.8(a) shows the median standard error in the Tycho Catalogue as a function of  $V_T$ . No difference can be seen between Hipparcos and non-Hipparcos stars. Figure 18.8(b) shows the much smaller standard error in the PPM Catalogue. Hipparcos stars have generally smaller errors than other stars probably because many Hipparcos stars, e.g. the IRS, are among the high precision subset of the PPM Catalogue. Figure 18.8(c) combines the internal errors of Tycho and Hipparcos, giving the internal standard error of ‘TYC–PPM’. The distribution of differences in proper motion, ‘TYC–PPM’, measured in units of the internal error, has its median around 0 and the 16th and 84th percentiles around  $-1$  and  $+1$ . The half difference between these two percentiles can be interpreted as the ratio between external and internal error. It is shown in Figures 18.8(d) and 18.8(e) for the two components of proper motion. For stars brighter than 9 mag the values are rather high because the systematic errors of the PPM Catalogue have been ignored, but these stars are not our main concern. At fainter than 9.5 mag the ratio lies at 1.05 for Hipparcos stars, but considerably higher for other stars with 1.25 as the minimum, reaching 1.5 at  $V_T = 10.5$  mag and 1.8 at  $V_T = 11$  mag. The latter two values are exactly the same as found for Tycho positions in the preceding section in the comparison with Hipparcos.

It is concluded that internal standard errors of Tycho proper motions need the same correctional factor as for positions. For brighter stars ( $V_T \simeq 7 - 9.5$  mag) Figure 18.4 shows that the ratio of external to internal error is in fact somewhat less than 1.0 for Hipparcos stars. If we now normalize Figures 18.8(d) and 18.8(e) to give the same ratios for Hipparcos stars as in Figure 18.4, the curves for non-Hipparcos stars will, of course, still lie 10 per cent higher than for Hipparcos stars, but now at a level of 1.05–1.1, which is again comparable to what was found for Tycho positions.

---

#### 18.4. Tycho Positions

---

It was demonstrated in Section 18.2, through comparisons with the Hipparcos Catalogue, that the Tycho and Hipparcos systems are practically identical. It was also shown that the standard errors in the Tycho Catalogue are too small for stars fainter than  $V_T \simeq 9.5$  mag. At  $V_T = 10.5$  mag a factor of 1.5 should be applied and at  $V_T = 11$  mag the factor is 1.8.

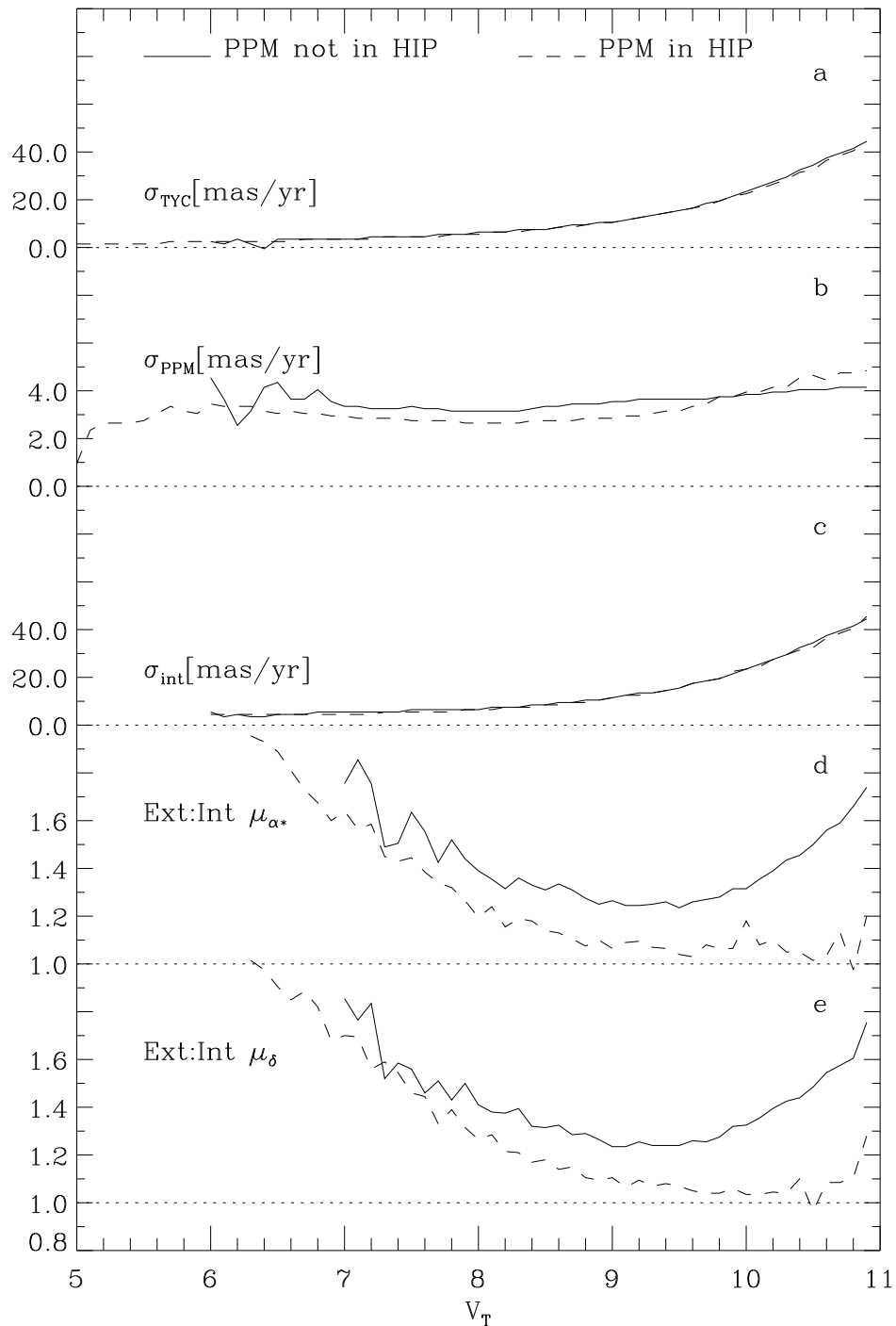


**Figure 18.8.** Median internal standard error of (a) the Tycho Catalogue proper motions, (b) of proper motions from the Catalogue of Positions and Proper Motions (PPM), and (c) of their difference. The ratio between external and internal errors of the Tycho Catalogue proper motions (d and e), see text. The high ratios for bright stars are only due to the rather simple method used for comparison, as explained in the text.

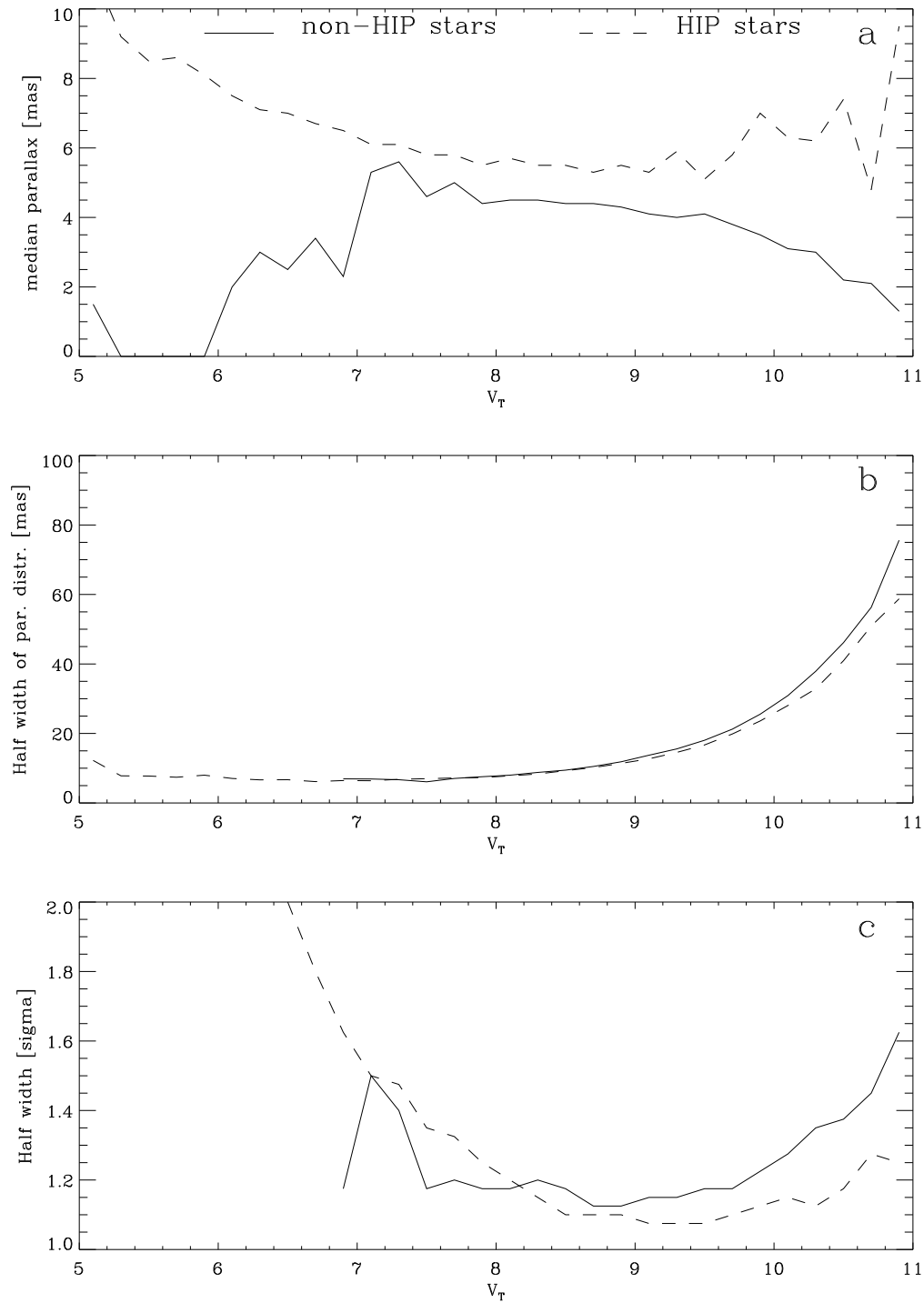


**Figure 18.9.** The median Tycho parallax for Hipparcos and non-Hipparcos stars is shown in (a). The half width of the parallax distribution, derived from the 16th and 84th percentiles, is shown in units of mas in (b) and in units of the internal standard error in (c). When the parallax is much smaller than the error, the curves in (c) represent the ratio between external and internal error. This assumption does not hold for the bright stars resulting in the steep rise. See the text for further explanation.

---

### 18.5. Tycho Proper Motions

---

It was shown in Section 18.2 that the Tycho proper motions agree systematically with the Hipparcos proper motion. The proper motions were also addressed in Section 18.3 in a comparison with the Catalogue of Positions and Proper Motions (PPM). The standard errors of Tycho proper motions were shown to need the same correction as for positions, i.e. no correction for stars brighter than  $V_T \simeq 9.5$  mag, at  $V_T = 10.5$  mag a factor of 1.5 should be applied and at  $V_T = 11$  mag the factor is 1.8.

---

### 18.6. Tycho Parallaxes

---

In the Tycho Catalogue there are 1132 non-Hipparcos stars with relative parallax errors less than 20 per cent, but in general the parallaxes are of low significance for individual stars. For larger samples, the Tycho parallaxes can be of value. There are, for example, more than 38 000 non-Hipparcos stars in the Tycho Catalogue with standard errors below 10 mas.

In Section 18.2 it was shown that the Tycho parallaxes agree with the Hipparcos parallaxes on a global scale. It was shown in Sections 18.2 and 18.3 that the internal standard errors for position and proper motion of non-Hipparcos stars in Tycho have been underestimated for stars fainter than  $V_T = 9$  mag. In order to test if the same is true for parallaxes we note that for faint stars, the standard error is generally much larger than the parallax. We can therefore assume that the true parallax is zero and get a conservative estimate of the external error. Figure 18.9 shows the median parallax (Figure 18.9(a)) which is much smaller than the half width of the distribution of parallaxes (Figure 18.9(b)) for the faint stars. The half width has been computed as the half difference between the 16th and 84th percentiles. Figure 18.9(c) shows the half width of the distribution of the parallax divided by the internal standard error. At the bright end the curve rises because the assumption of zero true parallax does not hold. At the faint end we find a ratio of external to internal error of 1.4 at  $V_T = 10.5$  mag and 1.7 at  $V_T = 11$  mag. These values are slightly smaller than what was found for position and proper motion.

C. Fabricius, V.V. Makarov



## 19. VERIFICATION OF THE TYCHO CATALOGUE: PHOTOMETRY

*This chapter discusses the photometric contents of the Tycho Catalogue and its epoch photometry annex. The systematic differences between the Tycho mean and ground-based magnitudes for 17 683 standard stars are well below 0.010 mag in the range  $V_T \simeq 4.25$  to 11.0 mag, and only few stars in this sample were found to be variable or at least suspected to be so in the course of analysis of the satellite data. The method and outcome of a Tycho variability search is described in detail. Finally, the Tycho magnitudes of double stars were compared with recent ground-based observations: pairs of equal brightness reveal too bright magnitudes in the Tycho Catalogue by about 0.05 mag and this bias increases to about 0.1 mag for other pairs.*

---

### 19.1. Tycho Mean Magnitudes

---

The majority of mean magnitudes in the Tycho Catalogue are flagged by ‘M’ or ‘N’ in Field T36 (Section 2.2, Volume 1) and are called ‘fully calibrated’ magnitudes. They were constructed using two different methods, namely median magnitudes for bright stars, de-censored magnitudes for faint stars, and using data from two different processing schemes, i.e. main processing and reprocessing. Photometrically, the major difference between main and reprocessing is the usage of different single-slit response functions (see Chapter 8) which is of importance only for very bright stars. The selection of the magnitudes is described in Section 11.5. A few thousand mean magnitudes in the catalogue, flagged by ‘D’ or ‘T’ in Field T36, have a different origin.

In the following, the fully calibrated Tycho mean magnitudes are checked for systematic differences between the four possible origins of the magnitudes. For this purpose, the Tycho magnitudes were compared with  $B_T$  and  $V_T$  magnitudes derived from ground-based observations for 17 683 stars, which is exactly the same standard star sample as used in Chapter 8. Figure 19.1 shows the difference for both Tycho channels between mean observed magnitudes in the Tycho Catalogue and ground-based magnitudes as a function of the ground-based magnitudes. The figure may be compared directly with Figures 8.3(a) and 8.3(b) which show the corresponding median magnitudes for the same stars, thus demonstrating the crucial correction of the de-censoring process for stars fainter than  $V_T \simeq 8.0$  mag. The median difference between Tycho and ground-based magnitudes is shown with a broken line in Figure 19.1 together with the 15th

and 85th percentiles of the distribution. Table 19.1 gives the corresponding median differences for both Tycho channels.

The systematic differences in  $V_T$  are below 0.005 mag for stars in the magnitude range 5.5 mag to 10.25 mag, but brighter stars seem to obtain too faint magnitudes while fainter stars may have obtained too bright magnitudes. This conclusion suffers however from the very small number of standard stars at both the bright and the faint ends of Table 19.1. Regarding the  $B_T$  channel, median differences are somewhat larger than for  $V_T$  when considering stars brighter than  $B_T = 7$  mag. This is a result of the (magnitude-independent) calibration carried out in the 4.5 mag to 9 mag interval for both channels separately. The median differences are smallest for the magnitudes where the bulk of standard stars is located. The calibration limit of 9 mag affects more the distribution of standard stars in  $B_T$  than that of  $V_T$  because only 69 per cent of stars in the sample were available for the calibration of the  $B_T$  channel while 83 per cent were available for the  $V_T$  channel.

The limit of 9 mag was, however, needed in the calibration process because no de-censoring was possible during this process. It may be noted in Figure 19.1 that the scatter is larger for  $B_T$  than for  $V_T$ . This is in accordance with the larger errors given for the ground-based  $B_T(\text{cat})$  magnitudes.

Differences between main and reprocessing calibration are below a few millimagnitudes for stars fainter than  $V_T \simeq 5$  mag and therefore negligible. For the very bright stars the improved estimation in reprocessing gave better mean magnitudes, and reprocessing magnitudes were therefore preferred over those from the main processing. The actual number of stars from the reprocessing in the Tycho Catalogue is however only 51 586. The processing origin of the data is not given in the Tycho Catalogue, but may be obtained from the flags in the Tycho Epoch Photometry Annex.

Table 19.1 also shows that no systematic differences remain from the usage of median magnitudes for stars brighter than  $V_T = 8.0$  mag and  $B_T = 8.5$  mag and de-censored values for fainter stars. This can also be seen from the distribution of stars with magnitude in Figure 16.19. The small artefact in the figure at  $B_T \simeq 10.95$  mag due to different de-censoring processings, discussed in Section 16.3, is not visible in Table 19.1.

In summary, calibration and de-censoring led to median systematic errors well below 0.01 mag in the ranges  $V_T \simeq 4.25$  to 11.0 mag and  $B_T \simeq 4.75$  to 11.5 mag, i.e. well down to the completeness limits. Outside these ranges too few standard stars are available to judge on the accuracy of calibration and de-censoring.

---

## 19.2. Doubtful Standard Stars

---

In principle, 17 683 stars were available for the Tycho photometric calibration. This number comprises an already ‘cleaned’ sample of the original set of stars, e.g. after removing obvious variable stars (see Section 8.3). The true numbers were only about 10 000 stars for the main processing and 13 600 for the reprocessing calibration, because only the magnitude range of 4.5 – 9.0 mag was used for the calibration processes. The complete sample of 17 683 stars was used when the results of photometric calibration (Section 8.2) and the accuracy of Tycho photometry (Section 19.1) were discussed.

**Table 19.1.** Median differences: Tycho Catalogue mean magnitudes minus ground-based magnitudes, as a function of the magnitude at the centre of a bin.

Magnitude	$B_T$		$V_T$	
	$N_{\text{stars}}$	Median	$N_{\text{stars}}$	Median
2.75	1	-	0	-
3.00	0	-	3	0.015
3.25	2	0.042	1	-
3.50	4	0.024	4	0.010
3.75	3	0.015	4	0.000
4.00	4	0.019	7	0.006
4.25	12	0.015	14	0.006
4.50	11	0.011	11	0.004
4.75	26	0.005	30	0.003
5.00	27	0.007	62	0.005
5.25	43	0.008	79	0.005
5.50	75	0.009	134	0.005
5.75	92	0.004	219	0.004
6.00	141	0.004	296	0.004
6.25	489	0.004	223	0.006
6.50	294	0.006	648	0.003
6.75	396	0.006	678	0.003
7.00	499	0.006	798	0.003
7.25	694	0.002	1041	0.003
7.50	910	0.001	1367	0.002
7.75	1113	-0.001	1724	0.002
8.00	1445	-0.002	2026	0.001
8.25	1704	-0.004	2007	0.001
8.50	1799	-0.002	1539	0.001
8.75	1836	-0.001	1135	0.000
9.00	1434	-0.002	850	0.002
9.25	997	0.000	652	-0.002
9.50	756	0.003	557	0.000
9.75	655	0.002	447	-0.003
10.00	585	-0.001	323	-0.004
10.25	511	0.001	220	-0.004
10.50	407	0.000	149	-0.006
10.75	308	-0.001	101	-0.007
11.00	207	0.000	52	0.005
11.25	174	0.003	10	-0.052
11.50	114	0.006	4	-0.140
11.75	74	0.013	2	-0.139
12.00	66	-0.009	0	-
12.25	21	-0.073	0	-
12.50	11	-0.117	0	-
12.75	9	-0.197	0	-

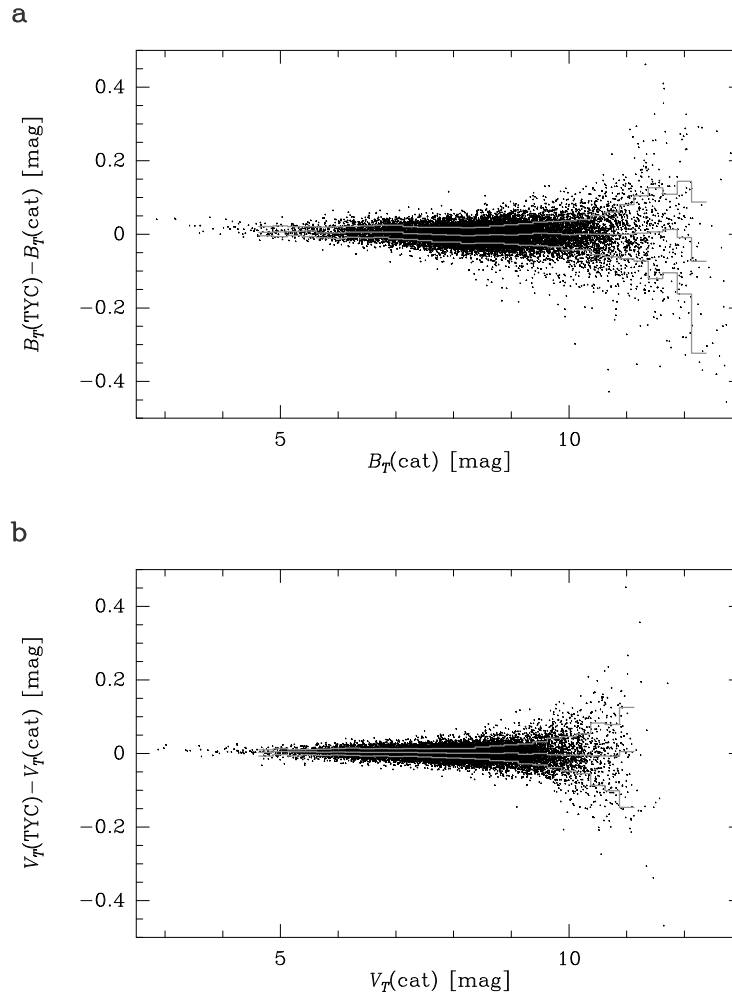


**Figure 19.1.** Tycho mean magnitudes of 17 683 standard stars. Each point represents (a) a  $B_T$  magnitude or (b) a  $V_T$  magnitude for one star, namely the difference between the Tycho mean magnitude and the ground-based magnitude ( $B_T(\text{cat})$  or  $V_T(\text{cat})$ ) versus the ground-based magnitude. The three lines give the median of this difference in 0.25 mag bins (middle) and the 15th and 85th percentiles of the distribution for a minimum of 15 stars per bin.

The ‘cleaned’ sample of standard stars thus included all stars believed to be constant at the beginning of the calibration process, already based on results from a first analysis of satellite data. Nevertheless, 584 standard stars in the Tycho Epoch Photometry Annex B, including 199 stars in the Tycho Epoch Photometry Annex A, are flagged as variable or suspected in either Hipparcos, Tycho or the General Catalogue of Variable Stars (GCVS) and the New Catalogue of Suspected Variable Stars (NSV), see Section 16.4. These stars, classified in Table 19.2, are discussed below.

158 stars were found by the Tycho variability analysis described in Section 19.3. This analysis is quite sensitive even to small variations in the light curve as can be seen when studying the 11 stars also found by Hipparcos variability analysis, e.g. the star TYC 7554–1099–1. (The remaining 147 stars were probably not Hipparcos stars.)

Among the 44 stars listed as variable or suspected variable in the GCVS/NSV only 11 were confirmed by the Hipparcos data and one star by Tycho. The latter star can not

**Table 19.2.** Doubtful standard stars.

Total	Single stars:			Combinations:			
	GCVS/NSV	Hipparcos	Tycho	Tycho Hipparcos	GCVS/NSV Hipparcos	GCVS/NSV Tycho	All
584	44	405	158	11	11	1	0

be shown to be definitely variable, and was not found as such from Hipparcos data, but it exhibits an increased scatter in the Tycho measurements.

In conclusion, all the 584 stars are only, with some reservation, constant enough for use as standards. Not all the 158 stars found in the Tycho variability analysis are definitely variable, but they showed an increased scatter which may be due to undiscovered duplicity or other effects. They should not be used for a photometric re-calibration of Tycho data. This is also true for the stars found to be variable during Hipparcos analysis, but the variability may be on such a low level that it would not harm Tycho calibration.

---

### 19.3. Tycho Suspected Variable Stars

---

#### Construction of the Flags T48 and T49

Two flags in the Tycho Catalogue indicate variability (T48) and duplicity (T49), see Section 2.2, Volume 1. Their construction was part of the photometry verification and is therefore described here rather than in Chapter 11.

Since duplicity may mimic variability in the Tycho measurements, the construction of the two flags could not be separated and the production of the flags was a far from straightforward procedure. The flags were derived by applying dedicated processes to results of the Tycho reduction chain. A procedure applied to the Tycho Photometric Observation Catalogue (TPOC, Section 11.4) yielded T48. The T49 flag required merged results from a procedure run on raw data and another one also applied to TPOC data. The flags were in fact the first derived quantities, constructed from preliminary versions of the Tycho Catalogue and its annex. Thus, providing a verification of the catalogue contents.

The flag in Field T50 (availability of epoch photometry) marks a selection of stars to be contained in the Tycho Epoch Photometry Annexes. A substantial part of the stars included in the Tycho Epoch Photometry Annex A consists of the stars flagged in Fields T48 and T49. This flagging was carried out as a two step procedure:

1. creation of two data bases containing all stars which are probably double or variable, respectively;
2. flagging of the stars in the Tycho Catalogue according to a well defined flag hierarchy.

The following three subsections describe the creation of the two data bases and the flag hierarchy used in flagging the star records in the Tycho Catalogue.

## Variability Data Base

The search for variability was carried out relative to the Tycho photometric precision, i.e. stars were considered to be 'potentially variable' if the variance of their observations exceeded the expected variance. The variances of the observations of stars were derived from the 15th and 85th percentiles of the actual magnitude distribution for all accepted transits. The expected variance was calculated using an empirical function derived from a carefully selected three-parameter fit to the distribution of the photometric standard errors against the number of observations of all standard stars and of a sample consisting of more than 50 000 randomly selected stars. The fit has been compared with a similar distribution for a second sample consisting of more than 10 000 stars flagged as variable and more than 6000 known variable stars selected from the Hipparcos Input Catalogue and cross-identified with the Tycho Photometric Observation Catalogue entries.

The resulting adopted procedure was very robust against single outliers. The procedure was applied to all stars satisfying the condition  $V_T \leq 9.5$  mag and  $N \geq 80$ , i.e.  $\approx 384\,000$  stars from the Tycho Catalogue. For fainter stars or stars having fewer observations the method of comparing an expected variance with the actual variance would not provide reliable results, since the expected variance was very unreliable beyond these limits. The function used in the search was:

$$F_{\text{err}} = 4.6 \times 1.75^m (N - 40)^{-0.71} \quad [19.1]$$

where  $F_{\text{err}}$  is the expected upper limit of the standard error of the mean magnitude of a non-variable star with  $V_T$  magnitude  $m$  and with  $N$  observations. Figure 19.2 shows lines of equal magnitude in a standard error versus  $N$  plane, calculated with Equation 19.1. Lines are drawn for the magnitudes given.

This simple model obviously fails for a small number of observations ( $N \leq 50$  for  $V_T = 6.5$  mag and  $N \leq 70$  for  $V_T = 10$  mag). In this range the correlation between  $N$  and the standard error vanishes.

As an example of the process, consider the 140  $\delta$  Scuti stars flagged in the Hipparcos Input Catalogue, 49 of which are also flagged in the Tycho Catalogue. Only 9 of the 49 are fainter than  $V_T = 8$  mag and 7 of these fainter ones have an amplitude larger than the one given in the Hipparcos Input Catalogue (some of them do not have an amplitude given). Most of the  $\delta$  Scuti stars have amplitudes around 0.1 mag and an unstable period around 0.1 days, thus Tycho was expected to find only the brightest ones. Most of the  $\delta$  Scuti stars not flagged in the Tycho Catalogue had too few transits or did not show any variability in the Tycho data. Similar comparisons have been carried out for variables of Algol and RR-Lyrae types. (Algol itself is not flagged as a Tycho variable because there are only few measurements during one of the minima within the satellite operation time, see Section 19.4).

## Duplicity Data Base

The search for double stars has been carried out using two independent procedures:

1. flagging of suspected double stars during Tycho Input Catalogue Update production in order to extract the raw photon counts during the detection process in reprocessing. The resulting data base of raw counts has been treated by a double peak fitting algorithm (Section 14.5). The number of input stars flagged in the

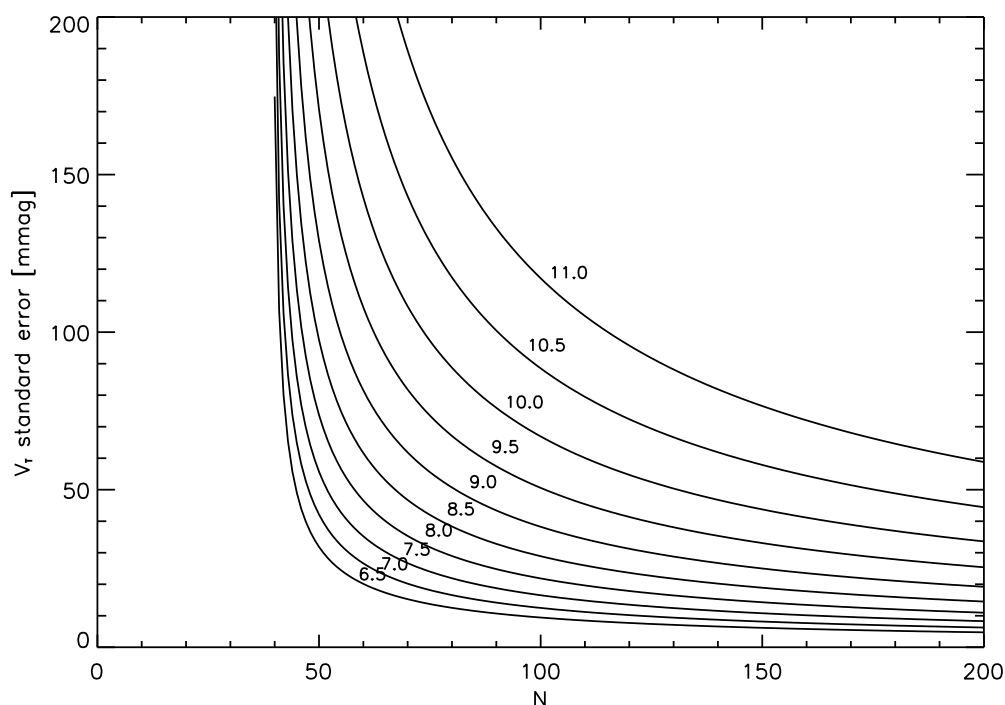


**Figure 19.2.** The lines show the empirical upper limit of the standard error of the mean magnitude for non-variable stars of 10 different magnitudes in the range from  $V_T = 6.5$  mag to  $V_T = 11.0$  mag.

Tycho Input Catalogue Update for this process was 22 083, collected from different sources. The method is called 'DP' hereafter;

2. the search for a correlation between the position angles of the slit and the measured magnitude for all stars brighter than  $V_T = 10.5$  mag (Section 14.6). This process was carried out for almost 500 000 stars. The method is called 'Ph' hereafter.

The duplicity data base was built up using input from these two sources. An overview of the results of the two methods is given in Table 19.3.

The duplicity data base contained data of all stars from both sources. There was a non-empty overlap between the two, and the internal flagging of the data base has been carried out applying the following precedence rule:

$$'D' \Rightarrow 'S' \Rightarrow 'Y' \Rightarrow 'Z'$$

This means, the data base flag was set to the highest indication found by either of the methods ('Z' indicates stars without an investigation of duplicity carried out).

The overlap of stars found to be 'double' or which showed some indication of duplicity in both input streams is given in Table 19.4.

Of the 22 083 stars contained in the candidate list (Section 14.3) for the DP-method, 16 194 stars did not show a significant indication of duplicity after DP-processing. 15 190 stars of this list could not be found by the Ph-method, either. On the other hand, by comparing the numbers contained in the Tables 19.3 and 19.4 it appears that about 75 per cent of the 'D' doubles found by the DP-method were also found by the Ph-method to be 'D' cases. As can be seen in the first two rows of the last column of Table 19.4

**Table 19.3.** Results of the two duplicity search methods. The letters are ‘D’ for double, ‘S’ for suspected double and ‘Y’ for having been treated, but no indication for duplicity found.

Method	D	S	Y
Double-peak (DP)	3239	2650	16194
Photometry (Ph)	7254	12672	478070

**Table 19.4.** Overlap between the internal flags in the duplicity data base. ‘DP’ is the ‘double-peak’ method and ‘Ph’ stands for the photometric method. The letters are ‘D’ for double, ‘S’ for suspected double, ‘Y’ for treated but no indication for duplicity found, and ‘Z’ not treated.

DP	D	S	Y	Z
Ph				
D	2415	588	249	4002
S	296	443	536	11397
Y	183	496	1687	475704
Z	346	1122	13722	556029

many stars got a flag solely because of the Ph-method. The reasons for this are first of all that the initial selection of the candidate list treated by the DP-method was not considered to be complete; and second that the DP and the Ph-methods had different separation sensitivity. The latter reason was also the decisive factor for the selection of the precedence rule given above.

### Flagging in T48 and T49

The final flagging procedure followed the fact that most of the double stars produced an apparent variability due to the long slits of the Tycho instrument. A hierarchical procedure was used to set flags T48 and T49. Any positive indication of duplicity was given precedence over an indication of variability for a given star. A description of the flagging procedure is given in Volume 1, Section 2.2.

### Examples of Tycho Phase Plots

Figures 19.3–19.5 show Tycho Epoch Photometry Annex A single observations for three periodic variables. The periods used to fold the lightcurves have been derived by a periodogram method and/or by a method called epoch folding. They agree with the periods found in the literature for these stars. Figure 19.3 shows the classical Cepheid SU Cas with TYC number 4313–1573–1 and a period of 1.94967 days. Figure 19.4 shows the double mode Cepheid TU Cas (TYC 3260–1095–1). The upper panel of Figure 19.4 shows the result of folding the lightcurve with the primary period of 2.13935 days. The lower panel shows the lightcurve folded with double the primary period, showing the typical behaviour of double mode Cepheids. Figure 19.5 shows the Mira variable R Car (TYC 8945–1871–1). This star has an amplitude of more than 4.5 mag and a period of 302.098 days. This figure shows how the errors of a single Tycho observation depend on the magnitude itself. The error bars shown in the plots are the  $1\sigma$  errors as given in the Tycho Epoch Photometry Annex A.

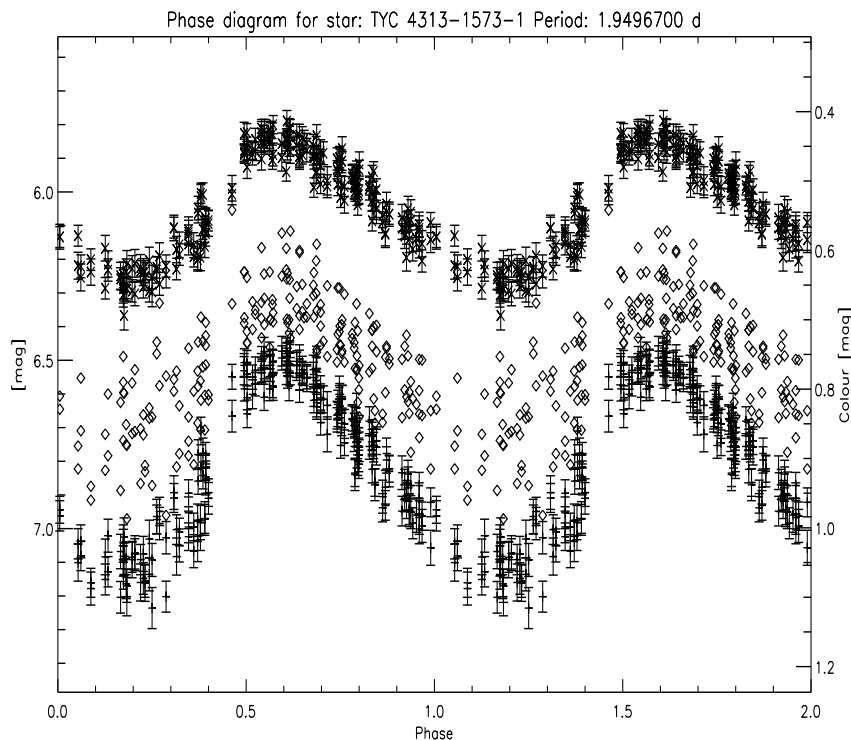


**Figure 19.3.** The phase diagram of the classical Cepheid *SU Cas*. The  $V_T$  observations are drawn with 'x' markers and error bars (upper curve). The  $B_T - V_T$  points are drawn with diamonds. For clarity no error bars are given for the colour. The  $B_T$  observations are drawn with + markers and their error bars. The magnitude axis is given at the left, the colour axis at the right.

---

#### 19.4. Comparison of Tycho and Hipparcos Epoch Photometry for Algol

---

Algol is a well-known bright eclipsing star contained in the Hipparcos Photometry Annex and in both Tycho Epoch Photometry Annexes as HIP 14576 and TYC 2851-2168-1. Due to its eclipses this star provides a suitable target to check the time scales of both Photometry Annexes. This section also compares the photometry in the different catalogues.

##### Mean and Single Transit Magnitudes

Algol was rather regularly and accurately observed by both the Tycho and Hipparcos instruments during the mission, providing a fair number of nearly simultaneous photometric estimations. Fortunately, both instruments observed a deep eclipse around JD 2 448 308.14, when the brightness had dropped by more than 1 mag (see Figure 19.6, upper panel for the observed  $V_T$  magnitudes). With a colour index of almost zero ( $B_T - V_T = -0.005 \pm 0.005$  mag) differences between  $H_p$  and  $B_T$  or  $V_T$  are small. Mean values from the Hipparcos Catalogue and the Tycho Catalogue are:  $H_p = 2.0970 \pm 0.0020$  mag and  $B_T = 2.100 \pm 0.003$  mag,  $V_T = 2.105 \pm 0.004$  mag. The good agreement between both catalogues demonstrates the good photometry available

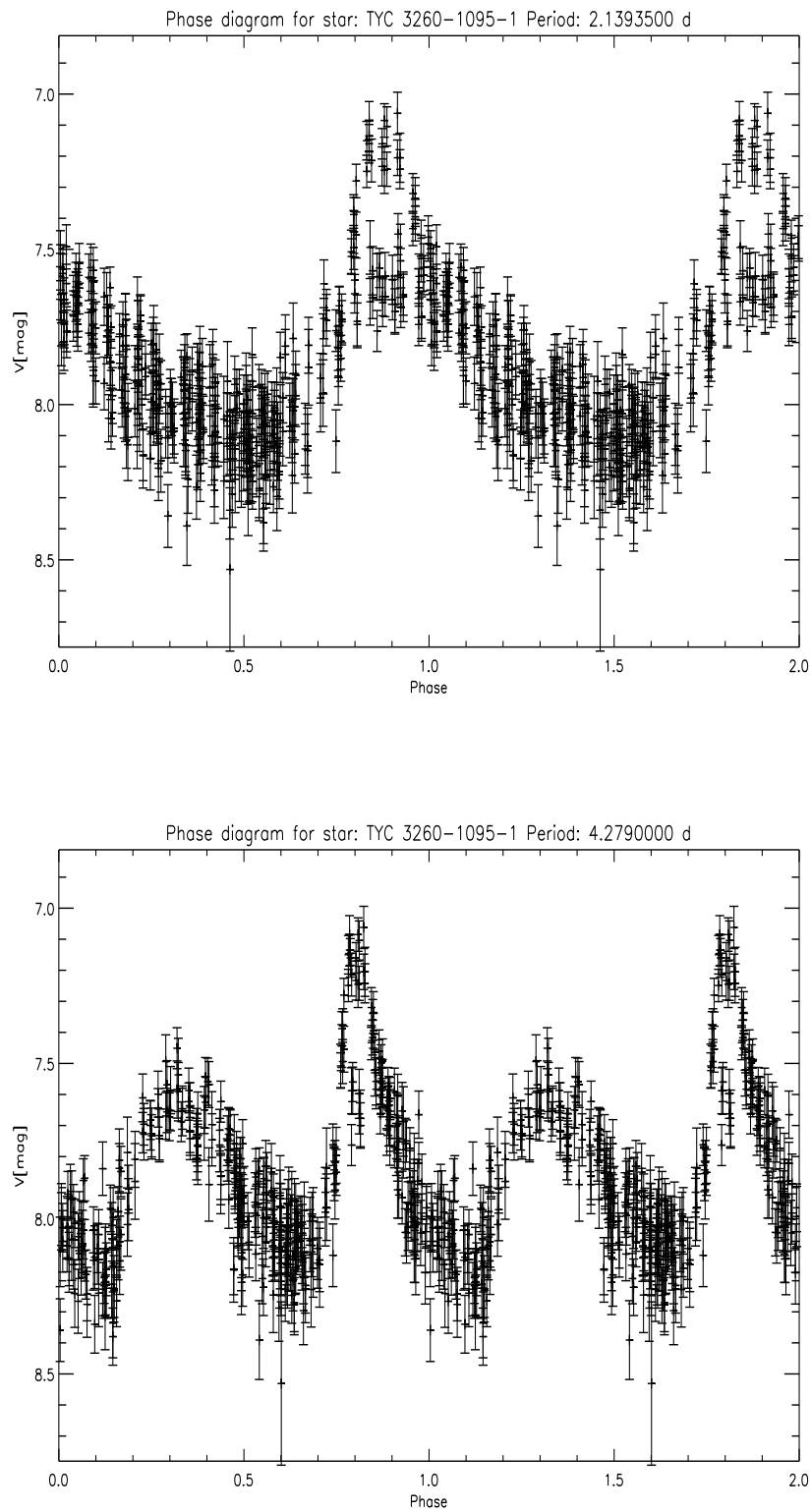


**Figure 19.4.** Phase diagrams for the double mode Cepheid TU Cas. The upper diagram shows the primary period of 2.13935 days, the lower diagram is folded with twice the primary period and shows the variable amplitude of most of the secondary mode peaks.

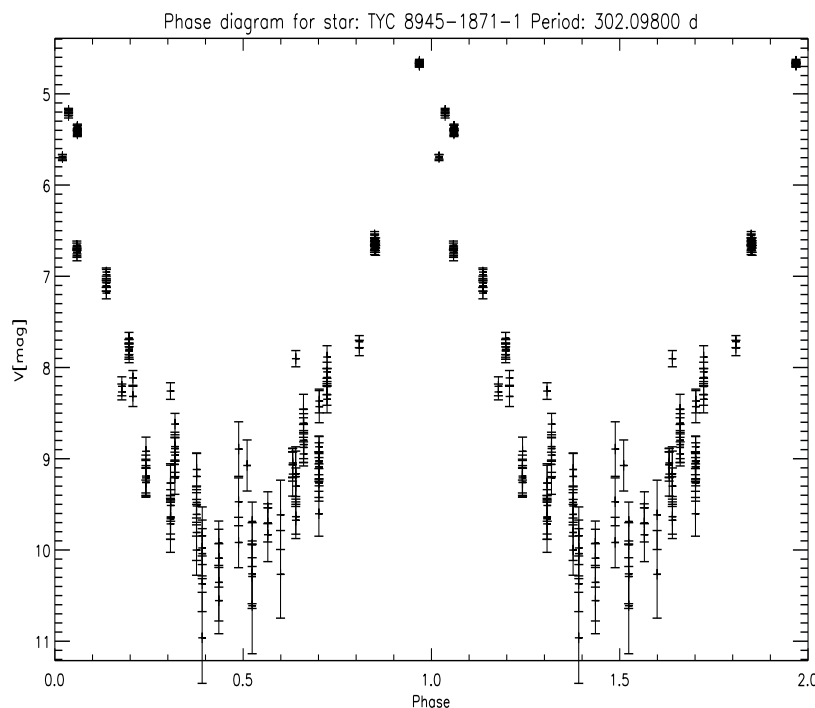


**Figure 19.5.** Phase diagram of the Mira type star *R Car* showing the increase of the errors of the Tycho single observations with magnitude.

when Tycho median magnitudes were derived from reprocessing data (i.e. using an estimation in the wings of the signal for very bright stars).

The differences  $H_p - B_T$  and  $H_p - V_T$  in observed magnitudes at the moments of quasi-simultaneous observations are shown in the two lower panels of Figure 19.6. A set of observations are called quasi-simultaneous if they were obtained during one passage across a field of view of the telescope in both the Hipparcos and Tycho experiment, i.e. within about 20 s of time. A star was first observed on the inclined slits of the star mapper, then on the vertical slits and finally on the main grid, according to the geometry of the instrument and the rotation of the satellite. The number of quasi-simultaneous observations can therefore be up to 3.

For clarity, no error bars for the Tycho magnitudes are shown in Figure 19.6. The typical values of the formal errors are about 0.01 mag in  $B_T$  and 0.009 mag in  $V_T$ , while the  $H_p$  magnitudes were measured with a much smaller formal error of approximately 0.003 mag. The scatter of the differences is 2 to 3 times larger than the expected standard error of the Tycho magnitudes. On the other hand, the scatter computed from the percentiles given in Tycho Epoch Photometry Annex is 0.02 mag for  $B_T$  and 0.03 mag for  $V_T$ . Both facts indicate that the formal errors given for the magnitudes of single transits in Tycho Epoch Photometry Annex (the photon noise and the parameter error, see Equation 8.4) do not include all error sources which may have been significant for the brightest stars. One important error source is the count rate compression during data transfer from the satellite to the ground (see Section 8.1). For a star as bright as Algol this could have introduced an additional error of up to 0.01 mag. Another error source for very bright stars was the limited knowledge of the scan velocity of the satellite.

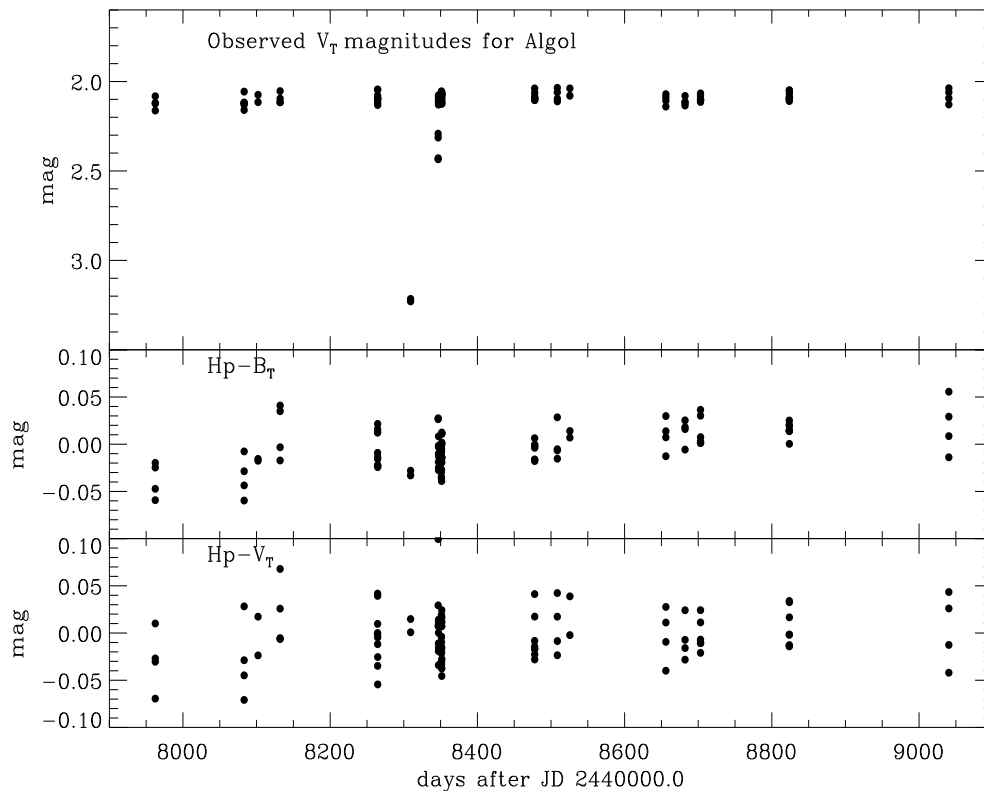


**Figure 19.6.**  $V_T$  magnitudes of Algol, observed by Tycho, and the differences in magnitudes for quasi-simultaneous observations in the Tycho and Hipparcos Epoch Photometry Annexes.

This had no consequences for fainter stars but it affected the estimation of the signal amplitudes in the wings of the signal during reprocessing.

### Timing Quantities

Timing quantities in the Tycho and Hipparcos Epoch Photometry Annexes have the same basic source, namely the counts of the on-board clock. In view of the completely independent and quite complicated data flows and reduction processes through which this primary timing and other subsidiary data have passed, it is useful to compare the times of quasi-simultaneous observations of Algol in the two annexes. Figure 19.7 shows the  $z$ -coordinates, as recorded in the Tycho Epoch Photometry Annex, versus the difference in barycentric Julian Date for quasi-simultaneous observations. As expected, the diamonds, representing observations on the vertical slits, are concentrated around a vertical line at about  $-11$  s, since they are hardly  $z$ -dependent. The gap of 11 s corresponds to the time needed for a star to move the distance of 30 arcmin between the vertical slits of the star mapper and the centre of the main grid, at a nominal velocity of  $165 \text{ arcsec s}^{-1}$ . At the same time, the filled circles clearly trace out the chevron geometry of the inclined slits. The scatter along the time axis of about 1 s is chiefly due to two circumstances: first, the timing of Hipparcos observations is not exactly centered on the middle of the main grid; and second, the timing quantities are rounded to  $10^{-5}$  days = 0.864 s in both annexes.

From this comparison it can be concluded that timing quantities are consistent in the two Epoch Photometry Annexes for this star. Given the fact that the Tycho data analysis

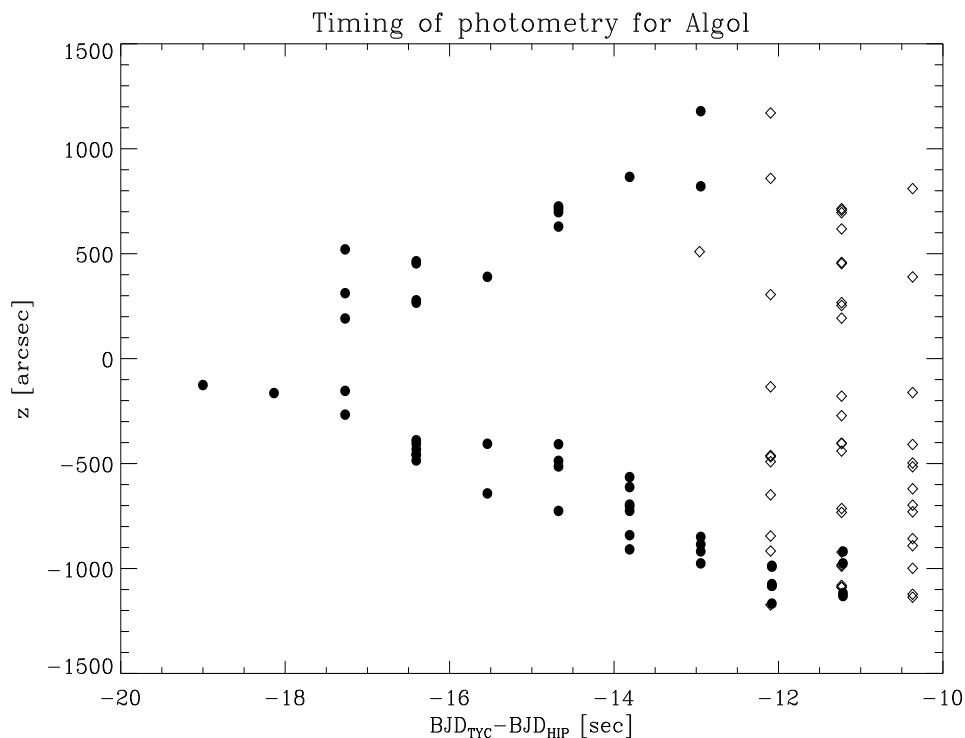


**Figure 19.7.** *z*-coordinates of individual crossings of Algol, as recorded in the Tycho Epoch Photometry Annex, versus the difference in time of observation on the star mapper and on the main grid. Diamonds mark transits over the vertical slits, circles over the chevron slits.

was not optimized to provide optimum photometry for very bright objects, Tycho yields very good mean magnitudes in the case of Algol (uncertainties for the brightest standard stars may be larger, especially for  $B_T$ , see Figure 19.1). However, the formal errors given in the Tycho Epoch Photometry Annex for magnitude estimations of single transits do not include all error sources. These additional errors are important for the bright stars only.

---

### 19.5. Tycho Photometry of Double Stars

---

The Tycho photometry in double or multiple systems was checked by comparison with two sets of ground-based measurements: the first set consisted of differences of magnitudes between the components, and the second set of absolute photometry.

The difference of  $V$  magnitudes between the components was measured by the European Network managed by Edouard Oblak (Oblak *et al.* 1992 and Lampens *et al.* 1997) for several hundred double stars from the Hipparcos programme. These data were obtained from CCD observations performed at various sites (La Palma, La Silla and Saint-Michel de Provence), and some measurements were delivered in advance of publication. Furthermore, a list of Tycho double stars was prepared with the following criteria: separations closer than 20 arcsec; pair belonging to the Hipparcos catalogue;

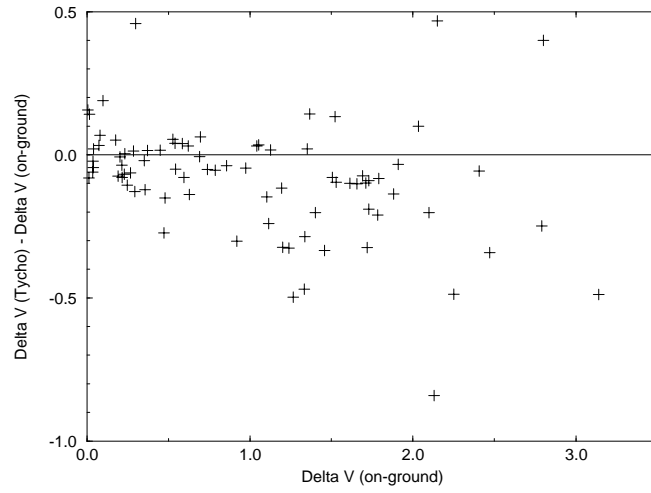


**Figure 19.8.** The bias of  $\Delta V$  derived from Tycho photometry.

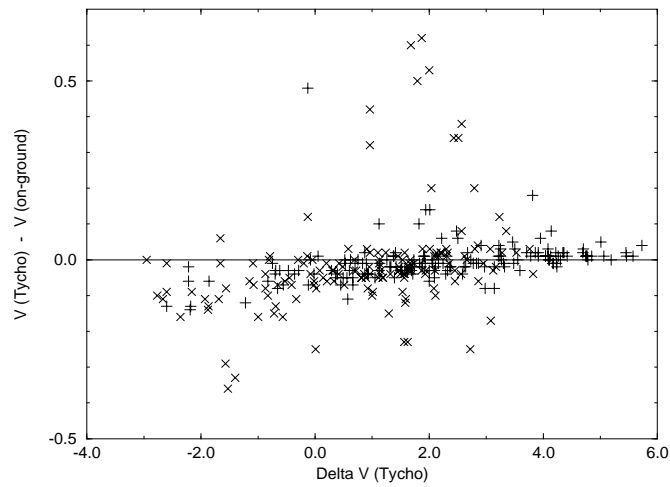


**Figure 19.9.** The bias of the Tycho magnitudes for double star components, related to the difference of magnitudes between the components. The negative  $\Delta V$  refer to secondary components, and the positive ones to primary components. The magnitudes derived from the median of Tycho individual measurements are represented by '+', and the magnitudes calculated by de-censoring are indicated by 'x'.

no variability found in Hipparcos photometry; and fully calibrated Tycho mean magnitudes (i.e. median or de-censored magnitudes). The Tycho  $V_T$  and  $B_T$  magnitudes of these stars were transformed into Johnson  $V$  magnitudes, and the differences between the components,  $\Delta V$ , were derived.

A cross-matching between the ground-based programme and the list of Tycho double stars provided 84 pairs. The offsets between the Tycho results and the ground-based measurements are plotted in Figure 19.8 as a function of the ground-based  $\Delta V$ . It appears from this figure that the  $\Delta V$  from Tycho are in agreement with the ground-based measurements when they are less than about 1 mag. For  $\Delta V$  between 1 and 2 mag, the Tycho photometry underestimates  $\Delta V$ . The bias could be about 0.1 mag. A bias in the double star photometry is not surprising because the Tycho Catalogue contains an excess of double stars due to the side lobes of the companion (see Section 16.2).

In order to confirm this feature, ground-based measurements of the  $V$  magnitudes were taken from the Hipparcos catalogue for some components of double stars. Only pairs closer than 20 arcsec, with Tycho photometry coming from the median or from de-censoring were considered. The stars classified as variable on the basis of the Hipparcos observations were discarded. A sample of 310 components was thus obtained, including 154 stars with  $V$  magnitudes derived from median  $V_T$ ,  $B_T$ , and 156 stars with  $V$  magnitudes coming from de-censored  $B_T$ ,  $V_T$ . The differences between the  $V$  magnitudes obtained from Tycho and the ground-based measurements are plotted in Figure 19.9 as a function of  $\Delta V$ . The  $\Delta V$  is defined as  $\Delta V = V_2 - V_1$ , where the index '1' refers to the component considered, and '2' to the other one.

It appears that the Tycho magnitudes are too bright when  $\Delta V$  is small. For  $\Delta V$  between -3 and +3 mag, the true magnitude of a double star component is about:

$$V_{1, \text{corrected}} = V_{1, \text{measured}} + 0.05 - \frac{0.1}{6} \Delta V \quad [19.2]$$

This formula may be applied to all the stars of the Tycho catalogue having a companion closer than the width of the star mapper slit group, i.e. 34 arcsec. However, it is only an average correction, since the exact one must depend also on the separation of the components (see Section 16.2). The bias of  $\Delta V$  found in Figure 19.8 is thus explained.

In conclusion, the Tycho magnitudes of double stars were compared to two different samples of ground-based measurements. It was found that the magnitudes of the stars were slightly biased, due to the contribution of the luminosity of the companions. The corrected magnitudes may be derived from Equation 19.2.



## 20. FUTURE PROSPECTS

*An outline is given on various future uses of Tycho Catalogue results. Improved proper motions may be derived by means of positions given in the Tycho Catalogue and the Astrographic Catalogue. More accurate reduction of photographic plates and CCD images may be based on the Tycho Catalogue. The search for new variable stars may be based on Tycho epoch photometry. The prospects of a second Tycho processing are briefly discussed, concluding that better values may be obtained for the fainter half million stars of the present Tycho Catalogue, and positions and magnitudes for a total of up to 3 million stars.*

---

### 20.1. Proper Motions Derived by Means of the Astrographic Catalogue

---

The median precision of the proper motion components in the Tycho Catalogue is about 30 mas/yr, while the typical proper motion of a star of magnitude 10 or 11 is of the order of 20 mas/yr. Thus, significant proper motions cannot be expected for the vast majority of the Tycho Catalogue stars from the Tycho data alone. The present section briefly outlines how this situation can be improved by the usage of ground-based data, most notably the Astrographic Catalogue.

#### **Existing Proper Motions**

About 10 per cent of the Tycho Catalogue stars are contained in the Hipparcos Catalogue. Thus, high-quality proper motions on the Hipparcos system with typical precisions between 1 and 2 mas/yr are available for these. The Catalogue of Positions and Proper Motions (PPM, Röser & Bastian 1991; Bastian *et al.* 1993) and its southern '90 000 Stars Supplement' (Röser *et al.* 1994) provide proper motions for about half of the Tycho Catalogue stars, with a typical precision of 4.5 mas/yr and 3.7 mas/yr on the northern and southern celestial hemispheres, respectively (see Volume 3, Chapter 19). However, these data suffer from rather large systematic errors. The regional distortions of the PPM system with respect to the Hipparcos system are of the order of 3 mas/yr on a 5 to 10° scale (again see Volume 3, Chapter 19, or Figure 18.7). Finally, the STAR-NET project (Röser 1996) has produced preliminary proper motions for practically all Tycho Catalogue stars. These are nominally on the PPM system and have an estimated precision of 5 to 7 mas/yr. The systematic errors are about 4 mas/yr, slightly larger than those of the Catalogue of Positions and Proper Motions.

## **The Astrographic Catalogue**

The Astrographic Catalogue is a photographic sky survey initiated in 1887 and carried through mainly between 1895 and 1910. For a description of this huge world-wide collaboration see Eichhorn (1974). The project resulted in more than 8 million position measurements for about 4 million stars. The precision of the plate measurements is now known to be mostly between 0.25 and 0.35 arcsec. However, due to the lack of a dense reference system with stars on all plates with a matching precision, and due to the lack of computing power, up to very recently these plate measurements had not been transformed into celestial coordinates of similar quality.

Between 1985 and 1993, the printed volumes containing the Astrographic Catalogue measurements were transferred into machine-readable form at the Sternberg Astronomical Institute, Moscow. A first reduction of these data onto the FK5 system was carried out in the course of the 'Catalogue of Positions and Proper Motions' project. The precision of that Catalogue and STARNET proper motions rests to a large extent on the Astrographic Catalogue as a very early and precise first epoch. The Catalogue of Positions and Proper Motions combined the Astrographic Catalogue with all existing high-precision astrographic sky surveys (most notably AGK2, AGK3, Yale and Cape zone catalogues, CPC-2 and FOKAT), while STARNET combined the Astrographic Catalogue with the Guide Star Catalog as sole second epoch.

## **The Tycho Reference Catalogue**

A combination of the Astrographic Catalogue with the Tycho Catalogue would give proper motions with a precision of about 2.5 mas/yr for practically all Tycho Catalogue stars. This is the basic idea of the Tycho Reference Catalogue project, a collaboration between scientists in Copenhagen, Lund, Moscow and Heidelberg. The major task to be performed in the framework of this project is a careful re-reduction of the Astrographic Catalogue (and the other astrographic sky surveys mentioned above) onto the Hipparcos system. The work is planned to be completed within about 2 years after the completion of the Tycho Catalogue.

The Tycho Reference Catalogue will surpass the Catalogue of Positions and Proper Motions (PPM) by a factor of 2.5 in the number of stars, and by a factor of 2 in the precision of the proper motions. The systematic errors should also be much smaller than in the PPM. With the very recent and very precise Tycho positions as second epoch, the median positional precision of the Tycho Reference Catalogue will stay below 60 mas for the next 15 years. With its mean density of 25 stars per square degree it will be the main reference catalogue for photographic astrometry for the near future.

The Tycho Reference Catalogue will be a very important supplement to the Hipparcos Catalogue for the study of galactic kinematics. If we define a 'significant' proper motion as one being at least 3 times as large as its mean error then in these terms, Hipparcos provides about 100 000 significant proper motions, the PPM about 200 000 (i.e. about 100 000 in addition to Hipparcos, but with the systematic errors mentioned above), and the Tycho Reference Catalogue will provide of the order of 700 000, i.e. 600 000 in addition to Hipparcos.

More details about the Tycho Reference Catalogue can be found in Röser & Høg (1993).

---

## 20.2. Reductions of Photographic Plates and CCDs using the Tycho Catalogue

---

The Tycho Catalogue will bring significant improvements to the present situation regarding reduction of wide field plates, both because of the larger star density than existing catalogues, and because of the better astrometric and photometric accuracy.

Astrometric and photometric quality have been discussed in the previous chapters. Concerning the star density, there is a factor of three to four with respect to current astrometric catalogues such as the SAO catalogue, frequently used in the past, or the more recent Catalogue of Positions and Proper Motions (PPM). The Tycho star density is eight to ten times larger than the Hipparcos star density.

A more detailed discussion of the use of Tycho data for Schmidt plate astrometric reductions has been presented by Robichon *et al.* (1995), as summarized in Volume 3, Section 19.5. This discussion was based on the use of preliminary Hipparcos and Tycho data as astrometric reference stars. The results obtained showed that the ultimate accuracy from a single Schmidt plate can be better than 0.10 arcsec for stars brighter than the Tycho limit of 11 mag. Actually, the modelling of Schmidt plate field distortions appears more reliable when the reduction is carried out using the numerous, though less accurate, data from Tycho, than when the Hipparcos data alone are used.

Obviously, the proper motions to be derived from the joint use of the Tycho Catalogue and the Astrographic Catalogue, as described in the previous section, will be of critical importance as soon as the photographic plates are taken at epochs significantly different from the Tycho mid-epoch.

The need for accurate proper motions for complementing Tycho data when exposures are obtained at dates only a few years from the Tycho mid-epoch will be even more acute for CCD data. It has been claimed that a precision of about 20 mas can be achieved (according to Zacharias *et al.* 1995 and Zacharias 1996, private communication) for CCD observations obtained with a wide-field astrograph, namely for the average of double exposures and for stars between 6 and 13.5 mag. The high star density of the Tycho Catalogue will be of great help for providing astrometric reference stars for large CCD frames.

For small-field applications, a still denser reference catalogue will be needed, which can be derived from a re-reduction of STARNET onto the Hipparcos system, or from the 3 million stars extended Tycho Catalogue described in Section 20.4.

---

## 20.3. Search for New Variables in the Epoch Photometry

---

A search for variable stars by means of the Tycho epoch photometry was performed among about 480 000 stars brighter than  $V_T = 10.5$  mag, as described in Section 19.3. This process was not based on all the transits valid for photometry, but only on those where photometric measurements were actually obtained. Therefore, if a variable star was too faint for detection of the Tycho transits during a part of the mission, it could be

detected as a variable star only if the variability appeared in the actual measurements. A search for variable stars taking also the non-detections into account, and the application of this method to all the Tycho stars is planned.

The importance of using the non-detections, was already seen in Tycho photometry, when the magnitudes of faint stars were 'de-censored' (see Chapter 9). The principle of de-censoring was to calculate the probability law of the magnitude that would have been measured if a measurement had been obtained. The de-censoring was used to convert the missing measurements into a distribution function that was added to the histogram of the magnitude measurements of any star. The  $V_T$  scatter of the faint stars was derived with this method.

The search for variable stars will be another application of de-censoring. The principle could be as follows: The probability law of the signal recorded for any transit would be computed, without considering whether the transit was detected or not. A theoretical histogram of the magnitude observations would then be derived, and it would be compared to the histogram actually obtained from de-censoring. The two histograms should be similar when the magnitude of the star is actually constant, but they should differ when it is variable.

---

#### 20.4. The Second Tycho Processing

---

All processing of Tycho observations described so far in this volume was based on detections at each group crossing above a certain signal-to-noise ratio (1.5 or 1.8).

Further improvement of the limiting magnitude by about 0.4 mag could be obtained by superposition of the photon counts for each star from two consecutive observations in the preceding and following fields of view. This was beyond the available capabilities with respect to software development and computing facilities when discussed in 1991.

A photon superposition for the whole mission would give a still higher gain and is planned for the near future. This idea was proposed in principle by Høg *et al.* (1982), but had to be abandoned in favour of the more modest approach described in this volume. A second Tycho processing of all raw counts should be based on the available satellite attitude, the Tycho Catalogue of one million stars, and an input catalogue of about 6 million stars from a new reduction of the Guide Star Catalog and the Astrographic Catalogue so that a position accuracy about 0.25 arcsec at the observation epoch is provided. This will facilitate the processing which is planned as a cooperative effort between scientists in Copenhagen and Heidelberg. This processing is expected to give better astrometric and photometric values for the fainter half of the present one million stars. The major reason is that an astrometric estimation based on very few photons does not achieve the Cramér-Rao limit (see Yoshizawa *et al.* 1985). An estimation based on all photons from many transits will come much closer to that limit. Furthermore, many transits of the faint stars were below the limit of signal-to-noise ratio for the detection and were thus completely lost. Good results are expected for altogether up to 3 million stars, brighter than about  $V = 12$  mag. Expected external standard errors at  $V = 11.0$  and 12.0 mag are respectively  $\sigma_{\alpha,\delta} \simeq 50$  and 100 mas and  $\sigma_V \simeq 0.10$  and 0.20 mag.

An illustration of the number of lost Tycho transits is provided by Figure 20.1. The number of stars observed by Tycho versus  $V_T$  magnitude is also shown (dotted). This,

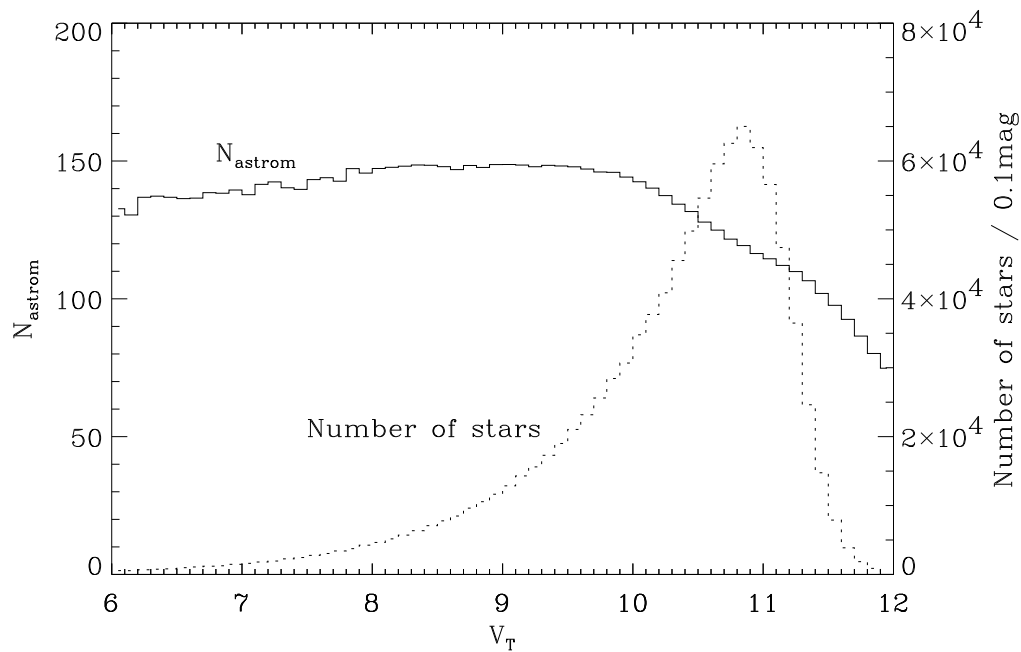


**Figure 20.1.** The number  $N$  of stars with a  $V_T$  magnitude actually observed by Tycho; the number of accepted astrometric transits,  $N_{\text{astrom}}$ .

therefore, does not include the stars in the similar Figure 17.1 having another magnitude than  $V_T$ . It was concluded in Section 17.1 and is also shown by the present figure that about 10 per cent of the stars on the sky with  $V_T = 11.5$  mag were detected by Tycho.

The curve for  $N_{\text{astrom}}$  shows that the number has a maximum of 150 transits at  $V_T \simeq 10$  mag, decreasing to typically 100 transits at  $V_T = 11.5$  mag due to a censoring of transits. The slight decrease towards brighter magnitudes is explained as due to the model for  $\sigma_u$  in Equation 7.8 giving too small values at bright magnitudes, leading to too tight rejection limits. It appears that about 90 per cent of the stars were lost at  $V_T = 11.5$  mag, and that about 30 per cent of the transits of the remaining stars were censored. For all stars on the sky with  $V_T = 11.5$  mag, including those not contained in the Tycho Catalogue, a larger fraction of about 50 per cent of the transits were censored. Further details on the number of transits are given in Section 16.4.

U. Bastian, D. Egret, J.-L. Halbwachs, E. Høg



## APPENDIX A REFERENCES

*Only literature explicitly cited in this volume is listed in the following. A complete bibliography of the Hipparcos project (including general literature and references related to the construction of the Hipparcos and Tycho Catalogues) can be found in Volume 2, Appendix D.*

- Arlot, J.E. 1982. New constants for Sampson-Lieske theory of the Galilean Satellites of Jupiter. *A&A*, 107, 305.
- Bastian, U., Röser, S., Yagudin, L. I., Nesterov, V.V. 1993. PPM Star Catalogue, Vols. III and IV, positions and proper motions of 197179 stars south of -2.5 degrees declination. *Astronomisches Rechen-Institut, Heidelberg*. Spektrum Akademischer Verlag, Heidelberg, Berlin, New York, 1993.
- Batrakov, Iu.V. et al. 1995. Ephemerides of minor planets for the year 1996. *Institute of Theoretical Astronomy, St Petersburg*.
- Brosche, P. 1966. Representation of systematic differences in positions and proper motions of stars by spherical harmonics. *Veröff. Astron. Rechen-Inst., Heidelberg*, No. 17. Verlag G. Braun, Karlsruhe.
- Couteau, P. 1990. Catalogue de 2550 étoiles COU. *Observatoire de la Côte d'Azur, Nice, France*.
- Didelon, P., Egret, D. 1987. Cross-matching SIMBAD and the Guide Star Catalogue for the Tycho Input Catalogue: First tests. *Bull. Inf. CDS*, 32, 27–36
- Dommanget, J. 1983. Un catalogue des composantes d'étoiles doubles et multiples. *Bull. Inf. CDS*, 24, 83-90
- Dommanget, J. 1989a. The CCDM astrometric catalogue for double and multiple stars. *Contributions of the Van Vleck Observatory*, 8, 77. (Star catalogues: a centennial tribute to A.N. Vissotsky).
- Dommanget, J. 1989b. Double Stars. In: Perryman M.A.C., Turon, C. *The Hipparcos mission*, ESA SP-1111, Vol. II, The Input Catalogue, 149–162
- Dourneau, G. 1993. Orbital elements of the eight major satellites of Saturn determined from a fit of their theories of motion to observations from 1886 to 1985. *A&A*, 267, 292.
- Egret, D., Didelon, P., McLean, B.J. 1988. Tycho Input Catalogue: Cross-matching the GSC with the SIMBAD data base. In: J. Torra, C. Turon (eds.), *The european astrometry*

- satellite Hipparcos. Scientific aspects of the input catalogue preparation II*, proceedings of a colloquium held at Sitges, Spain, 419–422
- Egret, D., Didelon, P., McLean, B.J. 1989. The Tycho Input Catalogue. In: Perryman M.A.C., Lindegren L., Murray C.A., Høg E., Kovalevsky J. *The Hipparcos mission*, ESA SP-1111, Vol. III, The Data Reductions, 427–436
- Egret, D., Wenger, M., Dubois, P. 1991. The SIMBAD astronomical data base. In: M.A. Albrecht, D. Egret (eds.), *Databases and on-line data in astronomy*, Kluwer Acad. Publishers, Dordrecht, 79–88
- Egret, D., Didelon, P., McLean, B.J., Russell, J.L., Turon, C. 1992. The Tycho Input Catalogue. Cross-matching the Guide Star Catalog with the Hipparcos INCA data base. *A&A*, 258, 217–222
- Eichhorn, H.K. 1974. *Astronomy of star positions*. Frederick Ungar Publishing Co., New York
- Fabricius, C. 1993. Comparison of the PPM and the Carlsberg Meridian Catalogues. In: A. Lopez Garcia et al. (eds.), *Second International Workshop on Positional Astronomy and Celestial Mechanics*, Universitat de València, 249
- Feigelson, E.D., Nelson, P.I. 1985. Statistical methods for astronomical data with upper limits. I. Univariate distributions. *ApJ*, 293, 192–213
- Frank L. A., van Allen J. A., Macagno E. 1964. Charged-Particle Observations in the Earth's Outer Magnetosphere. *J. Geophys. Res.*, 68 (3543)
- Gómez, A., Morin, D., Arenou, F. 1989. The INCA data base. In: Perryman M.A.C., Turon, C. *The Hipparcos mission*, ESA SP-1111, Vol. II, The Input Catalogue, 47–64
- Grenon, M., Mermilliod, M., Mermilliod, J.C. 1992. Hipparcos Input Catalogue III: Photometry. *A&A*, 258, 88–93
- Grewing, M., Høg, E. 1986. Hipparcos/Tycho: photometry and astrometry for more than 500 000 stars. In: J.P. Swings (ed.), *IAU Highlights of Astronomy, Vol. 7*, 707
- Grossmann, V., Baessgen, G., Evans, D.W., Grenon, M., Grewing, M., Halbwachs, J.L., Høg, E., Mauder, H., Snijders, M.A.J., Wagner, K., Wicenec, A. 1995. Results on Tycho photometry. *A&A*, 304, 110–115
- Halbwachs, J.L., Høg, E., Bastian, U., Hansen, P.C., Schwekendiek, P. 1992. Tycho star recognition. *A&A*, 258, 193–200
- Halbwachs, J.L., Bässgen, G., Bastian, U., Egret, D., Høg, E., van Leeuwen, F., Petersen, C., Schwekendiek, P., Wicenec, A. 1994. A preliminary list of stars from Tycho observations. *A&A*, 281, L25–L28
- Høg, E. 1985. Overview of the Tycho data analysis. In: C. Turon, M.A.C. Perryman (orgs.), *Scientific aspects of the Input Catalogue preparation*, proceedings of a colloquium held at Aussois, France, ESA SP-234, 225–230
- Høg, E. 1989. Overview of the Tycho data analysis. In: Perryman M.A.C., Lindegren L., Murray C.A., Høg E., Kovalevsky J. *The Hipparcos mission*, ESA SP-1111, Vol. III, The Data Reductions, 183–194
- Høg, E. 1995. Tycho astrometry from 30 months of the mission. In: E. Høg and P.K. Seidelmann (eds.) *Astronomical and Astrophysical Objectives of Sub-milliarcsecond Optical Astrometry*, IAU Symposium No. 166, The Hague, August 1994, Kluwer Academic Publishers, Dordrecht, 61–68.

- Høg, E., Wicenc, A. 1991. Tycho Assessment. *Adv. Space Research*, Vol. 11, No. 2, (2)35–(2)44
- Høg, E., Jaschek, C., Lindegren, L. 1982. Tycho - a planned astrometric and photometric survey from space. In: M.A.C. Perryman and T.D. Guyenne (eds.), *The scientific aspects of the Hipparcos space astrometry mission*, ESA SP-177, 21–26.
- Høg, E., Bastian, U., Egret, D., Grewing, M., Halbwachs, J.L., Wicenc, A., Bässgen, G., Bernacca, P.L., Donati, F., Kovalevsky, J., van Leeuwen, F., Lindegren, L., Pedersen, H., Perryman, M.A.C., Petersen, C., Scales, D., Snijders, M.A.J., Wesselius, P.R. 1992. Tycho data analysis. Overview of the adopted reduction software and first results. *A&A*, 258, 177–185
- Høg, E., Bastian, U., Halbwachs, J.L., van Leeuwen, F., Lindegren, L., Makarov, V.V., Pedersen, H., Petersen, C.S., Schwekendiek, P., Wagner, K., Wicenc, A. 1995. Tycho astrometry from half of the mission. *A&A*, 304, 150–159
- Isobe, T., Feigelson, E.D., Nelson, P.I. 1986. Statistical methods for astronomical data with upper limits. II. Correlation and regression. *ApJ*, 306, 490
- Jahreiß, H. 1989. The compilation of astrometric data. In: Perryman M.A.C., Turon, C. *The Hipparcos mission*, ESA SP-1111, Vol. II, The Input Catalogue, 115–128
- Jenkner, H., Lasker, B.M., Sturch, C.R., McLean, B.J., Shara, M.M., Russell, J.L. 1990. The Guide Star Catalogue. III. Production, data base organization and population statistics. *AJ*, 99, 2082–2154
- Kendall, M.G., Stuart, A. 1961. The advanced theory of statistics — Volume 2 : inference and relationship. Charles Griffin & Company Ltd, London, 1961, 1967
- Kukarkin, B.V., Kurochkin, N.E. 1947. *Peremennye Zvezdy*, 6, 93
- Lampens, P., Cuypers, J., Oblak, E., Duval, D. 1997. Accurate CCD photometry and astrometry results for HIPPARCOS visual double stars. In: J.A. Docobo and V. Tamazian (eds.), *Proceeding of the International Workshop Visual Double Stars: Formation, Dynamics and Evolutionary Tracks*, Santiago de Compostela, 29 July–1 August 1996, Astrophysics and Space Science Library Series, Kluwer Acad. Publishers, Dordrecht
- Lasker, B.M., Sturch, C.R., McLean, B.J., Russell, J.L., Jenkner, H., Shara, M.M. 1990. The Guide Star Catalogue. I. Astronomical foundations and image processing. *AJ*, 99, 2019–2058
- Lawson, C.L., Hanson, R.J. 1974. *Solving Least-Squares Problems*. Prentice-Hall
- Lindegren, L. 1977. Meridian observations of planets with a photoelectric multislit photometer. *A&A*, 57, 55–72
- Lindegren, L., Høg, E. 1977. Photoelectric meridian observations of Mars, Jupiter, Saturn, Uranus, Neptune and four minor planets. *A&A Suppl. Ser.* 30, 125–129
- Lindegren, L., et al. 1992. The NDAC data analysis consortium. Overview of the reduction methods. *A&A*, 258, 18–30
- Little, R.J.A., Rubin, D.B. 1987. *Statistical analysis with missing data*. Wiley series in probability and mathematical statistics, John Wiley & Sons
- Makarov, V.V., Høg, E. 1995. Random errors of Tycho astrometry. In: E. Høg and P.K. Seidelmann (eds.) *Astronomical and Astrophysical Objectives of Sub-milliarcsecond Optical Astrometry*, IAU Symposium No. 166, Kluwer Academic Publishers, Dordrecht, 376–378

- Oblak, E., Argue, A.N., Brosche, P., Cuypers, J., Dommanget, J., Duquenois, A., Froeschle, M., Grenon, M., Halbwachs, J.L., Jasiewicz, G., Lampens, P., Mermilliod, J.C., Mignard, F., Sinachopoulos, D., Seggewiss, W., van Dessel, E. 1992. The European Network of Laboratories: Visual Double Stars. In: H.A. McAlister, W.I. Hartkopf (eds.), *Proceeding of the IAU Colloquium 135, Atlanta, 5–10 April 1992, Complementary approaches to double and multiple star research*, ASP Conference Series, Vol. 32, 454–456
- Perryman, M.A.C., Lindegren, L., Murray, C.A., Høg, E., Kovalevsky, J. 1989. The Hipparcos Mission, ESA SP-1111
- Press, W.H., Flannery, B.P., Teukolsky, S.A., Vetterling, W.T. 1986. *Numerical recipes*. Cambridge University Press.
- Robichon, N., Turon, C., Makarov, V.V., Perryman, M.A.C., Høg, E., Froeschlé, M., Evans, D.W., Guibert, J., Le Poole, R.S., van Leeuwen, F., Bastian, U., Halbwachs, J.L. 1995. Schmidt plate astrometric reductions using preliminary Hipparcos and Tycho data. *A&A*, 304, 132–140
- Röser, S. 1996. An updated GSC as the astrometric reference for minor-planet observations. In: S. Ferraz-Mello *et al.* (eds) *Dynamics, Ephemerides and Astrometry of the Solar System*, IAU Symp. 172, 481–484
- Röser, S., Bastian, U. 1991. PPM Star Catalogue, Vols. I and II, positions and proper motions of 181731 stars north of  $-2.5$  degrees declination for equinox and epoch J2000.0. Astronomisches Rechen-Institut, Heidelberg. Spektrum Akademischer Verlag, Heidelberg, Berlin, New York
- Röser, S., Bastian, U., Kuzmin, A. 1994. PPM Star Catalogue — the 90 000 Stars Supplement. *A&A Suppl. Ser.*, 105, 301–303
- Röser, S., Høg, E., 1993. Tycho Reference Catalogue: a catalogue of positions and proper motions of one million stars. In: *Workshop Databases for galactic structure*, A.G. Davis Philip, B. Hauck, A.R. Upgren (eds.), L. Davis Press., 137–143.
- Russell, J.L., Lasker, B.M., McLean, B.J., Sturch, C.R., Jenkner, H. 1990. The Guide Star Catalogue. II. Photometric and astrometric models and solutions. *AJ*, 99, 2059–2081
- Scales, D.R., Snijders, M.A.J., Andreasen, G.K., Grenon, M., Grewing, M., Høg, E., van Leeuwen, F., Lindegren, L., Mauder, H. 1992. Tycho photometry calibration and first results. *A&A*, 258, 211–216
- Seber, G.A.F. 1977. *Linear Regression Analysis*, John Wiley & Sons, New York.
- Silvey, S.D. 1970. *Statistical Inference*. Penguin Books Ltd., Harmondsworth
- Spiegel, M.R. 1961. *Theory and Problems of Statistics*. McGraw Hill
- Sterken, C., Manfroid, J. 1992. *Astronomical Photometry - a guide*. *Astrophys. and Space Sci. Library*, Vol. 175, Kluwer Acad. Publishers, Dordrecht.
- Turon, C., Gómez, A., Crifo, F., Grenon, M. 1989. From scientific proposals to the INCA data base. In: Perryman M.A.C., Turon, C. *The Hipparcos Mission*, ESA SP-1111, Vol. II, The Input Catalogue, 7–22
- Turon, C., Arenou, F., Baylac, M.-O., Boumghar, D., Crifo, F., Gómez, A., Marouard, M., Mekkas, M., Morin, D., Sellier, A. 1991a. The Hipparcos INCA database In: M.A. Albrecht, D. Egret (eds.), *Databases and on-line data in astronomy*, Kluwer Acad. Publishers, Dordrecht, 67–78

- Turon., C., Gómez, A., Crifo, F., Crézé, M., Perryman, M.A.C., Morin, D., Arenou, F., Nicolet, B., Chareton, M., Egret, D. 1991b. The Hipparcos Input Catalogue. I. Star selection. *A&A*, 258, 74–81
- Turon, C., et al. 1992. The Hipparcos Input Catalogue. ESA SP-1136 (seven volumes).
- Turon, C., et al. 1993. Version 2 of the Hipparcos Input Catalogue. *Bull. Inf. CDS*, 43, 5-6
- Vienne, A., Duriez, L. 1995. TASS1.6: Ephemerides of the major Saturnian satellites. *A&A* 297, 588.
- Vityazev, V.V. 1994. The rotor: a new method to derive rotation between two reference frames. *Astron. Astrophys. Transactions*, 4, 195–218.
- Walter, H.G., Mignard, F., Hering, R., Froeschlé, M., Falin, J.L. 1986. Apparent and geometric star positions for the Hipparcos mission. *Manuscripta Geodaetica*, 11, 103–114
- Wicenec, A., Bässgen, G. 1992. Tycho background determination and monitoring. *A&A*, 258, 206–210
- Wicenec, A., van Leeuwen, F. 1995. The Tycho star mapper background analysis. *A&A*, 304, 160–167
- Worley, C.E., Douglass, G.G. 1984. The Washington Double Star Catalog. US Naval Observatory, Washington DC, USA.
- Yoshizawa, M., Andreasen, G.K., Høg, E. 1985. Astrometric and photometric estimators for Tycho photon counts. *A&A*, 147, 227–236
- Zacharias, N., de Vegt, C., Winter, L., Johnston, K. J. 1995. A radio-optical reference frame. VIII. CCD observations from KPNO and CTIO: Internal calibration and first results. *AJ*, 110, 3093



# INDEX

- ALADIN 245
- Algol 272, 275-279
- All-transits file 26, 117
- Amplitude estimation 63
- Apparent positions 43, 46, 65
- Astrographic Catalogue xii, 283-284
- Astrometric analysis 103-121, 159
- Astrometric content 220
- Astrometric disturbance 109
- Astrometric magnitude 117
- Astrometric parameters 117
- Astrometric processing 107
- Astrometric reference stars 223
- Astrometry 1-2, 27-28, 253-265
- Attitude and orbit data 45, 103
- Attitude estimation 11
- Attitude, satellite 17, 43
  
- $B_T$ , see magnitudes
- $B_T - V_T$ , see colour index
- Background 4, 17-20, 71, 140
  - , counts 20
  - , detector 11
  - , determination 51-55
  - , features 53-55
- Basic angle 112-116
- Basic signal processing 15
- Bias, magnitude 133, 144-145
- Bibliography, see Volume 2
- Bright stars 54, 152
  
- Calibration 26, 49, 127
  - , inclined slits 113
  - , instrument 43, 126
  - , magnitudes 84
  - , star mapper 5
  - , vertical slits 112-116
- Callisto 154, 205, 211
- Catalogue preparation 184
  
- CCD reductions 283-285
- CCDM Catalogue 36, 152, 193
- CDA Catalogue 34
- CDS (Strasbourg) 31-41
- Censoring, detections 141
  - , magnitudes 140
  - , see also de-censoring
- Cepheid variables 274
- Cerenkov radiation 18-20
- Ceres 212
- Chevron slits 3
- Close systems, binaries 243
  - , companions 74
  - , see also double stars
- Cloud plots 65-67, 99-100
- Clusters 243
- Colour index,  $B_T - V_T$  xii, 233-234, 237
  - , missing  $B_T - V_T$  179
- Colour-magnitude diagram 236
- Companion stars 76-81, 151
- Completeness 1, 24, 219, 243-252
  - , bright end 243
  - , faint end 250
- Copenhagen University Observatory 6
- Correction of systematic differences 164
- Correlation coefficients 230
- COU Catalogue 194
- Covariance matrix 160
- Cross references 252
- Cross-identifications 252, 257
  - , Guide Star Catalog 33
  - , Hipparcos Catalogue 170
  
- Dark current 18-20
- Data catalogue file 45
- Data delivery 45
- Data flow 6
- Data rates 57
- Data volumes xi, 26, 45-46, 75-77, 181-185

- De-censoring 10-13, 133-147
  - , magnitudes 11-12, 233
  - , procedure 138-144
  - , statistical model 134
- DE200 ephemeris 45, 155, 210
- DE403 ephemeris 210
- Decompression tables 57
- Delta Scuti stars 272
- Dense fields 243
- Detected transits 11
- Detection 10-13, 15, 17-25
  - , lines 78
  - , star transits 55
  - , threshold 137
- Detector background, see background
- Detectors 7
- Dichroic beam splitter 2-3
- Differences Tycho–Hipparcos, see Tycho–Hipparcos
- Differential rotation 112-116
- Digital filtering 15
- Distances between pairs 231
- DM Catalogue 252
- Double stars 1-2, 28, 36, 152, 170,
  - 191-204, 251, 257
  - , astrometry 198
  - , photometry 279-281
  - , photometry bias 281
- Duplicity data base 272
  
- Ecliptic latitude, dependency 225
- Elliptical transfer orbit 1
- Ephemerides, major planets 155
  - , minor planets 156, 210
  - , moons 155
- Ephemeris, see DE200, DE403
- Epoch photometry 2, 11-13, 150, 159,
  - 174, 178, 239-241
  - , annex A 27, 240-241, 274
  - , annex B 27, 240-241
  - , data flow 176
  - , physical sorting 175
  - , timing quantities 278
- Errors, external 258
  - , on magnitudes 143-145, 239
- ESO/SERC Schmidt survey 33
- ESOC 6, 45
- Estimation 20-22
- Europa 154
  
- $F_2$ , see goodness-of-fit
- $F_3$ , see signal-to-noise
- Faint stars 18-20
  
- False stars 79
  - , bright 245
- FAST Consortium 1, 9
- Field of view 113
- Filtering 20-25
  - , linear 23
  - , non-linear 23
- Format background 52
  
- Galactic latitude 31
- Galactic plane 19, 53-54
- Galilean moons 43
- Ganymede 154, 205, 211
- GCVS Catalogue 241, 252
- General Catalogue of Variable Stars, see GCVS
- Geneva Observatory 187
- Geneva standard star catalogue 177
- Geometric calibration 103, 111
- Geometry 45
- Givens rotations 107
- Glossary, see Volumes 1 and 3
- Goodness-of-fit ( $F_2$ ) 68, 227, 229, 255
- Grid assembly 45
- Group crossing 43
- Guide Star Catalog xii, 4, 16, 31, 245
  - , cross-identifications 33
  
- HD Catalogue 249, 252
- Hebe 215
- Heidelberg 6, 43
- Hexagon points 117
- High proper motion stars 35, 152, 251
- Hipparcos Catalogue 170
  - , comparison 255
  - , cross-identifications 170
- Hipparcos Input Catalogue 193
- Hipparcos reference frame 105
- Hipparcos reference stars 108
- Hipparcos–Tycho, differences 257
- Hubble Space Telescope 31
  
- ICRS reference system 105
- Identification of transits 91-101, 109
- Image, half-width 119
- INCA Data Base, see Input Catalogue Data Base
- Input Catalogue Data Base 16, 31-32
- Instrument calibration, see calibration
- Invalid transits 11
- Io 154
- Iris 216
  
- Jet firings 11, 45, 129

- Johnson magnitudes, see magnitudes  
 Jupiter 43, 52, 154
- Light bending 46  
 Linear digital filter 109
- Magnitudes 84  
 —,  $B_T$  9, 233  
 —,  $V_T$  9, 233  
 —, assessment 267-268  
 —, average  $V_T$  errors 238  
 —, censoring 135-136  
 —, Johnson 17  
 —, limiting 24  
 —, mean  $B_T/V_T$  142, 234  
 —,  $T$  11, 17, 82, 86  
 —, UBV 187  
 —, uncertain 179  
 —, see also statistics  
 Main processing 29, 109, 161  
 —, reprocessing 166  
 Major planet ephemerides, see ephemerides  
 Mars 43, 154  
 Maximum likelihood estimators 24  
 Measurements 10  
 Medium-scale irregularities 9-10, 114-116  
 Merging 161-164  
 Meridian circles xi  
 Millennium Star Atlas 243  
 Minor planets 43-45, 154  
 —, ephemerides 156  
 Missing Tycho magnitudes 179  
 Modulating grid 7  
 Monitor stars 36  
 Multiple stars, see double stars
- Nastrom 13  
 $N_{\text{photom}}$  13  
 $N_{\text{transits}}$  13  
 NDAC Consortium 1, 9  
 Neptune 43, 154, 205, 218  
 New Catalogue of Suspected Variable Stars, see NSV  
 Non-detections 11  
 Non-linear filter 59  
 Non-stellar images 36  
 Non-variable stars 237  
 NSV Catalogue 241, 252  
 Nutation 105
- Observation equations 105-107  
 Orbital ephemerides 45  
 Orbital position and velocity 43
- Overview of Tycho reductions 6
- Pair statistics 227  
 Pallas 213  
 Palomar Quick V Survey 33  
 Parallaxes 231-233, 265  
 —, see also statistics  
 Parasites 12, 109  
 —, flag 139  
 —, recording 97  
 Passbands 7, 9, 129  
 Payload, characteristics 7  
 PGC, see predicted group crossing  
 Phase plots 274  
 Photocathode 7  
 Photographic plate reductions 285  
 Photometric standard stars, see standard stars  
 Photometry 26, 178, 267-281  
 —, analysis 123-131  
 —, calibration 123, 189  
 —, catalogue content 233  
 —, disturbance 12  
 —, double stars 279-281  
 —, duplicity search 204  
 —, median magnitudes 125  
 —, photometric system 177  
 —, precision on sky 235  
 —, standard stars 9, 125, 187-189  
 Photosets 126  
 Poissonian behaviour of data 17-18, 51  
 Position angle of close double stars 202  
 Positions, see statistics  
 PPM Catalogue 194, 243-253, 283  
 —, comparisons 260-262  
 Precession 105  
 Precision 1, 27  
 —, dependence on colour 237  
 —, dependence on observations 237  
 —, in photometry 1-2  
 Predicted group crossing (PGC) 22, 57, 69, 91  
 —, see also prediction  
 Predicted transit times 12  
 Prediction 15  
 —, first 16  
 —, of group crossings 16-17, 43-50, 153  
 —, updating-2 91-93  
 —, updating-2 by attitude 16  
 —, updating-3 17, 93-96  
 —, updating-3 redoing 96  
 Processing summary 181-185  
 Proper motions 265  
 —, see also high proper motions

- , see also statistics
- , using PPM 283
- Quality classes 28, 117-118
- Quality control 66
- Quality flag 118, 121
- Quality index  $Q$ , see quality class
- Raw data rates 57
- Raw transit data stream 96
- Raw transits 22
- Recognition 15, 25, 73-90
- Reductions, overview 6
- Redundancy analysis 165
- Redundant companion stars 80
- Reference stars 36
- Reference system, see ICRS
- References 289
- Rejection of detections 12
- Reliability 250
- Reprocessing 29, 109, 149-157, 161
  - , data flow 150
  - , see main processing
- Revised standard star catalogue 188
- Rotation, grid 112-116, 169
- RR Lyrae variables 272
- Sampling frequency 5, 7
- Satellite data processing 43-71
- Satellite orbit comparison 65
- Saturn 43, 52, 154
- Scan fields 10
- Scanning law 5, 48
- Schedule xi, 17
- Schmidt plate astrometric reductions 285
- Second Tycho processing xii, 286-287
- Secondary components of double stars 199
- Separations 28
  - , limit 191
- Serendipity process 45, 251
- Serendipity stars 22, 25, 74, 81-84, 151
  - , mapping process 83
- Serendipity transits 83
- Shutter 45
- Side lobes 4, 23, 109-110
- Signal detection 15
- Signal-to-noise ( $F_s$ ) 12, 28, 61, 69, 118, 160, 229
- SIMBAD 245
- Simulations before launch 15, 28
- Single slit response, functions 5, 7, 57, 63
  - , inclined slits 8
  - , vertical slits 9
- Sirius 243
- Slit response functions, see single slit response
- Slit systems 3
- Solar flares 51-52
- Solar system objects 30, 43, 49, 205-218
  - , prediction 154
- Sorting 107, 184
- Spectral passbands, see passbands
- Spikes 4, 15, 19-20, 52, 58, 169
- Spurious non-detections 135, 138, 141, 242
- Standard errors 225, 253, 258
  - , astrometry 220, 231
  - , declination 226
  - , parallax 231
  - , photometry 220
  - , right ascension 226
  - , underestimate of 231, 262
- Standard stars 84, 126, 131, 152, 241
  - , doubtful 268
  - , for photometry 36
  - , photometric standard 187
- Star Constants Catalogue 159-160
- Star mapper, calibration 57, 103
  - , detection limit 2
  - , geometry 9, 104-107, 111
  - , overview 3
  - , properties 5
- STARNET 284
- Statistics, entries 219
  - , median  $V_T$  in ecliptic coordinates 224
  - , median  $V_T$  in galactic coordinates 224
  - , median  $B_T - V_T$  240
  - , median magnitude 12, 233
  - , median number of observations 225
  - , median parallax 227, 233
  - , median position 119
  - , median proper motion
  - , percentiles 143
  - , positions 262
  - , stars per square degree 222
  - , transits 13, 242
  - , Tycho-Hipparcos 170
  - , Tycho-PPM 261
- Stellar content 243-252
- Strasbourg 6, 31-41
  - , see also CDS
- Stray light 52
  - , sun 18-20
- Suspected variable stars 271-274
- Systematic differences Tycho-Hipparcos 170
- $T$  magnitudes, see magnitudes

- TDAC Consortium, composition xi-xii
- , organisation 3-5
- , overview 15-30
- Telemetry format 17
- Telemetry tapes 45
- Test processing 29
- TIC, see Tycho Input Catalogue
- Titan 43, 154, 211, 217
- Transits 10
  - , identification 26
  - , summary 25
  - , summary file 74-79
  - , time estimation 63
  - , times 103
- TYC, see Tycho Catalogue
- Tycho Catalogue, contents 219-242
  - , production 159-179
  - , see also astrometry/photometry
- Tycho counts, typical 18
- Tycho experiment approval xi
- Tycho Input Catalogue Revision 12, 15, 40, 73, 159
  - , content 25, 87
  - , properties 87
- Tycho Input Catalogue xii, 1, 15-16, 31-41, 73, 103
  - , access 48
  - , coordinates 37
  - , defects 149
  - , duplicate identifications 151
  - , flags 39
  - , format (ASCII) 38
  - , format (binary) 38
  - , identification 37
  - , magnitudes 37
  - , production 32
  - , properties 16, 31-32
  - , publication 41
  - , update 30, 149, 151-153
- Tycho interface document 46
- Tycho magnitudes 17
- Tycho Reference Catalogue 284
- Tycho–Hipparcos differences 163, 201
  - , parallaxes 173
  - , positions 171
  - , proper motions 172
- Tübingen 6
  
- Unit weight error 254-256
- Uranus 43, 154, 205, 218
  
- $V_T$ , see magnitudes
- Valid transits 11, 242
- Van Allen belts 4, 11, 17, 51, 56
- Variability 243
  - Variability data base 272
  - Variability flagging 274
- Variable stars, in epoch photometry 285
  - , suspected 271-274
- Venus 43, 52, 154
- Verification 121
  - , astrometry 253-265
  - , photometry 267-281
  - , results of de-censoring 144
  - , stellar content 243-252
- Vertical slits 3
- Vesta 214
  
- Walraven photometric system 187
- Washington Double Star Catalogue, see WDS
- WDS Catalogue 152, 193
- Wide companions 74, 191, 251
  
- Zodiacal light 19, 52-53